UNIVERSIDADE FEDERAL DO RIO DE JANEIRO

ALLAN AMORIM SANTOS

Tese de Doutorado

MITIGAÇÃO DE FLORAÇÕES DE CIANOBACTÉRIAS E SEUS METABÓLITOS: EFEITO DO PERÓXIDO DE HIDROGÊNIO E DEGRADAÇÃO BIOLÓGICA DE CIANOPEPTÍDEOS

Orientação: Valéria Freitas de Magalhães

Ana Beatriz Furlanetto Pacheco

RIO DE JANEIRO

2020

ALLAN AMORIM SANTOS

MITIGAÇÃO DE FLORAÇÕES DE CIANOBACTÉRIAS E SEUS METABÓLITOS: EFEITO DO PERÓXIDO DE HIDROGÊNIO E DEGRADAÇÃO BIOLÓGICA DE CIANOPEPTÍDEOS

Tese de Doutorado apresentada ao Programa de Pós-Graduação em Ciências Biológicas (Biofísica), Instituto de Biofísica Carlos Chagas Filho, Universidade Federal do Rio de Janeiro, como requisito parcial à obtenção do título de Doutor em Ciências Biológicas (Biofísica)

Orientador: Valéria Freitas de Magalhães
Ana Beatriz Furlanetto Pacheco

Rio de Janeiro
2020

FICHA CATALOGRÁFICA

Santos, Allan Amorim.

Mitigação de florações de cianobactérias: efeito do peróxido de hidrogênio e degradação biológica de cianopeptídeos. Allan Amorim Santos. – Rio de Janeiro: UFRJ / Centro de Ciências da Saúde, Instituto de Biofísica Carlos Chagas Filho, 2020.

ix, 242 f.: il.; 31 cm.

Orientadoras:Valéria Freitas de Magalhães e Ana Beatriz Furlanetto Pacheco.

Tese (doutorado) -- UFRJ, / Centro de Ciências da Saúde, Instituto de Biofísica Carlos Chagas Filho, Programa de Pós- Graduação em Ciências Biológicas (Biofísica), 2020.

Referências: f. 180-192.

1. Cianobactérias. 2. Microcistinas. 3. Qualidade da Água. 4. Biodegradação Ambiental. 5. Metagenômica. 6. Biofísica. - Tese. I. Magalhães, Valéria Freitas de. II. Pacheco, Ana Beatriz Furlanetto. III. UFRJ, CCS, Instituto de Biofísica Carlos Chagas Filho. IV. Título.

Ficha catalográfica elaborada pela equipe de Referência da Biblioteca Central do Centro de Ciências da Saúde da Universidade Federal do Rio de Janeiro.

AGRADECIMENTOS

Ao longo dessa caminhada de 4 anos não poderia deixar de compartilhar os meus agradecimentos a todas as pessoas envolvidas com contribuições diretas ou indiretas na elaboração desta tese de doutorado. Inicialmente, gostaria de agradecer a todos da minha família; mãe, pai, irmã, avó, tias e primos, além de minha namorada. Muito obrigado a todos vocês que estiveram e estarão presentes em todos os momentos da minha vida. Já na vida acadêmica, gostaria de agradecer as minhas orientadoras prof Valéria Magalhães e prof Ana Beatriz Pacheco (Bia) por todo apoio, suporte e paciência ao longo dos experimentos e experiências compartilhadas nessa jornada, desde a monografia apresentada ao Instituto Paulo de Goés, até o mestrado e o doutorado, realizados no Instituto de Biofísica Carlos Chagas Filho. Certamente o apoio de vocês fez tudo parecer mais fácil. Além disso, não poderia deixar de agradecer a prof Sandra Azevedo pelas conversas sempre construtivas em momentos oficiais ou de descontração, e por permitir que eu integrasse o laboratório de Ecofisiologia e Toxicologia de Cianobactérias (LETC), sob sua responsabilidade. Meus agradecimentos para todos os colegas e amigos que tive a oportunidade de cultivar dentro do LETC e de todos os laboratórios da UFRJ, nos quais pude realizar análises experimentais ou contar com algum tipo de ajuda durante esse período. Ressalto os meus profundos agradecimentos a todos os professores colaboradores dos artigos que compõem esta presente tese, bem como os autores dos trabalhos que pude colaborar. Além disso, não posso deixar de falar de todos os colegas que o doutorado me proporcionou tanto da Universidade Federal do Ceará como da Robert Gordon University em Aberdeen (Reino Unido). Não obstante, gostaria de agradecer ao prof Diogo Jurelevicius por aceitar ser o revisor desta tese, colaborando para uma melhor construção do texto, e também a todos os professores membros da banca examinadora por aceitarem a participar e contribuir com esta etapa de conclusão. Agradeço também a todos os órgãos de fomento (CNPq, CAPES e FAPERJ) pela disponibilização de recursos que proporcionaram a elaboração deste trabalho

Os meus mais sinceros agradecimentos a todos vocês!

EPÍGRAFE

"*A vida é aquilo que acontece enquanto você está fazendo outros planos*"

(John Lennon)

RESUMO

SANTOS, Allan Amorim. Mitigação de florações de cianobactérias: efeito do peróxido de hidrogênio e degradação biológica de cianopeptídeos. Rio de Janeiro, 2020. Tese (Doutorado em Ciências Biológicas – Biofísica) – Instituto de Biofísica Carlos Chagas Filho, Universidade Federal do Rio de Janeiro, Rio de Janeiro, Brasil, 2020.

As florações de cianobactérias estão se tornando cada vez mais recorrentes nos corpos hídricos do mundo inteiro, comprometendo a qualidade da água com efeitos danosos tanto para o ecossistema como para a saúde pública. Tal problemática está associada ao fato de cianobactérias serem organismos potencialmente produtores de compostos tóxicos para os seres humanos (cianotoxinas). O presente trabalho buscou investigar processos envolvidos na mitigação de florações de cianobactérias e biodegradação de cianopeptídeos. Primeiramente, foram avaliados os efeitos da aplicação de peróxido de hidrogênio nos parâmetros limnológicos (fatores físicos, químicos e fitoplâncton) e no bacterioplâncton de um reservatório de água usado para o abastecimento público de Fortaleza (CE). Também foi investigada a capacidade de biodegradação do peptídeo microcistina (cianotoxina) por uma comunidade microbiana de tamanho reduzido recuperada da lagoa de Jacarepaguá (RJ), além da degradação de microcistinas e outros peptídeos realizada por linhagens bacterianas isoladas. Os ambientes utilizados como modelo de estudo possuem histórico de florações de cianobactérias com o registro de dominância de gêneros como *Microcystis* e *Planktothrix*. O tratamento com H_2O_2, em escala de mesocosmos, resultou na supressão da floração de cianobactérias em até 72h, comparado a condição controle. No último tempo amostral (120h), houve um aumento de algas verdes na condição experimental de acordo com a análise de clorofila por fluorescência, evidenciando uma regeneração e readaptação deste grupo após o H_2O_2. Em paralelo, foi possível notar um pequeno aumento do grupo das cianobactérias, tanto pela análise de clorofila como metagenômica (16S rRNA), e que esteve relacionado principalmente ao gênero *Cyanobium*. Ainda, de acordo com a metagenômia, também foi observada uma modificação da composição do bacterioplâncton após o uso do H_2O_2, com a predominância do gênero *Exiguobacterium*. A capacidade de biodegradação de microcistina foi avaliada em amostras de água superficial da lagoa de Jacarepaguá (RJ), ao longo de 7 dias, a partir de comunidades microbianas de tamanho reduzido e obtidas por filtração. Assim, estas comunidades foram separadas em frações menores que 0.45 μm (<0.45) ou menores que 0.22 μm (<0.22). Ambas foram caracterizadas quanto à ultraestrutura por microscopia eletrônica de transmissão, e composição taxonômica por metagenômica (16S rRNA), nos tempos de incubação de 0 e 7 dias. Após 7 dias foram observadas alterações morfológicas em ambas as comunidades independente da presença de microcistina. A composição taxonômica de ambas as comunidades mudou em função do tempo e da presença/ausência de microcistina, em relação a composição selecionada inicialmente após a filtração (<0.45 ou <0.22). Na presença de microcistina, táxons já descritos como degradadores desta toxina aumentaram em abundância, especialmente representantes da ordem *Methylophilales*. Além de investigar a degradação de microcistina por consórcios microbianos, caracterizamos a degradação de diversos peptídeos purificados pelas bactérias *Sphingosinicella microcystinivorans* (cepa Y2) e *Paucibacter toxinivorans* (cepa 2C20). Foi possível observar a degradação de cinco variantes de microcistinas e outros cinopeptídeos ao longo de 7 dias apenas pela bactéria *P. toxinivorans*. Peptídeos de origens biológicas distintas também foram testados. *P. toxinivorans* apresentou taxas de degradação diferentes quando os peptídeos foram oferecidos individualmente ou misturados, observação relevante para futura aplicação em processo de remediação. Logo, este estudo contribuiu para a investigação acerca de

tecnologias alternativas no tratamento de água, voltadas para mitigação de florações de cianobactérias ou remediação de cianotoxinas, com perspectiva de otimizá-las como metodologias seguras, eficientes e disponíveis em maior escala.

Palavras-chave: Qualidade de água, florações de cianobactérias, tratamento alternativo, remediação, cianotoxinas, comunidade microbiana, metagenômica

ABSTRACT

SANTOS, Allan Amorim. Mitigation of cyanobacterial blooms: effects of hydrogen peroxide and biological degradation of cyanopeptides. Rio de Janeiro, 2020. Thesis (Doctoral thesis – Biological Sciences – Biophysics) – Institute of Biophysics Carlos Chagas Filho, Federal University of Rio de Janeiro, Rio de Janeiro, Brazil, 2020.

Cyanobacterial blooms are becoming increasingly recurrent in water bodies worldwide, affecting water quality with harmful effects on both the ecosystem and public health. This problem is associated with the fact that cyanobacteria can produce compounds potentially toxic to humans (cyanotoxins). The present work aimed to investigate processes involved in mitigating cyanobacterial blooms and cyanopetides biodegradation. We described the application of hydrogen peroxide in a reservoir used for public water supply in Fortaleza (CE) and its effects on limnological parameters (physical, chemical and phytoplankton factors) and bacterioplankton. The biodegradation capability of the peptide microcystin (cyanotoxin) by a small-sized microbial community recovered from the Jacarepaguá lagoon (RJ) was also investigated, in addition to the degradation of this cyanotoxin and other peptides by isolated bacterial strains. Both environments have cyanobacterial blooms report mainly dominated by *Microcystis* and *Planktothrix*. Treatment with H_2O_2, on a mesocosm scale, resulted in the suppression of cyanobacterial bloom within 72 h, in contrast to the control condition. In the last sampling time (120h) after treatment, there was an increase in green algae, according to the chlorophyll analysis by fluorescence, evidencing a regeneration and readaptation of this group. We also noticed a slight increase in cyanobacteria relative abundance, both by the chlorophyll analysis and metagenomics (16S rRNA), which was related to *Cyanobium* genus. According to this analysis, change in the composition of the bacterioplankton was also observed after treatment, leading to the predominance of *Exiguobacterium* genus. Using surface water samples from the Jacarepaguá lagoon (RJ), we investigated microcystin biodegradation over 7 days by small sized microbial communities, obtained by filtration and containing microorganisms smaller than 0.45 µm (<0.45) or smaller than 0.22 µm (<0.22). Both fractions were characterized for ultrastructure by transmission electron microscopy, and their composition was assessed by metagenomics (16S rDNA), at 0 and 7 days. After 7 days, microbial growth was observed in both fractions, accompanied by changes in cell size and morphology. The taxonomic composition of both bacterial communities changed according to time, the size initially selected (<0.45 or <0.22) and the presence / absence of microcystin. With the addition of microcystin, taxa already described as toxin degraders increased in abundance, especially representatives of the order *Methylophilales*. In addition to investigating microcystin degradation by microbial consortia, we characterized the degradation of several peptides by isolated bacterial strains *Sphingosinicella microcystinivorans* (Y2) and *Paucibacter toxinivorans* (2C20). We could detect degradation of five microcystins variants over 7 days by a *P. toxinivorans*. Other cyanopeptides or peptides of diverse biological sources were also tested. *P. toxinivorans* presented different degradation rates when the peptides were offered individually or mixed, a relevant point for future application in remediation processes. Therefore, this study contributed to the investigation of alternative technologies in water treatment, focusing on the mitigation of cyanobacterial blooms or remediation of cyanotoxins, with the perspective of optimizing them as safe, efficient and available methodologies on a larger scale.

Key words: Water quality, cyanobacterial bloom, alternative treatment, remediation, cyanotoxins, microbial community, metagenomics

LISTA DE ABREVIAÇÕES

ADDA: 3-amino-9-metoxi-10-fenil-2,6,8-trimetil-deca-4,6-ácido dienoico
AERUCY – aeruciclamidas
ALA - alanina
ANBP – anabaenopeptinas
ANOVA – análise de variância
ATP – adenosina trifosfato
BAC – do inglês "biologically activated carbono" - carvão biologicamente ativado
CAGECE – Companhia de água e esgoto do Ceará
COGERH – Companhia de gestão dos recursos hídricos do Ceará
CYCL – ciclosporina
D-MeASP: D-metilasparagina
DOC – do inglês "*dissolved organic carbon*" – carbono orgânico dissolvido
EROs – espécies reativas de oxigênio
FIB – fibrinopeptídeo
GLU - glutamina
H_2O_2 – peróxido de hidrogênio
LDA – do inglês "*linear discriminant analysis*" - análise do discriminante linear
LEFSE – do inglês "*linear discriminant analysis effect size*"
LEU-ENK – leucina-encefalina
MCs – microcistinas
MDHA: N-metildehidroalanina
MIB – 2-metilisoborneol
MRM – do inglês "multiple reaction monitoring" – monitoramento de múltiplas reações
nMDS – do inglês "*non-metric multidimensional scaling*"
OXYT - ocitocina
OTUs – do inglês "*operational taxonomic units*" – unidade taxonômica operacional
O_3^{-}• - radical superóxido
OH^{-}• - radical hidroxila
PBS – tampão fosfato-salino
PCA – análise das coordenadas principais
PCC – do inglês "*Pasteur culture collection*" – coleção de cultura do Instituto Pasteur
PCy - picocianobactéria
PERMANOVA – do inglês "*permutational analysis of variance*" – análise de variância permutacional
PICRUSt – do inglês "*phylogenetic investigation of communities reconstruction of unobserved states*"
POAs – processos oxidativos avançados
PVC – cloreto de polivinil
SNIS – Sistema Nacional de Informações sobre Saneamento
SOD – superóxido dismutase
TEM – do inglês "*transmission electron microscopy*" – microscopia eletrônica de tranmissão
TiO_2 – dióxido de titânio
TOC – do inglês "*total organic carbon*" – carbono orgânico total
UPLC – do inglês "*ultra performance liquid chromatography*" – cromatografia líquida de ultraperformance
UV – ultravioleta
WTP – do inglês "water treatment plant" – estação de tratamento de água

SUMÁRIO

1 INTRODUÇÃO GERAL

As comunidades microbianas habitam os mais diversos ecossistemas do planeta e possuem um grande impacto na manutenção das características ambientais, seja através da sua participação em ciclos biogeoquímicos (ciclo do carbono, nitrogênio, enxofre, entre outros), utilização de produtos naturais ou sintéticos para obtenção de energia, bem como pelas inúmeras associações bióticas e abióticas entre os componentes de um determinado sistema. Quando essas interações são afetadas por algum fator externo, o sistema poderá entrar em desequilíbrio, no qual algumas espécies serão resistentes a essa modificação enquanto outras mais susceptíveis apenas poderão retornar ao sistema de forma gradual, conforme o processo de resiliência. As consequências dos efeitos de um fator de desestabilização poderão estar relacionadas ao tempo de duração e permanência do agente causador do distúrbio (ALLISON & MARTINY, 2008; SHADE et al., 2012).

Cenários de desequilíbrio podem ser observados em ambientes terrestres e aquáticos. Como um exemplo de desequilíbrio da comunidade microbiana em ambientes aquáticos podemos mencionar o crescimento exacerbado de cianobactérias em um período relativamente curto, estabelecendo um evento conhecido como floração (“*bloom”*). Na floração, então, há uma dominância do grupo das cianobactérias em detrimento aos demais grupos do fitoplâncton, como por exemplo as algas verdes e diatomáceas. Eventos de floração são favorecidos em consequência da eutrofização (PAERL e OTTEN, 2013), que consiste em um aumento da concentração de nutrientes (principalmente fósforo e nitrogênio) em um nível que excede a capacidade de assimilação do ecossistema de um determinado ambiente aquático (REYNOLDS, 1987; 2006). Nas últimas décadas, esse cenário tem sido intensificado pela ação humana devido à urbanização acelerada e às práticas agrícolas, que acarretam numa intensa liberação de efluentes diretamente nos ambientes aquáticos, sem prévio tratamento.

Ambientes aquáticos estão sujeitos a diversas consequências danosas decorrentes de florações de cianobactérias. Por exemplo, a dominância desses organismos corresponde a um aumento da sua densidade celular, o que irá ocasionar em algum momento a decomposição desta biomassa por bactérias heterotróficas, levando à diminuição do teor de oxigênio dissolvido (PAERL e OTTEN, 2013). Além disso, o aumento da turbidez e a diminuição da transparência da água prejudicam o desenvolvimento de macrófitas, interferindo diretamente na cadeia alimentar, com uma possível diminuição da diversidade ecológica (PAERL, 2008).

Florações de cianobactérias são registradas em todo o mundo e já foram identificadas até em regiões pouco ocupadas pelo ser humano, como Antártica e Ártico (VINCENT, 2000; KLEINTEICH et al., 2018). Tal fato demonstra a enorme versatilidade adaptativa desses microrganismos, reflexo do seu longo processo evolutivo (CARMICHAEL, 2001; PAERL e OTTEN, 2013). Há evidências fósseis de células de cianobactérias datadas de aproximadamente 2,5 bilhões de anos, estimando-se sua origem por volta de 3,5 bilhões de anos (SCHOPF e WALTER, 1982; SCHOPF, 2000).

Sabe-se que as cianobactérias podem liberar diferentes tipos de moléculas para o ambiente, como ácidos orgânicos, carboidratos, proteínas e lipídeos através de secreção, exsudação ou lise celular (TONIETTO et al., 2014; KEHR e DITTMANN, 2015). Dentre essas moléculas, existem aquelas consideradas não essenciais ao metabolismo primário e definidas como metabólitos secundários. Em relação aos metabólitos secundários, podemos incluir as cianotoxinas de um modo geral. As cianotoxinas são classificadas de acordo com a estrutura química em peptídeos, alcalóides e lipopolissacarídeos, por exemplo. Além disso, são consideradas um fator de risco tanto para o ecossistema, associado a outros efeitos em consequência das florações, bem como para o abastecimento público. Neste último caso, a presença dessas cianotoxinas atreladas ao risco para a população humana se dá pela ineficiência do tratamento de água convencional na remoção dessas substâncias.

Em relação às cianotoxinas, para a maior parte não se sabe ao certo sua função para os organismos produtores. Entretanto, quando em contato direto com mamíferos (via inalação, ingestão, contato dérmico e administração intraperitoneal) agem em alguns tecidos específicos, podendo ocasionar desde irritações cutâneas até graves inflamações causadas por exposições agudas e crônicas. Dependendo da dose e via de exposição, as cianotoxinas podem levar ao óbito, incluindo os seres humanos, como foi reportado no Brasil em 1996, na cidade de Caruaru (PE), onde pacientes foram expostos a cianotoxinas durante terapia de hemodiálise (JOCHIMSEN et al., 1998; AZEVEDO et al 2002). Inclusive, o Brasil foi um dos primeiros países a adotar um limite de concentração de cianotoxinas em corpos d'água para abastecimento público. De acordo com a portaria 2.914 do Ministério da Saúde (BRASIL, MS 2011), que abrange uma normatização para a qualidade de água, quando há evidência de mais de 20.000 células de cianobactérias por mL o sistema de abastecimento deve ser interrompido e a concentração de cianotoxinas deve ser determinada, sendo o limite máximo estabelecido de 1 $\mu g\ L^{-1}$ para equivalentes de microcistina-LR e 3 $\mu g\ L^{-1}$ para equivalentes de saxitoxinas.

Além das cianotoxinas, tem sido observada a potencial toxicidade de outros metabólitos secundários produzidos por cianobactérias, acarretando efeitos citotóxicos em consequência da inibição de determinadas enzimas, comumente proteases (JANSSEN, 2019). Além disso, esses metabólitos podem atuar como aleloquímicos e inibir o crescimento de organismos autotróficos, por exemplo (LEÃO et al., 2010; JANSSEN, 2019). Dentre essas moléculas, as pertencentes à classe dos peptídeos são denominadas cianopeptídeos.

Mediante ao aumento da ocorrência de florações de cianobactérias e seus efeitos tóxicos, se faz necessário desenvolver e otimizar tratamentos alternativos de água nos ambientes impactados. No cenário ideal, o tratamento visa mitigar as florações de cianobactérias, além de eliminar os seus metabólitos até um nível desejável que não ofereça toxicidade aos organismos do ecossistema e aos seres humanos. Não obstante, alguns procedimentos já são aplicados em simultâneo a fim de se obter maior eficiência na melhoria da qualidade da água.

1.1 Controle do crescimento de cianobactérias

Devido ao aumento da ocorrência de florações de cianobactérias e, consequentemente, de suas toxinas nos corpos d'água em todo mundo nos últimos anos (MERILUOTO et al., 2017; SVIRČEV et al., 2019), algumas estratégias têm sido propostas como alternativa para controlar o crescimento desses microrganismos, sem efeito negativo na dinâmica do ecossistema. Para isso, é necessária a aplicação de métodos de baixo custo e com carácter mais específico na mitigação de florações de cianobactérias, evitando um contato direto de seus metabólitos com animais e o homem.

Dentre alguns métodos físicos, químicos e biológicos para este fim, a utilização de processos oxidativos avançados (POAs) tem sido constantemente abordada, devido a sua rápida velocidade de reação sem qualquer geração de subprodutos tóxicos para o ambiente (MATTHIJS et al., 2012; PESTANA et al., 2015; WEENINK et al., 2015; PARK et al., 2017; SCHNEIDER e BLÁHA, 2020). POAs são diferentes tecnologias que utilizam substâncias inorgânicas e, a partir de reações de oxidação, acarretam na geração de espécies reativas de oxigênio (EROs), sendo uma forma eficiente de alterar a composição e/ou decompor moléculas orgânicas (WAGGONER et al., 2017; WANG et al., 2017; GUAN et al., 2018).

Estudos prévios demonstraram que os POAs combinados a outros fatores, como a radiação ultravioleta, além dos processos biológicos convencionais, podem ser um sistema alternativo para remover de modo mais eficiente alguns compostos orgânicos durante o tratamento de água (LEKKERKERKER-TEUNISSEN et al., 2012; OLLER et al., 2011). Por exemplo, algumas estações de tratamento de água ao redor do mundo utilizam POAs com ozonização ou H_2O_2, seguidos de tratamento biológico, usando filtros de carvão biologicamente ativado (BAC) (BONNÉ et al., 2002; van DER HOEK et al., 1999; MARTIJN e KRUITHOF, 2012). Como outros exemplos, podemos citar a aplicação exclusiva de peróxido de hidrogênio (H_2O_2) ou sua associação à radiação ultravioleta (UV/ H_2O_2), além de dióxido de titânio (TiO_2), ozônio (O_3) e a reação de Fenton (LATIFI et al., 2009; MATTHIJS et al., 2012; WANG et al., 2017; JIN et al., 2019).

Alguns estudos avaliaram os efeitos de POAs não apenas em substâncias químicas, e matéria orgânica como um todo, mas também de forma direta na comunidade microbiana e no controle do crescimento de microrganismos (ALEXANDER et al., 2015; FAN & SONG, 2020; AP et al., 2020). O uso de POAs pode ser uma alternativa no controle de florações de cianobactérias e seus metabólitos. A aplicação de H_2O_2 surge como uma das alternativas mais viáveis dentre as estratégias de POAs, devido a facilidade de aplicação, baixo custo e seletividade contra cianobactérias em relação aos demais representantes do fitoplâncton, uma vez que algas verdes eucarióticas conseguem resistir ao tratamento aumentando em densidade em relação às cianobactérias (MATTHIJS et al., 2012; WEENINK et al., 2015; YANG et al., 2018). Alguns fatores podem explicar a maior sensibilidade das cianobactérias ao H_2O_2 comparado a organismos eucarióticos fotoautotróficos. Um é a ausência de uma organização e compartimentalização celular em organelas com membranas protetoras, como encontrado nos eucariotos. Outro motivo poderia ser a ausência da reação de Mehler nas cianobactérias, processo comumente encontrado em seres eucariontes fototróficos, que consiste na redução de moléculas de oxigênio resultando em radical superóxido ($O_2^{-}\bullet$) ou H_2O_2, por exemplo, a partir de elétrons provenientes da cadeia transportadora de elétrons, oriundos da atividade do fotossistema I (POLLE, 1996; ROBERTY et al., 2014). A presença de algumas flavoproteínas em cianobactérias estaria relacionada com a supressão da geração desses radicais. Dessa forma, no processo fotossintético haveria uma redução direta de O_2 para a produção de água, sem a formação de EROs intermediárias, como $O_2^{-}\bullet$, radical hidroxila ($OH^{-}\bullet$) ou H_2O_2 (HELMAN et al., 2003; ALLAHVERDIYEVA et al., 2013). Sendo

assim, as cianobactérias não possuiriam de um mecanismo enzimático completo e tão eficiente como o de eucariotos fototróficos para a eliminação das EROs (PASSARDI et al., 2007).

Independente da produção de EROs mediada pelos POAs usados no tratamento de água ou rejeitos, EROs são produzidas naturalmente em baixas concentrações em sistemas aquáticos, através de reações fotoquímicas que são atribuídas à biota, seja por procariontes ou eucariontes (MOSTOFA et al., 2013). Além disso, a presença de fotossensibilizadores naturais nas águas superficiais, como carbono orgânico dissolvido (COD) e matéria orgânica enriquecida com ácido húmico, pode ser outra fonte de EROs. A produção biológica de H_2O_2 por microrganismos supera a produção fotoquímica, especialmente em ambientes eutrofizados (CORY et al., 2016), e isso faz com que muitos sejam resistentes por possuírem um aparato eficiente de defesa contra o estresse oxidativo.

Por outro lado, o processo de mitigação de florações à base de H_2O_2 pode não degradar de maneira eficiente as toxinas eventualmente liberadas após a morte celular de cianobactérias (SCHNEIDER e BLÁHA, 2020). Além dos destinos naturais destas moléculas, como a degradação por microrganismos autóctones, muitos catalisadores biológicos podem ser otimizados e aplicados como alternativa após o tratamento oxidativo baseado em H_2O_2, uma vez que a eliminação de toxinas é necessária para a garantia de uma água potável e segura (SPOOF et al., 2020).

Mesmo com o aumento de estudos sobre o uso de moléculas oxidantes para a mitigação de florações de cianobactérias e suas toxinas, pouco se sabe sobre seus efeitos e consequências para a comunidade microbiana como um todo, em especial no bacterioplâncton. Ademais, a maior parte dos estudos avaliou a eficiência do tratamento usando espécies ou corpos d'água de ambientes temperados, o que não necessariamente se aplica aos efeitos em ambientes tropicais, que possuem uma carga orgânica mais elevada se comparado a ambientes temperados, podendo influenciar diretamente nos processos de oxidação e sua consequente eficiência (WEENINK et al., 2015; SPOOF et al., 2020).

1.2 Metabólitos secundários de cianobactérias, efeitos e remediação

Dentre os metabólitos secundários produzidos por cianobactérias, podemos citar como os mais estudados os peptídeos cíclicos conhecidos como microcistinas (MCs).

Essas moléculas apresentam mais de 200 análogos já descritos (MERILUOTO et al., 2017), sendo as principais cianotoxinas reportadas em florações tóxicas de água doce (MERILUOTO et al., 2017). São classificadas como hepatotoxinas e o que caracteriza sua ação biomolecular em mamíferos é a inibição das proteínas fosfatases 1 e 2A, acarretando hiperfosforilação e desorganização do citoesqueleto, o que leva a um dano tecidual, principalmente no fígado (YOSHIZAWA et al., 1990). Também já foram observados efeitos desta toxina em outros órgãos e tecidos, como trato gastrointestinal (MORENO et al., 2003; BOTHA et al., 2004), rins (NOBRE et al., 2001; LOWE et al., 2012, MORAES & MAGALHÃES, 2018) e pulmões (SOARES et al., 2007).

A estrutura química geral das MCs consiste em um heptapeptídeo cíclico (D-Ala-X-D-MeAsp-Z-Adda-DGlu-Mdha) com aminoácidos modificados (D-MeAsp: D-metilasparagina, Adda: 3-amino-9-metoxi-10-fenil-2,6,8-trimetil-deca-4,6-ácido dienoico e Mdha: N-metildehidroalanina) e L-aminoácidos em duas posições variáveis. Em relação às MCs já identificadas, a variante –LR (com os L-aminoácidos leucina e arginina nas posições variáveis) é uma das mais reportadas em florações de cianobactérias e uma das mais tóxicas (DIETRICH e HOEGER, 2005)

As MCs, têm sido estudadas com objetivos distintos, seja a caracterização da molécula, seu modo de ação em cultura de células e em organismos de diferentes níveis tróficos, principalmente mamíferos, seja a sua dinâmica no ambiente aquático. Muitos trabalhos já relataram o processo de bioacumulação em diferentes organismos (WILLIAMS et al., 1997; MAGALHÃES et al., 2001 e 2003), o processo de adsorção a partículas de sedimento (MORRIS et al., 2000; WORMER et al., 2011), além do processo de biodegradação por microrganismos presentes no próprio ambiente, na interface entre sedimento e água (JONES et al., 1994; CHEN et al., 2008; MOU et al., 2013; SONG et al., 2014; SANTOS et al., 2020).

Como as etapas inseridas ao longo do tratamento de água convencional não são capazes de eliminar essas moléculas, inúmeros estudos vêm buscando uma forma sustentável e ecológica de remediação, como a biorremediação, a filtração lenta e a utilização de POAs (como por exemplo pela aplicação de H_2O_2, O_3 e TiO_2) (HO et al., 2012; BARRINGTON et al., 2013; PESTANA et al., 2015; WU et al., 2017). Em relação a este último, pelo fato de o processo gerar radicais livres (por exemplo os radicais OH^{-}•), o que pode ser intensificado por reações de fotocatálise, ele seria capaz de decompor compostos orgânicos (SURI et al., 1993) como as próprias MCs (LAWTON et al., 2003; PESTANA et al., 2015; WU et al., 2017). Segundo Pestana et al. (2015) 11 análogos de

MCs, incluindo a MC-LR, puderam ser completamente oxidados em menos de 1 hora, o que facilitaria bastante a aplicação em uma estação de tratamento.

Em relação à biodegradação de MCs, muitos estudos têm relatado ao longo dos anos a ocorrência deste processo em ambientes dulcícolas com histórico de contaminação por esta toxina. Diferentes microrganismos, tanto da água como do sedimento, são capazes de degradar MCs (DZIGA et al., 2013; SONG et al., 2014; KUMAR et al., 2019), como linhagens bacterianas do gênero *Burkholderia* (LEMES et al., 2008), além de bactérias probióticas, como *Lactobacillus rhamnosus* (NYBOM et al., 2012) e também fungos, como o representante *Trichaptum abietinum* (JIA et al. 2012). A partir de linhagens de bactérias isoladas do ambiente foi possível caracterizar uma via enzimática responsável pela biodegradação (BOURNE et al., 1996 e 2001), o que é interessante do ponto de vista da aplicabilidade de um tratamento de água a partir de filtros biológicos, por exemplo. A via enzimática de degradação da MC-LR descrita até o momento (*mlr*), caracterizada por metalopeptidases, produz compostos intermediários como um peptídeo linear (NH2-Adda-Glu-Mdha-Ala-LeuMeAsp-Arg-OH), um tetrapeptídeo (NH2-Adda-Glu-Mdha-Ala-OH) e o aminoácido Adda (BOURNE et al., 1996; HARADA et al., 2004; DZIGA et al., 2016). Todas essas estrurturas apresentaram menor toxicidade, tanto em bioensaios com camundongos quanto em ensaios de inibição das proteínas fosfatases, se comparados à toxina íntegra. No entanto já se sabe que existem outras vias enzimáticas, ainda não descritas, envolvidas na degradação das MCs, uma vez que os genes da via *mlr* não foram detectados em alguns microrganismos isolados capazes de degradar, como representantes do gênero *Paucibacter*, *Stenotrophomonas*, *Aeromonas*, *Arthrobacter*, *Brevibacterium* e *Rhodococcus* (LI et al., 2017; KUMAR et al., 2019). Em paralelo, é importante considerar principalmente que no ambiente natural há consórcios microbianos atuantes com aparatos enzimáticos diversificados (EDWARDS et al., 2008; KUMAR et al., 2019).

Assim, do ponto de vista ecológico se torna pertinente compreender a atividade de biodegradação realizada por consórcios, onde diferentes indivíduos podem agir de forma sinérgica ou antagônica nesse processo (MOU et al., 2013; SONG et al., 2014; LI et al., 2016) resultando em diferentes produtos. Além disso, consórcios microbianos podem ser capazes de degradar não apenas a MC-LR, e possivelmente os subprodutos gerados, mas também outros metabólitos secundários, inclusive, outras substâncias consideradas poluentes (LEZCANO et al., 2017). Em relação a outras cianotoxinas, além das microcistinas, alguns autores observaram microrganismos isolados ou em consórcios capazes de degradar cilindrospermopsina, porém pouco se sabe a respeito dos

mecanismos envolvidos no processo (SMITH et al., 2008; DZIGA et al., 2016). Em relação as saxitoxinas, apesar de já ter sido evidenciada degradação por microrganismos de ambiente marinho e de água doce (DONOVAN et al., 2008; HO et al., 2012) um estudo apontou que esta seria a classe de cianotoxinas mais persistente em ambientes aquáticos, com baixa degradabilidade pela comunidade microbiana (HO et al., 2012).

Também vem crescendo o número de estudos sobre outros cianopeptídeos, como aeruginosinas, anabaenopeptinas, aeruciclamidas, cianobactinas, cianopeptolinas e microgininas. Tais moléculas apresentam diferentes atividades biológicas independente de sua origem, sendo descritos efeitos citotóxicos, antivirais e alelopáticos, dentre outros (BISTER et al., 2004; WELKER e VAN DOHREN, 2006; ERSMARK et al., 2008; SIVONEN et al., 2010; NIEDERMAYER, 2015). No entanto, pouquíssimos trabalhos relatam a atividade da microbiota na dinâmica e degradação dessas substâncias no ambiente aquático (KATO et al., 2007; BRIAND et al., 2016). Por exemplo, Briand et al. (2016) investigaram cultivos da cianobactéria *Microcystis sp*. em condições não-axênica e axênica e observaram biodegradação de cianopeptídeos pela comunidade heterotrófica.

Diante da necessidade da redução ou eliminação de cianotoxinas em ambientes aquáticos, dentre inúmeras outras substâncias consideradas nocivas à saúde humana, se faz necessário desenvolver propostas de mitigação das florações de cianobactérias e remediação de seus metabólitos potencialmente tóxicos. Dessa forma, é de extrema importância a otimização de tecnologias alternativas visando a eficácia do tratamento, em paralelo a segurança ecossistêmica, para que possam ser aplicadas em larga escala com a perspectiva de melhoramento da qualidade de água em função do abastecimento público ou do uso recreativo.

2 JUSTIFICATIVA

Em ambientes aquáticos, o aumento de florações de cianobactérias potencialmente tóxicas se deve à influência direta do homem, que vem acelerando e intensificando o processo de eutrofização, contribuindo com uma elevada carga de nutrientes. Essa situação contribui, de modo contínuo, a uma perda da qualidade da água, ameaçando a segurança hídrica. Em um cenário onde a cobertura de saneamento básico é mínima, esses problemas se tornam mais evidentes (SMITH e SCHINDLER, 2009). De acordo com o Instituto Trata Brasil e o Sistema Nacional de Informações sobre Saneamento (SNIS), no ano de 2018 o sistema de coleta de esgoto do Brasil atendeu apenas 53% da população, resultando em 100 milhões de pessoas sem acesso a esse tipo de serviço. Em consequência ao serviço de coleta, apenas 46% da população recebeu o devido tratamento para manutenção das condições básicas de saneamento (SNIS, 2019). Assim, o estudo e a aplicação de metodologias visando o melhoramento da qualidade de água bruta captada para tratamento, e o consequente abastecimento da população se tornam essenciais. Opções de tratamento alternativo surgem para suprir etapas ineficientes do tratamento convencional de água como, por exemplo, a eliminação de metabólitos secundários com potencial toxicidade. Além disso, esses tratamentos alternativos podem diminuir e controlar o crescimento cianobactérias dominantes no sistema aquático que alimenta as estações de tratamento de água.

No entanto, qualquer tipo de intervenção externa em um ambiente pode trazer consequências para o ecossistema. Neste trabalho procuramos abordar o efeito do uso de um POA através de um experimento de campo realizado em um reservatório de água usado para o abastecimento público de uma região tropical densamente povoada do semiárido brasileiro. Buscamos avaliar o efeito da aplicação única de peróxido de hidrogênio, não apenas no controle do crescimento de cianobactérias, mas também na composição da comunidade microbiana.

Uma outra abordagem alternativa para a remediação de metabólitos potencialmente tóxicos produzidos por cianobactérias é a exploração da capacidade natural de degradação dessas moléculas por representantes da comunidade microbiana. Em uma segunda etapa deste estudo, investigamos a degradação da microcistina por consórcios microbianos recuperados da lagoa de Jacarepaguá. O ambiente em destaque foi escolhido por ser um local historicamente impactado por florações tóxicas de cianobactérias. Além disso, resultados obtidos anteriormente pelo nosso grupo de pesquisa (SANTOS et al., 2020) sugeriram a degradação completa da MC-LR (10 ng mL^{-1}) ao longo de 7 dias por

consórcios microbianos recuperados após a filtração (filtros de 0.45 μm) da água intersticial da lagoa. Em paralelo, amostras de água usadas como controle negativo (filtrada em 0.22 μm) apresentaram uma diminuição da concentração da toxina, sugerindo a ocorrência do processo de degradação por microrganismos presentes nessa fração filtrada. Tal resultado supreendente mostrou-se promissor, uma vez que a degradação se repetiu a partir de outras coletas de água da lagoa a partir dessa fração de tamanho, sendo necessária uma melhor investigação e compreensão acerca de comunidades microbianas com tamanho reduzido. A existência de microrganismos denominados "nanobactérias", "ultramicrobactérias" ou "bactérias filtráveis", já foi observada em amostras ambientais provenientes do solo e de água subterrânea, por exemplo (SOINA et al., 2012; LUEF et al., 2015). No entanto, esses microrganismos representam uma fração microbiana vastamente subestimada e sua atividade metabólica nunca foi demonstrada. Sendo assim, neste estudo foi feita uma investigação aprofundada da participação de comunidades microbianas com estas características de tamanho na degradação de microcistina, caracterizando-as quanto à composição taxonômica e morfologia

Enquanto as microcistinas correspondem a uma pequena fração de peptídeos - e metabólitos secundários em geral - produzidos por cianobactérias, inúmeras moléculas com potencial toxicidade podem ser liberadas no ambiente aquático. Tal fato motiva a investigação de bactérias capazes de degradar essas moléculas presentes nos corpos d'água para uma posterior aplicação biotecnológica. No presente trabalho testamos a capacidade de degradação de linhagens bacterianas, já descritas como degradadoras de MCs, utilizando outros cianopeptídeos que foram adicionados de modo individual ou sob a forma de misturas. Esses experimentos visam mimetizar uma situação mais próxima da realidade encontrada nos ambientes aquáticos, além de buscar por processos eficientes de eliminação de múltiplos compostos com perspectivas para uma aplicação biotecnológica.

Logo, de modo abrangente, este estudo visa o estudo de abordagens alternativas para a mitigação de florações de cianobactérias e seus metabólitos, abrindo perspectivas de otimização destes processos para o potencial uso no tratamento de água, além da compreensão acerca de suas consequências para o ecossistema aquático.

3 OBJETIVOS

3.1 Objetivo geral

Investigar estratégias para o controle e remediação de florações de cianobactérias e seus metabólitos

3.2 Objetivos específicos

- Avaliar o uso de peróxido de hidrogênio como alternativa para a mitigação de florações de cianobactérias em um experimento de campo realizado em um reservatório de água para abastecimento (Capítulo 1);
- Estudar os efeitos do uso do peróxido de hidrogênio sobre a composição da comunidade do bacterioplâncton deste reservatório (Capítulo 2);
- Avaliar a capacidade de biodegradação da MC-LR por consórcios microbianos obtidos após a filtração da água de uma lagoa com histórico de contaminação por esta toxina (Capítulo 3);
- Caracterizar a ultraestrutura da comunidade microbiana destes consórcios por análises microscópicas na presença e ausência de MC-LR (Capítulo 3);
- Investigar a mudança da composição da comunidade bacteriana presente nestes consórcios incubados na presença e ausência da MC-LR (Capítulo 3);
- Avaliar a capacidade de duas linhagens bacterianas na biodegradação de diversos cianopeptídeos e peptídeos de origens biológicas distintas com diferentes estruturas químicas (Capítulo 4).

4 RESULTADOS E DISCUSSÃO (CAPÍTULOS)

4.1 Capítulo 1 (Improving water quality and controlling cyanobacterial bloom using hydrogen peroxide in a semiarid region reservoir used for drinking water)

Improving water quality and controlling cyanobacterial blooms using hydrogen peroxide in a semiarid region reservoir used for drinking water

Dayvson O. Guedes[1]**, Allan A. Santos[2]**, Mário U. G. Barros[1,3], Samylla Oliveira[1], Sandra M. F. O. Azevedo[2], Ana B. F. Pacheco[2], Valéria F. Magalhães[2], Carlos J. Pestana[4], Linda A. Lawton[4], José Capelo-Neto[1]

[1]Federal University of Ceará, Department of Hydraulic and Environmental Engineering, Fortaleza, Brazil.
[2]Biophysics Institute, Federal University of Rio de Janeiro, Brazil
[3]Water Resources Management Company, Fortaleza, Brazil.
[4]School of Pharmacy and Life Sciences, Robert Gordon University, Aberdeen, UK

** Authors contributed equally to the manuscript and both should be considered as the first author

Highlights

- Suppressive effects of H_2O_2 over phytoplankton community.

- Cyanobacteria, Green Algae, and Diatom were supressed for 72h, the duration of 10 mg L^{-1} of H_2O_2.

- Green Algae became the dominant phytoplankton group after H_2O_2 extinguishing.

- Cyanobacteria chlorophyll presented a discrete increase at 120h after H_2O_2 addition, suggesting a potential regrowth.

- H_2O_2 treatment had a high positive impact on cyanobacterial suppression and turbidity decreasing.

Abstract

Massive cyanobacterial blooms have increasingly been reported worldwide, presenting a challenge to conventional water treatment plants and increasing the risks to human health and aquatic ecosystems. Alternative water treatments, like advanced oxidative processes, have been proposed as the best solution to mitigate bloom-forming cyanobacteria as well as to minimize the potential of toxin production. Many researchers have suggested the use of hydrogen peroxide because of high sensitivity of cyanobacteria with no or little effects on other phytoplankton, or even zooplankton species. In this work, for the first time, we present an overview of the effects of hydrogen peroxide on limnological characteristics and chlorophyll concentration in a mesocosms system for 120h in a semiarid tropical Brazilian reservoir used for drinking water. The treatment was efficient supressing Cyanobacteria, Green Algae, and Diatom chlorophyll in comparison to the control condition. Additionally, cyanobacteria chlorophyll remained low and Green Algae became the dominant phytoplankton group until 120h with a discrete increase of cyanobacteria at this last sampling time, suggesting a possible regrowth. A pronounced increase in transparency and a decrease in cyanobacteria-related turbidity was also observed during the decrease of chlorophyll. Dissolved oxygen and pH decreased whereas dissolved organic carbon increased over cyanobacterial collapse until hydrogen peroxide extinction observed at 72h. Nutrients content did not change significantly, which could favor the phytoplankton regrowth after environmental conditions are favorable. According to the principal component analysis using all limnological parameters, the samples taken at 120h approached to the initial condition, suggesting a possible return of these conditions even with a low density of cyanobacteria.

Introduction

Toxic cyanobacterial blooms have increased worldwide, posing a risk to human health and aquatic ecosystem in general due to the production of toxins such as microcystins, cylinderspermopsin, and saxitoxins. Additionally, the intensification of agricultural, urban, and industrial activities associated with economic growth has contributed to anthropogenic eutrophication and higher intensity of cyanobacterial blooms (Neilan et al., 2013; Ibelings et al., 2014). Besides the production of toxins, cyanobacteria can produce taste and odor compounds such as MIB (2-methylisoborneol) and geosmin, which although have not been reported to be toxic, can attribute undesirable changes to the organoleptic characteristics of water (Olsen et al., 2016). Additionally, cyanobacterial blooms overburden water treatment plants operation, accumulating economical losses (Dodds et al., 2009).

Climate change has further intensified cyanobacterial blooms (O'Neil et al., 2012, Paerl and Paul, 2012; Bui et al., 2018; Maliaka et al., 2018). It is expected that the increase of temperature and nutrient loads in water bodies will enhance eutrophication (Moss et al., 2011) and exacerbated phytoplankton biomass with cyanobacteria dominance (Elliott, 2012).

The risks of human exposure to and the costs of treating water with secondary metabolites have led to an effort to investigate solutions for the control of water quality and cyanobacteria within the drinking water reservoir. Although approaches to decrease the abundance of cyanobacteria directly in water bodies do not attack the cause of eutrophication, they are relatively cheaper techniques, easier to manage (Jančula and Marsalek, 2011).

The use of pre-oxidation as a complement to conventional treatment has been applied to increase the efficiency of removing cyanobacteria and intracellular metabolites. Different oxidants such as ozone, chlorine, potassium permanganate, and chlorine dioxide have been tried to achieve this task and decrease the concentration of cyanobacteria and their secondary metabolites (Latifi et al., 2009; Sharma et al., 2012; Lu et al., 2018; Merel et al., 2020). The effectiveness of each oxidant depends on the physiology of the cells, the conditions of application, and the type of metabolite or toxin (Fan et al., 2014). In addition, each of these oxidants has disadvantages concerning the generation of toxic by-products in water (Capelo-Neto and Newcombe, 2017).

One of the alternatives to minimize the problems caused by cyanobacterial blooms mitigating risks of using traditional oxidants is the application of hydrogen peroxide (H_2O_2) directly to the water body (Matthijs et al., 2012; Sinha et al., 2018; Yang et al., 2018; Fan et al., 2019). H_2O_2 has the potential to be an effective algaecide with less environmental impact, given that cyanobacteria present higher sensitivity in comparison to other phytoplankton representant, without adding harmful substances from its composition (Yang et al., 2018) since it produces H_2O and O_2 as the main by-products. Its algaecide action occurs through the formation of hydroxyl radicals (•OH) under exposure to light, which inhibits the electron transportation and photosynthetic activity, causing cell death, mainly in cyanobacteria (Barrington et al., 2013, Latifi et al., 2009). Also, cyanobacteria are more sensitive to H_2O_2 than other phototrophs organisms present in the phytoplankton community due to their non-compartimentalized cellular structure which prevents them from neutralizing •OH (Drábková et al., 2007; Matthijs et al., 2012). Many studies have evaluated the application of H_2O_2 in laboratory-grown cyanobacteria cultures (Ho et al., 2010; Chang et al., 2018; Wang et al., 2019). However, cultivated strains may show adaptations that could modify their behavior in treatment conditions when compared to cyanobacteria in natural environments. Other researches have been investigating the use of H_2O_2 to control cyanobacteria in full-scale lakes in temperate regions and wastewater treatment plants (Matthijs et al., 2012; Barrington et al., 2013; Weenink et al., 2015; Yang et al., 2018). However, studies evaluating the effects of H_2O_2 on the physical-chemical characteristics of water, associated with impacts on the phytoplankton community in tropical reservoirs, especially cyanobacteria, have not been found in recent literature.

Therefore, we hypothesize that H_2O_2 applied *in situ* in reservoirs before the water treatment can improve the physical-chemical and limnological characteristics of the water, controlling the cyanobacteria community. Thus, this work aimed to evaluate the effects of H_2O_2 application on the physical-chemical characteristics of the water using pilot-scale experiments (mesocosms) within a tropical semiarid reservoir used for drinking water.

Methodology

Study area

This study was performed in Gavião reservoir, a water body used exclusively for public water supply to the Fortaleza Metropolitan Area in Ceará state, Brazil (Figure 1). Gavião reservoir is located at the coordinates 3º59'03''S and 38º37'13''W, in an altitude of 65 m relative to the sea level, it has a water storage capacity of 33,3 million m³ (COGERH, 2019). The water treatment plant (WTP) adjacent to Gavião reservoir uses a conventional water treatment technic (coagulation, direct filtration, and disinfection) and is managed by the Water and Wastewater Company of the State of Ceará (CAGECE).

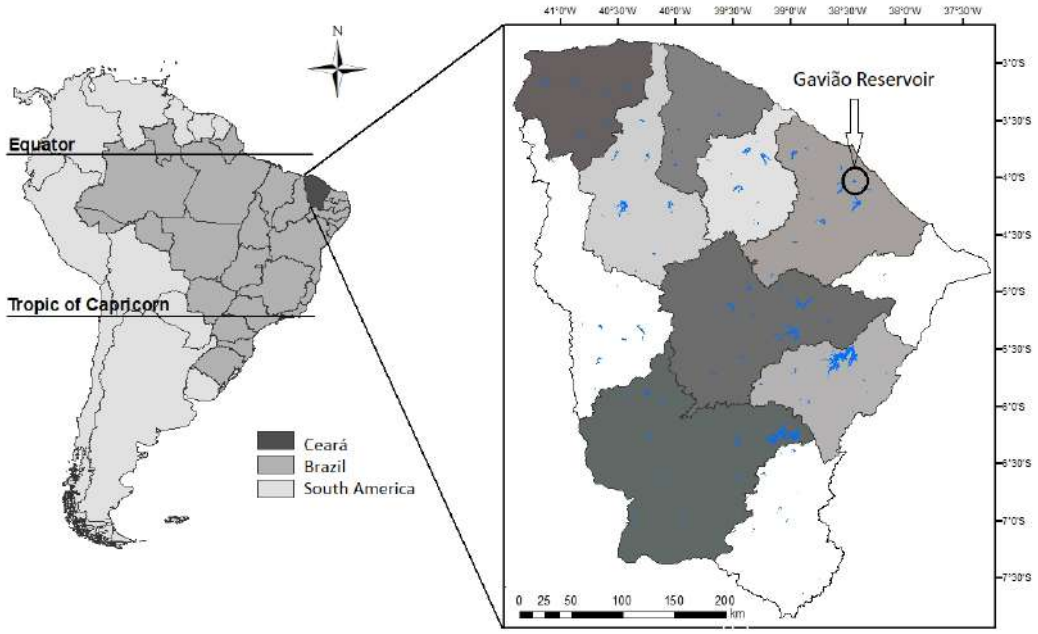

Figure 1: Gavião reservoir location. Source: Adapted from Barros et al. (2019).

Mesocosms experimental set-up

The experiment was carried out using reinforced, impermeable, and semi-transparent plastic bags (mesocosm), build in a cylindrical shape with 2 m length and with 1.5 m diameter (Figure 2A). Each mesocosm was kept open in water by a PVC structure composed as two arcs one at the top, above the water surface, and the other at the bottom of the mesocosm. All mesocosms were isolated from the surrounding waters, allowing no exchange between the internal and external water. The upper edge of the mesocosm was maintained about 50 cm above the water level by a floating structure also comprised of

PVC pipes. These floating structures that held the mesocosms were attached to a floating platform (Figure 2B) located in the lacustrine zone of the Gavião reservoir with an average depth of 10 m, near to the WTP intake point. Full-scale structures in the water can be seen in Figure 2C, D and E.

The water column depth (1.5 m) in the mesocosms was previously established to ensure that the experiment took place in the euphotic zone. The transparency was measured by Secchi disk (50 cm). The extent of the euphotic zone was calculated by multiplying the value of Secchi's disk depth by the K factor of 3, frequently used for tropical waters in Brazil (Esteves, 2011).

Six mesocosms were set up in two groups: three for control proposes (with no H_2O_2) and three considering the treatment conditions, with an initial H_2O_2concentration of 10 mg L^{-1}. Both conditions were performed in triplicates. The three pairs (control-treatment) of mesocosms were disposed of around the floating platform (Figure 2B). The dilution of H_2O_2 was prepared from a stock solution with a nominal concentration of 60% by weight (Sigma Aldrich®). During the experiment period, winds were weak to moderate and no rain or cloud cover was reported in the reservoir region. The experiment was started in February of 2019 with a duration of 120 hours.

Figure 1: Design of experimental platform, using illustration of individual mesocosms (A), the floating platform in top view (B) and real photographs of structure assembled in the Gavião reservoir (C, D and E).

Samples were taken immediately before the application of H_2O_2 (T0) and at times 24, 72, and 120h. For each sampling time, physical-chemical parameters were evaluated. All samples were collected from the center of the mesocosm in a depth of 75 cm using a Van Dorn bottle between 8:00 and 9:00 am, at the same time the H_2O_2 was added. Then, samples were transferred to 1 L amber glass flasks, refrigerated, and transported to the laboratory.

Physico-chemical analysis

The concentration of H_2O_2 in the stock solution was initially determined by iodometric titration according to Skellon and Wills (1948) and, throughout the experiment in the mesocosms treatment, a semi-quantitative method (Quantofix Peroxide 25 Macherey-Nagel, Germany) was used to determine when the H_2O_2 went extinct. The physical-chemical parameters were evaluated following procedures described in Table 1

Table 1: Parameter, method, and place of analysis

Parameter	Method/Equipment	Where
Transparency	Secchi disk	*in situ*
Temperature and pH	YSI probe model 60 - Yellow Springs Instruments, EUA	*in situ*
Dissolved oxygen	YSI probe model 55 - Yellow Springs Instruments, EUA	*in situ*
Conductivity	Conductivity meter 105A+, Orion Research, EUA	*in situ*
Turbidity	Hach model 2100P, EUA	Laboratory
True color	Genesys spectrophotometer 10S UV-Vis - Thermo Scientific, EUA	Laboratory
Total organic carbon (TOC) and dissolved carbon (DOC)	Sievers InnovOx Laboratory TOC Analyzer (General Electrics, USA)	Laboratory
Ammonia	4500-NH_3 C - APHA (2005)	Laboratory
Nitrite, nitrate, orthophosphate, sulfate, fluoride, and chloride.	Samples were filtered through a glass fiber 0.45-µm membrane before analyses using Dionex ICS-1100 (Thermo Scientific, EUA)	Laboratory

Chlorophyll-*a* concentration

Chlorophyll-*a* comprises the main pigment of photosynthetic activity and was used to evaluate the effect of hydrogen peroxide treatment on the natural phytoplankton community. The chlorophyll-*a* concentration estimation was carried out by PHYTO-PAM II Phytoplankton Analyzer (Walz, Germany), using four different wavelengths to excite chlorophyll-*a* by respective channels such as blue (470 nm), green (520) and red (645 and 665 nm). Then, it is possible to distinguish phytoplankton from different types of light-harvesting pigment antennae and estimate chlorophyll-*a* concentration values ($\mu g\ L^{-1}$) from cyanobacteria, green algae, and diatoms (Walz, 2003)

Statistical analysis

Multivariate analysis by PERMANOVA was applied to verify the effects of H_2O_2 over the time (0, 24, 72, and 120h) on all physical-chemical parameters evaluated, considering $\alpha = 0.05$. D'Agostino & Pearson normality test was applied to verify the distribution of data considering $p<0.05$. To support more specifically the difference within each parameter as an interaction consequence between control and treatment over the time, two-way ANOVA was used considering $\alpha = 0.05$ and uncorrected Fisher's LSD *post hoc* to detect the difference at the respective time level. To ordinate all data together, principal components analysis (PCA) was used following Kaiser rule that was chosen to take the most important components in the analysis since it selects eigenvalue above one criterion ($\lambda i > 1$), which explain the data variability (Fraga et al., 2016, Kaiser, 1958). To evaluate the ordination of samples, three groups were created considering the closest relationship between physical or chemical characteristics along with chlorophyll from the three phytoplanktonic groups. Group I had transparency, turbidity, true-color, and temperature; Group II had pH, dissolved oxygen, TOC and DOC; Group III had ammonium, nitrite, nitrate, and orthophosphate. To support the relationship between parameters with a clear association within each group, a Pearson correlation was applied considering $p<0.05$ and a minimal r-value of 0.7 to achieve greater strength of robustness. Statistical analysis was performed by R software version 1.3.959 and Graphpad Prism 8.0

Results

The time of 72h marked the extinction of H_2O_2 in all three mesocosms treatment. The multivariate analysis by PERMANOVA test supported the significant effect of H_2O_2 on water quality ($p = 0.02$; $F = 25.20$), with great interaction between time of exposure and treatment ($p = 0.024$; $F = 4.0793$), since all parameters were influenced by H_2O_2 until its extinction at 72h. All raw data as well as statistical analysis can be found in the Supplementary Information.

For the estimated chlorophyll analysis, all three phytoplankton groups were influenced by H_2O_2 over the time: Cyanobacteria ($p < 0.0001$, $F = 21.45$), Green Algae ($p < 0.0001$, $F = 58.38$) as well as Diatom ($p < 0.0001$, $F = 24.97$). Cyanobacteria showed the highest chlorophyll value at T0 (~ 35 µg L^{-1}), presenting a consistent decrease in all sampling times compared to the control condition, with complete elimination by 72h (Figure 3A). Green Algae chlorophyll also decreased significantly by 72h ($p = 0.0003$ for both) reaching 50% of reduction over this time. However, it showed a substantial increase at 120h ($p = 0.03$) reaching about 25 µg L^{-1} when the control condition showed only 13 µg L^{-1} (Figure 3B). Regarding the Diatoms group, the initial chlorophyll concentration (1 µg L^{-1}) was completely removed within 24h compared to the control condition ($p = 0.04$). A substantial increase occurred at 120h in the mesocosms treatment, reaching three times more chlorophyll than the control condition (Figure 3C).

Chlorophyll from Green Algae in the mesocosms from the treatment condition achieved a very similar concentration of cyanobacteria in the control condition at 120h (about 25 µg L^{-1}), two days after H_2O_2 extinction, which would suggest a substitution of bloom-forming phytoplankton group.

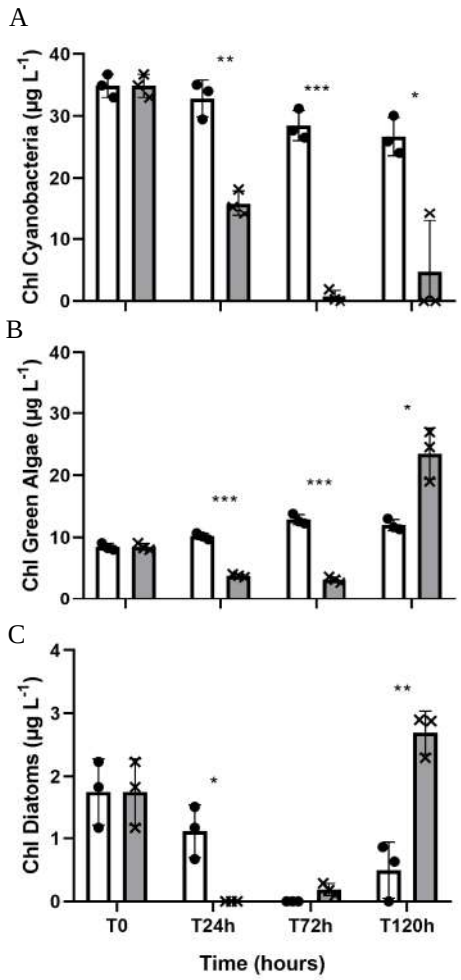

Figure 3: Chlorophyll estimation for the groups (A) Cyanobacteria, (B) Green Algae, and (C) Diatom over time. Results are expressed as the mean ± SD. Grey and white bars represent treatment with H_2O_2 and control conditions, respectively. The asterisks represent statistical difference between treatment and control, with * ($p<0.05$), ** ($p<0.01$), and *** ($p<0.001$).

The conductivity showed a significant variation over the time ($p = 0.005$, $F = 7.2$) with an increase in the treatment at 120h ($p = 0.0007$), reaching 585 µS cm^{-1} in comparison to 575 µS cm^{-1} from control. Nonetheless, no modification was observed over the time between the treatment and control condition for conductivity-related salts such as chloride ($p = 0.27$) and sulphate ($p = 0.57$) besides fluoride ($p = 0.57$) (Supplementary Figure 1). The parameters which demonstrated affinity or were correlated from a physical-chemical or biological standpoint were divided into three different groups, to achieve a comprehensive ordination using PCA over the time. Cyanobacteria, Green Algae, and Diatom chlorophyll were placed in all three groups to assess their interaction with the

other variables since they provide a reasonable estimate of the algal biomass (Bauzá et al., 2014).

Group I (transparency, turbidity, true-color, and temperature) was pooled in a bi-dimensional ordination in which the two highest components corresponded to 73.63% of the total variation, with the first component accounting for 46.5% of it (Figure 4A). The resulting PCA showed cyanobacterial chlorophyll and turbidity opposed to transparency, with their eigenvalues forming a 180º angle, indicating a high negative correlation between transparency and cyanobacterial chlorophyll ($p<0.001$; $r = -0.96$) as well as turbidity ($p<0.001r = -0.84$). That finding was also supported by Pearson correlation (Supplementary Table 1). No relationship between transparency and turbidity with the other chlorophyll groups was evidenced since their eigenvalues were positioned at approximately 90º. Additionally, cyanobacterial chlorophyll and turbidity are represented in the first quadrant alongside the control cluster, whereas transparency is in the third quadrant alongside the treatment samples (Figure 4B). This fact could be explained by the fact that cyanobacterial biomass influenced directly on turbidity with a high positive association ($p<0.001$; $r = 0.87$) (Supplementary Table 1). True-color and temperature had a poor correlation with these three chlorophylls, which can be observed according to their vector position and size, respectively (Figure 4A and Supplementary Table 1).

When clustered by time, samples at time 0h shared the same quadrant as cyanobacterial chlorophyll and turbidity whereas samples at time 72h shared the same quadrant as transparency, opposed (180º) to time 0h, suggesting an improvement in water quality. The cluster from samples 120h moved to the second quadrant towards the initial condition (time 0h), suggesting a return to a poor water quality scenario (Figure 4C). Moreover, green algae and diatom chlorophyll proximity to time 120h cluster may indicate that the worsening of water quality is due to the regrowth of these groups (Figure 4A and C).

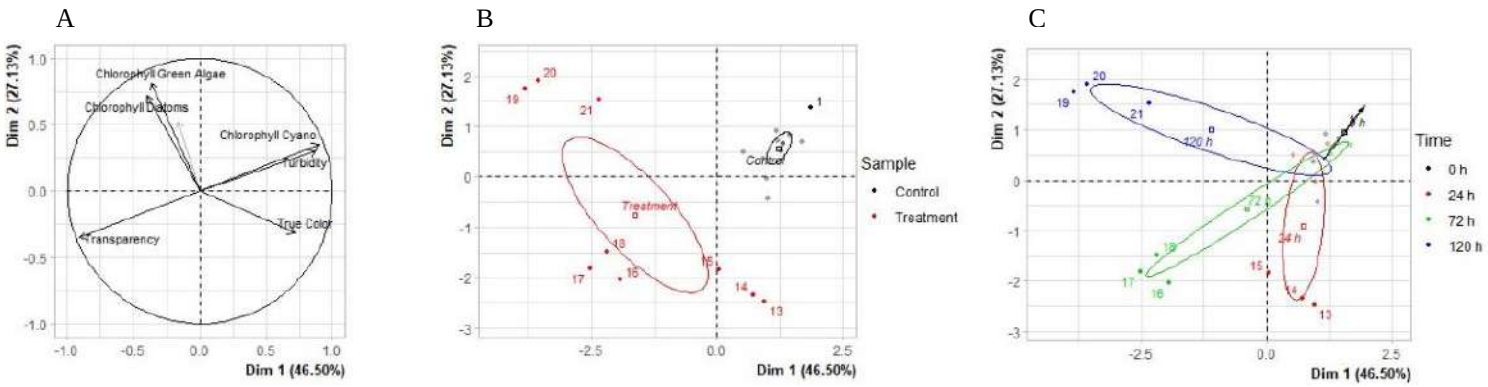

Figure 4: PCA ordination from Group I (transparency, turbidity, true-color, temperature, and the three chlorophylls) considering its eigenvectors (A) treatment and control experimental conditions comparison (B) and samples over time (C). PCA ordination was defined by components one and two, represented as Dim1 and Dim2. The small grey arrow in the second quadrant from (A) is related to the temperature eigenvector.

Within Group I, both transparency ($p < 0.0001$, $F = 69.67$) and turbidity ($p < 0.0001$, $F = 50.73$) were influenced by the treatment all sampling times (24, 72 and 120h) with transparency increasing from 60 to 110 cm while turbidity decreased from 15 to 6 NTU (Nephelometric Turbidity Units) from oh to 72h (Figure 5). The temperature did not show any significant change between the treatment and control and over the time ($p = 0.53$) while true-color showed a significant difference at time 120h ($p<0.0001$) (Supplementary Figure 2)

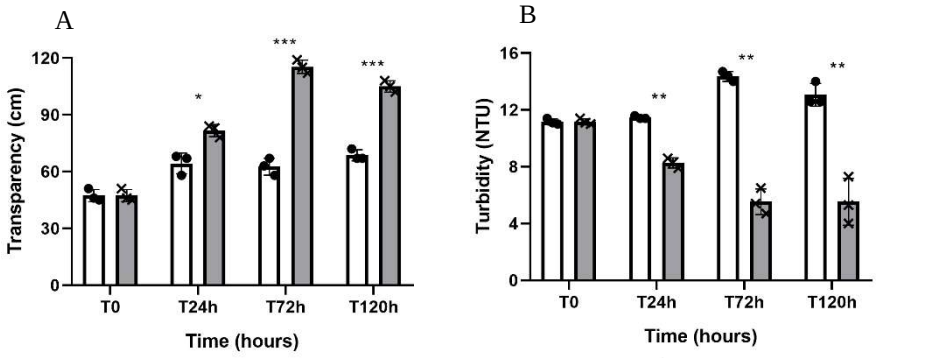

Figure 5: Effect of H_2O_2 on transparency (A) and turbidity (B) over the time. Results are expressed as the mean ± SD. Grey and white bars represent the treatment and control conditions, respectively. The asterisks represent the statistical difference between treatment and control with * ($p<0.05$), ** ($p<0.01$), and *** ($p<0.001$).

The cluster from Group II (pH, dissolved oxygen, DOC, and TOC) represented 70.8% of the total variability considering components one and two (Figure 6). Cyanobacterial chlorophyll shared the same quadrant with dissolved oxygen and pH, with the latter showing a strong association with cyanobacteria ($p<0.001$; $r = 0.82$) while dissolved oxygen had a significant but smaller correlation ($p = 0.006$; $r = 0.57$) (Figure 6A, Supplementary Table 1). Neither parameter showed any significant correlation with chlorophyll from Green Algae or Diatom, indicating that oxygen production and carbon dioxide consumption are mostly controlled by the cyanobacterial cells. In contrast, DOC and TOC did not show any significance to this group, according to their small eigenvectors represented by the grey arrows in the third quadrant (Figure 6A). As observed in the Group I, the control cluster was located in the first quadrant, opposed to the treatment cluster which was in the second and third quadrants, indicating a clear association between dissolved oxygen, pH, and cyanobacteria chlorophyll with the control condition (Figure 6B).

A B C

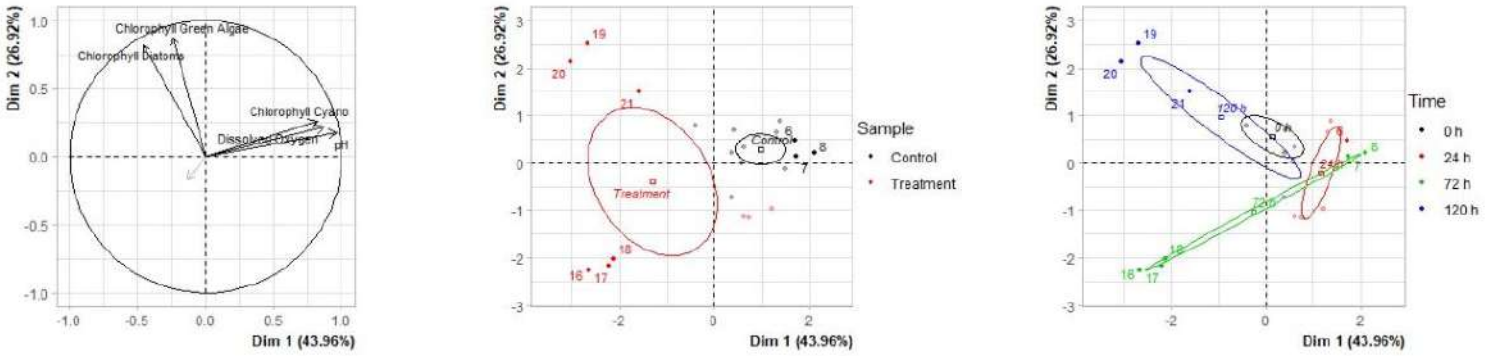

Figure 6: PCA ordination from Group II (pH, dissolved oxygen, DOC, and TOC and the three chlorophyll) considering its eigenvectors (A) treatment and control experimental conditions comparison (B) and samples over time (C). PCA ordination was defined by components one and two, represented as Dim1 and Dim2. The small grey arrow in the third quadrant (a) is related to the DOC and TOC eigenvector.

The pH was significantly altered after the H_2O_2 application when comparing control to treatment ($p<0.0001$, $F = 42.16$), decreasing from 9.2 to 8.1 at 72h time and from 9.0 to 8.3 at 120h. (Figure 7A). No significant change in TOC was observed throughout the treatment (Supplementary Figure 3), whereas DOC ($p = 0.003$, $F = 7.71$) and dissolved oxygen ($p<0.0001$, $F = 21.26$) decreased significantly at 72h compared to the control

condition (Figure 7B and 7C, respectively). The decrease of dissolved oxygen at 72h could be related to the collapse of the cyanobacteria community and photosynthetic activity at this time with consequent lower oxygen production. Moreover, when clustering samples by time, the same pattern encountered in Group I was observed, suggesting a return to the initial condition after the extinction of H_2O_2 (Figure 6C).

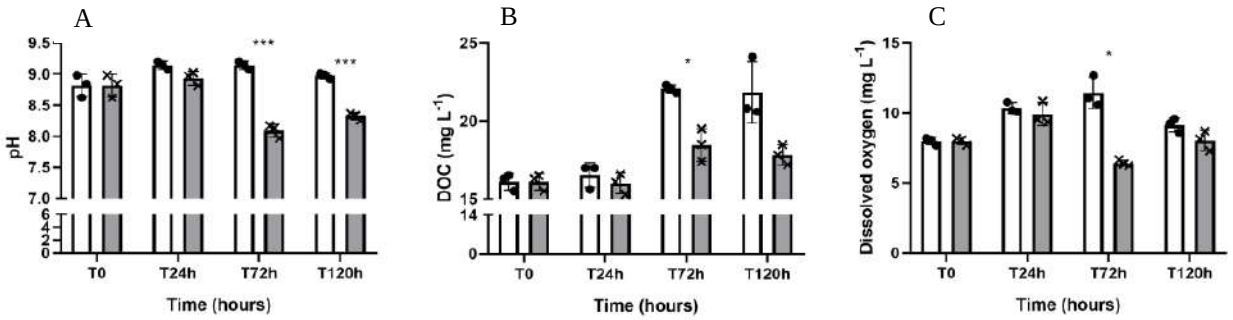

Figure 7: Effect of H_2O_2 on pH (A), DOC (B), and dissolved oxygen (C) over the time. Results are expressed as the mean ± SD. Grey and white bars represent the treatment and control conditions, respectively. In the figures A and B the y-axes were divided in two segments to identify the difference between both respective bars from control and treatment condition. The asterisks represent the statistical difference between treatment and control with * ($p<0.05$), ** ($p<0.01$), and *** ($p<0.001$).

Group III assembled all nutrients evaluated (ammonium, nitrite, nitrate, and orthophosphate), and, similar to the previous groups, the first two components contributed to 70% of the total variability. Even considering the high eigenvalues of green algae and diatoms chlorophyll in the second quadrant (Figure 8A and Supplementary Table 1), both showed a low relationship with nutrients due to the nearly 90 degrees between their eigenvectors. Regarding the cyanobacterial chlorophyll, its eigenvalue was lower than in the previous groups showing the smaller importance of Cyanobacteria to nutrients. Corroborating this, cyanobacterial chlorophyll did not present a significant correlation with nitrate ($p = 0.36$) nor with ammonia ($p = 0.13$).

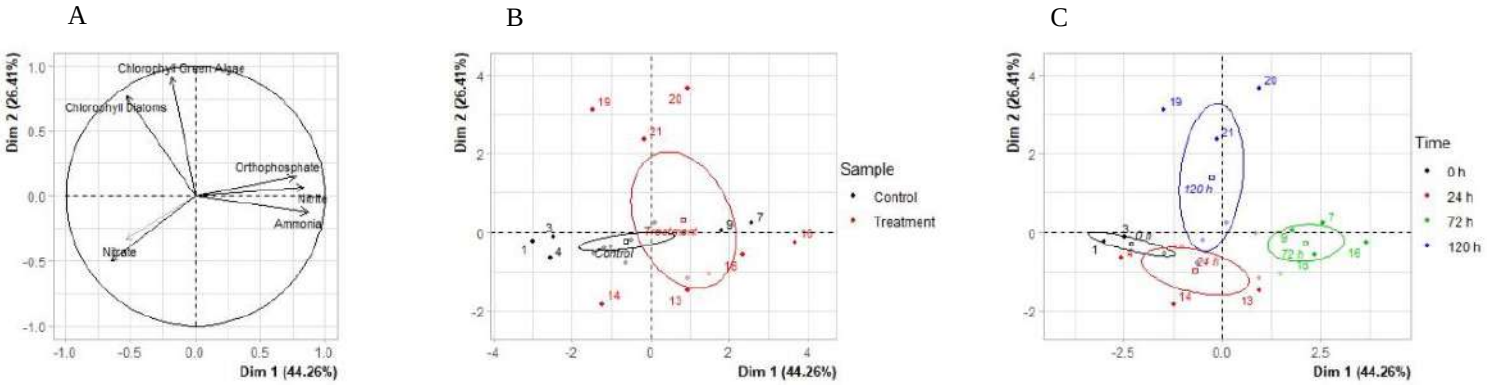

Figure 8: PCA ordination from Group III (orthophosphate, ammonia, nitrate, nitrite and the three chlorophyll) considering its eigenvectors (A) treatment and control experimental conditions comparison (B) and samples over time (C). PCA ordination was defined by components one and two, represented as Dim1 and Dim2. The small grey arrow in the third quadrant (a) is related to the cyanobacterial chlorophyll eigenvector.

When evaluating the influence of H_2O_2 treatment on nutrients, no significant difference of ammonia ($p = 0.59$), nitrite ($p = 0.73$), nitrate ($p = 0.50$) or orthophosphate ($p = 0.12$) was observed when comparing to the control sample (Supplementary Figure 4). Nonetheless, all nutrients were affected during the enclosure time for both treatment and control conditions. Considering samples clustered by treatment and control conditions, although distinct clusters can be observed, they are closer to each one than in the previous groups (Figure 8B) indicating a weaker effect of H_2O_2 over the four nutrients as compared to the other parameters evaluated. The same pattern observed in Groups I and II over the time was observed for Group III which is, clusters rotated way from the initial condition (0h) until 72h, and after that (120h) they moved towards the initial condition, only that, this time, in a counterclockwise manner (Figure 8C).

Discussion

In this research, for the first time, the application of H_2O_2 was used to mitigate a cyanobacteria-dominating phytoplankton bloom and to improve water quality parameters in a reservoir used for drinking water supply in the Brazilian semiarid region. Gavião reservoir has a recent history of cyanobacteria contamination, reported by the dominance of *Planktothrix agardhii* and *Raphidiopsis raciborskii* (Barros et al., 2019). A single dose of H_2O_2 was applied to achieve a final concentration of 10 mg L^{-1} and then, physical-chemical parameters and cyanobacteria, green algae, and Diatom chlorophyll were monitored for 120h (five days). This dose of H_2O_2 was used based on a previous

experiment performed in microcosm scale, using water from the same reservoir in which supressed cyanobacteria with a smaller negative effect on the rest of the phytoplankton community (Rocha, 2020). This investigation was previously performed since some studies reported that 5 mg L^{-1} of H_2O_2 would be enough to control cyanobacteria in a freshwater environment (Matthijs et al., 2012; Weenink et al., 2015). Fan et al. (2019) found that 10 mg L^{-1} effectively inhibited the growth of Cyanobacteria over 15 days with a subsequent dominance of eukaryotic green algae from the nineth day.

Using mesocosms with high volumes inserted into a reservoir, a decrease in the chlorophyll of cyanobacteria, green algae, and diatom groups immediately after the H_2O_2 application was observed. Additionally, a significant increase in green algae and diatom but not cyanobacteria was observed at 120h compared to the control samples, corroborating with other studies that found a higher sensitivity of cyanobacteria as compared to the other phytoplankton members (Barrington et al., 2013; Geer et al., 2016; Dziga et al., 2019, Yang et al., 2019). Sinhá et al. (2018) observed that a decrease of cyanobacteria was followed by an increase in the abundance of eukaryotic phytoplankton *Synedra sp.* and *Cladophora sp*., suggesting that these species would take advantage of the collapse of cyanobacteria to mobilize the available nutrients and regrow intensely. More specifically, a bloom-forming *Microcystis aeruginosa* was suppressed while an increase of *Chlorophytes* such as *Chlamydomonas sp.* was promoted (Wang et al., 2019). Although the composition of the phytoplankton community was not evaluated over the experiment, *Planktothrix sp.*, *Raphidiopsis sp.*, *Aulacoseira sp.,* and *Fragilaria sp.* were identified as the main species present in the raw water (data not shown).

An explanation for this selectivity and high sensitivity of cyanobacteria to H_2O_2 treatment could be attributed to the low capacity to produce enzymes in enough amounts to eliminate reactive oxygen species - ROS (Matthijs et al., 2012). Since ROS oxidize lipids and proteins, they can lead to a loss of membrane integrity in addition to the inactivation of enzymes, and eventually to cell death. As a mechanistic defense, eukaryotic algae use a high level of ascorbate peroxidase, not commonly found in cyanobacteria, to quickly reduce H_2O_2 before reaching the photosynthetic apparatus (Passardi et al., 2007; Shigeoka, 2002). Additionally, Matthijs et al. (2012) suggested that the Mehler reaction, or the lack of it, is an important way to explain the resistance or sensitivity against ROS. The Mehler reaction occurs in the photosynthetic system of eukaryotic algae producing superoxide radical, which is readily converted to H_2O_2 by superoxide dismutase and then eliminated by peroxidases (Latifi et al., 2009). This metabolism can explain the higher

resistance of eukaryotic algae when compared to the cyanobacterial group since cyanobacteria do not perform this reaction due to some flavoproteins that prevent the formation of superoxide radicals, then reducing O_2 directly to water (Helman et al., 2003; Latifi et al., 2009; Allahverdiyeva et al., 2011).

Transparency was increased and turbidity decreased over the time, especially at 72h, in association with the impacts on cyanobacterial cell numbers. Matthijs et al. (2012) observed transparencies from 40 to 60 cm over two months after an application of 2 mg L^{-1} of H_2O_2, mitigating a *Plantothrix*-dominating bloom but not increase transparency. Sinhá et al. (2018) did not observe a significant modification in the transparency, about 20 cm, using 2.5 and 4 mg L^{-1} over six weeks. On the other hand, in our experiment, an increase in transparency of 50 cm in comparison to the control condition was observed over the experimental time. This contradictory finding could be related to the higher concentration of H_2O_2 used in our mesocosm system, which was able to promote more intense modification to the cyanobacteria dynamics as well as to the physical-chemical characteristics of raw water.

In aquatic environments rich in organic matter, with concentrations higher than 5 mg L^{-1}, as found in eutrophicated tropical lakes, it is expected a less efficiency of oxidative treatments since a greater oxidizer demand it´s needed (Dargahi et al., 2015). Although H_2O_2 it is one of the most powerful oxidants, it does not have selectivity against any specific organic molecules and can react with many types of substances (Imlay, 2003; Parsons, 2004). Dargahi et al. (2015) observed a greater DOC degradation with higher dosages of H_2O_2 (10 mg L^{-1}) was enough to decrease about 30-40% of the organic matter over 30 minutes. Many factors could influence DOC degradation in natural freshwater, mainly to the speciation of the respective compounds. Here, we identified a significant decreases only in DOC after the H_2O_2 extinguishing, which could be associated with the biodegradation of organic compounds released after the oxidative processes (Chelme-Ayala et al., 2011; Metz et al., 2011), or even by an intense activity of H_2O_2-resistant microorganisms.

The pH and dissolved oxygen were also affected due to the decrease in photosynthetic activity. A decrease in pH after the H_2O_2 extinction (72h) was observed. Pflaumer (2016) also detected a decrease in pH values after H_2O_2 addiction while Crafton et al. (2019) observed a pH increase over ten days, instead. Dissolved oxygen concentration showed a pronounced decrease at 72h, also influenced by a decrease in primary production from the affected cyanobacteria, and a substantial increase at 120h related mainly to the green

algae bloom (Crafton et al., 2019) which became the phytoplankton-dominating microorganisms. In freshwater environments under natural conditions, many authors have suggested that considerable increases in pH and dissolved oxygen can be attributed to the exponential growth of cyanobacteria (Paerl et al., 2001; Gao et al., 2012) maintained as a massive bloom from high nutrients level.

Curiously, no changes were observed in nutrient content because of the H_2O_2 treatment for ammonia, nitrite, nitrate, and orthophosphate concentrations. Changes in nutrients concentration were not attributed to the treatment but rather to the water enclosure. Conversely, H_2O_2-based treatment was described as a trigger to reoligotrophication, an alternative equilibrium for the environment (Scheffer et al., 1993; Matthijs et al., 2012). Many studies have observed an increase in nutrient availability after H_2O_2 treatment with an increase in phosphate and ammonia that could be related by the cyanobacterial or any microbial cellular lysis (Matthijs et al., 2012; Bauzá et al., 2014; Sinha et al., 2018). The observation about significant impacts on nutrients could be associated with the bloom-forming cyanobacterial species, the redox potential of the water body, or even the associated microbial community able to quickly assimilate released nutrients. Additionally, we also observed that H_2O_2 treatment probably did not affect specific microbial activities, since for both control and treatment samples showed a decrease in nitrate at 72h along with an increase of nitrite and ammonia, suggesting a denitrifying process. Meanwhile, the maitnace of nutrient concentrations could signal an appropriate scenario for cyanobacterial regrowth over the time (Paerl and Otten, 2013). Finally, it is extremely important to understand the effects of oxidative treatment on microbial communities identifying susceptible/resistant microorganisms and the consequent effects on the composition and dynamics of aquatic environments, mainly those that can degrade toxins and other secondary metabolites (Dziga et al., 2019).

Conclusion

Cyanobacterial blooms are increasingly more frequent worldwide especially in drinking water reservoirs in the Brazilian semiarid region, which significantly increases the risks and costs of water treatment and making mitigating measures urgently needed. In this experiment, we evaluated the *in situ* application of H_2O_2 (10 mg L^{-1}) into Gavião reservoir using a mesocosms system by monitoring physical-chemical parameters as well as estimating the phytoplankton community chlorophyll. According to our findings, the natural phytoplankton community was affected by the selective suppression of

cyanobacteria and consequent green algae flourishing after the H_2O_2 extinguishing. Furthermore, we observed, along with cyanobacterial suppression, a high positive impact on transparency and turbidity, which could lead to better conditions for water treatment and the aquatic ecosystem. The treatment influenced other physical-chemical parameters evaluated, decreased pH, dissolved oxygen, and DOC. Meanwhile, H_2O_2-based treatment was not able to decrease nutrients content, indicating that an additional technique for the removal of nutrients would be important since cyanobacteria could quickly regrow and establish new blooms. The low concentration of cyanobacteria could indicate that the risks brought by toxins and other secondary metabolites are reduced if raw water is used before 120h from H_2O_2 application even toxin analyses were not performed. However, it is urgent to provide a toxin monitoring along an oxidative treatment, such as it promoted by hydrogen peroxide. After 72h, however, the problems caused by particulate and dissolved organic materials to water treatment plants are still present.

Acknowledgments

The authors would like to thank the Engineering and Physical Sciences Research Council (EPSRC) [EP/P029280/1], the Coordination for the Improvement of Higher Education Personnel - CAPES [PROEX 20/2016 and PrInt 88887.311806/2018-00], the Brazilian National Research Council – CNPq [403116/2016-3 and 304164/2017-8], the Ceará Research Support Foundation - FUNCAP [PNE-0112-00042.01.00 / 16] for funding this research. We also thank COGERH (Water Resources Management Company – form Portuguese “Companhia de Gerenciamento dos Recursos Hídricos do Estado do Ceará) workers and managers for the use their facilities.

References

Allahverdiyeva, Y., Ermakova, M., Eisenhut, M., Zhang, P., Richaud, P., Hagemann, M., Cournac., Aro, E-M., 2011. Interplay between Flavodiiron Proteins and Photorespiration in Synechocystis sp. PCC 6803. Journal of Biological Chemistry 286, (27), 24007-24014.

APHA. Standard Methods for Examination of Water and Wastewater. 21. ed. Washington, DC, American Public Health Association, American Water Works Association, Water Environment Federation, 2005.

Barrington, D.J., Reichwaldt, E.S., Ghadouani, A., 2013. The use of hydrogen peroxide to remove cyanobacteria and microcystins from waste stabilization ponds and hypereutrophic systems, Ecological Engineering 50, 86-94.

Barros, M.U.G., Wilson, A.E., Leitão, J.I.R., Pereira, S.P., Buley, R., Fernandez-Figueroa, E.G., Capelo-Neto, J., 2019. Environmental factors associated with toxic cyanobacterial blooms across 20 drinking water reservoirs in a semi-arid region of Brazil, Harmful Algae 86, 128-137.

Bauzá, L., Aguilera, A., Echenique, R., Andrinolo, D., Giannuzzi, L., 2014. Application of hydrogen peroxide to the control of eutrophic lake systems in laboratory assays, Toxins 6 (9), p. 2657-2675.

Bui, T., Dao, T-S., Vo, T. G., Lürling, M., 2018. Warming affects growth rates and microcystin production in tropical bloom-forming microcystis strains, Toxins 10 (3), 123.
Capelo-Neto, J., Neycombe, G., 2017. Oxidação de cianobactérias e seus metabólitos em sistemas de tratamento de água: o estado da arte. Engenharia Sanitária e Ambiental 22 (5), 829-840.

Chang, C.W., Huo, X., Lin, T. F., 2018. Exposure of Microcystis aeruginosa to hydrogen peroxide and titanium dioxide under visible light conditions: Modeling the impact of hydrogen peroxide and hydroxyl radical on cell rupture and microcystin degradation. Water Res. 141, 217–226.

Chelme-Ayala, P., El-Din, M.G., Smith, D.W., Adams, C.D., 2011. Oxidation kinetics of two pesticides in natural waters by ozonation and ozone combined with hydrogen peroxide. Water Res. 45(8), 2517-2526.

COGERH. Companhia de Gestão dos Recursos Hídricos, 2019. Rede de Monitoramento da Qualidade de Água. Governo do Estado do Ceará, Fortaleza. Last acessed 14th October 2019.

Crafton, E. A., Cutright, T. J., Bishop, W. M., Ott, D.W., 2019. Modulating the Effect of Iron and Total Organic Carbon on the Efficiency of a Hydrogen Peroxide-Based Algaecide for Suppressing Cyanobacteria, Water, Air, and Soil Pollution 230 (56).

Dargahi, A., Pirsaheb, M., Hazrati, S., Fazlzadehdavil, M., Khamutian, R., Amirian, T., 2015. Evaluating efficiency of H_2O_2 on removal of organic matter from drinking water. Desalination and Water Treatment 54 (6), 1589-1593.

Dodds, W. K., Bouska, W. W., Eitzmann, J. L., Pilger., T.J., Pitts, K.L., Riley, A.J., Schloesser, J.T., Thornbrugh, D.J., 2009. Eutrophication of U.S. freshwaters: Analysis of potential economic damages, Environmental Science and Technology 43 (1), 12-19.

Drábková, M., Admiraal, W., Maršálek, B., 2007. Combined exposure to hydrogen peroxide and light-selective effects on cyanobacteria, green algae, and diatoms, Environmental Science and Technology 41 (1), 309-314, 2007.

Dziga, D., Tokodi, N., Drobac, D., Kokocinski, M., 2019. The Effect of a Combined Hydrogen Peroxide-MlrA Treatment on the Phytoplankton Community and Microcystin Concentrations in a Mesocosm Experiment in Lake Ludoš, Toxins 11 (12), 725.

Elliott., J. A., 2012. Is the future blue-green? A review of the current model predictions of how climate change could affect pelagic freshwater cyanobacteria, Water Research 46 (5), 1364-1371.2012.

Esteves, F. A., 2011. Fundamentos de limnologia, 137-166, Interciência, Rio de Janeiro.

Fan, J., Hobson, P., Ho, L., Daly, R., Brookes, J., 2014. The effects of various control and water treatment processes on the membrane integrity and toxin fate of cyanobacteria, Journal of Hazardous Materials 264, 313-322.

Fan, F., Shi, X., Zhang, M., Liu, Changqing, L., Chen, Kaining., 2019. Comparison of algal harvest and hydrogen peroxide treatment in mitigating cyanobacterial blooms via an in situ mesocosm experiment. Science of the Total Environment 694, 133721.

Fraga, A. B., Lima Silva, F., Hongyu, K., Santos, D. S., Murphy, W., Lopes, F. B., 2016 .Multivariate analysis to evaluate genetic groups and production traits of crossbred Holstein × Zebu cows, Tropical Animal Health and Production 48 (3), 533-538.

Gao, Y., Cornwell, J. C., Stoecker, D. K., Owens, M. S., 2012. Effects of cyanobacterial-driven pH increases on sediment nutrient fluxes and coupled nitrification-denitrification in a shallow fresh water estuary. Biogeosciences 9,(7), 2697-2710.

Geer, T. D., Kinley, C. M., IwinskI, K. J., Calomeni, A. J., Jr, J. H. R., 2016. Comparative toxicity of sodium carbonate peroxyhydrate to freshwater organisms, Ecotoxicology and Environmental Safety 132, 202-211.

Ger, K. A., Urrutia-Cordero, P., Frost, P. C., et al. "The interaction between cyanobacteria and zooplankton in a more eutrophic world", Harmful Algae, v. 54, p. 128–144, 2016. DOI: 10.1016/j.hal.2015.12.005.

Helman, Y., Tchernov, D., Reinhold, L., Shibata, M., Ogawa, T., Schwarz, Ohard, I., Kaplan, A., 2003. Genes Encoding A-Type Flavoproteins Are Essential for Photoreduction of O2 in Cyanobacteria, Current Biology 13 (3), 230-235.

Ho, L., Kayal, N., Trolio, R., Newcombe, G., 2010. Determining the fate of Microcystis aeruginosa cells and microcystin toxins following chloramination. Water Sci. Technol. 62, 442-450.

Ibelings, B. W., Backer, L. C., Kardinaal, W. E. A., Chorus, I., 2014. Current approaches to cyanotoxin risk assessment and risk management around the globe. Harmful Algae (40), 63-74.

Imlay, J.A., 2003. Pathways of oxidative damage. Annu. Rev. Microbiol. 57, 395-418.

Jančula, D., Maršálek, B., 2011 Critical review of actually available chemical compounds for prevention and management of cyanobacterial blooms", Chemosphere 85 (9), 1415 - 1422.

Kaiser, H. F., 1958. The varimax criterion for analytic rotation in factor analysis, Psychometrika 23 (3), 187-200.

Latifi, A., Ruiz, M., Zhang, C. C., 2009. Oxidative stress in cyanobacteria. FEMS Microbiology Reviews 33 (2), 258-278.

Lu, S., Wang, N., Wang, C., 2018. Oxidation and biotoxicity assessment of microcystin-LR using different AOPs based on UV, O3 and H2O2. Front. Environ. Sci. Eng. 12, 12. https://doi.org/10.1007/s11783-018-1030-2

Maliaka, V., Faassen, E.J., Smolders, A.J., Lürling, M., 2018. The Impact of Warming and Nutrients on Algae Production and Microcystins in Seston from the Iconic Lake Lesser Prespa, Greece. Toxins 10.

Matthijs, H. C. P., Visser, P. M., Reeze, B., Meeuse, J., Slot, P.C., Wijn, G., Talens, R., Huisman, J., 2012. Selective suppression of harmful cyanobacteria in an entire lake with hydrogen peroxide, Water Research 46 (5), 1460-1472.

Merel, S., Yan, S., Song, W., 2020. Conventional Disinfection and/or Oxidation Processes for the Destruction of Cyanotoxins/Cyanobacteria. In Water Treatment for Purification from Cyanobacteria and Cyanotoxins (eds A.E. Hiskia, T.M. Triantis, M.G. Antoniou, T. Kaloudis and D.D. Dionysiou). doi:10.1002/9781118928677.ch6

Metz, D.H., Meyer, M., Dotson, A., Beerendonk, E., Dionysiou, D.D., 2011. The effect of UV/H_2O_2 treatment on disinfection by-product formation potential under simulated distribution system conditions. Water Res. 45(13), 3969-3980.

Moss, B., Kosten, S., Meerhoff, M., Battarbee, R. W., Jeppesen, E., Mazzeo, N., Havens, K., Lacerot, G., Liu, Z., de Meester, L., Paerl, H., Scheffer, M., 2011. Allied attack: climate change and eutrophication. Inland Waters: Journal of the International Society of Limnology, 1(2), 101-105.

Neilan, B. A., Pearson, L. A., Muenchhoff, J., Moffitt, M. C., Dittmann, E., 2013. Environmental conditions that influence toxin biosynthesis in cyanobacteria. Environmental microbiology 15(5), 1239-1253.

O'Neil, J. M., Davis, T. W., Burford, M. A., Gobler, C. J., 2012. The rise of harmful cyanobacteria blooms: The potential roles of eutrophication and climate change, Harmful Algae 14, 313-334.

Olsen, B. K., Chislock, M. F., Wilson, A. E., 2016. Eutrophication mediates a common off-flavor compound, 2-methylisoborneol, in a drinking water reservoir, Water Research 92, 228-234.

Paerl, H. W., Fulton, R. S., Moisander, P. H., Dyble, J., 2001. Harmful Freshwater Algal Blooms, With an Emphasis on Cyanobacteria, The Scientific World Journal 1, 76-113.

Paerl, H. W. and Paul, V. J., 2012. Climate change: Links to global expansion of harmful cyanobacteria, Water Research 46 (5), 1349-1363.

Passardi, F., Zamocky, M., Favet, J., Jokopitsch, C., Penel, C., Obinger, C., Dunand, C., 2007. Phylogenetic distribution of catalase-peroxidases: Are there patches of order in chaos?", Gene 397 (1–2), 101–113.

Parsons, S., 2004. Advanced Oxidation Processes for Water and Wastewater Treatment. IWA Publishing, London.

Paerl, H.W. and Otten, T.G., 2013. Harmful Cyanobacterial Blooms: Causes, Consequences, and Controls. Environmental Microbiology. 65(4):995-1010. doi: 10.1007/s00248-012-0159-y.

Pflaumer, A. L., 2016. Hydrogen Peroxide in Eutrophic Lake Taihu, China: Addition Effects on Phytoplankton and Diel Variability in Natural Concentrations. 95 f. University of North Carolina at Chapel Hill Graduate School, 2016.

Walz, 2003. PHYTO-PAM. System Components and Principles of Operation. . Effeltrich, Heinz Walz GmbH.

Rocha, M.A.M., 2020. Effects of hydrogen peroxide on the phytoplankton community of a reservoir in the tropical semi-arid region of Brazil. Dissertion for conclusion of Master degree - Civil Engineering) - Centro de Tecnologia, Programa de Pós-Graduação em Engenharia Civil: Saneamento Ambiental, Universidade Federal do Ceará, Fortaleza, 2020.

Sharma, V.K., Triantis, T.M., Antoniou, M.G., He, X., Pelaez, M., Han, C., Song, W., O'Shea, K.E., de la Cruz, A.A., Kaloudis, T., Hiskia, A., Dionysiou, D.D., 2012. Destruction of microcystins by conventional and advanced oxidation processes: A review. Separation and Purification Technology, 91, 3-17. https://doi.org/10.1016/j.seppur.2012.02.018

Scheffer, M., Hosper, S.H., Meijer, M.L., Moss, B., Jeppesen, E., 1993. Alternative equilibria in shallow lakes. Trends in Ecology and Evolution 8 (8), 275-279.

Shigeoka, S., 2002. Regulation and function of ascorbate peroxidase isoenzymes, Journal of Experimental Botany 53 (372), 1305-1319.

Sinha, A. K., Eggleton, M. A., Lochmann, R. T., 2018. An environmentally friendly approach for mitigating cyanobacterial bloom and their toxins in hypereutrophic ponds: Potentiality of a newly developed granular hydrogen peroxide-based compound, Science of The Total Environment 637–638, 524-537.

Skellon, J.H. and Wills, E.D., 1948. Iodimetric methods of estimating peroxidic oxygen. Analyst 73, 78. https://doi.org/10.1039/an9487300078

Wang, B., Song, Q., Long, J., Song, G., Mi, W., Bi, Y., 2019. Optimization method for Microcystis bloom mitigation by hydrogen peroxide and its stimulative effects on growth of chlorophytes. Chemosphere 228, 503–512.

Weenink, E. F. J., Luimstra, V. M., Schuurmans, J. M., Van Herk, M. J., Visser, P. M., Matthijs, H. C., 2015. Combatting cyanobacteria with hydrogen peroxide: a laboratory study on the consequences for phytoplankton community and diversity, Frontiers in Microbiology 6, 1-15.

Yang, Z., Buley, R. P, Fernandez-Figueroa, E. G, Barros, M. U. G, Rajendran, S., Wilson, A.E., 2018. Hydrogen peroxide treatment promotes chlorophytes over toxic cyanobacteria in a hyper-eutrophic aquaculture pond. Environmental pollution 240, 590-598.

4.2 Capítulo 2 (Effect of hydrogen peroxide on the bacterioplankton community from a drinking water reservoir in Brazilian semiarid region)

Effect of hydrogen peroxide on bacterioplankton community from a drinking water reservoir in Brazilian semiarid region

Allan Amorim Santos[1], Dayvson Guedes[2], José Capelo-Neto[2], Carlos Pestana[3], Christine Edwards[3], Linda Lawton[3], Sandra Azevedo[1], Valeria Magalhães[1], Ana Beatriz Pacheco[1]

[1]Biophysics Institute, Federal University of Rio de Janeiro, Brazil

[2]Federal University of Ceará, Department of Hydraulic and Environmental Engineering, Fortaleza, Brazil.

[3]School of Pharmacy and Life Sciences, Robert Gordon University, Aberdeen, UK

Abstract

Cyanobacterial blooms occur in freshwater bodies worldwide mainly because of anthropogenic eutrophication. Some alternatives have been suggested to suppress these events with low risks to the ecosystem. The reactive oxygen species (ROS)-based advanced oxidative processes (AOPs) comprise efficient and safe methods for water or effluent treatment. Hydrogen peroxide (H_2O_2) application affects preferentially cyanobacteria over other phytoplankton members. However, there is little information on its impact on the bacterioplankton. Here, we have assessed the effect of H_2O_2 to the planktonic community, emphasizing cyanobacteria and heterotrophic bacteria. Mesocosms were set up in a eutrophic reservoir used for water supply. After H_2O_2 treatment, physical-chemical parameters were evaluated and the composition of bacterial communities was followed by high-throughput sequencing (16S SSU rRNA) and compared to that of the control condition throughout five days. The original *Planktothrix*-

dominating cyanobacterial bloom was suppressed after H_2O_2 addition. Other *Cyanobacteria* (*Microcystis*, *Cyanobium* and *Raphidiopsis*) also decreased to <1%. After 120 h, cyanobacterial OTU (operational taxonomic unit) abundance began to increase but was dominated by *Cyanobium.* Other bacterial OTUs were resistant to H_2O_2 application and increased in relative abundance 24-72 h after the treatment such as *Exiguobacterium*, *Deinococcus* and *Paracoccus*. After 120 h, these genera decreased substantially and a novel bacterial community profile was observed. Our results revealed the microbial community dynamics after AOP treatment beyond the effect on cyanobacteria. Changes in the relative abundance of specific taxa could be used to anticipate the regrowth of cyanobacteria after H_2O_2 extinction.

Keywords: Blue-Green Algae bloom, Advanced Oxidative Process, Remediation, Metagenomics, Exiguobacterium

Introduction

The worldwide increase of harmful cyanobacterial blooms in freshwater is directly related to anthropogenic eutrophication and at present, this is the main concern regarding drink water quality (Pearl and Otten, 2013; Meriluoto et al., 2017; Huisman et al., 2018). The best way to control cyanobacterial blooms in aquatic environments is the interruption of nutrient input to the water body (Meriluoto et al., 2017), however, this is a challenging and long-term measure. As short-term solution, some strategies have been proposed to efficiently and selectively control cyanobacterial blooms. It must be noted that some blooms can be toxic, and thus, these strategies must also target cyanotoxins avoid human or animal exposure. Ideally, reliable and low cost procedures should be available to mitigate cyanobacterial blooms.

Among biological, chemical or physical approaches that have been applied to mitigate cyanobacterial blooms and remove cyanotoxins, advanced oxidative processes (AOPs) are increasing in importance due to the speed, efficiency and harmless by-products-compounds generated (Matthijs et al., 2012; Pestana et al., 2015; Weenink et al., 2015; Park et al., 2017; Schneider and Bláha, 2020). AOPs are oxidative methods that produce free radicals, such as hydroxyl radicals, which are able to degrade many organic compounds being widely used for wastewater treatment (Vallejo et al., 2015).

Previous studies in temperate regions have emphasized the potential of hydrogen peroxide (H_2O_2) for controlling cyanobacterial blooms (Matthijs et al., 2012; Lurling et al., 2014; Weenink et al., 2015) while preserving eukaryotic phytoplankton (Yang et al., 2018). Matthijs et al. (2012) evaluated an application *in situ* of H_2O_2 into a mesotrophic lake to suppress *Planktothrix* bloom. After the addition of 2 mg L^{-1} of H_2O_2, the density of cyanobacteria diminished within three days while no negative effect was observed on eukaryotic phytoplankton and zooplankton.

The higher sensitivity of cyanobacteria to H_2O_2 as compared to eukaryotic phototrophs can be explained by the presence of compartmentalised organelles protected by membranes in the former. In addition, the absence of Mehler reaction, as found in higher plants and algae, in cyanobacteria can contribute to this selectivity since some flavoproteins can suppress the superoxide radical ($O_2^{-}\bullet$) generated in the photosynthetic electron flow. Thus, excess of electrons resulting from respiration are donated to the oxygen acceptor and water is produced without an intermediary production of reactive species of oxygen (ROS) such as superoxide or hydroxyl radical as well as H_2O_2 (Helman et al., 2003; Allahverdiyeva et al., 2013). However, cyanobacteria do not possess a robust and well-developed ROS-eliminating enzymatic machinery to protect against free radical produced in photosynthesis as green algae or higher plants (Passardi et al., 2007).

However, H_2O_2-based treatments may mitigate cyanobacterial blooms but might not degrade the toxins released in the process (Schneider and Bláha, 2020). Other steps should be applied after the H_2O_2-based oxidising treatments, since toxin degradation is needed to ensure safe drinking water. Previous studies have demonstrated that AOPs combined with ultraviolet (UV) radiation, H_2O_2, ozone or photo-Fenton processes, besides conventional biological processes, offer an optimised system to effectively remove organic compounds during water treatment (Lekkerkerker-Teunissen et al., 2012, Oller et al., 2011). Several water treatment companies utilise AOPs followed by biological treatment in drinking water production, such as ozonation or UV/H_2O_2 with biological activated carbon (BAC) filtration (Bonné et al., 2002, Van Der Hoek et al., 1999; Martijn and Kruithof, 2012).

In contrast to the alternative treatment using AOPs, H_2O_2 and reactive oxygen species (ROS) can be naturally found in small concentrations as the result of photochemical reactions as well as due to the metabolism of prokaryotes and eukaryotes (Mostofa et al. 2013). Additionally, the presence of natural photosensitizers in surface water, such as dissolved organic carbon (DOC) and humic acid-enriched organic matter may enhance ROS. The biological production of H_2O_2 by microorganisms overwhelm the photochemical production especially in eutrophic waters (Cory et al. 2016). Although the investigation of the effects of oxidants against phytoplankton is raising, little is still known regarding the effects on other representative microorganisms of the bacterioplankton community.

Bacteria vary in their susceptibility or resistance to ROS-producing treatments as AOPs by UV/H_2O_2 addition. The main cellular damage of ROS occurs in macromolecules, DNA/RNA, lipids or proteins (Latifi et al., 2009), which are exposed in specific sites such as cation-interacting and iron-sulphur bindings, cysteine residues or haem groups (Imlay,

2006, 2008; Stadtman and Levine, 2006; Yan, 2009). The defence mechanism involved in cell survival rests on preventing or eliminating ROS (eg: HO•, O_2•$^-$, H_2O_2) using specific enzymatic pathways or non-enzimatic agents (Daly, 2009). In addition to the enzymes (eg.: catalase, peroxidase and dismutase) and non-enzymatic agents (eg.: carotenoids, flavonoids, ascorbic acid and polyphenols), the ratio of intracellular manganese to iron concentrations is also important. A higher concentration of manganese than iron can increase resistance to protein oxidation (Daly, 2009).

A previous study reported bacterial phyla detected after a singlet oxygen ($^1O_2$) or H_2O_2 treatment in a humic lake from the north region of Germany (Glaeser et al., 2014). Using DGGE analysis, under increasing concentrations of oxidants, they observed that three genera of Proteobacteria (*Polynucleobacter*, *Limnohabitans*-related phylotype and *Novosphingobium*) were not affected by $^1O_2$ (0.2-2 µM) but decreased in abundance after H_2O_2 addition (5-10 µM). Actinobacteria members were sensible to $^1O_2$ but resistant to H_2O_2. Thus, among the diverse bacterioplankton community, bacterial taxa differ in antioxidant defences and after the oxidant is applied into the water, changes on the dynamics of bacterial communities are expected. Moreover, Baltar et al. (2013) observed that H_2O_2 presented great effects on bacterioplankton from Northest Atlantic. After 24h, the addition of H_2O_2 revealed a strong inhibition of enzymatic activies such as glucosidase, leucine aminopeptidase and alkaline phosphatase. Simultaneously, they observed a reduction about 36-100% on prokaryotic heterotrophic production as well as affecting prokaryote growth besides a hydrolysis of organic matter in comparison to those samples with no H_2O_2.

In a previous study (Guedes et al., 2020), we evaluated the effectiveness of H_2O_2 for the mitigation of a cyanobacterial bloom in a reservoir with high UV-solar irradiation. The treatment was applied to mitigate a *Planktothrix*-dominating bloom in a hypereutrophic

reservoir used for drinking water supply in the semiarid of Northeast Brazil. Here, we assessed the effects of the H_2O_2 treatment on the bacterioplankton community using high-throughput sequencing (16S SSU rRNA). We hypothesized that the treatment would affect not only *Cyanobacteria* phyla but also heterotrophic bacterial taxa since a modification on oxidative potential makes susceptible and resistant bacteria over the process. Thus, after H_2O_2 extinction a novel bacterial community profile would emerge, different from the original one.

Methodology

Study area and experimental set-up

This study was carried out in the Gavião reservoir, located in a semi-arid region in Northeast of Brazil (3º59'03''S and 38º37'13''W). It is used as a public drinking water supply to inhabitants of Fortaleza, a city of about 4 million inhabitants. This reservoir receives urban run-off and is highly impacted, presenting a eutrophic condition. This situation is enhanced by the prolonged retention time (> 12 months) (Barros et al., 2017; Cogerh, 2017, Barros et al., 2019). The reservoir location receives a high solar radiation reaching approximately 5 kWh m^{-2} day^{-1}, 8h per day and the annual average atmospheric temperature is 32 °C (FUNCEME, 2017; Barros et al., 2019). These factors may enhance the results of the advanced oxidation process *in situ*. The water treatment plant adjacent to the reservoir is managed by the Water Company of Ceará (Cagece) and the Gavião reservoir by Water Management Company of Ceará (Cogerh).

For the experiment set up, reservoir water was enclosed in six cylindrical mesocosms made with flexible semi-transparent plastic bags of 1.5 m in diameter and 2.0 m in depth. The transparency of the water column was previously measured to ensure that the

experiment took place in the euphotic zone. The cylindrical shape of each mesocosm was maintained by two arcs of polyvinyl chloride (PVC), one floating at the top and the other at the bottom of the structure. The upper PVC arc was fixed to a rigid floating structure made of PVC pipes (Supplementary Figure 1A). The PVC structures were attached to a floating platform comprised a wood deck supported by six empty plastic barrels to ensure fluctuation. The platform allowed easy access for sampling (Supplementary Figure 1B). The mesocosms were located in the lacustrine zone of the reservoir, next to the intake point of the water treatment plant. All mesocosms were submerged but allowing no exchange between internal and external water. A detailed description of the experiment can be found in Guedes et al., 2020.

Three mesocosms served as the control group (with no H_2O_2) and three mesocosms corresponded to treatment (receiving an initial H_2O_2 concentration of 10 mg L-1). The H_2O_2 diluted solution was prepared from a stock solution of H_2O_2 (60% by weight – Sigma Aldrich®). Both conditions were tested in triplicates and maintained for 120 hours in the reservoir. After application, the concentration of H_2O_2 was estimated throughout the experiment using a semi-quantitative method with colorimetric strips (MQuant™ Peroxide-Test, Merck®). H_2O_2 extinguished in 72h and the physical-chemical parameters were measured over the experiment were detailed in Guedes et al. (2020).

Sample processing and DNA extraction

Samples were taken from the reservoir at time 0 before the H_2O_2 application (n=3). At each sampling time (24, 72, and 120h), aliquots of 300 mL of water were taken from each mesocosm and refrigerated until reaching the laboratory. Then, samples were filtered

through a 0.22 μm Steritop™ filter units (Merck Millipore®, Massachusetts, US) and the resulting filters were frozen at -80 ºC until DNA extraction.

DNA was extracted from the cells collected in the filters using a DNA Fecal/Soil Microbe Miniprep kit (Zymo® Research, California, US), following the standard protocol. Purified DNA was quantified using the Qubit BR DNA assay in the Qubit fluorimeter (ThermoFisher Scientific®, Massachusetts, US). The v4 region of the bacterial 16S rDNA gene was amplified by polymerase chain reaction (PCR) using primers F515 and R806 (5' GTGCCAGCMGCCGCGGTAA 3' and 5'GGACTACHVGGGTWTCTAAT 3', respectively) as described by Caporaso et al., 2011. For each DNA sample, amplifications were performed in triplicate in 25 μL reactions containing 12.5 μL of HiFi HotStart ReadyMix (KAPA Biosystems®), 0.2 μM of each primer and 10 ng of DNA. Incubation conditions consisted of an initial denaturation step at 95 °C for 3 min followed by 25 cycles of amplification (95 °C for 30 s, 55 °C for 30 s and 72 °C for 30 s) and a final step of 72 °C for 5 min. Replicates were pooled and then purified using magnetic beads Agencourt AMPure XP (Beckman Coulter®, California, US). A second PCR was performed to incorporate dual indices following the standard recommendation from Illumina® MiSeq system protocol (16S Metagenomic Sequencing Library Preparation). After a second purification step with magnetic beads, libraries were quantified using the Qubit BR DNA assay in the Qubit fluorimeter (ThermoFisher Scientific®, Massachusetts, US) and then mixed in equimolar amounts to be sequenced.

Sequencing and bioinformatics analysis

Sequencing was performed using the MiSeq Reagent kit v2 (2 x 150 base pairs) in a MiSeq Platform, according to the manufacturer's instructions. The resulting (.fastq) files were recovered and the paired-end reads were joined using Mothur v.1.43 (Schloss et al.

2009). Criteria to exclude low-quality reads were length <260 base pairs, ambiguous characters ('N'), >8 homopolymers and nucleotide mismatches to the primer and/or barcode. The resulting high-quality reads were aligned using the SILVA reference database (Quast et al. 2013), trimmed, filtered and pre-clustered with diff = 2. Chimeras were detected using VSEARCH and then excluded (Rognes et al. 2016). Taxonomic classification was carried out using the SILVA database with a confidence threshold of 80%. Sequences not assigned as Bacteria or classified as chloroplast, mitochondria, Archaea or unknown were discharged. Taxa with only one or two sequences were removed. The total number of sequences in each sample was randomly normalized to equal that of the sample with the lower number of sequences. Then, the sequences were clustered into operational taxonomic units (OTUs) using a sequence similarity cut-off of 97%. The taxonomic assignment of OTUs was performed according to SILVA database (release date December 16, 2019).

The composition of microbial communities was evaluated according to the relative abundance of taxa (Phylum and Order levels), considering only those OTUs that contributed more than 1% to total sequences. Results were represented considering the average values of triplicates (Supplementary Material). Rarefaction curves were constructed considering alpha diversity indexes. Shannon diversity index, Sobs richness and evenness were calculated for each sample using the Mothur v1.43 software.

Sequence information for this project is available at the NCBI database (BioProject accession number PRJNA659532).

Statistical analysis

- **Differential composition of bacterial communities**

From each sample, a table including OTU frequencies was used as input to perform a permutational multivariate analysis of variance using two factors (two-way PERMANOVA, $p<0.05$). Experimental conditions (with or without H_2O_2) and time (0, 24, 72 and 120 h) were tested as factors for two-way analysis influencing to the composition of bacterial communities. The null hypothesis was rejected if the p-value was < 0.05, assuming the alternative hypothesis that there was a significant effect of H_2O_2 on bacterial community structure over time. A non-metric multidimensional scaling (nMDS) was applied to ordinate the 22 samples based on OTU composition using a dissimilarity matrix based on Bray Curtis distance. A hierarchical clustering dendrogram was also constructed based on Bray Curtis distance of dissimilarity.

A mixed-effects model of ANOVA was used to evaluate differences on alpha diversity (Richness and Shannon index) considering $p<0.05$ and Sidak's multiple comparison tests. These analyses and charts were performed in Graphpad Prism 8.0 (GraphPad Software, LaJolla California, US)

We performed a linear discriminant analysis (LDA) and effect Size (LEfSe) (Segata et al., 2011) to select bacterial taxa with a significant contribution ($p<0.05$) to the differentiation between groups (treatment and control) considering sampling time as subgroups. LEfSe analysis was carried out according to the Hutlab Galaxy web framework application (http://huttenhower.sph.harvard.edu/galaxy/) using a threshold for LDA score of 3.0 (log 10 transformed) and a cladogram was constructed based on order level (Segata et al., 2011). The statistical analysis consisted of a two-tailed nonparametric Kruskal-Wallis test and an unpaired Wilcoxon test to reveal significant differences in OTU relative abundance comparing treatment and control (considering all replicates) over the time. Then, LDA with LefSe was performed to estimate the effect size considering the most abundant OTUs with significant different distributions between the

conditions. We also used a similarity percentage analysis (SIMPER) (Clarke, 1993) to select the main OTUs that contributed to the differentiation between control and treatment analysing each sampling time separately (24, 72 and 120 h).

- **Relationship between OTUs and physical-chemical parameters**

Those OTUs selected by SIMPER were used to test for correlations with physical-chemical parameters. According to previous results of our group (Guedes et al., 2020), we selected physical-chemical parameters that proved relevant to describe the effects of the H_2O_2 treatment over time, besides chlorophyll α values from phytoplankton groups: cyanobacteria, green algae, and diatom. The following physical-chemical parameters presented statistical difference comparing treatment and control: transparency and turbidity (which were significantly different in all sampling times), pH (different in 72 h and 120h), dissolved O_2 (DO) and dissolved organic carbon (DOC) (different in 72 h) and conductivity (different in 120h) (Table 1). We carried out a canonical correspondence analysis (CCA) combining these parameters with the major OTUs. These OTUs corresponded to those selected by SIMPER analysis and that presented a relative contribution higher than 1% or cumulative contribution of 50% or more at each sampling time (24, 72 or 120h). The CCA was represented using the PAST3 software (Hammer et al., 2001). A correlation matrix using Spearman ($p<0.01$ and a threshold for r value = ±0.6) was constructed to calculate significant associations among physical-chemical parameters and OTUs included in the CCA.

Results

We investigated the effects of H_2O_2 used to mitigate a cyanobacterial bloom exploring the impacts on the bacterioplankton community. H_2O_2 concentration extinguished 72h

after application (data not shown), and we have followed physical-chemical parameters, chlorophyll and bacterial community composition until 120h.

Physical-chemical parameters affected by H_2O_2

According to previous results (Guedes et al., 2020) we observed that transparency, turbidity, pH, DOC, DO and conductivity were affected by the treatment and presented different values in comparison to control over the time. More specifically, transparency increased and turbidity decreased at all sampling times (24, 72 and 120h) whereas pH decreased at 72 and 120h. DO and DOC concentrations decreased significantly only at 72h whereas conductivity slightly decreased at 120h (Table 1).

Table 1: Limnlogical parameters affected by the H_2O_2 addition over the time comparing treatment and control conditions according to Guedes et al., 2020. The parameters that presented a significant difference ($p<0.05$) between control and experimental group at each sampling time are labeled in bold. The values represent mean and standard deviation (n=3). The abreviations mean: DOC – dissolved organic carbon; DO – dissolved oxygen; Chl – chlorophyll; NTU – nephelometric turbidity unit.

Parameters	Initial time (T0)	T 24h		T 72h		T 120h	
		Control	Treatment	Control	Treatment	Control	Treatment
Transparency (cm)	47.30±3.2	**64.33±5.5**	**81.67±3.2**	**62.67±4.5**	**115.30±3.5**	**68.67±2.9**	**105.00±3**
Turbidity (NTU)	11.17±0.2	**11.47±0.1**	**8.27±0.35**	**14.37±0.35**	**5.53±0.9**	**13.07±0.8**	**5.53±1.7**
Conductivity ($\mu S\ cm^{-1}$)	568±3.1	565±1.15	567.33±1.5	573±1.15	580.33±3.5	**574±1**	**582±0.6**
pH	8.81±0.2	9.14±0.1	8.93±0.1	**9.14±0.07**	**8.09±0.1**	**8.97±0.05**	**8.32±0.06**
DOC ($mg\ L^{-1}$)	16.10±0.5	16.53±0.8	16.00±0.7	**22.07±0.25**	**18.47±1.05**	21.83±2	17.83±0.65
DO ($mg\ L^{-1}$)	8.00±0.3	10.35±0.4	9.91±0.8	**11.45±1.1**	**6.42±0.2**	9.14±0.5	8.05±0.7
Chl Cyanobacteria ($\mu g\ L^{-1}$)	34.89±1.9	**32.85±3**	**15.90±2.07**	**28.48±2.4**	**0.72±1.01**	**26.69±3.06**	**4.75±8.2**
Chl Green Algae ($\mu g\ L^{-1}$)	8.47±0.5	**10.17±0.5**	**3.82±0.3**	**12.87±0.8**	**3.18±0.5**	**12.00±0.9**	**23.51±4.1**
Chl Diatom ($\mu g\ L^{-1}$)	1.74±0.5	1.11±0.4	0±0	0±0	0.19±0.1	**0.50±0.45**	**2.69±0.3**

Diversity and composition of bacterial communities

After normalization, 32221 sequences were considered in each sample to describe the bacterial communities (Supplementary Table 1). The sample T3M5 (no H_2O_2 at 72h) was lost during DNA processing and could not be analysed.

Rarefaction curves approached saturation with coverage of bacterial diversity reaching 97-98% for all samples (Supplementary Table 1 and Supplementary Figure 2). The clustering of samples according to the test condition revealed an average similarity of 60% within each group. The treatment and control groups presented a dissimilarity between 70-80% (Supplementary Figure 3). Considering Shannon diversity indexes and sobs richness estimation the addition of H_2O_2 did not affect richness at any time ($p=0.07$, $F=5.58$) (Figure 1A) but decreased community diversity ($p=0.001$, $F=63.51$) at 24 and 72 h compared to the control condition (Figure 1B). This indicated that compositional changes occurred on bacterial communities after H_2O_2 addition without a decrease in the number of species.

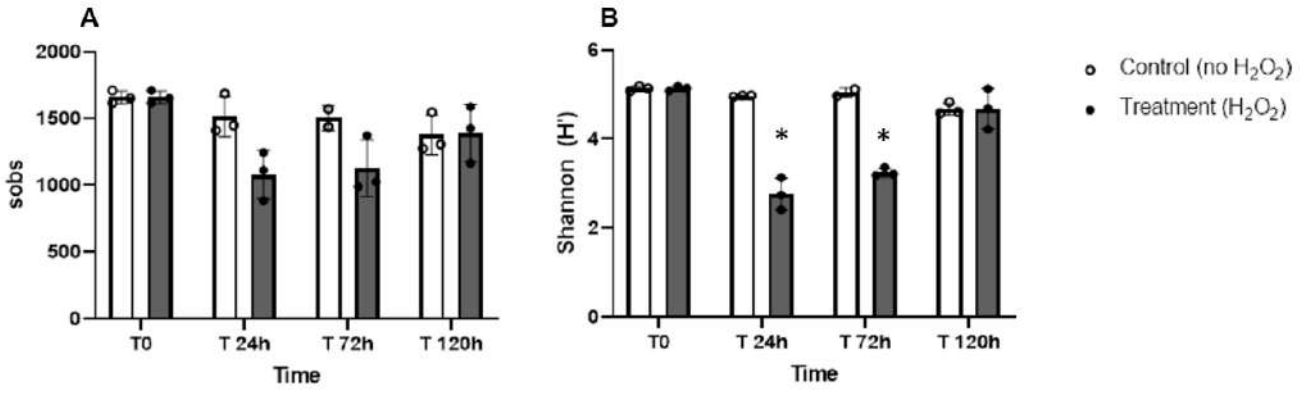

Figure 1: Alpha diversity considering sobs richness (A) and Shannon diversity (B) of samples from each condition (treatment x control) over the time. Grey and white bars represent the treatment and control conditions, respectively. Asterisks mean significant differences between control and treatment at each sampling time ($p<0.05$) considering mixed-effects model ANOVA ($p<0.05$) using Sidak's as *post hoc* test.

Ordination of samples corresponding to treatment and control conditions over the time was represented in non-metric multidimensional scaling (nMDS) to visualize differences among groups. Samples corresponding to the two conditions distributed distantly. Samples corresponding to treatment at different times were also separated, with replicate samples grouped (Figure 2). Samples collected 24 and 72 h after H_2O_2 addition were more similar than that recovered at 120 h. These differences were confirmed by two way PERMANOVA for treatment vs. control ($p<0.0001$, $F = 26.562$) and treatment over the time, 24, 72, 120 h ($p<0.0001$, $F=4.516$) with the interaction between these factors ($p<0.03$) (Supplementary Table 2).

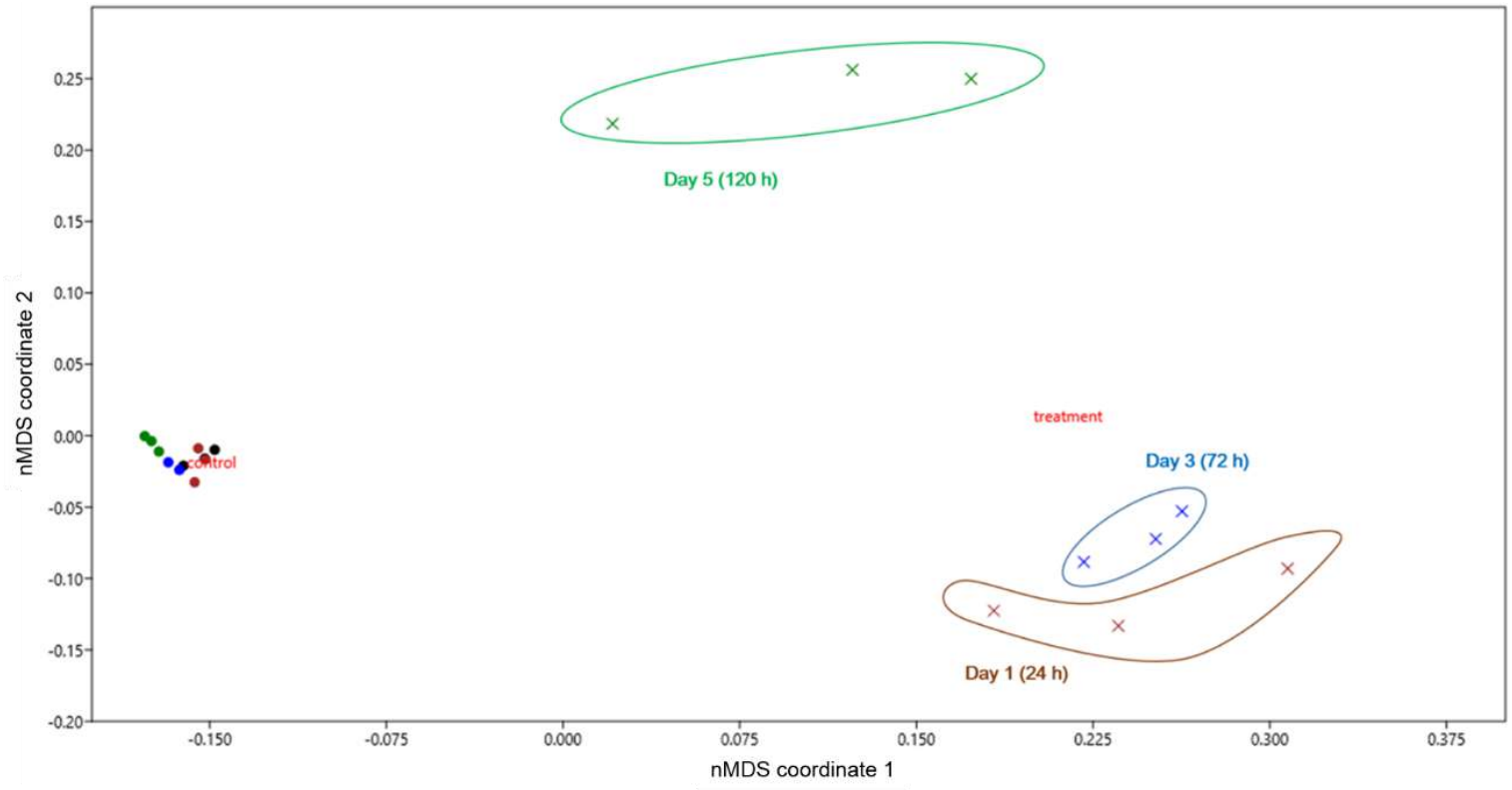

Figure 2: Ordination of samples according to the bacterial community composition by non-metric multidimensional scaling (nMDS) using Bray-Curtis distance. Samples correspond to control or H_2O_2 treatment collected over the time, 24, 72 and 120 h, n=3.

The composition of bacterial communities at the phylum level changed over time after H_2O_2 addition (Figure 3, Supplementary Table 3). The original community was mainly composed of *Actinobacteria* (21%), *Cyanobacteria* (20%), *Plantomycetes* (15%) and *Proteobacteria* (11%), followed by *Verrucomicrobia* (9%), *Chloroflexi* (8%) and *Bacteroidetes* (7%). Few changes were observed in the control condition over the time. An increase of Cyanobacteria relative abundance occurred at 24 h (25%) and 72 h (27%), and then returning at 120h to a value similar to the initial abundance. *Actinobacteria* relative abundance continuously decreased throughout the time reaching 11% at 120h, while *Verrucomicrobia* increased to 21% at the final time. In contrast, in the treatment condition the composition of the bacterial community was strongly affected. Samples collected at 24 and 72 h were more similar, showing a notable expansion of *Firmicutes* passing from 0.2% at time 0 to 40-50%. Other phyla that increased in abundance in these samples were *Deinococcus* (from 0.01% at time 0 to 7-11%) and *Proteobacetria* (from 11% at time 0 to 17-23%). In parallel, *Actinobacteria, Verrucomicrobia*, *Planctomycetes* and *Chloroflexi* decreased in abundance. After 120h, the community profile of the treated samples was dissimilar from time 0 and also from control at this time, including as dominant phyla *Bacteroidetes* (19%), *Verrucomicrobia* (24%) as well as *Proteobacetria* (26%) (Figure 3).

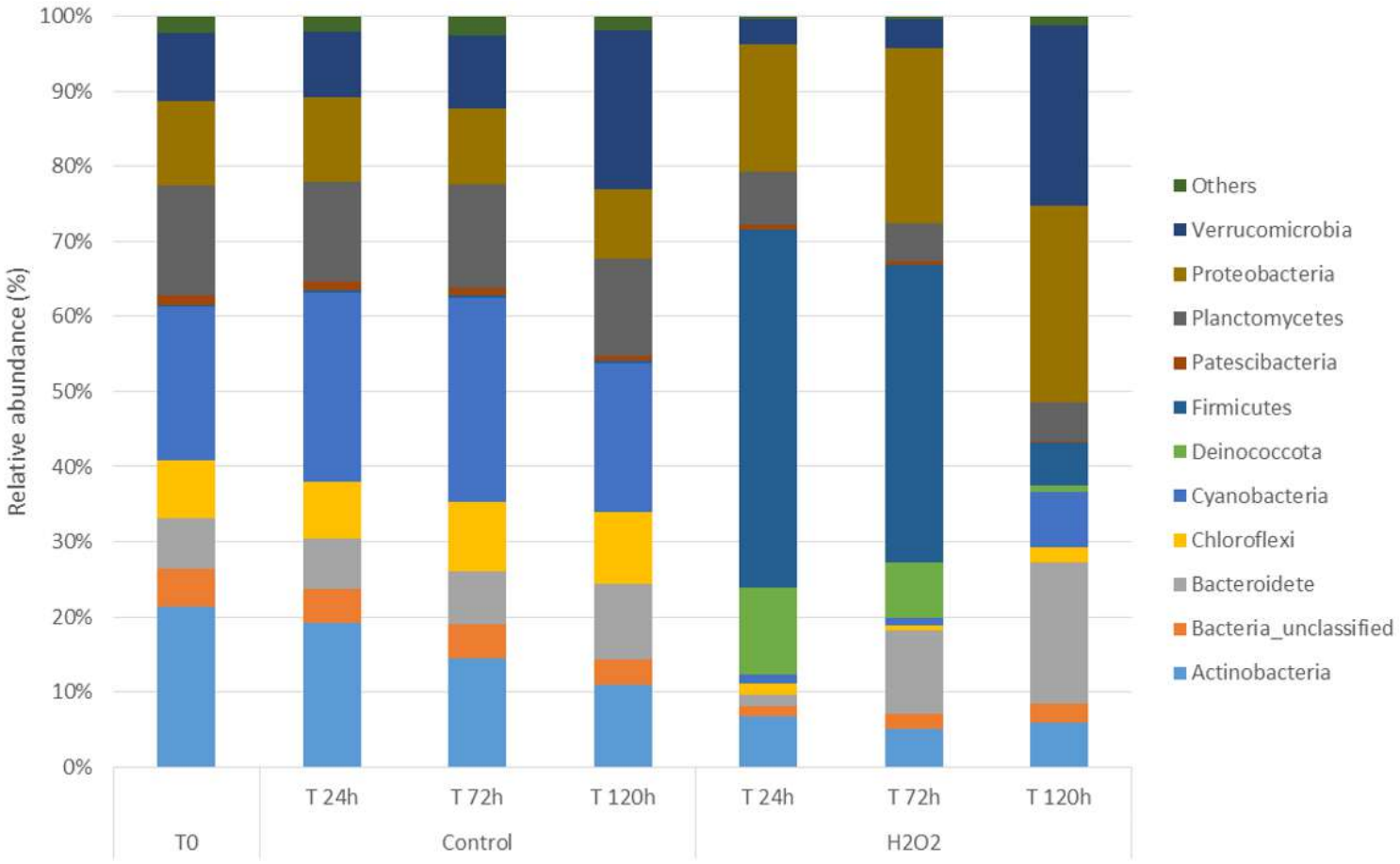

Figure 3: Relative abundance of bacterial OTUs at phylum level at time 0 and in control or treatment (H_2O_2 addition) after 24, 72 and 120h.

Effect of H_2O_2 on *Cyanobacteria*

The H_2O_2 treatment decreased the relative abundance of *Cyanobacteria* from 20% at time 0 to 1% at 24 and 72 h and 7% after 120 h. We investigated whether the composition of the cyanobacterial community had also been affected (Figure 4). *Cyanobium*, *Planktothrix* and *Microcystis* were the dominant genera in the original cyanobacterial community accounting for 30, 27 and 16%, respectively. In the control condition, they remained as the main genera until the end of the experiment. In the treatment condition, after a drastic decline in cyanobacterial abundance, *Microcystis* was dominant accounting for 60% of all cyanobacterial OTUs at 24 h, while *Cyanobium* corresponded to 20%. From 72 h to 120 h, *Microcystis* abundance decreased (10 and 5%, respectively) while C*yanobium* abundance increased (53 and 64%, respectively). *Plantothrix* abundance remained low after the treatment (4-8%). Thus, at the end of the experiment, when cyanobacterial abundance tended to increase, the community composition differed from the original one (Figure 4).

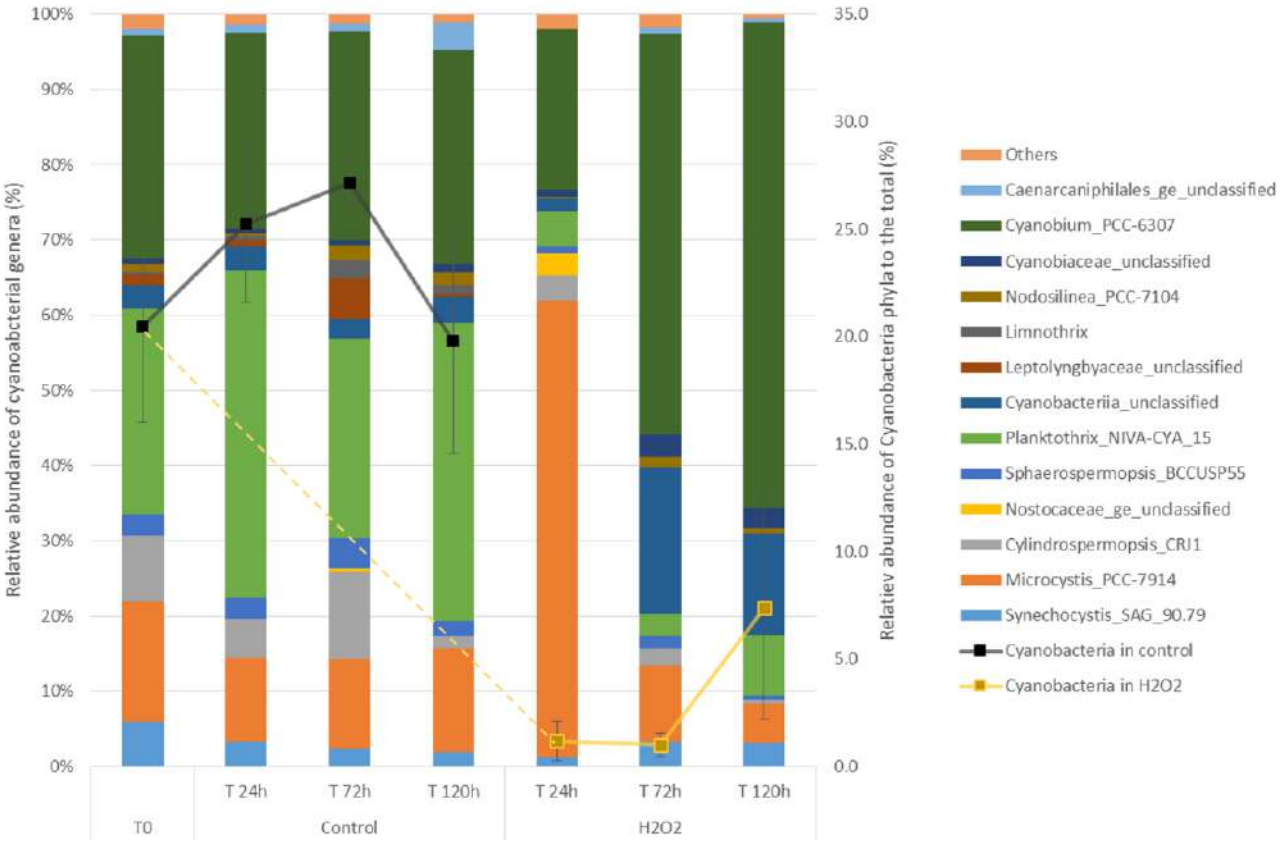

Figure 4: Relative abundance of OTUs representing from *Cyanobacteria* genera (bar chart). The lines represent the relative abundance of *Cyanobacteria*.

Main bacterial taxa distinguishing control and H_2O_2 treatment

To highlight the main taxa associated with the differentiation of bacterial communities in control and treatment conditions, regardless of time, we performed LDA and LEfSe analysis using the relative abundances of OTUs as input. The taxonomic distribution of the main bacterial taxa present in each condition is represented in a cladogram (Figure 5A). Bacterial taxa identified after the H_2O_2 treatment included members of *Exiguobacteriaceae* (*Firmicutes*), *Deinococcaceae* (*Deinococcus*), *Rhodobacteriaceae* (*Proteobacteria*), *Sphingobacteriaceae* and *Spirosomaceae* (*Bacteroidetes*). In the control condition, main bacterial families were affiliated with more diverse families/phyla, *Caldilineaceae* (*Chloroflexi*), *Mycobacteriaceae* (*Actinobacteria*), *Pirellulaceae* and *Phycisphaeraceae* (*Planctomycetes*), *Chthoniobacteraceae* (*Verrucomicrobia*) and *Microcystaceae*, *Synechococcaceae*, *Nostocaceae*, and *Phormidiaceae* (*Cyanobacteria*).

Considering the LDA score (log10) with a cut-off of 3.0, we selected 67 OTUs that contributed to the discrimination of treatment and control (Figure 5B). Restricting to those OTUs above a threshold of 3.5, in the treatment the dominant genera were *Exiguobacterium*, *Deinococcus*, *Paracoccus* and *Rhizobium*. At 24 and 72 h, the relative abundance of *Exiguobacterium* reached 40-50%. *Paracoccus* corresponded to 4-9% and *Deinococcus* had an abundance of 10%, while their abundance was close to zero in the control condition or at time 0 (T0) (Supplementary Figure 4). In the control condition, the most representative taxa were *Terrimicrobium sp.* (4%), an unclassified genus of *Chthoniobacteraceae* (3%) (Supplementary Figure 5) and the *Cyanobacteria* genera *Planktothrix* (6-10%), *Microcystis* (3%), *Cyanobium* (3%) and

Cylindrospermospis/Raphidiopsis (1%) (Supplementary Figure 6). Other taxa characteristic of the control condition were *Mycobacterium* and unclassified genera of *Solirubrobacterales*, *Caldilineaceae*, *Chloroflexaceae* and *Pirellulaceae* (Figure 5B).

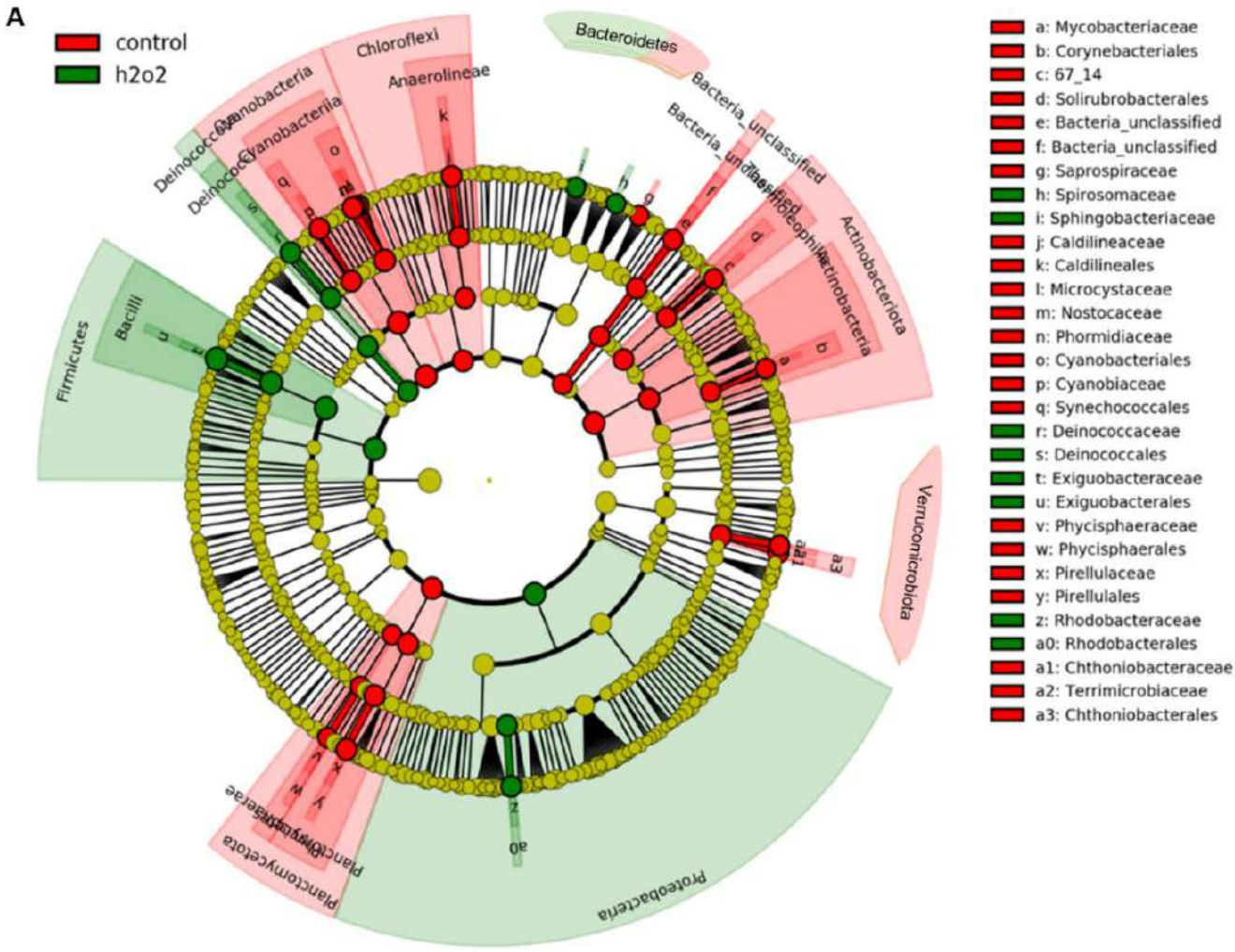

B

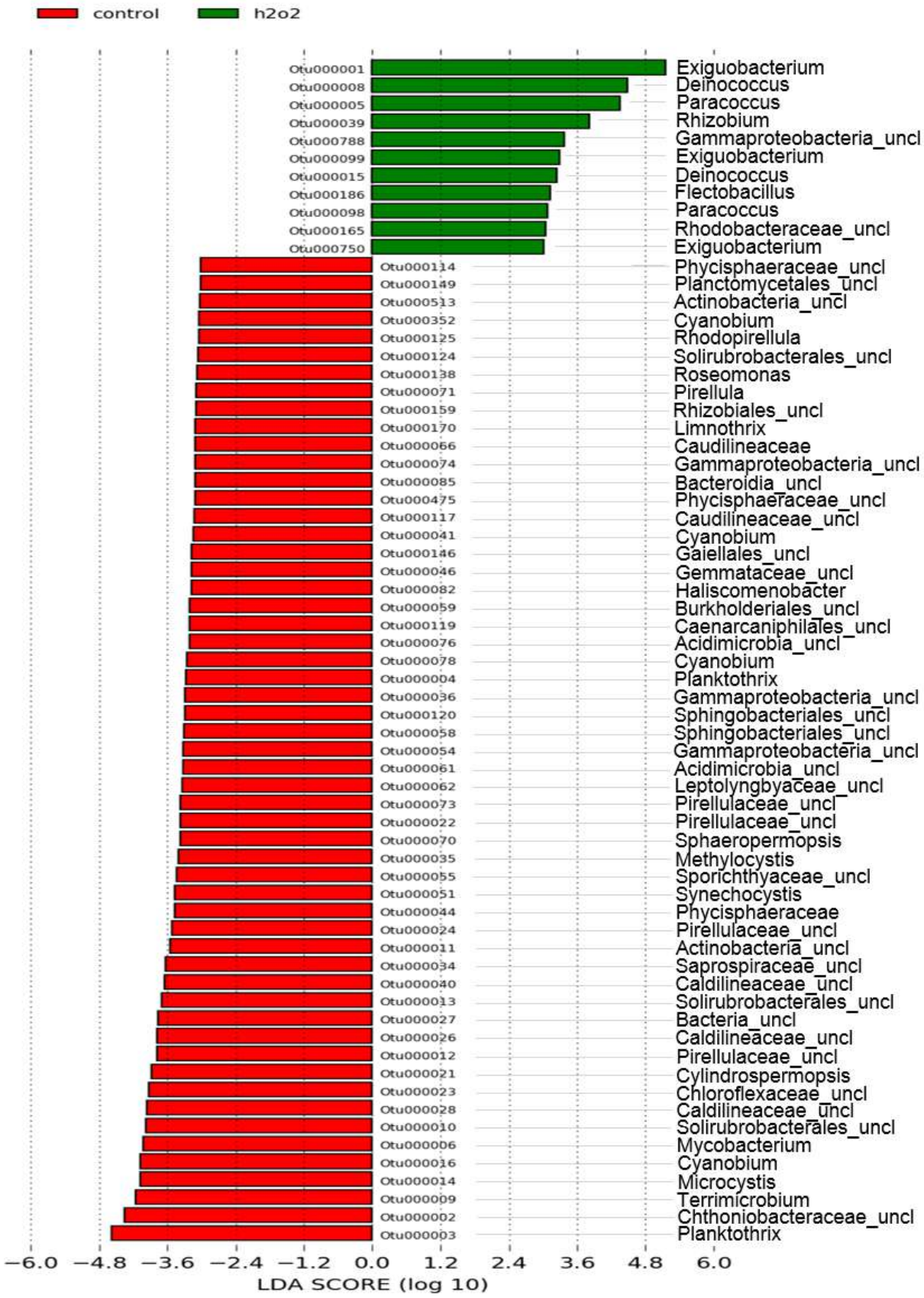
control
h2o2
Otu000001 Exiguobacterium
Otu000008 Deinococcus
Otu000005 Paracoccus
Otu000039 Rhizobium
Otu000788 Gammaproteobacteria_uncl
Otu000099 Exiguobacterium
Otu000015 Deinococcus
Otu000186 Flectobacillus
Otu000098 Paracoccus
Otu000165 Rhodobacteraceae_uncl
Otu000750 Exiguobacterium
Otu000114 Phycisphaeraceae_uncl
Otu000149 Planctomycetales_uncl
Otu000513 Actinobacteria_uncl
Otu000352 Cyanobium
Otu000125 Rhodopirellula
Otu000124 Solirubrobacterales_uncl
Otu000138 Roseomonas
Otu000071 Pirellula
Otu000159 Rhizobiales_uncl
Otu000170 Limnothrix
Otu000066 Caudilineaceae
Otu000074 Gammaproteobacteria_uncl
Otu000085 Bacteroidia_uncl
Otu000475 Phycisphaeraceae_uncl
Otu000117 Caudilineaceae_uncl
Otu000041 Cyanobium
Otu000146 Gaiellales_uncl
Otu000046 Gemmataceae_uncl
Otu000082 Haliscomenobacter
Otu000059 Burkholderiales_uncl
Otu000119 Caenarcaniphilales_uncl
Otu000076 Acidimicrobia_uncl
Otu000078 Cyanobium
Otu000004 Planktothrix
Otu000036 Gammaproteobacteria_uncl
Otu000120 Sphingobacteriales_uncl
Otu000058 Sphingobacteriales_uncl
Otu000054 Gammaproteobacteria_uncl
Otu000061 Acidimicrobia_uncl
Otu000062 Leptolyngbyaceae_uncl
Otu000073 Pirellulaceae_uncl
Otu000022 Pirellulaceae_uncl
Otu000070 Sphaeropermopsis
Otu000035 Methylocystis
Otu000055 Sporichthyaceae_uncl
Otu000051 Synechocystis
Otu000044 Phycisphaeraceae
Otu000024 Pirellulaceae_uncl
Otu000011 Actinobacteria_uncl
Otu000034 Saprospiraceae_uncl
Otu000040 Caldilineaceae_uncl
Otu000013 Solirubrobacterales_uncl
Otu000027 Bacteria_uncl
Otu000026 Caldilineaceae_uncl
Otu000012 Pirellulaceae_uncl
Otu000021 Cylindrospermopsis
Otu000023 Chloroflexaceae_uncl
Otu000028 Caldilineaceae_uncl
Otu000010 Solirubrobacterales_uncl
Otu000006 Mycobacterium
Otu000016 Cyanobium
Otu000014 Microcystis
Otu000009 Terrimicrobium
Otu000002 Chthoniobacteraceae_uncl
Otu000003 Planktothrix
−6.0 −4.8 −3.6 −2.4 −1.2 0.0 1.2 2.4 3.6 4.8 6.0
LDA SCORE (log 10)

Figure 5: Linear discriminant analysis coupled to effect size (LEfSe) of bacterial abundance in treatment and control. (A) Phylogenetic representation of differentially distributed bacterial taxa according to LEfSe in each condition (treatment or control) at phylum to family level (B). Taxa with significant difference distribution between treatment (H_2O_2) and control (no H_2O_2) groups were selected using a p value <0.05 and a LDA score (log10) >3.0.

Bacteria that presented a major contribution to community structure after H_2O_2 extinguished were identified in comparison to the control condition at 120 h based on LEfSe analysis (Figure 6). The top 15 taxa in the treatment were graphically represented in a cladogram showing that the majority of them were members of *Proteobacteria* (families *Comamonadaceae*, *Sphingomonadaceae*, *Caulobacteraceae*, *Rhizobiaceae*, *Rhodobacteraceae*) and *Bacteroidetes* (families *Sphingobacteriaceae*, *Flavobacteriaceae*, *Spirosomaceae*, *Chitinophagaceae*) (Figure 6). Other taxa were attributed to *Firmicutes (Exiguobacteriaceae)*, *Verrucomicrobia (Rubritaleaceae* and *Verrucomicrobiaceae)*, *Cyanobacteria (Cyanobiaceae)* and an unclassified phylum. According to the LEfSe analysis, the five most relevant OTUs in the treatment condition after extinction of H_2O_2 were *Luteolibacter sp*. (~15%), *Exiguobacterium sp.* (~5%), *Comamonadaceae unclassified* (~3%), *Spirosomaceae sp.* (~3%) and *Prosthecobacter sp.* (~3%) (Supplementary Figure 7).

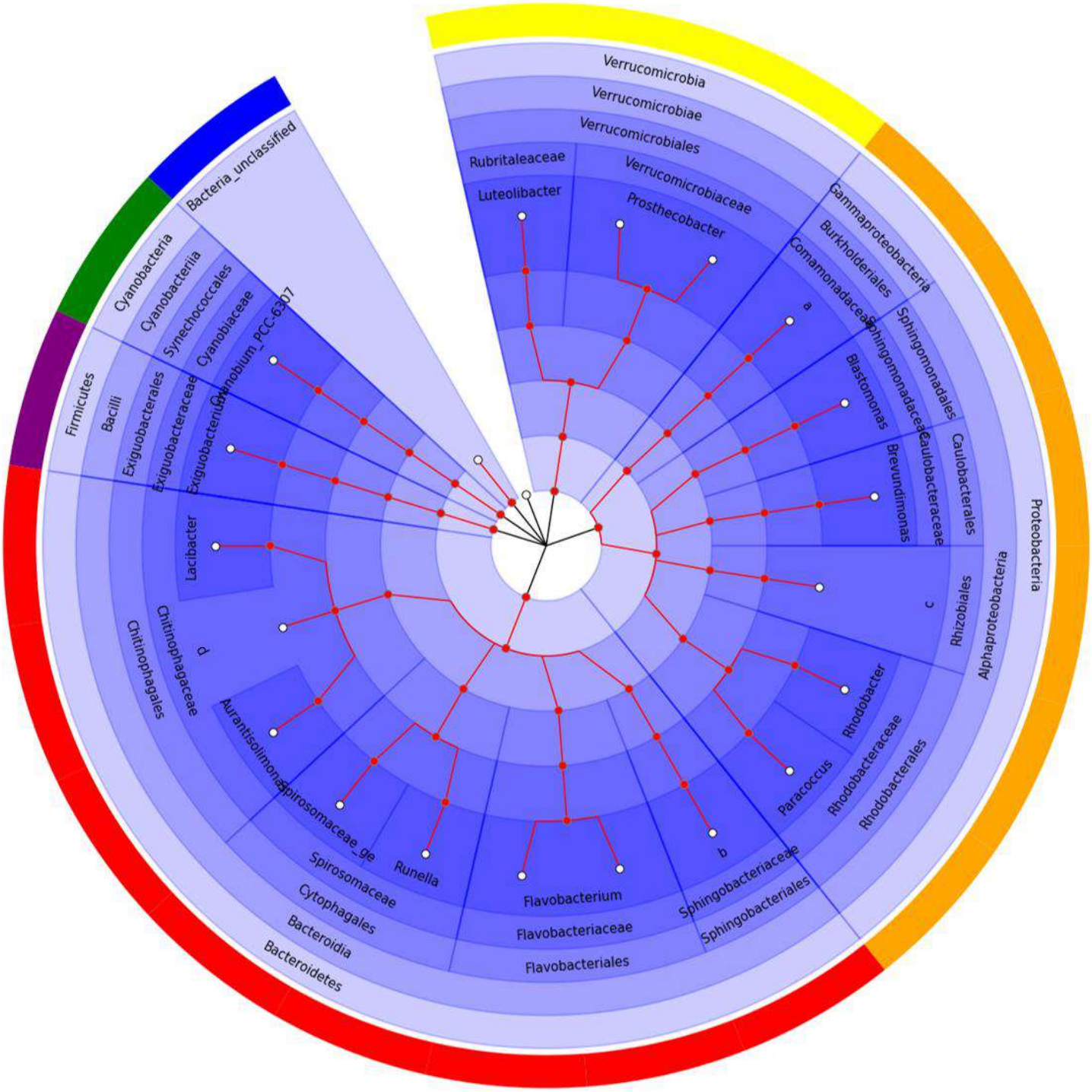

Figure 6: Cladogram constructed using the top-fifteen OTUs represented at the H_2O_2 treatment condition after 120h based on LEfSe analysis comparing to the control. The letters within specific clades mean a: *Comamonadaceae unclassified*; b: *Sphingobacteriaceae unclassified*; c: *Allorhizobium-Neorhizobium-Pararhizobium-Rhizobium*; d: *Chitinophagaceae unclassified*.

Correlation between bacterial groups and physical-chemical parameters

After we have obtained a general picture of OTUs that were differently represented in control and treatment conditions by LEfSe analysis, we further detailed the contribution of individual bacterial OTUs at each sampling time performing SIMPER analysis (Supplementary Table 4). Considering these OTUs, we tested their correlation with chlorophyll and physical-chemical parameters that were affected by the H_2O_2 treatment (Guedes et al., 2020) (Table 1). These data were ordinated by CCAs, considering each sampling time (24, 72, and 120h) (Figure 7). In the control condition, all sampling times grouped and turbidity, transparency and cyanobacterial chlorophyll were the main factors contributing to this condition. The high turbidity was positively correlated with an uncultured *Chthoniobacteraceae* (OTU000002) ($p = 0.0001$) and *Cyanobium* (OTU000016) ($p = 0.000002$) (r-value of 0.75 and 0.84, respectively). Cyanobacterial chlorophyll was positively correlated to an OTU from *Sporichthyaceae* (OTU000007) ($p = 0.0002$) ($r = 0.73$) (Supplementary Table 5). *Microcystis* (OTU000014) showed the strongest correlation to both factors (r-value of 0.79 for turbidity; and 0.88 for cyanobacterial chlorophyll). In addition, turbidity and cyanobacterial chlorophyll were positively correlated to *Planktothrix* (OTU000003), *Microcystis* (OTU000014), *Cylindrospermopsis/Raphidiopsis* (OTU000021) as well as the heterotrophic bacteria *Mycobacterium* (OTU000006), *Terrimicrobium* (OTU000009), a *Solirubrobacterales* member (OTU000010) and a *Caldilineaceae* member (OTU000028); with a correspondent negative correlation with transparency (Supplementary Table 5). As an early effect of H_2O_2 addition (24 h), when transparency increased and cyanobacterial chlorophyll decreased, a significant positive correlation between transparency and *Exiguobacterium* (OTU000001) ($p = 0.00006$; $r = 0.77$), *Paracoccus* (OTU000005) ($p = 0.00001$; $r = 0.80$) and *Deinococcus* (OTU000008) ($p = 0.00002$; $r = 0.79$) was observed

(Figure 7). Simultaneously, a significant negative correlation was estimated between these three OTUs and cyanobacteria chlorophyll (r-value of -0.71, -0.74 and -0.75, respectively) (Figure 7 and Supplementary Table 5).

At 72h, the transparency as well as turbidity were still significantly different in the two conditions and at this sampling time pH, DOC and DO decreased in H_2O_2 samples compared to control samples (Table 1). In the control condition, cyanobacterial OTUs that correlated positively with turbidity also showed a significant positive correlation to pH, including *Planktothrix* (OTU000003) (r = 0.7), *Microcystis* (OTU000014) (r = 0.66) and *Cylindrospermopsis/Raphidiopsis* (OTU000021) (r = 0.64). The heterotrophic bacteria *Mycobacterium* (OTU000006) (r = 0.64) and a *Caldilineaceae* member (OTU000028) (r = 0.7) also correlated positively with these factors. In the treatment, the genera *Exiguobacterium* (OTU000001), *Paracoccus* (OTU000005) and *Deinococcus* (OTU000008) were still positively correlated with transparency ($p<0.01$) (r value of 0.77, 0.80 and 0.79 respectively), and also an unclassified *Sphingobacteriaceae* (OTU000025) (p = 0.001, r = 0.66) (Figure 7). The genera *Rhizobium* (OTU000039) (p = 0.0002) and *Flavobacterium* (OTU000042) (p = 0.004) were positively correlated with transparency (r-value of 0.66, 0.73 and 0.6, respectively) and negatively correlated to the turbidity (r = -0.65 and -0.74, respectively) and pH (r = -0.62 and -0.80, respectively). *Flavobacterium* (OTU000042) (p = 0.0001) also showed a negative correlation with DO_2 (r = -0.75). No significant correlation was observed between any OTU and DOC (Figure 7, supplementary table 5).

In the control condition at 120 h, high turbidity, pH and chlorophyll α (*Cyanobacteria*) were relevant factors and positive correlations were observed with OTUs already cited for the early sampling times. In the treatment condition, conductivity and transparency increased while pH slightly decreased, but was still different from the control condition,

whereas chlorophyll of green algae and diatoms increased (Table 1). A positive correlation was established between some OTUs and both conductivity and transparency: *Blastomonas* (OTU000065) (conductivity: p = 0.000002, r = 0.84; transparency: p = 0.00001, r = 0.68), *Rhodobacter* (OTU000081) (conductivity: p = 0.0001, r = 0.75; transparency: p = 0.0001 r = 0.80), *Lacibacter* (OTU000160) (conductivity: p = 00002, r = 0.80; transparency: p = 0.0003, r = 0.75) and an unclassified *Spirosomaceae* (OTU000037) (conductivity: p = 0.000009, r = 0.82; transparency: p = 0.0009, r = 0.72). The abundance of an unclassified *Sphingobacteriaceae* (OTU000025) was related only to conductivity, (p = 0.00005, r = 0.77). OTUs negatively correlated with conductivity were *Mycobacterium* (OTU000006) (p = 0.003, r = -0.62), an uncultured *Solirubrobacterales* (OTU000010) (p = 0.0009, r = -0.67). OTUs negatively related to pH were *Spirosomaceae* (OTU000037) (p =0.0001, r = -0.74), *Rhizobium* (OTU000039) (p =0.003, r = -0.62), *Flavobacterium* (OTU000042) (p = 0.00001, r = -0.80), *Blastomonas* (OTU000065) (p = 0.0004, r = -0.71), *Rhodobacter* (OTU000081) (p = 0.002, r = -0.63) and *Lacibacter* (OTU0000160) (p = 0.0004, r = -0.71) (Figure 7, Supplementary Table 5). Although *Luteolibacter* (OTU000017) (p = 0.2), *Comamonadaceae* unclassified (OTU000029) (p = 0.6) and *Prosthecobacter* (OTU000088) (p = 0.2) were related to the treatment condition at 120h, they did not present a significant correlation with physical chemical factors (Supplementary Table 5). Moreover, green algae chlorophyll was positively correlated to *Cyanobium sp.* (OTU000016) (p = 0.003, r = 0.62) that maintained its presence in the control condition and a slight increase in the treatment samples. Meanwhile, *Prosthecobacter sp.* (OTU000088) was positively related to diatom chlorophyll (p = 0.0001, r = 0.74), whereas a *Comamonadaceae* unclassified (OTU00029) was positively related to the both factors (r = 0.6 for green algae and 0.73 for diatom group).

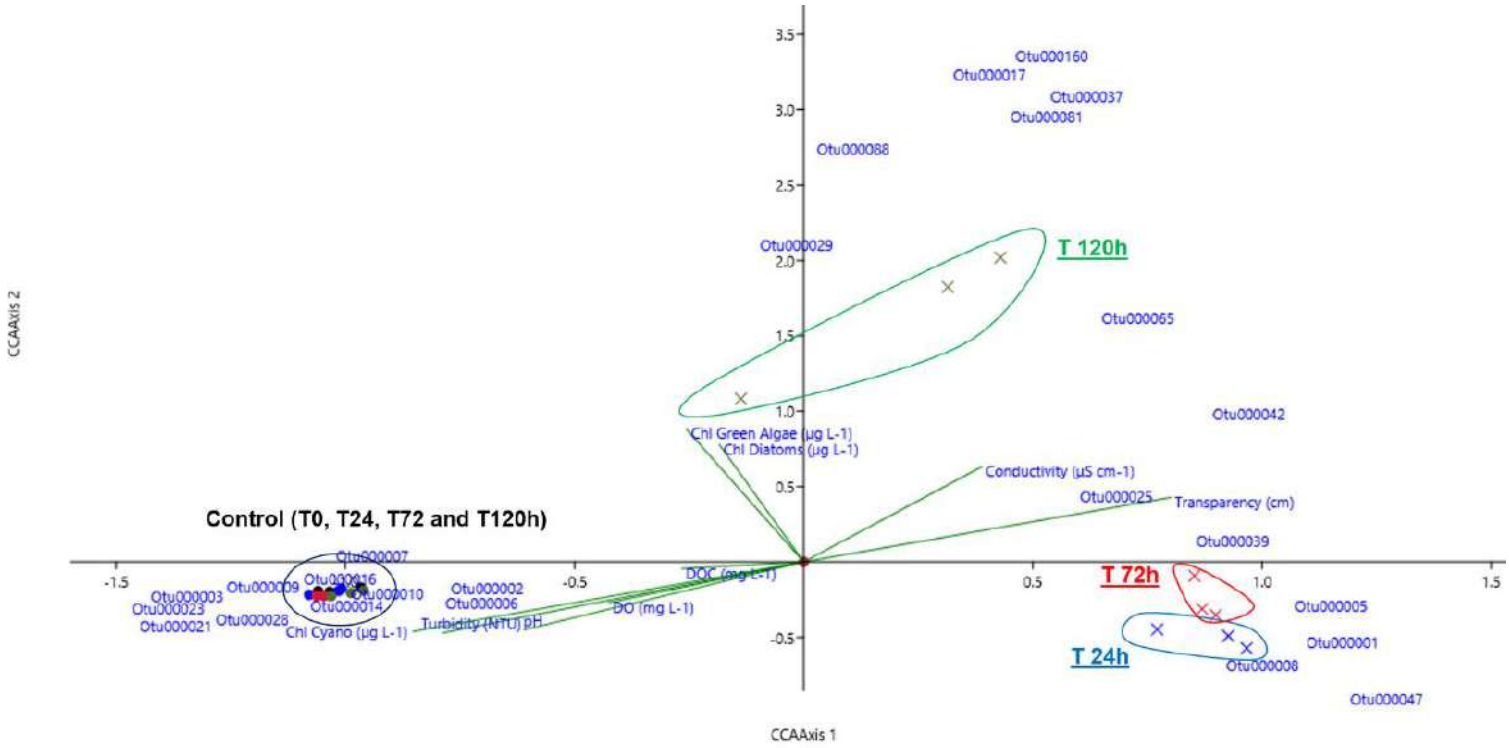

Figure 7: Canonical correspondence analysis (CCA) considering the main OTUs that contributed to the differentiation between control and treatment at each sampling time (by SIMPER) and physical chemical parameters significantly different at each time.

Discussion

In this study, we conducted a metagenomics analysis to investigate the effect of a hydrogen peroxide treatment, primarily directed to reduce a cyanobacterial bloom, on the bacterioplankton community of a reservoir located in a semi-arid region. A concentration of 10 mg L^{-1} was applied and the effect was evaluated over 120 hours (5 days) with sampling at 24, 72 and 120 h. Guedes et al. (2020), described changes in physical-chemical parameters and chlorophyll α concentration after the treatment. The hydrogen peroxide extinguished in 72 h, and at this time, we have registered the lowest cyanobacterial chlorophyll concentration and the highest transparency. Here, we have detailed how the composition of the bacterial community changed due to this treatment, compared to control conditions in which it remained stable.

The community diversity was lower in the treatment than in the control condition at 24 and 72 h, with no change in richness. Yang et al. (2017) evaluated the effect of H_2O_2 (7 mg L^{-1}) on bacterial communities from a wastewater effluent after 10 and 60 min but did not observe any difference in bacterial diversity or richness, only minor changes in the relative abundance of specific taxa. Wang et al. (2017) described a dose-dependent effect of residual H_2O_2 on bacterial diversity after sand-filtration. Higher bacterial diversity was observed in the lowest concentration of H_2O_2 (0.25 mg L^{-1}) and decreased with increasing H_2O_2 concentrations (1.0, 3.0 and 5.0 mg L^{-1}). Additionally, these authors observed a decrease of about 40% in microbial metabolic activity as measured by ATP production at the highest H_2O_2 concentration (5 mg L^{-1}), despite the occurrence of DOC degradation in these conditions. DOC degradation was attributed to the growth and activity of aerobic bacteria, since more O_2 was released over the oxidative process (Wang et al., 2017). Here, we did not evaluate the bacterial metabolic activity, but data from Guedes et al., 2020 showed that DOC concentration decreased at 72 h after H_2O_2 addition compared to the control condition. This could result from metabolic activities that promoted the oxidation of organic matter releasing smaller molecules that could be more easily degraded by the remaining microorganisms (Chelme-Ayala et al., 2011, Metz et al., 2011). However, in the present study we could not observe a significant correlation between DOC and the relative abundance of specific bacterial OTUs, which could further support this idea. In addition, the lower DOC and DO concentrations 72 h after the treatment could be related to the suppression of cyanobacterial cells and an increasing in the consumption of dissolved carbon by resistant heterotrophic bacteria.

The bacterial community composition changed 24 h after the treatment in comparison to the initial time (T0) and the respective control, with *Cyanobacteria*, *Actinobacteria* and *Verrucomicrobia* decreasing in abundance whereas *Firmicutes*, *Proteobacetria* and

Deinococcus increased. A similar profile was observed at 72 h, with a relative increase of *Bacteroidetes*. Additional changes were observed at 120 h with an increase of *Proteobacteria, Bacteroidetes* and *Verrucomicrobia*. Moreover, a slight increase in *Cyanobacteria* was observed at this final time.

In the control condition, the high relative abundance of cyanobacteria was related to a *Planktothrix* bloom also including *Cylindrospermospsis/Raphidiopsis*, as previously enumerated by microscopy analysis (data not shown). *Cyanobacteria* commonly reported as dominant in the Gavião reservoir include *Planktothrix agardhii* and *Raphidiopsis raciborskii* (previously *Cylindrospermospsis raciborskii*) (Barros et al., 2019; Pestana et al., 2019). We identified sequences not only from these genera but also from *Microcystis* and *Cyanobium,* with high abundance. Both are unicellular genera that might be underestimated using microscopy counting in comparison to large filamentous species such as *P. agardhii* and *R. raciborskii*. Especially *Cyanobium sp.* that is a picoplanktonic cyanobacteria difficult to detect in natural samples by optical microscopy (Callieri, 2008; Callieri et al., 2012).

All cyanobacteria taxa decreased in abundance after the treatment, confirming that in the phytoplankton community, this group is more susceptible to H_2O_2 than green algae and diatoms (Barrington and Ghadouani, 2008; Matthijs et al., 2012; Spoof et al., 2020). Matthijs et al. (2012) applied H_2O_2 (2 mg L^{-1}) into an entire lake dominated by *P. agardhii* in the Netherlands and observed a sharp collapse of cyanobacterial cells from $6x10^5$ to 10^3 over 10 days. The suppression was maintained for 7 weeks using a concentration 5 times lower than the one applied here and the authors did not observe any effects on other phytoplankton groups. Here, using 10 mg L^{-1} of H_2O_2 we have observed that both green algae and diatom groups were suppressed over 72 h, and then increased at 120 h, as evaluated by chlorophyll measurement (Guedes et al., 2020). From

chlorophyll analysis, Guedes et al. (2020) estimated that cyanobacteria were undetectable at 72 h after the treatment. However, our metagenomics analysis showed that DNA sequences from four different cyanobacterial genera could be identified at this moment. In addition, after H_2O_2 extinction, we observed an increase in the relative abundance of cyanobacterial sequences at 120 h, suggesting regrowth of this group, although with a composition different from the original one. After the treatment, *Cyanobium* was the main genus dominating the cyanobacterial community in the mesocosm but sequences from *Planktothrix* and *Microcystis* were also detected. Picoplanktonic cyanobacteria like *Cyanobium* (0.2 – 2 µm) are abundant but underestimated in freshwater systems (Komárek, 2003; Callieri, 2008; Gaysina et al., 2019, Cabello-Yeves et al., 2017; Guedes et al., 2018). Picocyanobacteria would be dominant in many freshwater systems along with other filamentous genera (Li et al., 2019). They have been described in oligo-mesotrophic environments (Callieri, 2008; Gaysina et al., 2019) and also in a hypereutrophic reservoir in Brazil (Guedes et al., 2018). Representative species of picocyanobacteria can reach a growth rate of 0.5 d^{-1} in oligotrophic marine environments (Cruz and Neuer, 2019). In our experiment, as the cyanobacterial bloom was supressed by H_2O_2, *Cyanobium* with its relatively faster growth rate may have benefited from the alleviation of competition with other cyanobacteria and the availability of nutrients, which has not decreased due to H_2O_2 treatment (Helbling et al., 2001; Callieri, 2010; Leblanc et al., 2018). Thus, long-term microscopy analysis, chlorophyll measurements and molecular tools would be important to monitor the development of the remaining cyanobacterial community and optimize mitigation strategies.

The collapse of cyanobacterial blooms after oxidative processes can lead to the release of cyanotoxins, such as microcystins. The residual concentration of H_2O_2 can be insufficient to oxidise completely the released toxin. As a result, high concentrations of microcystins

can still be detected in the water 24h after H_2O_2 application (Lürling et al., 2014; Spoof et al., 2020). In our study, we did not evaluate the concentration of cyanotoxins but we consider that this issue should be investigated for evaluation of water consumption risks from Gavião reservoir.

Besides *Cyanobacteria*, the abundance of other phyla decreased after the H_2O_2 treatment. This was the case of *Actinobacteria*, *Verrucomicrobia*, *Planctomycetes* and *Chloroflexi*, indicating that members of these phyla were also sensible to the oxidative process. Conversely, we could point some bacterial taxa that resisted to the H_2O_2 treatment. They included *Firmicutes*, *Proteobacteria* and *Deinoccoci* members. More specifically, within *Firmicutes* the main genus in the treatment condition was *Exiguobacterium* (*Bacillales*). Many species of *Exiguobacterium* are found in aquatic environments, both seawater and freshwater (White et al., 2019). Some strains have been isolated from microbialites and/or microbial mats (White et al., 2013a; Ordoñez et al., 2013; 2015; Gutiérrez-Preciado et al., 2017). The cosmopolitan distribution of *Exiguobacterium* members may be related to its adaptability to extreme environmental conditions such as a wide range of temperature, pH and salinity (White et al., 2013a; Mlewski et al., 2018) and also high UV intensity (Strahsburger et al., 2018). Additionally, an inherent characteristic of this genus is the intense activity of catalase (Yumoto et al., 2004; Pitt et al., 2007), which can be directly related to its resistance to H_2O_2. Takebe et al. (2007) observed that laboratory cultures of *Exiguobacterium oxidotolerans* (T-2-2T strain) in the mid-exponential growth phase were able to grow in continuously added H_2O_2 concentrations between 5-200 mM every 2 hours from cultivation. In this case, the strong tolerance to H_2O_2 in the mid-log phase shows the importance of growth stage for protective-stimulation defence. Although there was no significant changes on intracellular catalase activity, a substantial increase on extracellular catalase activity was observed without any association to cell disruption

since malate dehydrogenase marker enzyme was not detected in the supernatant. Additionally, catalase configures one of the most important defence since there was no any bacterial growth in 10 mg L^{-1} of H_2O_2 after the addition of a catalase inhibitor. Moreover, members of *Exiguobacterium* (and *Firmicutes* in general) synthesize carotenoid pigments. All isolated strains from this genus present the complete pathway for carotenoid C_{30} synthesis (White et al., 2019), which might contribute to ROS quenching as well as protect against to photo-damage.

The OTU assigned as *Exiguobacterium* (OTU000001) showed a positive correlation with transparency and a negative correlation with turbidity, factors also related to the collapse of cyanobacteria. While *Exiguobacterium sp.* (OTU000001) abundance increased substantially in 24 and 72 h after treatment, *Planktothrix*, *Cyanobium*, *Microcystis* and *Raphidiopsis* abundances decreased. Curiously, Tian et al. (2012) showed that *Exiguobacterium sp.* isolated from Lake Taihu had an intense algicidal activity against diverse cyanobacteria inhibiting the growth of *Planktothrix sp.* (82.9%), *Synechococcus sp*. (78.7%) and *Chroorococcus sp*. (75.6%) in 2 days, without any activity against green algae. The inhibitory effect was attributed to uncharacterized extracellular compounds. Thus, due to its high resistance against H_2O_2, the *Exiguobacterium* strains were able to grow more efficiently than *Cyanobacteria*. The possible inhibitory effects of *Exiguobacterium* over cyanobacterial growing also deserve to be investigated. Then, *Exiguobacterium* abundance decreased and *Cyanobium* dominated the cyanobacterial community.

According to the LeFSe analysis and relative abundance values, *Paracoccus sp.* (OTU000005) and *Deinococcus sp.* (OTU000008) contributed in similar proportions (4 – 10%) to the bacterial communities of treated samples (24 and 72 h). Members from both genera are known to produce enzymes involved in bacterial defence against the

deleterious effects of oxidative stress (Wang and Schellhorn, 1995; Baker et al., 1998). *Deinococcus* is known for its capacity to survive in diverse extreme environmental conditions such as ionization, UV radiation and desiccation (Daly, 2009; Fredrickson et al., 2008). Ionization and UV radiation can mediate and intensify the production of ROS. The defence mechanism involves a complex between Mn^{+2} and inorganic phosphate or amino acids/small peptides to remove and decompose reactive species as superoxide or hydrogen peroxide (Berlett et al., 1990; Daly et al., 2004). *Deinococcus radiodurans* cells have high catalase activity and increase it when exposed to H_2O_2. When pre-treated with sub-lethal doses of H_2O_2 (5 or 10 mM), cells became resistant to higher concentrations of H_2O_2 (80 mM). The pre-treated strain was also more resistant to UV light and γ rays, showing the potential to enhance survival to diverse stress factors (Wang and Schellhorn, 1995; Slade and Radman, 2011). This resistance is associated with the transcriptional regulator OxyR, which regulates catalase activity and ROS scavenging strategies when the cell is exposed to H_2O_2 (Chen et al., 2008; Yin et al., 2010).

Paracoccus is a genus from *Proteobacteria* that can be found in microbiomes of pristine and polluted aquatic environments (Lasek et al., 2018). Members of this genus possess many enzymes involved in H_2O_2 elimination as oxidases and peroxidases. Baker et al. (1998) identified a family of cytochrome c in *Paracoccus* genomes including a cytochrome c peroxidase as well as cytochrome c oxidase that probably decompose H_2O_2 resulting from the respiratory metabolism or other kinds of ROS. *Paracoccus denitrificans* is a model to study the eukaryotic cell respiratory activity since it is very similar to the mitochondrial electron transport chain (Stouthamer, 1992; Baker et al., 1998) and it has been described as a protomitochondrion (John and Whatley, 1975). Additionally, as *Paracoccus* is capable to produce continuously many ROS over the respiratory process it uses some well-studied enzymatic or non-enzymatic systems against

the oxidative stress to scavenge all of cell-damage ROS (Kirankumar et al., 2013; Sedláček and Kučera, 2019).

These resistant bacteria benefited from an oxidative environment created after H_2O_2 addition but did not maintain relative high abundances after H_2O_2 extinction. After 120 h they decreased in abundance substantially while other taxa increased, including *Cyanobium*. A major contributor at this later time was *Luteolibacter sp.* that increased in abundance after the treatment in comparison to the control condition. A close correlation between this genus and picocyanobacteria has been previously reported, more specifically during a *Synechococcus*-dominated cyanobacterial bloom in a Brazilian reservoir (Guedes et al., 2018), which indicates a potential relationship between this heterotrophic bacteria and picocyanobacteria growth in natural environments. Additionally, Cardman et al. (2014) suggested that members of *Verrucomicrobia*, including *Luteolibacter sp.* could be involved in algal polysaccharide degradation in marine environments.

These results indicate that further investigation using metagenomics approaches can confirm the prevalence of specific bacterial taxa after the oxidising process and subsequent community composition changes that precede cyanobacterial regrowth. In this scenario, it is important to know which resistant bacteria dominate the bacterioplankton after an oxidising treatment for water treatment purposes since they could imply to risks for water consumption. In addition, understanding the dynamics of microbial communities after H_2O_2 treatment could reveal bacterial taxa potentially useful in biomonitoring conditions before the return of cyanobacterial blooms.

Conclusion

Using a mescosm system installed in a eutrophic drinking water reservoir, we simulated the use of H_2O_2 to mitigate cyanobacterial blooms. Here we investigated the effects of

this treatment on the bacterioplankton community. The original *Planktothrix* dominated bloom was suppressed 72 h after H_2O_2 addition to the mesocosms, the time of H_2O_2 extinction. Other genera of Cyanobacteria were also drastically reduced. In a later time (120 h) *Cyanobium* and *Microcystis* started to increase in abundance, indicating a possible regrowth of cyanobacteria after H_2O_2 extinction. The main bacterial taxa with higher resistance against oxidative treatment were *Exiguobacterium*, *Deinococcus* and *Paracoccus*, genera well known by their increased resistance to oxidative stress. They predominated at 24-48 h after treatment but at 120 h, a novel community profile was apparent and these genera decreased in abundance. The composition of the novel bacterioplankton community at the end of the experiment was different from the original one. Thus, H_2O_2 imposes a stress condition upon the whole bacterioplankton with profound changes in the relative abundances of almost all phyla. After the extinction of the oxidising agent, both cyanobacteria and heterotrophic bacteria re-established with different contributions to the bacterioplankton community.

Acknowledgments

The authors would like to thank the Engineering and Physical Sciences Research Council (EPSRC) [EP/P029280/1], the Coordination for the Improvement of Higher Education Personnel - CAPES [PROEX 20/2016 and PrInt 88887.311806/2018-00], the Brazilian National Research Council – CNPq [403116/2016-3 and 304164/2017-8], the Ceará Research Support Foundation - FUNCAP [PNE-0112-00042.01.00 / 16] for funding this research. We would also like to thank Cogerh and Cagece for their support.

References

Allahverdiyeva, Y., Mustila, H., Ermakova, M., Bersanini, L., Richaud, P., Ajlani, G., et al. (2013). Flavodiiron proteins Flv1 and Flv3 enable cyanobacterial growth and

photosynthesis under fluctuating light. Proc. Natl. Acad. Sci. U.S.A. 110, 4111–4116. doi: 10.1073/pnas.1221194110

Baker, S.C., Ferguson, S.J., Ludwig, B., Page, M.D., Richter, O.M., van Spanning, R.J. (1998). Molecular genetics of the genus Paracoccus: metabolically versatile bacteria with bioenergetic flexibility. Microbiology and molecular biology reviews: MMBR, 62(4), 1046–1078.

Baltar, F., Reinthaler, T., Herndl, G. J., Pinhassi, J. (2013). Major effect of hydrogen peroxide on bacterioplankton metabolism in the Northeast Atlantic. PloS one, 8(4), e61051. https://doi.org/10.1371/journal.pone.0061051

Barrington, D.J. and Ghadouani, A. (2008). Application of hydrogen peroxide for the removal of toxic cyanobacteria and other phytoplankton from wastewater. Environ Sci Technol 42:8916–8921. https://doi.org/10.1021/es801717y

Barros, M.U.G., Lopes, I.K.C., Farias, W.R.L., Capelo, J.C., Carvalho, S.M.C., 2017. Impact of filamentous cyanobacteria on the water quality of two tropical reservoirs. Braz. J. Water Res. 22 E.6. http://dx.doi.org/10.1590/2318-0331.011716072

Barros, M.U.G., Wilson, A.E., Leitão, J.I.R., Pereira, S.P., Buley, R.P., Fernandez-Figueroa, E.G., Capelo-Neto, J. (2019). Environmental factors associated with toxic cyanobacterial blooms across 20 drinking water reservoirs in a semi-arid region of Brazil. Harmful Algae, 86, 128–137. https://doi.org/10.1016/j.hal.2019.05.006

Barnese, K., Gralla, E.B., Cabelli, D.E., Valentine, J.S. (2008). Manganous phosphate acts as a superoxide dismutase. J. Am. Chem. Soc. 130:4604–4606.

Berlett, B.S., Chock, P.B., Yim, M.B., Stadtman, E.R. (1990). Manganese (II) catalyzes the bicarbonate-dependent oxidation of amino acids by hydrogen peroxide and the amino acid-facilitated dismutation of hydrogen peroxide. Proc. Natl. Acad. Sci. USA 87:389–393

Cabello-Yeves, P. J., Haro-Moreno, J. M., Martin-Cuadrado, A. B., Ghai, R., Picazo, A., Camacho, A., Rodriguez-Valera, F. (2017). Novel Synechococcus Genomes Reconstructed from Freshwater Reservoirs. Frontiers in microbiology, 8, 1151. https://doi.org/10.3389/fmicb.2017.01151

Callieri, C. (2008). Picophytoplankton in freshwater ecosystems: the importance of small-sized phototrophs. Freshw. Rev. 1 1–28. doi: 10.1608/FRJ-1.1.1

Callieri, C. (2010). Single cells and microcolonies of freshwater picocyanobacteria: a common ecology. J. Limnol. 69:257–277. https://doi.org/10.4081/jlimnol.2010.257

Callieri, C., Cronberg, G., Stockner, J.G. (2012). ”Freshwater picocyanobacteria: single cells, microcolonies and colonial forms,” in Ecology of Cyanobacteria II: Their Diversity in Time and Space 2nd Edn ed. Whitton B. A. (Berlin: Springer;) 229–269.

Caporaso, J. G., Lauber, C. L., Walters, W. A., Berg-Lyons, D., Lozupone, C. A., Turnbaugh, P. J., Noah Fierer, N., & Knight, R. (2011). Global patterns of 16S rRNA diversity at a depth of millions of sequences per sample. Proc Natl Acad Sci USA 108, 4516–4522. http://doi.org/10.1073/pnas.1000080107

Cardman, Z., Arnosti, C., Durbin, A., Ziervogel, K., Cox, C., Steen, A.D., Teske, A. (2014). Verrucomicrobia are candidates for polysaccharide-degrading bacterioplankton in an arctic fjord of Svalbard, Appl. Environ. Microbiol.80:3749–3756. Doi: 10.1128/AEM.00899-14

Chelme-Ayala, P., El-Din, M.G., Smith, D.W., Adams, C.D. (2011). Oxidation kinetics of two pesticides in natural waters by ozonation and ozone combined with hydrogen peroxide. Water Res. 45(8):2517-2526. doi:10.1016/j.watres.2011.02.007

Chen, H., Xu, G., Zhao, Y., Tian, B., Lu, H., Yu, X., Xu, Z., Ying, N., Hu, S., Hua, Y. (2008). A novel OxyR sensor and regulator of hydrogen peroxide stress with one cysteine residue in Deinococcus radiodurans. PLoS One. 2008;3(2):e1602. doi:10.1371/journal.pone.0001602Clarke, K. R. (1993). Non-parametric multivariate

analyses of changes in community structure. Austral Ecology, 18(1), 117–143. doi:10.1111/j.1442-9993.1993.tb00438.x

Cogerh (Companhia de Gestao de Recursos Hidricos do Ceará), (2017). Rede de monitoramento da qualidade de água. Governo do Estado do Ceará, Fortaleza. Last accessed June 2020.

Cory, R.M., Davis, T.W., Dick, G.J., Johengen, T., Denef, V.J., Berry, M.A., Page, S.E., Watson, S.B., Yuhas, K., Kling, G.W. (2016). Seasonal Dynamics in Dissolved Organic Matter, Hydrogen Peroxide, and Cyanobacterial Blooms in Lake Erie. Front. Mar. Sci. 3:54. doi: 10.3389/fmars.2016.00054

Cruz, B.N. and Neuer, S. (2019). Heterotrophic Bacteria Enhance the Aggregation of the Marine Picocyanobacteria Prochlorococcus and Synechococcus. Frontiers in microbiology, 10, 1864. https://doi.org/10.3389/fmicb.2019.0186

Daly, M.J., Gaidamakova, E.K., Matrosova, V.Y., Vasilenko, A., Zhai, M., Venkateswaran, A., Hess, M., Omelchenko, M.V., Kostandarithes, H.M., Makarova, K.S., Wackett, L.P., Fredrickson, J.K., Ghosal, D. (2004). Accumulation of Mn(II) in Deinococcus radiodurans facilitates gamma-radiation resistance. Science. 306:1025–1028. doi: 10.1126/science.1103185

Daly, M.J. (2009). A new perspective on radiation resistance based on Deinococcus radiodurans. Nat Rev Microbiol 7: 237–245. doi: 10.1038/nrmicro2073

Fredrickson, J.K, Li, S.M., Gaidamakova, E.K., Matrosova, V.Y., Zhai, M., Sulloway, H.M., Scholten, J.C., Brown, M.G., Balkwill, D.L., Daly, M.J. (2008) Protein oxidation: key to bacterial desiccation resistance? ISME J 2: 393–403. doi: 10.1038/ismej.2007.116

Funceme (Fundação Cearense de Meteorologia e Recursos Hídricos), 2017. Last accessed June 2020. Website: http://www.funceme.br/

Gaysina, L.A., Saraf, A. Singh, P. (2019). Cyanobacteria in Diverse Habitats. Chapter 1 in Cyanobacteria: From Basic Science to Applications. Mishra, A.K., Tiwari, D.N., Rai,

A.N. [Edts], Academic Press 1st edition. 1–28. doi:10.1016/b978-0-12-814667-5.00001-5

Glaeser, S.P., Berghoff, B.A., Stratmann, V., Grossart, H.P., Glaeser, J. (2014). Contrasting Effects of singlet oxygen and hydrogen peroxide on bacterial community composition in a humic lake. PLoS One.9(3):e92518.doi:10.1371/journal.pone.0092518

Guedes, I.A., Rachid, C., Rangel, L.M., Silva, L., Bisch, P.M., Azevedo, S., Pacheco, A. (2018). Close Link Between Harmful Cyanobacterial Dominance and Associated Bacterioplankton in a Tropical Eutrophic Reservoir. Frontiers in microbiology, 9, 424. https://doi.org/10.3389/fmicb.2018.00424

Guedes, D., Santos, A., Barros, M., Oliveira, S., Pestana, C., Lawton, L., Azevedo, S., Magalhães, V., Pacheco, A., Capelo-Neto, J. (2020). Improving water quality and controlling cyanobacterial bloom using hydrogen peroxide in a semiarid region reservoir used for drinking water. Dissertion for conclusion of Master degree - Civil Engineering - Centro de Tecnologia, Programa de Pós-Graduação em Engenharia Civil: Saneamento Ambiental, Universidade Federal do Ceará, Fortaleza, 2020.

Gutiérrez-Preciado, A., Vargas-Chávez, C., Reyes-Prieto, M., Ordoñez, O.F., Santos-García, D., Rosas-Pérez, T., et al. (2017). The genomic sequence of Exiguobacterium chiriqhucha str. N139 reveals a species that thrives in cold waters and extreme environmental conditions. PeerJ. 5:e3162. doi: 10.7717/peerj.3162

Helbling, E.W., Villafañe, V., Buma, A., Andrade, M., Zaratti, F. (2001). DNA damage and photosynthetic inhibition induced by solar ultraviolet radiation in tropical phytoplankton (Lake Titicaca, Bolivia). European Journal of Phycology 36: 157–166. doi: https://doi.org/10.1017/S0967026201003122

Helman, Y., Tchernov, D., Reinhold, L., Shibata, M., Ogawa, T., Schwarz, R., et al. (2003). Genes encoding a-type flavoproteins are essential for photoreduction of O-2 in cyanobacteria. Curr. Biol. 13, 230–235. doi: 10.1016/S0960-9822(03)00046-0

Huisman, J., Codd, G.A., Paerl, H.W., Ibelings, B.W., Verspagen, J.M.H., Visser, P.M., (2018). Cyanobacterial blooms. Nat Rev Microbiol. 16(8):471-483. doi:10.1038/s41579-018-0040-1

Imlay, J.A. (2006). Iron-sulphur clusters and the problem with oxygen. Mol Microbiol. 59(4):1073-1082. doi:10.1111/j.1365-2958.2006.05028.x

Imlay, J.A. (2008). Cellular defenses against superoxide and hydrogen peroxide. Annu Rev Biochem. 77:755-776. doi:10.1146/annurev.biochem.77.061606.161055

John, P. and Whatley, F.R. (1975). Paracoccus denitrificans and the evolutionary origin of the mitochondrion. Nature. 254(5500):495-498. doi:10.1038/254495a0

Kirankumar, B., Guruprasad, B.K., Santoshkumar, M., Anand, S.N., Karegoudar, T.B. (2013). The response of Paracoccus sp. SKG to acetonitrile-induced oxidative stress. Extremophiles. 17(6):1037-1044. doi:10.1007/s00792-013-0585-x

Komárek, J. (2003). Coccoid and colonial cyanobacteria. In: Wehr, J.D., Sheath, R.G. (Eds.), Freshwater Algae of North America. Ecology and Classification. Academic Press, Amsterdam/Boston/London/New York/Oxford/Paris/San Diego/San Francisco/Singapore/Sydney/Tokyo, pp. 59–116.

Lasek, R., Szuplewska, M., Mitura, M., Decewicz, P., Chmielowska, C., Pawłot, A., Sentkowska, D., Czarnecki, J., Bartosik, D. (2018). Genome Structure of the Opportunistic Pathogen Paracoccus yeei (Alphaproteobacteria) and Identification of Putative Virulence Factors. Frontiers in microbiology, 9, 2553. https://doi.org/10.3389/fmicb.2018.02553

Latifi, A., Ruiz, M., Zhang, C.C. (2009). Oxidative stress in cyanobacteria. FEMS Microbiol Rev. 33(2):258-278. doi:10.1111/j.1574-6976.2008.00134.x

Leblanc, K., Quéguiner, B., Diaz, F., Cornet, V., Michel-Rodriguez, M., de Madron, X.D., Bowler, C., Malvyia, S., Thyssen, M., Grégori, G., Rembauville, M., Grosso, O., Poulain, J., de Vargas, C., Pujo-Pay, M., Conan, P. (2018). Nanoplanktonic diatoms are

globally overlooked but play a role in spring blooms and carbon export. Nat Commun 9, 953. https://doi.org/10.1038/s41467-018-03376-9

Li, H., Alsanea, A., Barber, M., Goel, R. (2019). High-throughput DNA sequencing reveals the dominance of pico- and other filamentous cyanobacteria in an urban freshwater Lake. Sci Total Environ.661:465-480. doi:10.1016/j.scitotenv.2019.01.141

Lürling, M., Meng, D., Faassen, E. J., 2014. Effects of hydrogen peroxide and ultrasound on biomass reduction and toxin release in the cyanobacterium, Microcystis aeruginosa. Toxins, 6(12), 3260–3280. https://doi.org/10.3390/toxins6123260

Matthijs, H.C.P., Visser, P.M., Reeze, B., Meeuse, J., Slot, P.C., Wijn, G., Talens, R., Huisman, J. (2012). Selective suppression of harmful cyanobacteria in an entire lake with hydrogen peroxide. Water Res 46:1460–1472. https://doi.org/10.1016/j.watres.2011.11.016

Meriluoto, J., Spoof, L., Codd, G.A. (Eds.) (2017). Handbook of Cyanobacterial Monitoring and Cyanotoxin Analysis, 1st edition. Wiley 576p. ISBN: 978-1-119-06868-6.

Metz, D.H., Meyer, M., Dotson, A., Beerendonk, E., Dionysiou, D.D. (2011). The effect of UV/H2O2 treatment on disinfection by-product formation potential under simulated distribution system conditions. Water Res. 45(13):3969-3980. doi:10.1016/j.watres.2011.05.001

Mlewski, E.C., Pisapia, C., Gomez, F., Lecourt, L., Soto Rueda, E., Benzerara, K., et al. (2018). Characterization of pustular mats and related rivularia-rich laminations in oncoids from the Laguna Negra lake (Argentina). Front. Microbiol. 9:996. doi: 10.3389/fmicb.2018.00996

Mostofa, K.M.G., Liu, C-Q., Sakugawa, H., Vione, D., Minakata, D., Wu, F. (2013). Photoinduced and microbial generation of hydrogen peroxide and organic peroxides in natural waters. In: Mostofa KMG, Yoshioka T, Mottaleb A, Vione D (eds)

Photobiochemistry of organic matter: principles and practices in water environments. Springer, Berlin, pp 139–207

Ordoñez, O., Lanzarotti, E., Kurth, D., Gorriti, M., Revale, S., Cortez, N. et al (2013). Draft genome sequence of the polyextremophilic Exiguobacterium sp. strain S17, isolated from hyperarsenic lakes in the Argentinian Puna. Genome Announc. 1:e00480-13. doi: 10.1128/genomeA.00480-13

Ordoñez, O., Lanzarotti, E., Kurth, D., Cortez, N., Farias, M.E., Turjanski, A.G. (2015). Genome comparison of two Exiguobacterium strains from high altitude andean lakes with different arsenic resistance: identification and 3D modeling of the Acr3 efflux pump. Front. Environ. Sci. 3:50. doi: 10.3389/fenvs.2015.00050

Park, J.A., Yang, B., Park, C., Choi, J.W., van Genuchten, C.M., Lee, S-H. (2017). Oxidation of microcystin-LR by the Fenton process: Kinetics, degradation intermediates, water quality and toxicity assessment. Chemical Engineering Journal, 309, 339-348. https://doi.org/10.1016/j.cej.2016.10.083

Pestana, C., Capelo Neto, J., Lawton, L., Oliveira, S., Carloto, I., Pessoa, H. (2018). The effect of water treatment unit processes on cyanobacterial trichome integrity. Science of The Total Environment. 659. 10.1016/j.scitotenv.2018.12.337.

Passardi, F., Zamocky, M., Favet, J., Jakopitsch, C., Penel, C., Obinger, C., et al. (2007). Phylogenetic distribution of catalase-peroxidases: are there patches of order in chaos? Gene 397, 101–113. doi: 10.1016/j.gene.2007.04.016

Pitt, T.L., Malnick, H., Shah, J., Chattaway, M.A., Keys, C.J., Cooke, F.J., Shah, H.N. (2007). Characterisation of Exiguobacterium aurantiacum isolates from blood cultures of six patients. Clin Microbiol Infect.13(9):946-948. doi:10.1111/j.1469-0691.2007.01779.x

Rognes, T., Flouri, T., Nichols, B., Quince, C., Mahé, F. (2016). VSEARCH: a versatile open source tool for metagenomics. PeerJ, 4, e2584. https://doi.org/10.7717/peerj.2584

Schneider, M. and Bláha, L. (2020). Advanced oxidation processes for the removal of cyanobacterial toxins from drinking water. Environ Sci Eur 32, 94. https://doi.org/10.1186/s12302-020-00371-0

Sedláček, V. and Kučera, I. (2019). Modifications of the Aerobic Respiratory Chain of Paracoccus Denitrificans in Response to Superoxide Oxidative Stress. Microorganisms, 7(12), 640. https://doi.org/10.3390/microorganisms7120640

Segata, N., Izard, J., Waldron, L., Gevers, D., Miropolsky, L., Garrett, W., Huttenhower, C. (2011). Metagenomic biomarker discovery and explanation. Genome Biol. 12(6):R60. Published 2011 Jun 24. doi:10.1186/gb-2011-12-6-r60

Sies, H. (2017). Hydrogen peroxide as a central redox signaling molecule in physiological oxidative stress: Oxidative eustress. Redox biology, 11, 613–619. https://doi.org/10.1016/j.redox.2016.12.035

Slade, D. and Radman, M. (2011). Oxidative stress resistance in *Deinococcus radiodurans*. Microbiology and molecular biology reviews: MMBR, 75(1), 133–191. https://doi.org/10.1128/MMBR.00015-10

Spoof, L., Jaakkola, S., Važić, T., Häggqvist, K., Kirkkala, T., Ventelä, A-M., Kirkkala, T., Svircev, Z., Meriluoto, J. (2020). Elimination of cyanobacteria and microcystins in irrigation water—effects of hydrogen peroxide treatment. Environ Sci Pollut Res 27, 8638–8652. https://doi.org/10.1007/s11356-019-07476-x

Stadtman, E. and Levine, R. (2006). Chemical Modification of Proteins by Reactive Oxygen Species. RedoxProteomics (eds). doi: 10.1002/0471973122.ch1.

Strahsburger, E., Zapata, F., Pedroso, I., Fuentes, D., Tapia, P., Ponce, R., Valdes, J. (2018). Draft genome sequence of Exiguobacterium aurantiacum strain PN47 isolate from saline ponds, known as “Salar del Huasco”, located in the Altiplano in the North of Chile. Brazilian Journal of Microbiology, 49(1), 7-9. https://doi.org/10.1016/j.bjm.2017.03.011

Stouthamer, A.H. (1992). Metabolic pathways in Paracoccus denitrificans and closely related bacteria in relation to the phylogeny of prokaryotes. Antonie Van Leeuwenhoek. 61(1):1-33. doi:10.1007/BF00572119

Takebe, F., Hara, I., Matsuyama, H., Yumoto, I. (2007). Effects of H2O2 under low- and high-aeration-level conditions on growth and catalase activity in Exiguobacterium oxidotolerans T-2-2T. J Biosci Bioeng. 104(6):464-469. doi:10.1263/jbb.104.464

Tian, C., Liu, X., Tan, J., Lin, S., Li, D., Yang, H. (2012). Isolation, identification and characterization of an algicidal bacterium from Lake Taihu and preliminary studies on its algicidal compounds. J Environ Sci (China).24(10):1823-1831. doi:10.1016/s1001-0742(11)60983-2

Vallejo, M., Fresnedo San Román, M., Ortiz, I., Irabien, A. (2015). Overview of the PCDD/Fs degradation potential and formation risk in the application of advanced oxidation processes (AOPs) to wastewater treatment. Chemosphere.118:44-56. doi:10.1016/j.chemosphere.2014.05.077

Veal, E.A., Day, A.M., Morgan, B.A. (2007). Hydrogen peroxide sensing and signaling. Mol Cell. 26(1):1-14. doi:10.1016/j.molcel.2007.03.016

Wang, P. and Schellhorn, H.E. (1995). Induction of resistance to hydrogen peroxide and radiation in Deinococcus radiodurans. Can J Microbiol.41:170–176

Wang, F., van Halem, D., Liu, G., Lekkerkerker-Teunissen, K., van der Hoek, J.P. (2017). Effect of residual H2O2 from advanced oxidation processes on subsequent biological water treatment: A laboratory batch study. Chemosphere. 185:637-646. doi: 10.1016/j.chemosphere.2017.07.073.

Weenink, E.F., Luimstra, V.M., Schuurmans, J.M., Van Herk, M.J., Visser, P.M., Matthijs, H.C. (2015). Combatting cyanobacteria with hydrogen peroxide: a laboratory study on the consequences for phytoplankton community and diversity. Front Microbiol.6:714. doi:10.3389/fmicb.2015.00714

White, R.A. III, Grassa, C.J., Suttle, C.A. (2013a). Draft genome sequence of Exiguobacterium pavilionensis strain RW-2, with wide thermal, salinity, and pH tolerance, isolated from modern freshwater microbialites. Genome Announc. 1:e00597-13. doi: 10.1128/genomeA.00597-13

White, R.A. III, Soles, S.A., Gavelis, G., Gosselin, E., Slater, G.F., Lim, D.S., Leander, B., Suttle, C.A. (2019). The Complete Genome and Physiological Analysis of the Eurythermal Firmicute Exiguobacterium chiriqhucha Strain RW2 Isolated From a Freshwater Microbialite, Widely Adaptable to Broad Thermal, pH, and Salinity Ranges. Front. Microbiol. 9:3189. doi: 10.3389/fmicb.2018.03189

Yan, L.J. (2009). Analysis of oxidative modification of proteins. Curr Protoc Protein Sci. Chapter 14:Unit14.4. doi:10.1002/0471140864.ps1404s56

Yang, Y., Cheng, D., Li, Y., Yu, L., Gin, K. Y.-H., Chen, J. P., Reinhard, M. (2017). Effects of monochloramine and hydrogen peroxide on the bacterial community shifts in biologically treated wastewater. Chemosphere, 189, 399–406. doi:10.1016/j.chemosphere.2017.09.087

Yang, Z., Buley, R.P., Fernandez-Figueroa, E.G., Barros, M.U.G., Rajendran, S., Wilson, A.E. (2018). Hydrogen peroxide treatment promotes chlorophytes over toxic cyanobacteria in a hyper-eutrophic aquaculture pond. Environ Pollut.240:590-598. doi:10.1016/j.envpol.2018.05.012

Yin, L., Wang, L., Lu, H., Xu, G., Chen, H., Zhan, H., Tian, B., Hua, Y. (2010). DRA0336, another OxyR homolog, involved in the antioxidation mechanisms in Deinococcus radiodurans. J Microbiol. 48(4):473-479. doi:10.1007/s12275-010-0043-8

Yumoto, I., Hishinuma-Narisawa, M., Hirota, K., Shingyo, T., Takebe, F., Nodasaka, Y., et al. (2004). Exiguobacterium oxidotolerans sp nov., a novel alkaliphile exhibiting high catalase activity. Int. J. Syst. Evol. Microbiol. 54, 2013–2017. doi: 10.1099/ijs.0.63129.0

4.3 Capítulo 3 (Filterable bacterioplankton able to degrade microcystin)

Filterable bacterioplankton able to degrade microcystin

SANTOS, A.A., [1] KEIM, C.N., [2] MAGALHÃES, V.F[1]*, PACHECO, A.B.F[3]*[a]

[1]*Laboratory of Ecophysiology and Toxicology of Cyanobacteria, Carlos Chagas Filho Biophysics Institute, Federal University of Rio de Janeiro, Rio de Janeiro, RJ, Brazil*

[2]*Laboratory of Geomicrobiology, Institute of Microbiology Paulo de Goés, Federal University of Rio de Janeiro, Rio de Janeiro, RJ, Brazil*

[3] *Laboratory of Biological Physics, Carlos Chagas Filho Biophysics Institute, Federal University of Rio de Janeiro, Rio de Janeiro, RJ, Brazil*

*both authors contributed equally

[a]corresponding author: biafp@biof.ufrj.br

Highlights

-Filterable plankton (< 0.45 or < 0.22 μm) hold metabolically active cells that degrade MC.

-These microbial communities include diverse morphologies and phylogenies.

-The microbial community structure differed based on the original size selection.

-MC shifted the structure of these communities compared with samples without MC.

-An underestimated fraction of water microbial community participates in MC degradation.

Abstract

Cyanobacterial blooms affect biotic interactions in aquatic ecosystems, including those involving heterotrophic bacteria. An example is the biodegradation of microcystin by microbial consortia, an interesting topic from ecological and biotechnological perspectives. Microcystin is a toxic, cyclic peptide with widespread occurrence in freshwater bodies impacted by cyanobacterial blooms, representing an ecological and water quality problem. The Jacarepaguá Lagoon, Rio de Janeiro city, Brazil, is an example of this situation. Here, we show microcystin degradation by microbes from the lagoon water that are able to pass through 0.45 or 0.22-μm membrane filters. Cells from both filtrates were incubated over 7 days at 25 ºC with or without microcystin-LR. At days 0 and 7, bacterial communities were recovered and characterized by transmission electron microscopy and 16S rDNA sequencing. Both size fractions grew during the incubation period and contained metabolically active cells capable of degrading microcystin. In addition, incubation led to changes in both cell size and morphology. Communities originating from different size fractions (<0.45 μm and <0.22 μm) shared some operational taxonomic units (OTUs) but diverged in taxonomic composition. The presence of microcystin shifted the structure of these communities in comparison to those maintained without toxin, with a clear enrichment of taxa known to degrade microcystin. Our results point to the existence of nano-sized microbial cells that are capable of passing through the filters, that grow in size and number, and that can degrade cyanotoxin. These findings suggest a widespread occurrence of microcystin-degrading microorganisms in cyanobacterial impacted environments.

Keywords: Cyanobacterial bloom; Cyanotoxin; Biodegradation; Metagenome; Ultramicrobacteria; Nanobacteria

Introduction

The occurrence of freshwater cyanobacterial blooms is increasing worldwide, raising concerns about water quality mainly due to the presence of secondary metabolites that act as potent toxins to animals, known as cyanotoxins (Ferrão-Filho and Kozlowsky-Suzuki, 2011; Huisman et al., 2018). The exacerbated increase in cyanobacteria biomass in water bodies also affects the ecosystem, unbalancing different trophic levels (Paerl and Otten, 2013). *Cyanobacteria* establish diverse biotic interactions with heterotrophic bacteria, protists, zooplankton, and viruses, which involve mutualism, parasitism, grazing and predation (Pal et al., 2020). Bacterial interactions can occur in the cyanobacterial phycosphere with colonizing heterotrophic bacteria, where the remineralisation of organic matter and nutrient exchange occur, favouring all parties involved (Li et al., 2018; Woodhouse et al., 2018). Interactions can also be antagonistic, as exemplified by cyanolytic bacteria (Osman et al., 2017).

A particular aspect of the close interaction between these groups is the biodegradation of cyanotoxins by heterotrophic bacteria (Dziga et al., 2013). This issue has been mostly explored for microcystin (MC) degradation. MCs are the most common cyanotoxins in freshwater, and MC-LR is one of the more toxic and frequent variants amongst the other 250 already described variants (Szlag et al. 2015; Bouaïcha et al 2019).

The biodegradation of MC by bacteria was first described in *Sphingomonas* (Jones et al., 1994, Bourne et al., 1996). Then, diverse microorganisms capable of degrading MC were identified, belonging to different genera (Dziga et al., 2013; Li et al. 2017; Kumar et al., 2019). The best-characterized MC degradation pathway involves three Mlr enzymes that cooperate to linearize the cyclic peptide and decompose it, releasing non-toxic products (Bourne et al., 1996, Dziga et al., 2012; Shimizu et al., 2012). It is now recognized that phylogenetically diverse bacteria are able to degrade MC, including some strains lacking

mlr genes (Dziga et al., 2013; 2017). Indeed, the identification of other intermediaries and products of MC biodegradation indicate the existence of additional biochemical pathways (Dziga et al., 2013; 2017).

The study of isolated strains allowed the identification of MC-degrading bacteria and revealed the biochemical bases of this process, whereas other investigations have explored MC degradation by microbial consortia, a situation closer to that of natural aquatic environments (Christoffersen et al., 2002; Mou et al., 2013, Briand et al., 2016; Dziga et al., 2017). Some authors have concluded that these complex microbial communities are more efficient in toxin degradation than individual strains isolated from these communities (Yang et al., 2018; Ramani et al., 2012). The origin of the bacterial community also affects the degradation efficiency. In combination with physical-chemical characteristics of the natural environment, prior exposure to MC in water bodies with a history of cyanobacterial blooms favours the persistence of MC degraders and affects their abundance, metabolic activity and diversity (Christoffersen et al., 2002; Hyenstrand et al., 2003; Dziga et al., 2013; 2017).

In line with these observations, we chose to investigate the potential for MC biodegradation in Jacarepaguá Lagoon, a highly eutrophic coastal lagoon impacted by untreated sewage discharge, industrial effluents, and a disordered urban occupation on the margins, which has been historically subjected to toxic cyanobacterial blooms dominated by the MC-producing genus *Microcystis*. MC concentrations as high as 980 $\mu g\ L^{-1}$ have been reported in seston samples from this lagoon (Magalhães et al. 2001; Ferrão-Filho et al. 2002a; de Magalhães et al., 2017). In a recent study, we demonstrated that microorganisms recovered from sediments and interstitial water were able to degrade MC and contributed to the dynamics of the toxin in Jacarepaguá Lagoon (Santos et al., 2020). In that study, biodegradation assays were carried out with microbial fractions

selected by filtration through 0.45-µm pore membranes to avoid the interference of suspended particles that could adsorb MC. The observation of MC degradation mediated by small-sized microorganisms in samples collected at different times prompted us to further explore the diversity of filterable microorganisms from the lagoon surface water and to test their ability to degrade MC. Some studies have reported the cultivation of filterable microorganisms in either natural water or culture media using simple or complex organic matter as carbon and energy sources (Hahn et al., 2003; Wang et al., 2007; Liu et al., 2019). However, the potential of these small cells for the biodegradation of structurally complex and unusual molecules has not yet been investigated.

This effort was also motivated by recent reports on the characterization of ultra-small microbial communities found in both surface and groundwater (Wang et al., 2007; Luef et al., 2015, Bruno et al., 2017). Advances in high-throughput sequencing technologies and the development of metagenomics approaches allowed the exploration of microbial communities directly from their environment, immensely expanding our dimension of microbial diversity and providing access to previously unknown, uncultivable taxa. This led to the recognition that a minority of microbial phyla has a cultivated representative. For those phyla composed exclusively of uncultured representatives, the term Candidate Phyla was adopted. These groups are also referred to as "microbial dark matter", indicating that they include a great microbial (both Archaea and Bacteria) biomass and biodiversity with almost unknown physiology, metabolic profiles, and ecological roles (Solden et al., 2016). Environmental genome sequencing revealed that most of these Candidate Phyla presented small genomes (<1 Mb) lacking primary biosynthetic pathways, thus indicating that these organisms cooperate and depend on other members of the community to sustain their metabolism (Luef et al., 2015; Solden et al., 2016). The selection of groundwater samples after passage through a 0.2-µm filter revealed that the

small sized genomes of Candidate Phyla corresponded to ultra-small cells (median cell volume: $0.009 \pm 0.002\ \mu m^3$) with varied morphologies (Luef et al., 2015). Additionally, filtration of water samples from a treatment plant (10000 MWCO, more stringent than a 0.2 μm pore filter) resulted in the recovery of ultra-small microorganisms that were characterized by high-throughput DNA sequencing, revealing the diverse composition of bacterial communities in this system (Bruno et al., 2017). However, the metabolic activities of these small cells has not been investigated

Here we tested MC biodegradation by nano-sized plankton fractions from Jacarepaguá Lagoon surface water, and characterized their morphology and taxonomic composition before and seven days after incubation with or without MC.

Methodology

Field Work

Water samples were collected from the Jacarepaguá Lagoon (22°59'00.4" S, 43°24'36.2" W), Rio de Janeiro city, Brazil. The lagoon has a surface area of 3.7 km² and an average depth of 3 m and is part of a lagoonal complex that includes three other coastal lagoons in the urban area of the city. Jacarepaguá Lagoon is oligohaline and highly eutrophic due to the discharge of untreated urban effluents, as well as those from industries and hospitals. This environment is also highly impacted by cyanobacterial blooms, which have been recorded in the last 20 years (Magalhães et al., 2001; de Magalhães et al., 2017). Water was collected at a depth of 0.5 m near the shore on different dates: September and November 2016, September and November 2017. Water samples were conditioned in polypropylene bottles and transported to the laboratory within an hour.

Processing of water samples to obtain filterable plankton fractions

To obtain the filterable plankton fractions used in the experiments, water samples were filtered through glass fibre prefilter membranes (Sartorius®) to remove large suspended material. The volume of water varied according to the collection dates: 2 L in September 2016 and 5 L in November 2016, September and November 2017. The first filtrate was centrifuged (12600 g for 30 minutes at 10 ºC), and the pellet was suspended in a residual volume to obtain a concentrated suspension (concentrated 10 times in relation to the original volume, resulting in 200 mL from 2 L samples and 500 mL from 5 L samples). Samples from September 2016 were filtered only using 0.45 μm membranes to generate <0.45-μm fractions. In November 2016, September 2017 and November 2017, the volume of the concentrated suspensions was divided in two equal aliquots, which were filtered through membranes of different pore sizes (cellulose acetate, Sartorius®). An aliquot was filtered through 0.45-μm-pore membrane to provide a filtrate containing a plankton fraction smaller than 0.45 μm (<0.45 μm); the other one was filtered through a 0.22-μm-pore membrane, resulting in a filtrate containing a plankton fraction smaller than 0.22 μm (<0.22 μm).

An aliquot of water filtered through a 0.45-μm-pore membrane was autoclaved and used as a negative control in the MC-LR biodegradation assays. In November 2016 and November 2017, samples for TEM and DNA extraction were obtained from freshly filtered plankton concentrates to characterize the original microbial community and compare it with the communities recovered after 7 days with or without MC, as described below and illustrated in Supplementary Figure 1.

MC-LR biodegradation assays

The assays were performed with plankton fractions of different sizes (< 0.45 μm or < 0.22 μm) obtained from a lagoon water (item 2.2). In each case, filtrates were incubated under

two conditions: (i) with the addition of MC-LR (20 ng.mL^{-1}) to test for biodegradation; (ii) without MC-LR to evaluate the community survival under laboratory conditions. As a negative control, MC-LR was added to an aliquot of autoclaved filtrate (0.45-µm-pore membrane).

For incubation with or without MC-LR, 90 mL of each filtrate (previously concentrated 10 times in relation to the lagoon water) was divided in triplicate and maintained in each condition over 7 days at 25 ºC in sterile flasks. To evaluate biodegradation, 1-mL aliquots were obtained immediately after the experimental set-up (T0) and on day 7, filtered through 0.22-µm-pore membranes and stored at -20 ºC until MC-LR analysis. The MC-LR added to the filtrates was obtained as described below (2.4).

For samples collected in November 2016 and November 2017 at T0, 40 mL of each filtrate was collected for DNA extraction (these volumes corresponded to suspensions concentrated 10 times in relation to the lagoon water), and at day 7, 15 mL of each sample was obtained for DNA extraction. For samples collected in November 2017, at the initial time (T0), 30 mL of each filtrate was collected for transmission electron microscopy, and at day 7, 15 mL of each replicate were collected and pooled. A general description of the experimental set-up is presented in Supplementary Figure 1.

MC-LR extraction and purification

Cyanobacterial cultivation, MC-LR extraction and purification were performed according to Santos et al., 2020. The purified MC-LR was quantified by LC-MS/MS according to Spoof et al. (2003). The detection limit was 0.1 ng.mL^{-1}, and the quantification limit was 0.5 ng.mL^{-1}.

Transmission electron microscopy (TEM)

Samples from MC-LR biodegradation assays performed in November 2017 (< 0.22-μm or < 0.45-μm communities, with or without MC-LR) were collected at the initial (T0) and final (T7) incubation times. For the initial time (T0), a volume of 30 mL was collected; at the final time (T7), 15 mL of each replicate was collected and pooled. These samples were further concentrated by ultracentrifugation (68000 x g, 40 minutes, 4 ºC), resulting in cell suspension volumes ranging from 300-450 μL.

The cell suspensions were fixed in a glutaraldehyde solution (2.5%) and kept at 4 ºC. Later, the cells were rinsed three times in cacodylate buffer and three times in distilled water, deposited on 300 mesh copper grids coated with Formvar films (0.5% chloroform), and negatively stained with 2% uranyl acetate. The samples were observed using a Jeol JEM 1200 EX at 80 kV.

DNA extraction and 16S rDNA high-throughput sequencing.

Samples from the MC-LR biodegradation assays conducted in November 2016 and November 2017 (<0.22-μm or <0.45-μm fractions) were collected at the initial (T0) and final (T7, with and without MC-LR) times for DNA extraction. Aliquots (40 mL at T0 and 15 mL at T7) from the biodegradation assays containing the <0.45-μm fraction were filtered onto 0.22-μm-pore membranes, and the cells recovered in the filters were used for DNA extraction (community between <0.45 and >0.22-μm). Thus, this community was expected to contain a cellular fraction > 0.22 μm. For DNA extraction from the biodegradation assays using the <0.22-μm fraction, aliquots (40 mL at T0 and 15 mL at T7) were filtered onto 0.025-μm-pore membranes to recover the cells on the filters. The filters were stored at -80 ºC until DNA extraction. In cases in which the microorganisms were maintained without MC-LR (both <0.22-μm and <0.45-μm communities), the

replicate samples were pooled on day 7 and filtered as described above for DNA extraction.

DNA extraction was performed using a DNA Fecal/Soil Microbe Miniprep kit (Zymo® Research) following standard instructions. The resulting DNA samples were quantified using the Qubit dsDNA BR assay (Thermo Fisher Scientific®) and a Qubit fluorometer (Thermo Fisher Scientific®). The variable region (v4) of the bacterial 16S rRNA gene was amplified by the polymerase chain reaction (PCR) using primers F515 (5' GTGCCAGCMGCCGCGGTAA 3') and R806 (5'GGACTACHVGGGTWTCTAAT 3') (Caporaso et al., 2011). For each sample, three PCRs were performed and then pooled. The amplifications were performed in 25-μL reactions containing 12.5 μL of HiFi HotStart ReadyMix (KAPA Biosystems®), 0.2 μM of each primer and 10 ng of DNA. The PCR programme consisted of an initial denaturation step at 95 °C for 3 min followed by 25 cycles of amplification (95 °C for 30 s, 55 °C for 30 s and 72 °C for 30 s) and a final step of 72 °C for 5 min. The products were purified using magnetic beads (Agencourt AMPure XP, Beckman Coulter®) and subjected to a second PCR to incorporate dual indices as described in the 16S Metagenomic Sequencing Library Preparation Protocol for the Illumina® MiSeq system. After a second purification step with magnetic beads, the libraries were quantified using a Qubit fluorometer (Thermo Scientific®), and their concentrations were normalized. Pooling of the libraries, denaturation and sequencing were performed as recommended in the 16S Metagenomic Sequencing Library Preparation Protocol for the Illumina® MiSeq system. For samples collected in November 2016, sequencing was performed on a HiSeq platform (Illumina®) using the HiSeq Reagent Kit v3. For samples collected in November 2017, sequencing was performed on a MiSeq platform (Illumina®) using the MiSeq Reagent Kit v2 (2 × 150 base pairs).

Bioinformatics analysis

The resultant output files (.fastq file) were processed using Mothur software v.1.43 (Schloss et al., 2009). Sequences were assembled as paired-end reads forming unique contigs. The following criteria were used to eliminate low-quality reads: average quality (window size = 50) < 30, length in base pairs (< 254 bp), presence of ambiguous characters ('N'), maximum of 8 homopolymers, and nucleotide mismatches to the primer and/or barcode. The remaining reads were aligned using the SILVA reference database (Quast et al., 2013), trimmed and filtered. The sequences were then pre-clustered with diff = 2. Chimeras were detected using the VSEARCH software and excluded (Rognes et al., 2016). Taxonomic classification was carried out using the RDP database with a confidence threshold of 80%. Sequences not assigned as bacteria or classified as chloroplast, mitochondria, archaea or unknown were discarded. Singletons and doubletons were removed, and for each experiment, the number of sequences in the samples was normalized to equal the sample with the smaller number of sequences. For each date, the resulting sequences were used as input to generate a distance matrix and were clustered into operational taxonomic units (OTUs) (sequence similarity cutoff of 97%). The taxonomic assignment of OTUs was performed using the RDP database (release date February, 2016).

The composition of microbial communities was evaluated for each date according to the relative abundance of taxa (Phylum and Order level), considering only those OTUs that contributed more than 1% to the total sequences. To estimate the alpha diversity, species richness and diversity indexes were calculated using Mothur (software v.1.43). Venn diagrams were also constructed in Mothur considering the sobs richness.

The PICRUSt approach (gene prediction with phylogenetic investigation of the community reconstruction of unobserved states) was used to predict the functional

attributes of the bacterial communities used in the MC biodegradation assays (November 2016 and November 2017). For this analysis, only the main OTUs contributing to the differentiation of the communities (based on size and presence of MC) were considered.

PICRUSt (Galaxy, online version) (Langille et al., 2013) used a .biom file as input was obtained from the taxonomy assignment performed in the Green Genes database (version 13.8_99), following the software pipeline. Functions were assigned according to the Kyoto Encyclopaedia of Genes and Genomes (http://www.kegg.jp).

This project is available in the NCBI (National Center for Biotechnology Information) database under the bioproject study accession number PRJNA629884, as well as the biosample and sequence read archive (SRA).

Statistical analysis

For each date, the OTU composition of the samples was used to generate an ordination plot by nMDS (non-metric multidimensional scaling) as well as hierarchical clustering dendrograms constructed based on Bray-Curtis similarity. These analyses were performed using the Past3 software (Hammer et al., 2001). Two-way PERMANOVA was carried out to evaluate differences in community composition for samples from November 2016 and November 2017 considering groups by cellular size (< 0.22 μm and < 0.45 μm) and by the presence/absence of MC-LR. Two-way ANOVA was also carried out to evaluate differences in diversity and richness between communities able to degrade MC-LR over 7 days, considering size and date as groups.

A Wilcoxon-Mann-Whitney unpaired test ($p<0.05$) was used for pairwise comparisons between samples (T0 x T7), (T7 +MC x T7 -MC) and (T7 +MC <0.22 μm and T7 +MC < 0.45 μm). These analyses were performed using Past3 software (Hammer et al., 2001) and GraphPad Prism 8.4.

A similarity percentages procedure (SIMPER) analysis (Clarke, 1993) was performed to estimate the contribution of each OTU to the differentiation between communities of different sizes and between communities that received or did not receive MC. To visualize the top OTUs indicated by the SIMPER analysis, heatmaps were constructed using GraphPad Prism 8.4 for Windows (GraphPad Software, La Jolla California USA).

Results

MC-LR degradation by nanoscale microbial communities

We collected water from a coastal lagoon that has historically been impacted by cyanobacterial blooms (with a dominance of *Microcystis sp.*) and tested the ability of the plankton fractions that were able to pass through either 0.45-µm or 0.22-µm-pore filters to degrade MC-LR. Concentrated cell suspensions were incubated with purified MC-LR over 7 days, and the toxin concentrations were measured at initial and final times (Table 1).

Microorganisms present in the <0.45-µm filtrates obtained in September and November 2016 and in September and November 2017 effectively reduced the MC-LR concentrations by 80% - 99% in 7 days. Incubation of MC-LR with microorganisms selected in <0.22-µm filtrates in November 2016, September and November 2017 also resulted in decreased toxin concentrations (reduction of 70 - 99%) after 7 days, with different efficiencies according to the sampling date. In contrast, MC-LR concentrations remained unaltered after 7 days of incubation in the control condition, corresponding to water samples filtered using 0.45-µm membranes and autoclaved, thus eliminating living microorganisms.

Table 1: Ratio of final/initial MC-LR concentrations (Cf/C0) after incubation with Jacarepaguá Lagoon water filtered through membranes (<0.45-µm and <0.22-µm pore size). Water samples were obtained in September and November 2016 and 2017. The negative control corresponds to lagoon water filtered through 0.45-µm-pore membranes and autoclaved.

	Ratio of residual MC-LR after 7 days of incubation (C_f/C_0)								
	<0.45 µm			<0.22 µm			Negative control		
Sept/16	0.010	0.588	0.013	x	x	x	x	x	x
Nov/16	0.021	0.015	0.011	0.014	0.011	0.011	x	x	x
Sept/17	0.011	0.010	0.010	0.023	0.728	0.006	0.962	0.546	1.081
Nov/17	0.005	0.007	0.007	0.290	0.005	0.643	0.959	0.842	1.115

TEM observations

Samples obtained from the <0.45-µm lagoon water fractions presented few microbial cells at day 0, with some showing typical morphologies of prokaryotes, as exemplified in Figure 1a. Most cells were elongated, rod-shaped or ovoid and > 0.45 µm long and < 0.45 µm wide.

Conversely, no typical prokaryotic cell morphologies were observed in the < 0.22-µm fractions. Instead, we observed mainly thin filamentous structures with very small diameters (Figure 2A-E). Common structures included filaments with and without polymeric extracellular structures resembling capsules (Figure 2A-B), thin segmented structures that could consist of multicellular filaments or multiple cell divisions without complete separation (Figure 2C), and other structures that might have represented secreted vesicles or cell debris (Figure 2 D-E), as well as structures typical of viruses (not shown).

Cells were clearly more abundant after 7 days of incubation in both the < 0.45-µm and the < 0.22-µm fractions, with and without MC. The originally < 0.45-µm cell fraction

incubated with MC-LR over 7 days showed larger cells (> 0.45 μm) that were mostly rod-shaped, with some showing flagella and/or polymeric substances reminiscent of capsules (Figure 1B and C), which is compatible with the macroscopic mucoid aspect apparent in these samples (not shown). Similarly, the originally <0.45-μm filtrate incubated over 7 days without MC-LR contained larger cells in comparison to the initial sample, with some showing flagella and/or extracellular polymers resembling bacterial capsules (Figure 1C). Samples originally selected as <0.22 μm changed after 7 days of incubation with MC-LR originating larger cells with abundant extracellular polymers resembling capsules (Figure 2F) as well as flagella (not shown). Different cell types were observed, such as spirilla (Figure 2F), vibria, rods, and bacilli (not shown). Similarly, after 7 days of incubation without MC-LR, the originally < 0.22-μm fraction presented larger cells (Figure 2G), showing a lower morphological diversity compared to the < 0.22-μm samples incubated with MC-LR (Figure 2F-G). Interestingly, extracellular polymers were less frequent in the <0.22-μm samples incubated without MC-LR. As observed for the <0.45-μm cellular fraction, a macroscopically dense mucous material was observed in the < 0.22-μm samples with MC-LR (data not shown).

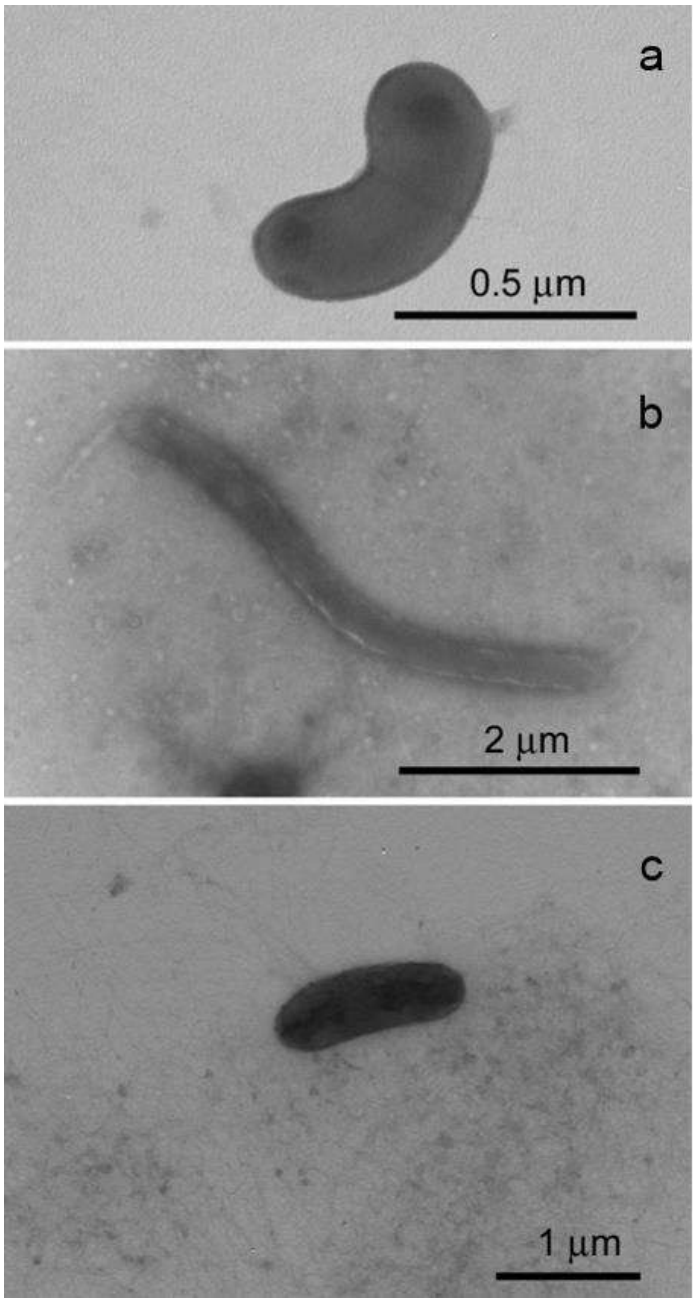

Figure 1: Representative transmission electron micrographs of microorganisms recovered from lagoon water filtered through 0.45-µm-pore membranes. (A) at time 0, (B) after 7 days of incubation with MC-LR and (C) after 7 days of incubation without MC-LR. Note the septum for cell division in the cell in “A”, amphitrichous flagella in “B”, and abundant polymers resembling a bacterial capsule in “C”.

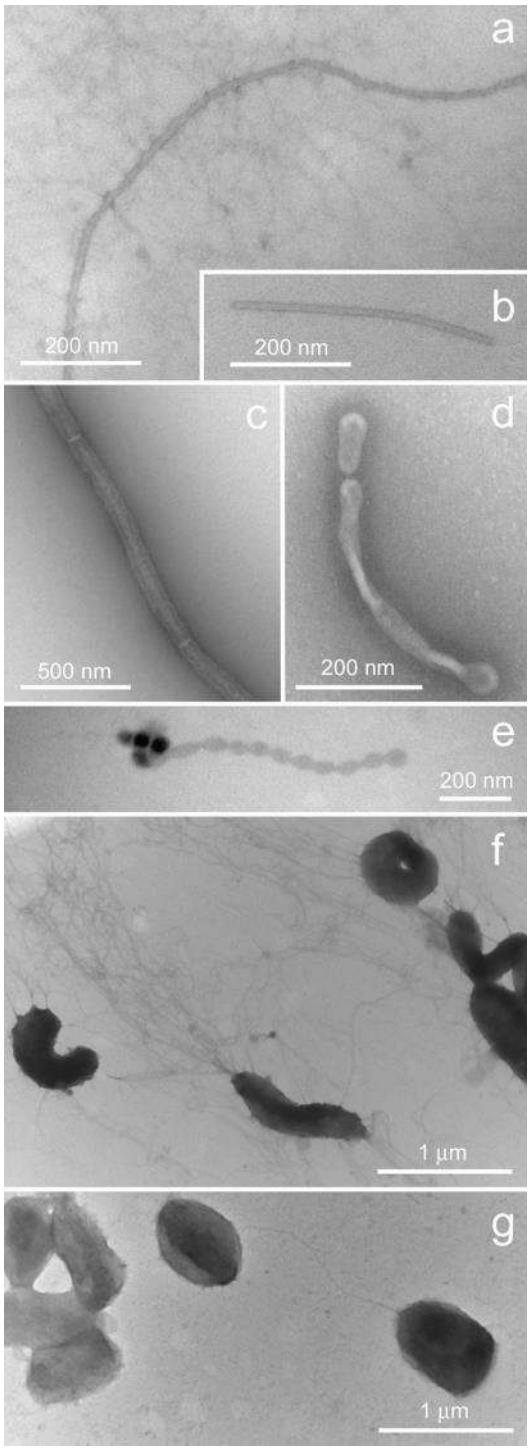

Figure 2: Representative transmission electron micrographs of microbial fractions recovered from the lagoon water filtered through 0.22-µm-pore membranes. Samples retrieved (A-E) at time 0, (F) after 7 days of incubation with MC-LR, and (G) after 7 days of incubation without MC-LR. Note the predominance of spirilla and abundant extracellular polymers in “F”, and the presence of short rods and ovoid cells in “G”.

Characterization of microbial communities in filtered fractions by metagenomics analysis

- **General profile of bacterial communities**

Cells were recovered from biodegradation assays to characterize the composition of the bacterial communities originally selected by different pore size filters (< 0.45 or < 0.22 μm) at time 0 and after 7 days with or without MC-LR. The sequencing analysis was performed with samples collected in November 2016 and November 2017.

Samples with the same date were normalized to an equal number of sequences for comparison (Table 2). Rarefaction curves approached saturation with sufficient coverage of bacterial diversity, reaching approximately 99% (November 2016) and 94% (November 2017) (Table 2 and Supplementary Figure 2). Diversity (Shannon) and richness (sobs) indexes were estimated for these bacterial communities (Table 2). In November 2016, the diversity and richness of the original <0.22-μm community were higher at day 0 and decreased after incubation with MC-LR. Considering the <0.45-μm community, we did not recover the original community, but after 7 days of incubation, a higher richness was estimated in samples without versus with MC-LR.

Table 2: Sequencing information and diversity indexes for microbial communities collected in November 2016 and November 2017.

Date	Days of incubation	Cell fraction/ condition	Number of sequences		Sobs	Coverage	Shannon	Simpson	Evenness
			Before normalization	After normalization					
Nov 2016	T0	<0.22	56181	54046	773	0.994	3.00	0.103	0.45
	T7	<0.22 +MCb	82658	54046	305	0.997	2.86	0.115	0.50
		<0.22 +MCc	72760	54046	511	0.995	2.89	0.127	0.46
		<0.45 +MCa	63804	54046	263	0.998	1.55	0.513	0.27
		<0.45 +MCc	72760	54046	671	0.994	2.30	0.302	0.35
		<0.45 no MC	54046	54046	899	0.995	2.72	0.259	0.40
Nov 2017	T0	<0.45	5486	2086	288	0.924	3.86	0.077	0.68
	T7	<0.22 +MCa	10580	2086	199	0.931	2.73	0.158	0.51
		<0.22 +MCb	3302	2086	217	0.933	2.75	0.155	0.51
		<0.22 +MCc	12384	2086	187	0.941	2.21	0.277	0.42
		<0.22 no MC	6438	2086	165	0.947	2.81	0.127	0.55
		<0.45 +MCa	5977	2086	219	0.951	4.00	0.03	0.74
		<0.45 +MCb	3363	2086	214	0.948	3.68	0.05	0.68
		<0.45 +MCc	2086	2086	218	0.948	3.70	0.05	0.68
		<0.45 no MC	15138	2086	259	0.932	4.01	0.043	0.72

In November 2017 after 7 days of incubation, the <0.22-µm fractions showed a higher estimated richness for samples with MC-LR, on average, than those without MC-LR. The original <0.45-µm community presented similar values of richness and diversity to the communities recovered after 7 days with MC-LR and lower than those incubated without MC-LR. We tested whether the estimated richness (number of observed species) or diversity (Shannon index) of communities able to degrade MC-LR after 7 days would be

different according to size (<0.45 and <0.22 µm) or collection dates (November 2016 and November 2017). The richness and diversity were higher for communities collected in November 2016 than for those obtained in November 2017, but they were similar for communities originally selected by different sizes (Supplementary Figures 3 and 4).

- **Differential composition of bacterial communities**

Figure 3 shows the ordination of samples collected on different dates and grouped according to the original size of the microbial communities and according to the presence of MC-LR. In November 2016, a very low amount of DNA was obtained from the < 0.45-µm fraction at T0, and thus it could not be analysed. The same problem occurred for the <0.22-µm fraction after 7 days without MC-LR. For the <0.45-µm fraction after 7 days without MC-LR, the cell densities were also low, leading to a low recovery of DNA, and replicates were pooled (Supplementary Table 1). According to the ordination analysis and two-way PERMANOVA (Supplementary Table 2), the composition of the bacterial communities was significantly different according to the size and to presence/absence of MC-LR ($p<0.05$), with an interaction between these factors (Figure 3A). More specifically, pairwise comparisons were performed (Wilcoxon-Mann-Whitney test, $p<0.05$) and indicated different bacterial community profiles for <0.45-µm samples incubated with and without MC for 7 days ($p<0.001$). For the originally < 0.22-µm community, the initial composition (T0) changed after 7 days of incubation with MC-LR ($p<0.001$). Additionally, the composition of the < 0.22-µm and < 0.45-µm samples incubated with MC for 7 days was different ($p<0.001$) (Supplementary Table 3). On average, 828 species were observed in < 0.45-µm bacterial communities incubated over 7 days, but only 18% of them were shared between communities with or without MC. The original < 0.22-µm community (T0) shared only 18% (215/1163) of species with the corresponding fraction incubated for 7 days with MC-LR. The composition of the < 0.22-

μm and < 0.45 μm samples incubated with MC over 7 days shared 30% (312/1051) of species (Supplementary Figure 5).

In November 2017, for < 0.45-μm fractions, samples from T0 and from T7 without MC-LR resulted in low recovery of DNA and were pooled. The < 0.22-μm fraction at T0 resulted in low recovery of DNA and could not be analysed. Samples < 0.22-μm at T7 without MC-LR were also pooled (Supplementary Table 1). The original < 0.45-μm sample at T0 was located distantly from the other samples (Figure 3B), but the separation of T7 groups according to the presence/absence of MC-LR or size was not so evident.

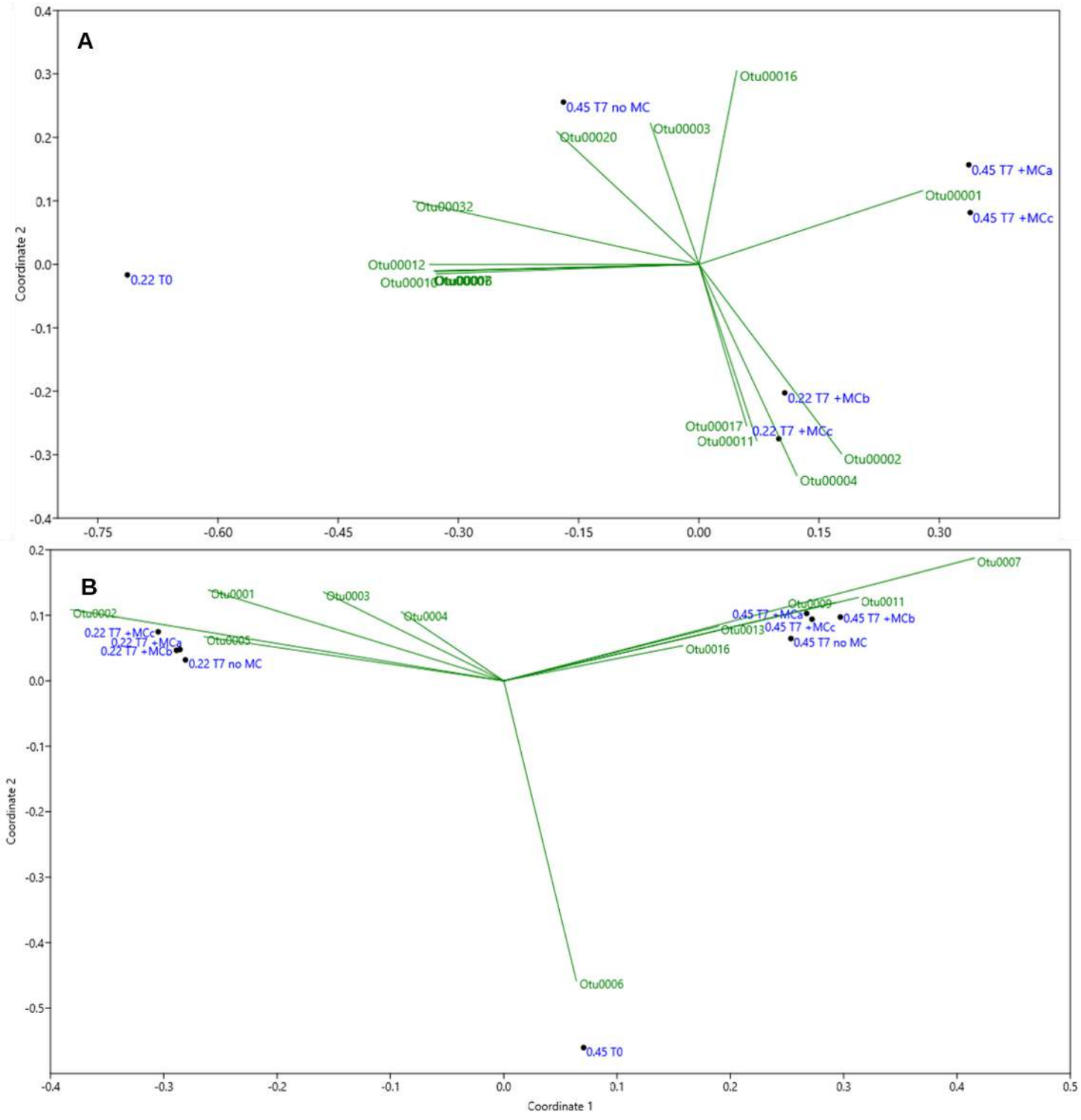

Figure 3: Non-metric Multidimensional Scaling (nMDS) plots in two-dimensions (2D) showing the ordination of samples collected on different dates and recovered from biodegradation assays. Samples are grouped according to the original size of the microbial communities (<0.45 μm or <0.22 μm) and according to the presence/absence of MC-LR during 7 days of incubation. (A) Samples from November 2016, bacterial communities

of different sizes (<0.45 μm and <0.22 μm). The <0.45-μm cellular fraction after 7 days without MC-LR represents a pool of three replicates (T7 no MC). (B) Samples from November 2017, bacterial communities of different sizes (<0.45 μm and <0.22 μm). Samples incubated for 7 days without MC-LR represent a pool of 3 (T7 no MC). Plots were based on the Bray-Curtis matrix distance with a similarity metric of 97%, and in B and C, vectorization was attributed to the main OTUs that contributed to the difference between groups according to SIMPER analysis.

Yet, two-way PERMANOVA (Supplementary Table 2) indicated significant differences in bacterial composition according to the filter pore size used, as well as the presence/absence of MC-LR ($p<0.05$), with interaction between these variables. Pairwise comparisons (Wilcoxon-Mann-Whitney test, $p<0.05$) indicated that different communities were present in < 0.45-μm samples incubated with and without MC-LR for 7 days, as well as in < 0.45-μm samples obtained at T0 and at T7 with MC-LR. Conversely, for the < 0.22-μm fractions after 7 days, samples maintained with or without MC-LR were not significantly different. Considering samples by filter pore size, the < 0.22-μm and < 0.45-μm fractions incubated with MC over 7 days were significantly different ($p<0.001$) (Supplementary Table 3). From a total of 603 species identified in < 0.45-μm communities (on average 257 for each sample), samples from T0 and T7 with MC-LR shared only 7% of species, those from T0 and at T7 without MC-LR shared only 10% of species, and samples incubated with or without MC-LR for 7 days shared 30% of species (Supplementary Figure 5).

Considering those groups that degraded MC-LR after 7 days in the November 2016 and November 2017 samples, the communities differed according to the filter pore size and the sampling date (two-way PERMANOVA, $p<0.05$) (Supplementary Table 2).

The taxonomic composition (Order level) of the bacterial communities from MC-LR biodegradation assays was estimated from the relative abundance of OTUs (Figure 4).

For samples collected on the same date, similarity was evaluated considering the filter pore size (< 0.45 and < 0.22 μm), presence/absence of MC-LR, incubation time, and replicates.

In November 2016 (Figure 4A), the pool of samples corresponding to the < 0.22-μm fraction at T0 was less than 10% similar to the samples incubated for 7 days (with or without MC-LR). The predominant phyla at T0 were *Actinobacteria* (63%) and *Proteobacteria* (31%) (Supplementary Table 4), and the major orders were *Actinomycetales* (28%), *Gammaproteobacteria unclassified* (23%) and *Actinobacteria unclassified* (16%). The communities recovered after 7 days with MC-LR from both pore size fractions (< 0.45 and < 0.22 μm) formed a group with 70% similarity. The major components of these communities were members of the phylum *Proteobacteria* (> 85%) and orders *Methylophilales* (29-34% in the < 0.22-μm community and 65–76% in the < 0.45-μm community), *Rhodobacterales* (4-5% in the < 0.22-μm community and 4-7% in the < 0.45-μm community) and *Pseudomonadales* (28-36% in the < 0.22- μm community and 7-12% in the < 0.45-μm community). After 7 days of incubation, the samples spiked with MC-LR were only 10% similar to the pool of samples without MC-LR (< 0.45 μm). In the latter, *Methylophilales* was a minor group (1.5%), whereas *Burkholderiales* was the dominant group (69%) in the < 0.45-μm fraction.

In the November 2017 samples (Figure 4B), the bacterial community (< 0.45 μm) of the original sample (T0) was clearly different from that recovered after 7 days. The original community was rich in *Actinobacteria* (62%), particularly the orders *Actinobacteria unclassified* (23%) and *Actinomycetales* (24%). The communities recovered after 7 days were distributed in two groups according to the original size selection. In the case of the < 0.22-μm fractions, one replicate of T7 with MC-LR grouped with the pool of samples T7 without MC-LR, and the other two replicates grouped together. In all samples

incubated for 7 days, *Proteobacteria* was the most abundant phylum (68-99%). For the < 0.45-µm fractions, in samples that received MC-LR, the dominant order was *Methylophilales* (20-33%). In the pool of samples maintained without MC-LR, the major orders were *Rhodobacterales* (23%), *Burkholderiales* (13%), *Rhizobiales* (13%) and *Pseudomonadales* (10%). In < 0.22 -µm fractions incubated with MC-LR, the dominant order was *Methylophilales* (61-78%), while in the < 0.22-µm samples without MC-LR, *Methylophilales* was less abundant (31%), and the major order was *Pseudomonadales* (45%).

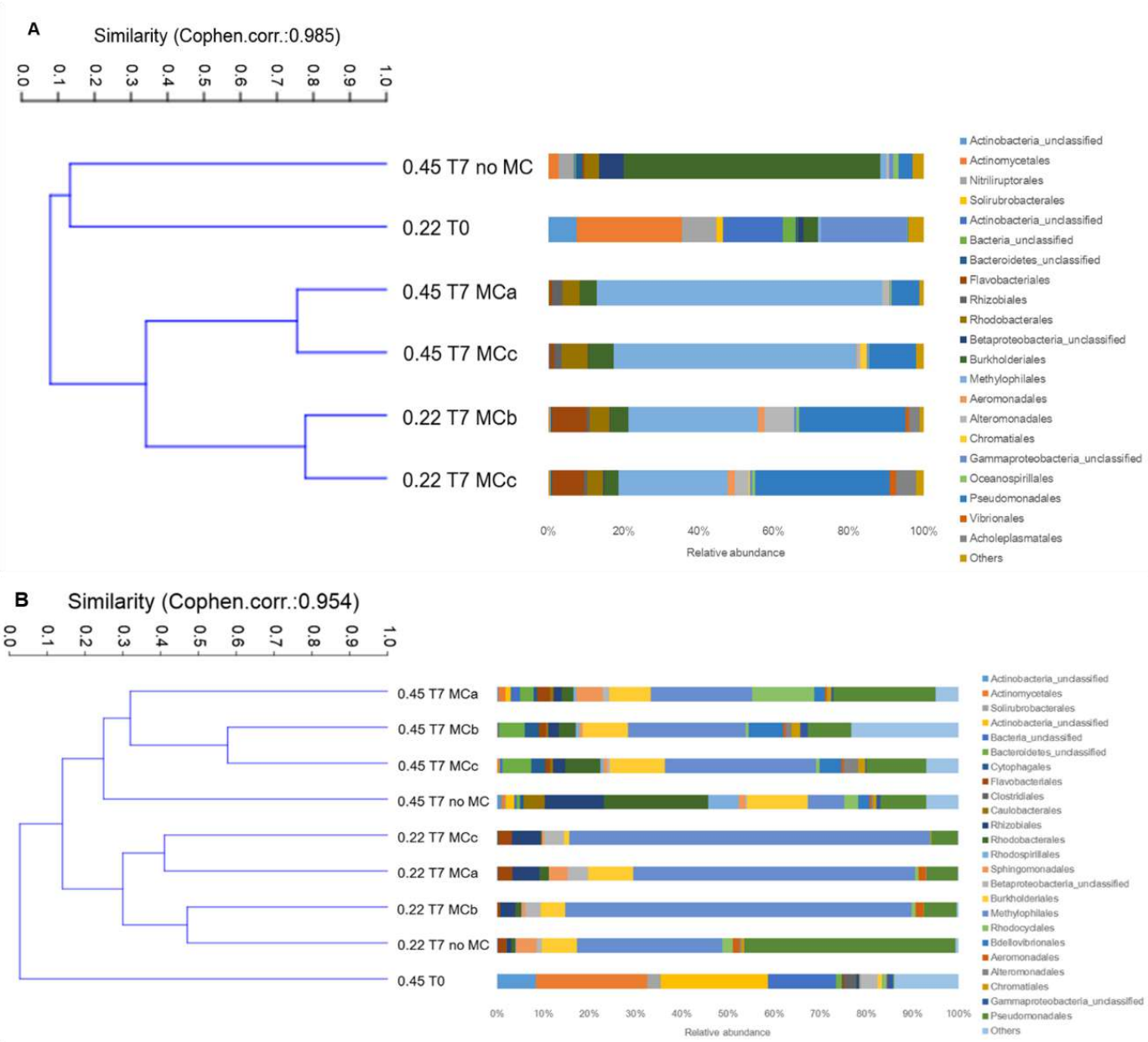

Figure 4: Bacterial composition at the Order level (considering abundance over 1%) and clustering (using Bray-Curtis as the dissimilarity distance) of the samples collected in (A) November 2016 and (B) November 2017 corresponding to microbial fractions <0.45 μm and <0.22 μm at T0 and after 7 days of incubation with or without MC-LR. Samples from T0 and T7 without MC-LR correspond to pools. Samples from T7 with MC-LR are shown as replicates.

In summary, the composition of samples collected on different dates suffered a considerable shift after incubation for 7 days in laboratory conditions, and the addition of MC-LR at the beginning of the experiment clearly led to an enrichment of *Methylophilales*. In those samples maintained for 7 days without MC-LR, this was a minor component. Communities originating from < 0.22-μm and < 0.45-μm fractions had different compositions.

Then, we detailed the main OTUs contributing to the difference between the groups according to filter pore size and presence/absence of MC-LR using SIMPER analysis (Supplementary Tables 5 and 6). These OTUs were plotted as vectors in the nMDS ordinations of samples from each date (Figure 3). In November 2016, four OTUs were responsible for 50% of the distinctiveness in relation to size (Figure 5, Supplementary Table 5). *Methylophilales(o) Methylophilus(g)* (OTU 0001) and *Burkholderiales(o) Hydrogenophaga(g)* (OTU 0003) were enriched in < 0.45-μm communities, while *Pseudomonadales(o) Acinetobacter(g)* (OTU 0004) and *Methylophilales(o) Methylophilus(g)* (OTU 0002) were more abundant in < 0.22-μm communities. In relation to the presence of MC-LR, the predominant OTUs were *Methylophilales(o) Methylophilus(g)* (OTU 0001), *Pseudomonadales(o) Acinetobacter(g)* (OTU 0004), and *Methylophilales(o) Methylophilus(g)* (OTU 0002), which accounted for 30% of the differentiation from communities without MC-LR. Considering only the < 0.45-μm fraction and comparing communities incubated for 7 days with or without MC-LR, the

main OTU enriched in samples that degraded MC-LR was *Methylophilales(o) Methylophilus(g)* (OTU 0001). After 7 days of incubation without MC-LR, the main taxa were *Burkholderiales(o) Hydrogenophaga(g)* (OTU 0003) and *Aucaligenageae unclassified(g)* (OTU 0020).

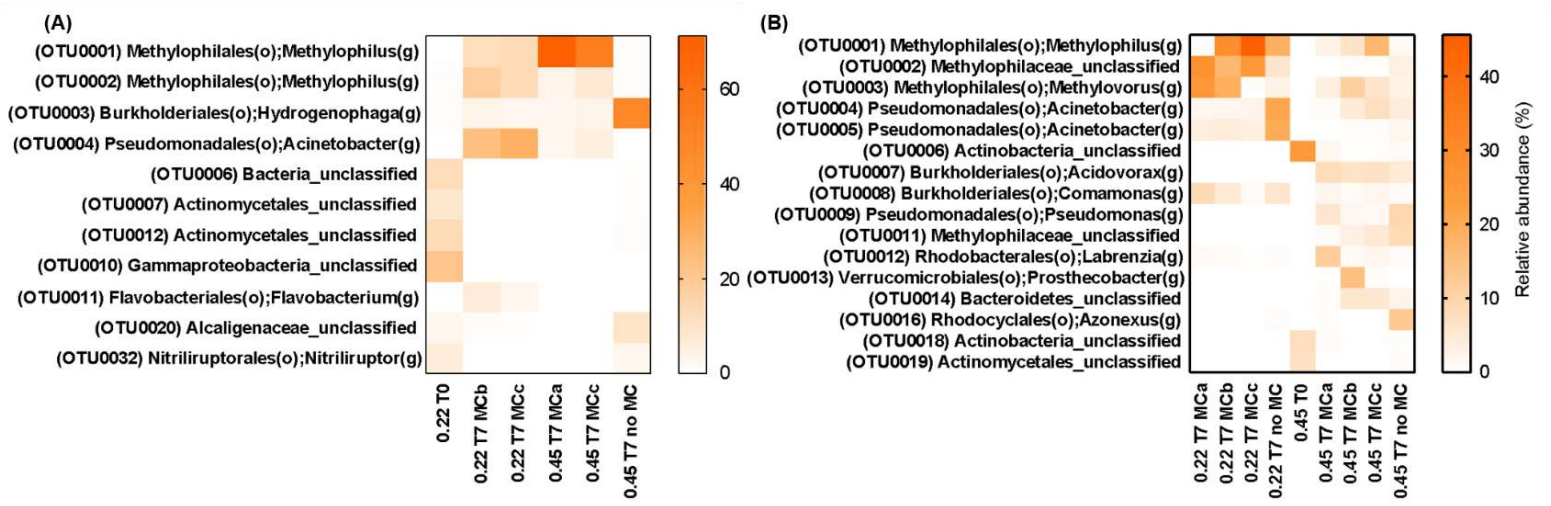

Figure 5: Heatmap representing the relative abundance of OTUs that contributed to the differentiation of groups (SIMPER analysis) according to the size and presence/absence of MC-LR in (A) November 2016 and (B) November 2017. Only OTUs that contributed with more than 1% or together contributed to 50% of the differentiation are included.

Considering only the < 0.22-µm communities, we compared the original samples (T0) with those that degraded MC after incubation for 7 days. In the initial sample, predominant OTUs were *Gammaproteobacteria unclassified* (OTU 0010), *Actinomycetales unclassified* (OTU 0012), *Bacteria unclassified* (OTU 0006) *and Nitriliruptorales(o) Nitriliruptor(g)* (OTU 0032). In < 0.22-µm samples with MC-LR, the main taxa were *Pseudomonadales(o) Acinetobacter(g)* (OTU 0004) and *Methylophilales(o) Methylophilus(g)* (OTU 0002). Independent of the filter pore size, *Methylophilus* (*Methylophilales*) and *Acinetobacter* (*Pseudomonadales* order) were dominant genera in samples incubated with MC-LR.

In November 2017 samples, a greater diversity of OTUs contributed to the variability of communities by size, as well as by the presence/absence of MC-LR (Figures 3 and 5, Supplementary Table 6). *Methylophilales(o) Methylophilus(g)* (OTU 0001), *Methylophilaceae unclassified* (OTU 0002), *Methylophilales(o) Methylovorus(g)* (OTU 0003), and *Pseudomonadales(o) Acinetobacter(g)* (OTU 0004 and 0005) were the main OTUs in < 0.22 -µm communities, contributing 38% for filter pore size differentiation. In the < 0.45-µm communities, enriched taxa included *Actinobacteria unclassified* (OTU 0006), *Burkholderiales(o) Acidovorax(g)* (OTU 0007), *Pseudomonadales(o) Pseudomonas(g)* (OTU 0009), *Methylophilaceae unclassified* (OTU 0011), *Verrucomicrobiales(o) Prosthecobacter(g)* (OTU 0013) and *Rhodocyclales(o) Azonexus(g)* (OTU0016). The original (T0) sample was rich in *Actinobacteria unclassified* (OTU 0006). After 7 days, samples that degraded MC-LR presented a higher contribution of *Burkholderiales(o) Acidovorax(g)* (OTU 0007), *Pseudomonadales(o) Pseudomonas(g)* (OTU0009), *Methylophilaceae unclassified* (OTU 0011), *Verrucomicrobiales(o) Prosthecobacter(g)* (OTU 0013). In contrast, the main contributor in communities incubated without MC-LR was *Rhodocyclales(o) Azonexus(g)* (OTU0016), which differed from T0 and from MC-LR added samples.

In the <0.22 -µm fractions, day 7 samples maintained with MC-LR were mainly characerized by *Methylophilales(o) Methylophilus(g)* (OTU 0001), *Methylophilaceae unclassified* (OTU 0002), *Methylophilales(o) Methylovorus(g)* (OTU 0003) and *Burkholderiales(o) Comamonas(g)* (OTU 0008), while *Pseudomonadales(o) Acinetobacter(g)* (OTUs 0004 and 0005) was associated with samples incubated without MC-LR.

- **Taxa exclusively found in ultra-small bacterial communities**

We selected those OTUs that were only found in the <0.22 -µm fractions, irrespective of the date, to further investigate the diversity of these nanoscale bacteria (Figure 6, Supplementary Table 7). From a total of 48 OTUs, the most numerous groups were unclassified bacteria and *Proteobacteria*. The genera *Azospirillum* and *Insolitispirillum* (*Alphaproteobacteria*), *Zoogloea* and an unidentified Methylophilaceae (*Betaproteobacteria*), *Halobacteriovorax* and *Geobacter* (*Deltaproteobacteria*), *Acinetobacter*, *Catenovulum* and *Thioalkalimicrobium* (*Gammaproteobacteria*) were included. *Acholeplasma*, a member of *Mollicutes* (Tenericutes), was repeatedly identified. We also identified OTUs from *Actinobacteria*, including *Mycobacterium* and several unidentified OTUs from *Actinomycetales*. Within *Bacteroidetes*, OTUs from *Cryomorphaceae* (*Flavobacteriales*) were present. Three OTUs corresponded to *Spirochaetes*.

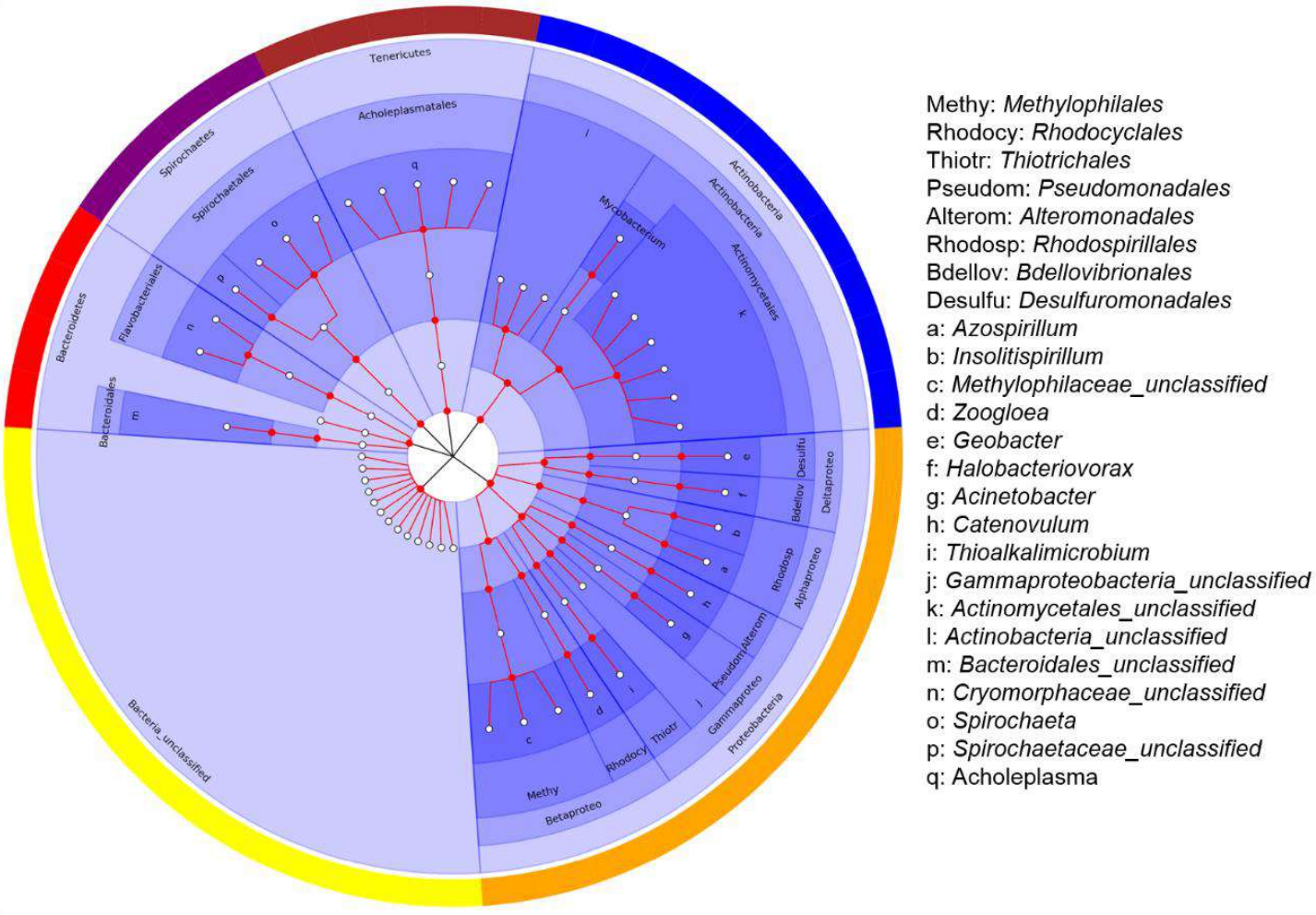

Figure 6: Cladogram representing OTUs exclusively identified in <0.22-µm fractions.

- **Functional prediction based on bacterial community composition**

We applied the gene prediction with phylogenetic investigation of communities reconstruction of unobserved states (PICRUSt) to estimate the functional potential of the bacterial communities, considering those OTUs pointed (by SIMPER) as the main contributors to the differentiation of the bacterial communities. Figure 7 shows the relative abundances of the most represented gene functions. In November 2016 (Figure 7A), transporters distinguished the < 0.22-µm communities at T0. After 7 days, communities were enriched in gene categories related to secretion, motility, and ribosome. These categories were more abundant in < 0.45-µm communities with MC than < 0.45-µm communities without MC and in < 0.22-µm communities with MC. In contrast, butanoate metabolism was less represented in T7 communities compared with T0 communities. For other predicted functions (DNA repair and transcription factors, for example), an overall similarity in relative abundance was apparent for the tested samples. For samples from November 2017 (Figure 7B), comparison of < 0.45-µm and < 0.22-µm communities showed that methane metabolism was more abundant in the fraction selected by the 0.22-µm pore size, whereas propanoate and amino and nucleotide sugar metabolism were more evident in the < 0.45-µm fraction. At the initial time (T0), the < 0.45-µm community was richer in amino sugar and nucleotide sugar metabolism, amino acid metabolism and degradation, butanoate metabolism, the TCA cycle, and glycolysis than the < 0.45-µm community after 7 days. No evident differences were noted in the comparison of < 0.45-µm communities maintained over 7 days with or without MC. In < 0.22-µm communities after 7 days of incubation, those with no MC showed an increase in functions related to butanoate and propanoate metabolism, but all other functions were better represented in samples incubated with MC.

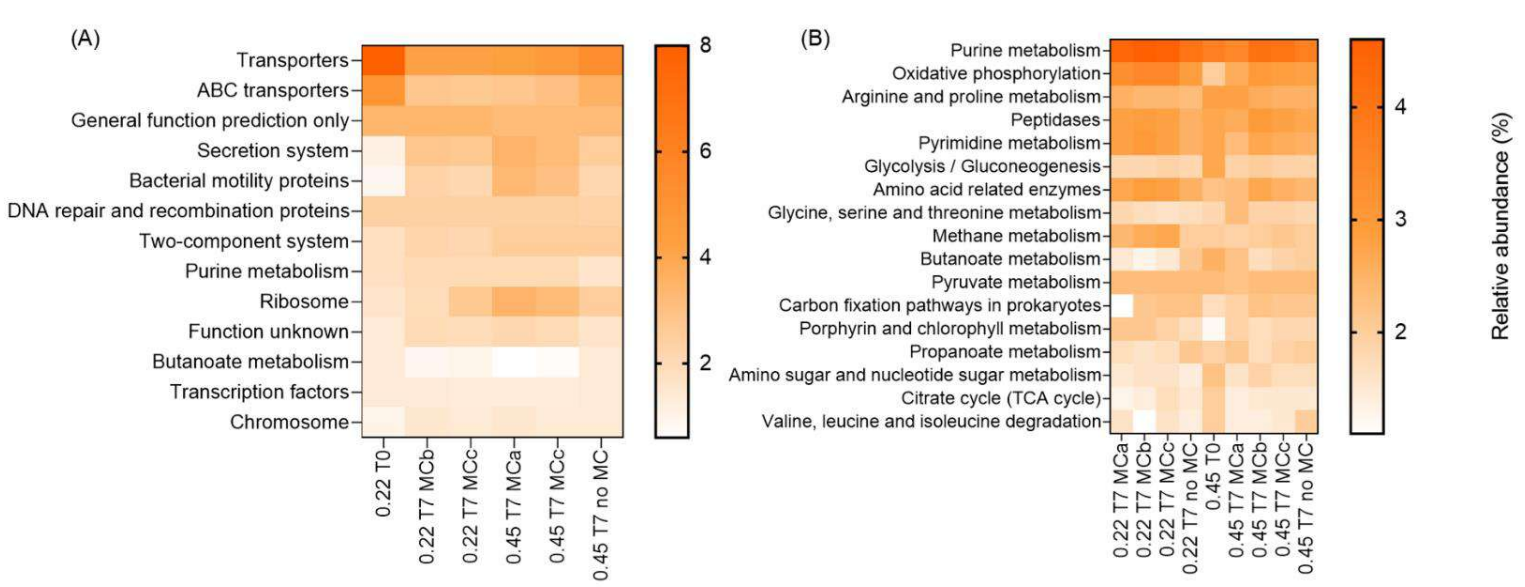

Figure 7: Heatmap representing the relative abundance of functional categories based on the composition of the bacterial communities from (A) November 2016 and (B) November 2017. Only OTUs previously selected as major contributors to the differentiation of the samples maintained with or without MC-LR and from samples of different sizes were considered.

Discussion

We detected MC biodegradation by microbial communities recovered from filtered (< 0.22-µm and < 0.45-µm fractions) surface water of a coastal lagoon historically contaminated with MC. Microorganisms were morphologically and taxonomically diverse, and the communities contained metabolically active cells capable of degrading MC. In a previous work, we showed MC-LR biodegradation by microbial communities recovered as < 0.45-µm fractions from the interstitial water of the same lagoon (SANTOS et al., 2020). Filtering through 0.45-µm membranes was used to avoid thin sediment particles that could adsorb MC and interfere with MC concentration measurements (SONG et al., 2014). In the present study, we further investigated MC degradation by size-selected filterable fractions of surface water plankton, which passed through either

0.45 or 0.22-μm pore membrane filters, and characterized these communities using 16S rDNA sequencing and TEM.

TEM of samples retrieved just after filtration (T0) revealed small prokaryotic cells with varied morphologies in the < 0.45-μm samples, whereas the samples < 0.22-μm showed no obvious cellular morphologies. On this date, bacterial DNA could be retrieved only from < 0.45-μm fractions. In the biodegradation assays, the size-selected cells survived, grew in size, and reproduced over 7 days in the lagoon water under laboratory conditions, as evidenced by the increase in both cell size and abundance observed by TEM, as well as by the more efficient DNA recovery from samples at day 7 than at T0. More specifically, after 7 days of incubation, there were plenty of unmistakable prokaryotic cells in the TEM samples of the < 0.22-μm fraction, which implies that some cells passed through pore filters and grew in size and number during the following 7 days, in both MC-containing and MC-free conditions. To identify the parent cells of T0 samples filtered through 0.22-μm pores, we found a few structures that could be filterable cells, such as long and thin filaments. Some structures somewhat resembled the multi-septate starved cells of *Mycobacterium smegmatis* shown by Wu et al. (2016). Similarly, the ultra-small cells in the < 0.22-μm fraction could represent either starved, or resting, resistance, and/or dispersal cells, which could grow and reproduce after larger, metabolically active cells and predator zooplankton have been removed by filtration. Thus, nutrient availability, stable conditions, and elimination of competing groups and predators have probably cooperated to favour growth over 7 days. Indeed, after 7 days TEM images indicated reproduction (septa), cell growth (larger and more abundant cells), motility (flagella) and excretion of polymeric substances (abundant thin fibres), all of which are energy-costing cellular processes. Many of these features were observed for

both size fractions, suggesting that these communities were not limited by nutrients at this point.

Ghuneim et al. (2018) discussed the effect of cell structure and environmental conditions on filterability, suggesting three distinct types of filterable bacteria: (i) small dimensions regardless of external factors; (ii) an absence of rigid cell walls enabling the cells to pass through pores smaller than cell diameters; or (iii) starvation and/or senescence potentially leading to a decreased cell size. The comparison of sample morphology before and after 7 days of incubation showed distinct shapes and sizes, indicating a large contribution from starved, resting, resistant, senescent, and/or dispersal cells that were able to reproduce when more favourable conditions were established, i.e., during incubation. Accordingly, most cells were larger than the pore sizes used to select the original community, indicating a growth in cell size. This phenomenon is similar to observations by Wang et al. (2007) and Liu et al. (2019), which showed that only a fraction of filterable cells incubated in lake or river water passed through the same pore size filters used to select initial inocula, indicating size growth during incubation. Moreover, the shift in bacterial community composition observed in the metagenomics analysis after incubation indicated growth of selected groups from the original community. Sequencing of the original (T0) samples collected in November 2016 (< 0.22 μm) and November 2017 (< 0.45 μm) revealed that *Actinobacteria* and *Proteobacteria* were the major phyla present in the samples. Indeed, these are the most commonly found groups in freshwater (Newton et al., 2011). Luef at al. (2015) sequenced communities of different sizes from groundwater and noted that the composition of the larger cell fractions (< 1.2 μm and > 0.2 μm) was different from the smaller fractions (< 0.2 μm and > 0.1 μm). In contrast, in the larger size fraction, *Proteobacteria* was the major phylum, and in the ultra-small fraction, the most commonly classified bacteria belonged to Candidate Phyla *WWE3*,

OP11 and *OD1*. Bruno et al. (2017) identified the *Parcubacteria* superphylum as a major group in samples of ultra-small cells from a water treatment plant, contributing ~ 30% of the microbial community. The difference in composition of small and ultra-small communities in different studies can be attributed to the diverse aquatic environments from which those samples were recovered. For example, the composition of ultra-small bacterial communities from groundwater is markedly different from that of contaminated groundwater or surface freshwater (Luef et al., 2015).

We were particularly interested in nanoscale bacterial cells originally isolated from the < 0.22-μm fractions, since very little is known about the community able to pass through 0.22-μm filter as well as this is the first observation for its MC-LR-biodegradation capacity. Thus, we detailed OTUs found only in this size fraction. Additionally, *Actinobacteria* and *Proteobacteria*, taxa from *Bacteroidetes*, *Tenericutes* and *Spirochaetes*, were identified. For some of these taxa, cells with reduced dimensions have been previously described. *Actinobacteria* isolates obtained from freshwater lakes with contrasting trophic states in Europe and Asia consisted of short spirilla with very small cell volumes (< 0.1 μm^3), showing thin Gram-positive cell walls (Hahn et al., 2003). In the present study, *Mycobacterium sp.* was the only *Actinobacteria* genus identified in the < 0.22-μm fractions. Interestingly, a resting stage consisting of short rods 1.4 ± 0.3 μm has been observed in *M. smegmatis* and in two other cultivated mycobacterial strains when exposed to mild starvation (Wu et al., 2016).

Proteobacteria in < 0.22 μm fractions included a variety of taxa, for some of which small cells have been previously reported. We identified OTUs from *Methylophilaceae*, a family of methylotroph aquatic bacteria that can use methanol and other one-carbon compounds as carbon and energy sources. Five genera have been described (*Methylotenera*, *Methylobacillus*, *Methylophilus*, *Methylovorus*, and *Ca.*

Methylopumilus), which can be found in both water and sediments (Salcher et al., 2019) and increase in abundance during cyanobacterial blooms (Salcher et al., 2015). Two freshwater strains isolated in Lake Zurich (Switzerland) (Candidatus *Methylopumilus*) presented a small cell size (median 0.041 μm^3 during stationary growth and 0.075 μm^3 during exponential growth phase). Similarly, small cells were observed in the lake in spring (0.048 μm^3-0.055 μm^3) and even smaller cells in autumn (0.03 μm^3) (Salcher et al., 2015).

Azospirillum and *Insolitispirillum* are genera from *Rhodospirillaceae* (*Proteobacteria*) that have also been described as ultra-small cells. These are purple non-sulphur bacteria found in ponds, sewage and illuminated anoxic zones. *Azospirillum* is a well-characterized genus with nitrogen fixing, non-spore forming cells. The generation of dormant forms in the species *A. brasilense* was reported under nitrogen limitation, with the formation of cyst-like resting cells with distinct morphologies, stress resistance, and long-term viability (Mulyukin et al., 2009).

Acinetobacter (*Proteobacteria*) are coccoid rods that are widely distributed in nature as free-living cells in soil and diverse aquatic habitats such as freshwater, sewage and wastewater treatment plants (Zhang et al., 2009). Growing cells are typically 1.5–2.5 μm long and 1.0–1.5 μm wide, but they can adopt a smaller coccoid shape in stationary phase (Garrity, 2012), which could explain the recovery of this genus in the <0.22-μm fractions.

Thioalkalimicrobium (*Proteobacteria*) is a chemolithoautotrophic group that inhabits the aerobic mixolimnion layer of lakes. The cells are small with an open ring-shape, diameter of 0.5–0.8 μm and width of 0.3–0.4 μm (Kappler et al., 2016), in principle compatible to their presence in the < 0.22-μm communities.

Halobacteriovorax (previously *Bdellovibrio, Proteobacteria*) is a micro-predatory bacteria that inhabit estuarine and marine environments, thus exerting a significant role

in bacterial cell death (typically *Vibrio* species) in aquatic ecosystems (Williams et al., 2016). Cells in the attack phase are 0.2-0.4 μm in width and 0.75-1.0 μm in length and can be recovered after filtration through 0.22 μm pore membranes (Richards et al., 2016). *Acholeplasma* is a mycoplasma (*Mollicutes* class, *Tenericutes*) that presents filamentous or spherical cells (0.3 μm) without a cell wall (Garrity, 2012). *Acholeplasma* can be found in soil and wastewater, although it is also known as a common contaminant of cell cultures. To avoid contamination, culture media must be filtered through 0.1-μm filters because mycoplasmas can pass through the more commonly used 0.22-μm membranes. Long incubation times in nutrient limitation and stress conditions favour the formation of small resistant cells (Folmsbee et al., 2010, Chernov et al., 2011).

Spirochaeta are free living bacteria that are common in aquatic environments, and their unique helical shape with long (ca. 25 μm up to 60 μm) and slender (average diameter of 0.23 μm) cells (Wirth et al., 2016) probably favoured their filtration through 0.2-μm pores.

Cryomorphaceae (*Bacteroidetes*) was also identified herein as ultra-small cells. In marine and freshwater ecosystems, members of this group were found associated with phytoplankton and algal blooms. Common traits of these bacteria are carotenoid pigments, aerobic respiration and rod- to filamentous-shaped cells with varied cell dimensions (Bowman, 2020). Some species present small cells, for example, *Phaeocystidibacter luteus* with a length of approximately 1.0–1.5 μm and diameter of 0.2–0.4 μm (Zhou et al., 2013) and *Vicingus serpentipes* rods with 0.2 to 0.8-μm-wide coccoid cells (Wiese et al., 2018).

For the other OTUs identified in our < 0.22-μm fractions, taxonomic identification revealed bacterial groups for which ecological traits were compatible with the characteristics of the site of sample isolation, but we could not find published reports

relating these genera to ultra-small cells. This phenomenon occurred for the genus *Zoogloea* (family *Rhodocyclaceae*, *Proteobacteria*) that includes the non-spore-forming bacteria found in aquatic habitats and is common in sewage or treatment systems. Cell aggregates are found embedded in a gelatinous matrix but are not particularly small (width, 0.6–0.9 μm; length, 1.1– 2.0 μm) (Shao et al., 2009). Cultivated *Geobacter* strains are obligate anaerobes, which can oxidize organic compounds to CO_2 through the reduction of extracellular electron acceptors as insoluble Fe and Mn oxides, an important step in the natural cycling of carbon, Fe, Mn, and other elements. Laboratory strains of *Geobacter* have not been specifically considered as small cells, although the type strain of the species *G. luticola* is 0.6-1.9 μm in length and 0.2-0.4 μm in width (Viulu et al., 2013). The finding that both the environment and incubation conditions in the present work were aerobic indicate that those cells present in our samples would not behave as classic *Geobacter*, which could be associated to new species. In *Catenovulum* (*Alteromonadaceae*, *Proteobacteria*), the cells are rod-shaped, facultatively anaerobic, and agar-hydrolytic, and they were found in marine sediment or marine algae. Cell dimensions of type strains vary in length and diameter (0.7–1.2 μm in width and 1.5–3.0 μm in length), and they are not characteristically small (Shi et al., 2017). In summary, <0.22-μm communities, similarly to 0.45-μm communities, included microorganisms with a varied phylogenetic distribution.

In our assays, bacteria were incubated in lagoon water. The Jacarepaguá lagoon receives untreated domestic and industrial discharges, containing both organic contaminants and inorganic nutrients, which can generally support *Cyanobacteria* and heterotrophic microbial communities (Salloto et al., 2012; De Magalhães et al., 2017). The addition of MC to lagoon water possibly provided a richer nutrient environment for filterable plankton communities, as noted by the increased recovery of DNA after 7 days in samples

with added MC in comparison to samples without MC. Additionally, for the communities originally selected as < 0.22 μm, the addition of MC apparently resulted in a more diverse set of cell morphologies and coincided with the deposition of extracellular polymeric fibres. Previous studies on MC biodegradation conducted in minimal medium (only salts and vitamins) indicated that MCs represent a complementary nutritional source for bacteria upon degradation (Lezcano et al., 2016; Móron-Lopez et al., 2017).

The taxonomic composition of the communities from the water lagoon changed after incubation for 7 days in laboratory conditions, as indicated by a minority of taxa shared between T0 and T7 in both size factions, with and without MC. In November 2016, *Actinobacteria* was the major group in the initial community, which decreased to 0% after 7 days, whereas *Proteobacteria* represented 31% of the OTUs at T0 and increased to > 85% after 7 days. A similar shift in these two phyla was noted in the November 2017 samples. Similarly, Li et al. (2016) described shifts in the composition of lake sediment bacterial communities in response to MC-LR biodegradation. Comparing communities at the initial and final times, when MC-LR was undetectable, they noted that both *Proteobacteria* (39%) and *Actinobacteria* (25%) dominated in the original sample, whereas only *Proteobacteria* was predominant (87%) after degradation.

The presence of *Proteobacteria* after 7 days of incubation was associated with a relatively high abundances of genera assigned as *Methylophilales*, *Pseudomonadales* and *Burkholderiales*. The recovery of these taxa originating from nanoscale cellular fractions indicated that these OTUs were present as small cells in the natural sample and, as suggested by microscopy analysis, generated larger cells during incubation. Typical cell morphologies and sizes described for a bacterial genus are usually derived from isolated strains in culture. Natural samples can reveal a more diverse set of cell shapes and sizes, as illustrated by our microscopy images, as well as by results from other studies (Schauer

and Hahn, 2005; Luef et al., 2015, Yang et al., 2016). Morphological changes reflecting physiological responses to a changing environment can be related to the increased abundance of predicted functions associated with transporters in the < 0.22-μm samples at T0. In the natural environment, competition for dissolved organic matter and nutrients as well as stressful conditions would favour higher surface-to-volume ratios and an increase in active transport systems. Under stable laboratory conditions, cells could probably sustain growth and modify their shape, as supported by the relative increase in gene functions associated with translation, secretion, motility, oxidative phosphorylation, and nucleotide and amino acid metabolism predicted for communities after 7 days, especially in those that degraded MC.

Considering that a clear shift occurred in the composition of the bacterial communities after 7 days of incubation in the laboratory, we next asked whether the resulting communities would differ according to their original size selection. To address this question, we compared the < 0.45-μm and < 0.22-μm communities after 7 days in the presence of MC. There was no difference in diversity or richness comparing communities originally selected by different pore size filters, but they were significantly different in composition. In these MC-degrading communities, the dominant genera were *Methylophilus* and other unclassified genera of *Methylophilaceae*, which were present in both size fractions, although individual OTUs presented a relatively higher abundance depending on the pore-sized filter selection. Additionally, in the < 0.45-μm fractions, *Pseudomonas* and *Acidovorax* predominated, whereas in the < 0.22-μm fractions, *Acinetobacter* was more representative. Other OTUs were exclusively detected in the < 0.22-μm fractions, as discussed above. Thus, the structure of the bacterial communities after 7 days of incubation also differed based on their original size selection.

Bacterial communities were maintained in the presence or absence of MC, and we could test whether the toxin would affect the course of the community shift over time. In November 2016 and November 2017, samples with and without MC were significantly different, and a similar shift in community composition was observed. In 2016, the major components in both size fractions incubated with MC were *Methylophilus* (*Methylophilales*) and *Acinetobacter* (*Pseudomonadales*). In the <0.45-μm samples without MC-LR, *Methylophilus* was a minor group, whereas *Hydrogenophaga* (*Burkholderiales*) was a dominant group. In the 2017 samples, those that degraded MC-LR presented a higher contribution of *Acidovorax* (*Burkholderiales*), *Prosthecobacter* (*Verrucomicrobiales*), *Pseudomonas*, *Comamonas* (*Burkholderiales*), *Methylophilus*, *Methylovorus* and the unclassified genera of *Methylophilaceae*.

Pseudomonas and *Acinetobacter*, as well as *Methylophilaceae* genera, have been previously detected in MC-degrading samples from the interstitial water of the same lagoon (Santos et al., 2020), and they have also been described as MC-degraders in other studies (Ho et al. 2012; Li et al. 2016; Massey and Yang, 2020). Other taxa, such as *Acidovorax, Comamonas* and *Prosthecobacter*, have also been previously reported to degrade MC, or they are enriched in toxin-degrading consortia (Ding et al., 2020). A similar result has been reported in the characterization of lake sediment samples before and after MC degradation (Li et al., 2016), leading to the conclusion that a shift in the bacterial composition was largely due to MC-LR assimilation. The shift involved the increase in numerous *Proteobacteria* orders, including *Methylophilales* and *Bulkholderiales*, which was also enriched in our experiments with MC-LR. Curiously, *Sphingomonadaceae* OTUs were not identified as major components in our MC-degrading communities, which has been reported in another environment (Bukowska et al., 2018). From these experiments, we can conclude that bacterial communities

maintained with and without MC diverged in composition, and the presence of MC led to the selection of taxa associated with its degradation.

The environmental samples studied herein were collected from a coastal lagoon that is highly impacted by urban pollution, where recurrent cyanobacterial blooms have resulted in an environment contaminated with MC (Salloto et al., 2012; De Magalhães et al., 2017). The dynamics of MC in this shallow lagoon involve different aspects, including sorption to the sediment and biodegradation. We have previously reported that microbial communities associated with the sediment exhibit high diversity, including bacteria capable of degrading MC-LR and groups known to thrive under extreme conditions (Santos et al., 2020). In the present study, we extended this observation to bacteria obtained from surface water and selected by their small cellular size.

Conclusion

This study revealed that both < 0.45-μm and < 0.22-μm fractions exhibited microorganisms of varied morphology and contained metabolically active cells capable of degrading MC. Despite sharing several OTUs, the communities originating from the different size fractions diverged in taxonomic composition. For both size-selected fractions, incubation under laboratory conditions favoured growth and led to morphological changes and an increased cell size. The presence of MC shifted the structure of these communities in comparison to samples maintained in the absence of MC, with a clear enrichment of taxa known to degrade MC. Our results reveal that filterable bacteria constitute a diverse and underestimated fraction of microbial communities, which participate in the dynamics of cyanotoxins in natural environments.

Acknowledgements

This work was supported by the National Council of Scientific and Technological Development - CNPq (473468/2013-1), and Rio de Janeiro State Foundation to Support Research - FAPERJ (E-26110.604/2014). We would like to acknowledge Engineering and Physical Sciences Research Council (EPSRC – United Kingdom) (project EP/P029280/1).

Additionally, we thankfully acknowledge to Dr. Leonardo Andrade and Ms. Mair M. M. Oliveira for the helpful support in microscopy analysis and sample preparation as well as and Prof Sandra Maria Feliciano de Oliveira e Azevedo for fruitful discussions.

References

Bouaïcha, N., Miles, C.O., Beach, D.G., Labidi, Z., Djabri, A., Benayache, N.Y., Nguyen-Quang, T. (2019). Structural Diversity, Characterization and Toxicology of Microcystins. Toxins, 11(12), 714. https://doi.org/10.3390/toxins11120714

Bourne, D.G., Jones, G.J., Blakeley, R.L., Jones, G.J., Negri, A.P., Riddles, P. (1996). Enzymatic pathway for the bacterial degradation o;f the cyanobacterial cyclic peptide toxin microcystin LR. Appl. Environ. Microbiol. 62, 4086–4094.

Bowman, J.P. (2020). Out From the Shadows–Resolution of the Taxonomy of the Family Cryomorphaceae. *Frontiers in Microbiology*, *11*, 795. https://doi.org/10.3389/fmicb.2020.00795

Briand, E., Humbert, J.F., Tambosco, K., Bormans, M., Gerwick, H. (2016). Role of bacteria in the production and degradation of Microcystis cyanopeptides. Microbiology open. Jun; 5(3): 469–478. Published online 2016 Feb 25. doi: 10.1002/mbo3.343

Bruno, A., Sandionigi, A., Rizzi, E., Bernasconi, M., Vicario, S., Galimberti, A., Cocuzza, C., Labra, M., Casiraghi, M. (2017). Exploring the under-investigated "microbial dark matter" of drinking water treatment plants. Sci. Rep. 7. https://doi.org/10.1038/srep44350.

Bukowska, A., Kaliński, T., Chróst, R.J. (2018). Degradation of microcystins by water and bottom sediment bacterial communities from a eutrophic freshwater lake. *Aquat. Microbl. Ecol.* 82, 129–144. doi: 10.3354/ame01887

Caporaso, J.G., Lauber, C.L., Walters, W.A., Berg-Lyons, D., Lozupone, C.A., Turnbaugh, P.G., Fierer, N., Knight, R. (2011). Global patterns of 16S rRNA diversity at a depth of millions of sequences per sample. PNAS 108, 4516–4522. https://doi.org/10.1073/pnas.1000080107.

Chernov, V.M., Chernova, O.A., Medvedeva, E.S., Mouzykantov, A.A., Ponomareva, A.A., Shaymardanova, G.F., Gorshkov, O.V., Trushin, M.V. (2011). Unadapted and adapted to starvation Acholeplasma laidlawii cells induce different responses of Oryza sativa, as determined by proteome analysis. *Journal of proteomics*, *74*(12), 2920-2936. doi: 10.1016/j.jprot.2011.07.016

Christoffersen, K., Lyck, S., Winding, A. (2002). Microbial activity and bacterial community structure during degradation of microcystins. Aquat. Microb. Ecol. 27, 125–136. doi: 10.3354/ame027125

Clarke, K.R. (1993). Non-parametric multivariate analyses of changes in community structure. Australian Journal of Ecology 18: 117-143

De Magalhães, L., Noyma, N.P., Furtado, L.L., Mucci, M., Van Oosterhout, F., Huszar, V.L.M., Marinho, M.M., Lurling, M., (2017). Efficacy of coagulants and ballast compounds in removal of cyanobacteria (Microcystis) from water of the tropical lagoon Jacarepaguá (Rio de Janeiro, Brazil). Estuaries Coasts 40 (1), 121–133. https://doi.org/10.1007/s12237-016-0125-x.

Ding, Q., Liu, K., Song, Z., Sun, R., Zhang, J., Yin, L., Pu, Y. (2020). Effects of Microcystin-LR on Metabolic Functions and Structure Succession of Sediment Bacterial Community under Anaerobic Conditions. *Toxins (Basel)* 12(3):183. doi:10.3390/toxins12030183

Dziga, D., Wasylewski, M., Szetela, A., Bocheńska, O., Wladyka, B. (2012). Verification of the role of MlrC in microcystin biodegradation by studies using a heterologous expressed enzyme. Chem. Res. Toxicol. 25, 1192–1194.

Dziga, D., Wasylewski, M., Wladyka, B., Nybom, S., Meriluoto, J. (2013). Microbial degradation of microcystins. Chem. Res. Toxicol. 26, 841–852. https://doi.org/10.1021/tx4000045

Dziga, D., Maksylewicz, A., Maroszek, M., Budzyńska, A., Napiorkowska-Krzebietke, A., Toporowska, M., Meriluoto, J. (2017). The biodegradation of microcystins in temperate freshwater bodies with previous cyanobacterial history. Ecotoxicol. Environ. Saf. 145, 420–430. https://doi.org/10.1016/j.ecoenv.2017.07.046

Ferrão-Filho, A., Domingos, P., Azevedo, S.M.F.O. (2002). Influences of a Microcystis aeruginosa Kützing bloom on zooplankton populations in Jacarepaguá Lagoon (Rio de Janeiro, Brazil), Limnologica. 32:(4)295-308. doi: 10.1016/S0075-9511(02)80021-4

Ferrão-Filho, A.S. and Kozlowsky-Suzuki, B. (2011). Cyanotoxins: bioaccumulation and effects on aquatic animals. *Mar Drugs*. 9(12):2729-2772. doi:10.3390/md9122729

Folmsbee, M., Noah, C., McAlister, M. (2010). Nutritional Effects on the Growth, Cell Size, and Resistance to Stress of Acholeplasma laidlawii. *PDA journal of pharmaceutical science and technology*, *64*(6), 581-592.

Garrity, G.M. (2012). Bergey's manual of systematic bacteriology: Volume one: the Archaea and the deeply branching and phototrophic bacteria. Springer Science & Business Media

Ghuneim L-A. J., Jones D. L., Golyshin, P. N., Golyshina, O. V. (2018). Nano-sized and filterable Bacteria and Archaea: Biodiversity and function. Frontiers in Microbiology 9: 1971. doi: 10.3389/fmicb.2018.01971

Hahn, M.W., Lünsdorf, H., Wu, Q., Schauer, M., Höfle, M., Boenigk, J., Stadler, P. (2003). Isolation of novel ultramicrobacteria classified as actinobacteria from five freshwater habitats in Europe and Asia. Appl Environ Microbiol. 2003;69(3):1442-1451. doi:10.1128/aem.69.3.1442-1451.2003

Hammer, O., Harper, D., Ryan, P. (2001). PAST: Paleontological Statistics Software Package for Education and Data Analysis. Palaeontologia Electronica. 4. 1-9.

Ho, L., Sawade, E., Newcombe, G. (2012). Biological treatment options for cyanobacteria metabolite removal - a review. Water Res. 46 (5), 1536–1548. https://doi.org/10.1016/j.watres.2011.11.0

Huisman, J., Codd, G.A., Paerl, H.W., Ibelings, B.W., Verspagen, J.M.H., Visser, P.M., (2018). Cyanobacterial blooms. *Nat Rev Microbiol*. 16(8):471-483. doi:10.1038/s41579-018-0040-1

Hyenstrand, P., Rohrlack, T., Beattie, K., Metcalf, J., Codd, G., Christoffersen, K. (2003). Laboratory studies of dissolved radiolabelled microcystin-LR in lake water. Water research. 37. 3299-306. doi: 10.1016/S0043-1354(03)00180-5.

Jones, G.J., Bourne, D.G., Blakeley, R.L. Doelle, H. (1994). Degradation of the cyanobacterial hepatotoxin microcystin by aquatic bacteria. Nat. Toxins 2, 228-235

Kappler, U., Davenport, K., Beatson, S., Lapidus, A., Pan, C., Han, C., Montero-Calasanz, M., Land, M., Hauser, L., Rohde, M., Göker, M., Ivanova, N., Woyke, T., Klenk, H., Kyrpides, N. (2016). Complete genome sequence of the haloalkaliphilic, obligately chemolithoautotrophic thiosulfate and sulfide-oxidizing γ-proteobacterium Thioalkalimicrobium cyclicum type strain ALM 1 (DSM 14477 T). *Standards in genomic scien*ces, 11(1), 38. doi:10.1186/s40793-016-0162-x

Kumar, P., Hegde, K., Brar, S.K., Cledon, M., Kermanshahi-Pour, A. (2019). Potential of biological approaches for cyanotoxin removal from drinking water: A review. Ecotoxicol Environ Saf. 172:488-503. doi:10.1016/j.ecoenv.2019.01.066

Langille, M., Zaneveld, J., Caporaso, J., McDonald, D., Knights, D., Reyes, J., Clemente, J., Burkepile, D., Vega Thurber, R., Knight, R., Beiko, R., Huttenhower, C. (2013). Predictive functional profiling of microbial communities using 16S rRNA marker gene sequences. Nat Biotechnol 31, 814–821. https://doi.org/10.1038/nbt.2676

Lezcano, M.A., Moron-Lopez, J., Agha, R., Lopez-Heras, I., Nozal, L., Quesada, A., El-Shehawy, R. (2016). Presence or absence of mlr genes and nutrient concentrations co-determine the microcystin biodegradation efficiency of a natural bacterial community. Toxins 8:E318. doi: 10.3390/toxins8110318

Li, J., Shi, G., Mei, Z., Wang, R., Li, D. (2016). Discerning biodegradation and adsorption of microcystin-LR in a shallow semi-enclosed bay and bacterial community shifts in response to associated process. Ecotoxicol. Environ. Saf. 132, 123–131. https://doi.org/10.1016/j.ecoenv.2016.05.033

Li, J., Li, R., Li, J. (2017). Current research scenario for microcystins biodegradation - A review on fundamental knowledge, application prospects and challenges. Sci Total Environ. 595:615-632. doi:10.1016/j.scitotenv.2017.03.285

Li, Q., Lin, F., Yang, C., Wang, J., Lin, Y., Shen, M., Zhao, J., (2018). A large-scale comparative metagenomic study reveals the functional interactions in six bloom-forming microcystis-epibiont communities. *Frontiers in microbiology*, *9*, 746

Liu, J., Li, B., Wang, Y., Zhang, G., Jiang, X., Li, X. (2019). Passage and community changes of filterable bacteria during microfiltration of a surface water supply. Environment International 131: 104998. doi: 10.1016/j.envint.2019.104998

Luef, B., Frischkorn, K., Wrighton, K., Holman, H-Y., Birarda, G., Thomas, B., Singh, A., Williams, K., Siegerist, C., Tringe, S., Downing, K., Comolli, L., Banfield, J. (2015). Diverse uncultivated ultra-small bacterial cells in groundwater. Nat Commun 6, 6372. https://doi.org/10.1038/ncomms7372

Magalhães, V.F., Soares, R.M., Azevedo, S.M.F.O. (2001). Microcystin contamination in fish from the Jacarepaguá Lagoon (Rio de Janeiro, Brazil): ecological implication and human health risk. Toxicon 39:(7), 10077–11085. https://doi.org/10.1016/S0041-0101(00)00251-8.

Massey, I.Y. and Yang, F. (2020). A Mini Review on Microcystins and Bacterial Degradation. *Toxins*, *12*(4), 268. https://doi.org/10.3390/toxins12040268

Morón-López, J., Nieto-Reyes, L., El-Shehawy, R., (2017). Assessment of the influence of key abiotic factors on the alternative microcystin degradation pathway(s) (mlr −): A detailed comparison with the mlr route (mlr +). Sci. Total Environ. 599, 1945–1953. https://doi.org/10.1016/j.scitotenv.2017.04.042. 600.

Mou, X., Lu, X., Jacob, J., Sun, S., Heath, R. (2013). Metagenomic identification of bacterioplankton taxa and pathways involved in microcystin degradation in Lake Erie. PLoS One. 8(4):e61890. doi:10.1371/journal.pone.0061890

Mulyukin, A. L., Suzina, N. E., Pogorelova, A. Y., Antonyuk, L. P., Duda, V. I., El-Registan, G. I. (2009). Diverse morphological types of dormant cells and conditions for their formation in *Azospirillum brasilense*. *Microbiology*, *78*(1), 33-41.

Newton, R.J., Jones, S.E., Eiler, A., Mcmahon, K.D., Bertilsson, S. (2011). A guide to the natural history of freshwater lake Bacteria. Microbiol. Mol. Biol. Rev. 75 (1), 14–49.https://doi.org/10.1128/MMBR.00028-10.

Osman, O.A., Beier, S., Grabherr, M., Bertilsson, S. (2017). Interactions of freshwater cyanobacteria with bacterial antagonists. Appl. Environ. Microbiol. 83, 1–18. doi: 10.1128/AEM.02634-16

Paerl, H.W. and Otten, T.G. (2013). Blooms bite the hand that feeds them. Science 342 (6157), 433–434. https://doi.org/10.1126/science.1245276.

Pal, M., Yesankar, P.J., Dwivedi, A., Qureshi, A. (2020). Biotic control of harmful algal blooms (HABs): A brief review [published online ahead of print, 2020 May 3].*J Environ Manage*. 268:110687. doi:10.1016/j.jenvman.2020.110687

Quast, C., Pruesse, E., Yilmaz, P., Gerken, J., Schweer, T., Yarza, P., Peplies, J., Glöckner, F.O. (2013). The SILVA ribosomal RNA gene database project: improved data processing and web-based tools. Nucleic Acids Res. 41 (Database issue), D590–6. https://doi.org/10.1093/nar/gks1219.

Ramani, A., Rein, K., Shetty, K.G., Jayachandran, K. (2012). Microbial degradation of microcystin in Florida's freshwaters. Biodegradation 23, 35. https://doi.org/10.1007/s10532-011-9484-y.

Richards, G.P., Fay, J.P., Uknalis, J., Olanya, O.M., Watson, M.A. (2016). Purification and host specificity of predatory Halobacteriovorax isolates from seawater. Applied and environmental microbiology, 82(3), 922-927. doi: 10.1128/AEM.03136-15

Rognes, T., Flouri, T., Nichols, B., Quince, C., Mahé, F. (2016). VSEARCH: a versatile open source tool for metagenomics. PeerJ, 4, e2584. https://doi.org/10.7717/peerj.2584

Salcher, M.M., Neuenschwander, S.M., Posch, T., Pernthaler, J. (2015). The ecology of pelagic freshwater methylotrophs assessed by a high-resolution monitoring and isolation campaign. *The ISME journal*, *9*(11), 2442-2453.

Salcher, M.M., Schaefle, D., Kaspar, M., Neuenschwander, S.M., Ghai, R. (2019). Evolution in action: habitat transition from sediment to the pelagial leads to genome streamlining in Methylophilaceae. *ISME J*. 13(11):2764-2777. doi:10.1038/s41396-019-0471-3

Salloto, G., Cardoso, A., Coutinho, F., Pinto, L., Vieira, R., Chaia, C., Lima, J., Albano, R., Martins, O., Clementino, M. (2012). Pollution Impacts on Bacterioplankton Diversity in a Tropical Urban Coastal Lagoon System. PLoS ONE 7(11): e51175. https://doi.org/10.1371/journal.pone.0051175

Santos, A.A., Rachid, C., Pacheco, A.B, Magalhães, V. (2020). Biotic and abiotic factors affect microcystin-LR concentrations in water/sediment interface. Microbiol Res.236:126452. doi:10.1016/j.micres.2020.126452

Schauer, M. and M.W. Hahn. (2005). Diversity and phylogenetic affiliations of morphologically conspicuous large filamentous bacteria occurring in the pelagic zones of a broad spectrum of freshwater habitats. Appl. Environ. Microbiol. 71:1931-1940. doi:10.1128/AEM.71.4.1931–1940.2005

Schloss, P.D., Westcott, S.L., Ryabin, T., Hall, J.R., Hartmann, M., Hollister, E.B., Lesniewski, R.A., Oakley, B.B., Parks, D.H., Robinson, C.J., Sahl, J.W., Stres, B., Thallinger, G.G., Van Horn, D.J., Weber, C.F. (2009). Introducing mothur: opensource, platform-independent, community-supported software for describing and comparing microbial communities. Appl. Environ. Microbiol. 75 (23), 7537–7541. https://doi.org/10.1128/AEM.01541-09.

Shao, Y., Chung, B.S., Lee, S.S., Park, W., Lee, S.S., Jeon, C.O. (2009). Zoogloea caeni sp. nov., a floc-forming bacterium isolated from activated sludge. *International journal of systematic and evolutionary microbiology*, *59*(3), 526-530.

Shimizu, K., Maseda, H., Okano, K., Kurashima, T., Kawauchi, Y., Xue, Q., Utsumi, M., Zhang, Z., Sugiura, N. (2012). Enzymatic pathway for biodegrading microcystin-LR in Sphingopyxis sp. C-1. J. Biosci. Bioeng. 114, 630–634. doi:10.1016/j.jbiosc.2012.07.004

Solden, L., Lloyd, K., Wrighton, K. (2016). The bright side of microbial dark matter: Lessons learned from the uncultivated majority. Current Opinion in Microbiology. 31. 217-226. 10.1016/j.mib.2016.04.020.

Spoof, L., Vesterkvist, P., Lindholm, T., Meriluoto, J. (2003). Screening for cyanobacterial hepatotoxins, microcystins and nodularin in environmental water samples by reversed-phase liquid chromatography-electrospray ionisation mass spectrometry. J Chromatogr A 1020:105–119

Szlag, D.C., Sinclair, J.L., Southwell, B., Westrick, J.A. (2015). Cyanobacteria and Cyanotoxins Occurrence and Removal from Five High-Risk Conventional Treatment Drinking Water Plants. Toxins (Basel). 7(6):2198-2220. Published 2015 Jun 12. doi:10.3390/toxins7062198

Viulu S, Nakamura K, Okada Y, Saitou S, Takamizawa K. Geobacter luticola sp. nov., an Fe(III)-reducing bacterium isolated from lotus field mud. Int J Syst Evol Microbiol.63(Pt 2):442-448. doi:10.1099/ijs.0.039321-0

Wang, Y., Hammes, F., Boon, N., Egli, T. (2007). Quantification of the Filterability of Freshwater Bacteria through 0.45, 0.22, and 0.1 μm Pore Size Filters and Shape-Dependent Enrichment of Filterable Bacterial Communities. Environ. Sci. Technol. 2007, 41, 7080-7086. https://doi.org/10.1021/es0707198

Wiese, J., Saha, M., Wenzel-Storjohann, A., Weinberger, F., Schmaljohann, R., Imhoff, J.F. (2018). Vicingus serpentipes gen. nov., sp. nov., a new member of the Flavobacteriales from the North Sea. *International journal of systematic and evolutionary microbiology*, *68*(1), 333-340. doi: 10.1099/ijsem.0.002509

Williams, H.N., Lymperopoulou, D.S., Athar, R., Chauhan, A., Dickerson, T.L., Chen, H., Laws, E., Berhane, T-K., Flowers, A., Bradley, N., Young, S., Blackwood, A., Murray, J., Mustapha, O., Blackwell, C., Tung, Y., Noble, R. (2016). *Halobacteriovorax*, an underestimated predator on bacteria: potential impact relative to viruses on bacterial mortality. The ISME journal, 10(2), 491-499. doi: 10.1038/ismej.2015.129

Wirth, R., Ugele, M., Wanner, G. (2016). Motility and Ultrastructure of Spirochaeta thermophila. *Frontiers in Microbiology*, *7*, 1609. doi: 10.3389/fmicb.2016.01609

Woodhouse, J.N., Ziegler, J., Grossart, H.P., Neilan, B.A (2018). Cyanobacterial community composition and bacteria–bacteria interactions promote the stable occurrence of particle-associated bacteria. *Frontiers in microbiology*, *9*, 777. doi: 10.3389/fmicb.2018.00777

Wu, M-L., Gengenbacher, M., Dick, T. (2016). Mild nutrient starvation triggers the development of a small-cell survival morphotype in Mycobacteria. Frontiers in Microbiology 7: 947. doi: 10.3389/fmicb.2016.00947

Yang, D.C., Blair, K.M., Salama, N.R.. (2016). Staying in Shape: the Impact of Cell Shape on Bacterial Survival in Diverse Environments. Microbiol Mol Biol Rev. 80(1):187-203. doi:10.1128/MMBR.00031-15

Yang, F., Guo, J., Huang, F., Massey, I., Huang, R., Li, Y., Wen, C., Ding, P., Zeng, W., Liang, G. (2018). Removal of microcystin-LR by a novel native effective bacterial community designated as YFMCD4 isolated from Lake Taihu. Toxins 10 (9), 363. https://doi.org/10.3390/toxins10090363

Zhang, Y., Marrs, C. F., Simon, C., Xi, C. (2009). Wastewater treatment contributes to selective increase of antibiotic resistance among Acinetobacter spp. *Science of the Total Environment*, *407*(12), 3702-3706. doi: 10.1016/j.scitotenv.2009.02.013

Zhou, Y., Su, J., Lai, Q., Li, X., Yang, X., Dong, P., Zheng, T. (2013). Phaeocystidibacter luteus gen. nov., sp. nov., a member of the family Cryomorphaceae isolated from the marine alga Phaeocystis globosa, and emended description of Owenweeksia hongkongensis. *International journal of systematic and evolutionary microbiology*, 63(3), 1143-1148. https://doi.org/10.1099/ijs.0.030254-0

4.4 Capítulo 4 (Biodegradation of cyanobacterial and non-cyanobacterial peptides by *Paucibacter toxinivorans*)

Biodegradation of cyanobacterial and non-cyanobacterial peptides by *Paucibacter toxinivorans* 2C20

Allan Amorim Santos[ab], Valeria Freitas de Magalhães[a], Christine Edwards[b] and Linda A. Lawton[b]

[a] Biophysics Institute, Federal University of Rio de Janeiro, 373 Avenida Carlos Chagas Filho, Rio de Janeiro, Brazil

[b] School of Pharmacy and Life Sciences, Robert Gordon University, The Sir Ian Wood Building, Garthdee Road, Aberdeen, AB10 7GJ, United Kingdom

Abstract

Cyanobacterial bloom is increasing worldwide due to the high level of pollution and nutrients in water bodies, which make a public health concern because cyanobacteria cells might be potential toxigenic organisms. Regarding compounds with toxicity distinctive, there are a large number of peptides produced by them, of which microcystins are the most reported as well as toxic. Nonetheless, other cyanopeptide metabolites might present a potential toxicity and disturbance to the ecosystem. When cyanobacteria cells release their intracellular metabolites into the water, conventional water treatment is inefficient to eliminate them. Thus, many approaches have been studied to solve it. Biodegradation, for example, plays an important role in environment dynamics, and it could be used as an alternative water treatment by isolated bacteria or even by a bacterial community. Here, we evaluated the capability of two already known MC-degrading bacteria to diminish the concentration of five MC variants (MC-LR, DM-LR, MC-RR, MC-LF and MC-YR), four non-MC cyanopeptides (anabaenopeptin A and B, aerucyclamide A and D), and non-cyanobacterial peptides (cyclosporine A,

fibrinopeptide B, leucine-enkephalin and oxytocin) over seven days of incubation. In addition, we evaluated the MC-LR degradation rate along a peptide mix composed of all eight previously tested cyanopeptides and in a *Microcystis aeruginosa* crude extract. Two bacteria were used and *Paucibacter toxinivorans* was efficiently able to degrade all cyanopeptides over 7 days incubation when individually added, except for MC-LR and –RR which were decreased approximately 85 and 90%, respectively. Moreover, when MC-LR was added into the peptide mix, the degradation rate decreased throughout incubation time and in the *Microcystis* crude extract was completely degraded over three days. *Paucibacter* had its biodegradation capacity decreased in the peptide mix not only for MC-LR but also for all four other MCs while non-MCs were not detected even at time 0. Furthermore, *Paucibacter* showed a great metabolic diversity to degrade non-cyanobacterial peptides efficiently over 7 days. This excludes oxytocin that was degraded about 50%, perharps due to its amino acid bonds. Thus, from a high biodegradation capacity for different peptides and great MC-LR degradation in cyanobacterial senescent scenarios, *Paucibacter toxinivorans* could be optimized as a potential biological tool for water treatment purposes.

Key-words: Cyanobacterial bloom; Cyanotoxins; Cyanopeptides; Secondary metabolites; Bacteria; Biodegradation

Introduction

Microbial communities have been described as crucial in the recycling and/or fixation of carbon, nitrogen, sulfur, and other elements on a global scale since they were first observed in previous century (Winogradsky, 1889 and 1890; Beijerinck, 1901). The phytoplankton community, for instance, displays an important role in aquatic environments mainly due to their oxygenic activity as primary producers. Among this group, cyanobacteria have been increasing worldwide and dominating water bodies that are heavily impacted by anthropogenic pollution from agricultural to domestic and industrial effluents (Parikh et al., 2006; Qin et al., 2015). Moreover, harmful cyanobacterial blooms can cause detrimental effects on aquatic ecosystems, particularly as they release a range of bioactive metabolites, many of which may be toxic to different trophic levels (Paerl and Otten, 2013).

An example are microcystins (MCs), the most reported cyanotoxins worldwide and ones with potential carcinogenic (Szlag et al., 2015; Meriluoto et al. 2017). MCs are cyclic heptapeptides that can include diverse L-amino acids in two variable positions and chemical variations in all their constituent amino acids. These variations generate about 250 congeners of this molecule, which MC-LR (with leucine in position two and arginine in position four) is one of most toxic and reported MCs (Szlag et al. 2015; Meriluoto et al. 2017; Bouaïcha et al., 2019). Regardless of MCs, cyanobacteria can produce many other peptides that are secondary metabolites from non-ribosomal synthetase pathways or polyketide synthetase. The latter includes such potentially toxic peptides as aeruginosins, microginins, anabaenopeptins, cyanopeptolins, cyclamides and microvidirins (Welker and von Dohren, 2006). When these kind of compounds are released into the water, many of them can maintain their stability regardless of environmental conditions and even steps of conventional water treatment, making it difficult to eliminate them from water (Harada et al., 1996; Ho et al., 2012). Then, bacterial biodegradation offers a safe alternative and low cost form for remediation of contaminated water from the toxic cyanobacterial compounds. The exploitation of biodegrading bacteria in water treatment has been increasing as a promising alternative to conventional approaches (Kumar et al., 2019).

Regarding MCs biodegradation, many authors have been contributing to the knowledge of isolated bacteria or microbial communities on the dynamics of biodegradation in different conditions (Jones et al., 1994; Edwards et al., 2008; Mou et al., 2013; Lezcano

et al., 2016; Kumar et al., 2019). For example, some studies have reported differences in nutrient availability and lag phase of bacteria as essential characteristics for biodegradation and its respective application on treatment approaches (Kumar et al., 2019).

Nonetheless, there is only one enzymatic pathway that has been described for MC-LR biodegradation, coded by *mlr* genes, to generate four enzymes MlrA, B, C and D by isolated *Sphingomonas* bacteria (Bourne et al., 1996 and 2001). The three first enzymes (MlrA, B and C) seem to make a linearization of cyclic structure by a hydrolytic cleavage at the Arg-Adda peptide bond. Then, the linearized MC-LR (H-Adda-Glu-Mdha-Ala-Leu-Me-Asp-Arg-OH) was hydrolyzed at the Ala-Leu peptide bond resulting in the formation of the tetrapeptide (H-Adda-Glu-Mdha-Ala-OH). MlrD is then involved in MC transportation to the outside membrane.

Although no other degradation pathway has been elucidated until now, authors have considered bacteria or microbial communities in general able to degrade MCs without any *mlr* genes, suggesting that further pathways are involved in biodegradation (Rapala et al., 2005; Edwards et al., 2008; Mou et al., 2013; Lezcano et al., 2016; Dziga et al., 2013 and 2017). Besides *mlr* genes undetection, there are other evidences to cover multiple pathways such as the nature of cleavage at specific amino acid bonds, the respective mode of enzymatic action and intermediates compounds generated by the process (Edwards et al., 2008; Dziga et al., 2013; Kreitz, 2016).

Among different degradation pathways, some isolated *mlr*+ or *mlr*- bacteria have been evaluated in order to compare their capability for MCs biodegradation in different culture conditions such as nutrient loading, temperature and cell density, all of which could influence the biodegradation process over a water treatment purpose (Park et al., 2001; Lezcano et al., 2016; Morón-Lopez et al., 2017). *mlr*+ *Sphingosinicella microcystinivorans* Y2 strain (Park et al., 2001; Saito et al., 2003; Maruyama et al., 2006) and *mlr*- *Paucibacter toxinivorans* 2C20 strain (Rapala et al., 2005) showed efficient degradation of MC-LR, -RR or –YR. With a particular focus on nutrient supply, Lezcano et al. (2016) observed a greater biodegradation from Y2 strain (*mlr*+) than 2C20 strain (*mlr*-) in environments with low nutrient availability such as minimal salt medium or reservoir water in which Y2 degraded over 24h and 2C20 over 50 hours. When both bacteria were supplied by diluted R2A culture media, *P. toxinivorans* 2C20 took a relatively long time of 120 hours to degrade 80% while *S. microcystinivorans* Y2 reached

total degradation in just over ten hours. In addition, Morón-Lopez et al., (2017) showed that *mlr*- bacteria was less efficient at degrading MC-LR after the addition of P, N and C and that temperatures ranging from 22º C to 32º C did not play an important role in biodegradation capability.

In addition to MCs biodegradation, few studies have evaluated the biodegradation of other cyanobacterial peptides. For example, in their observations of a cytoplasmic extract of *Sphingosinicella sp.* B-9 that was able to degrade MC-LR, Kato et al. (2007) observed enzymes that could also hydrolyze peptide bonds of a range of non-microcystins cyclic cyanopeptides without any lag time. In addition, the authors suggested that this fact is inherent to MC-degrading bacteria. Meanwhile, Kreitz (2016) observed a slight biodegradation of anabaenopeptins A and B – approximately 5% and 37% respectively – by MC-degrading *P. toxinivorans*.

Moreover, Briand et al. (2016) showed the ability of a natural bacterial community, recovered from *Microcystis* mucilage and added to an axenic *Microcystis* PCC 7806, in degrading extracellular cyanopeptides such as aerucyclamides and cyanopeptolines instead of MCs over three weeks. Recently, Torunska-Sitarz et al. (2018) examined a natural community able to degrade another toxic peptide nodularin, structurally very similar to MCs and observed an ability to degrade peptides from anabaenopeptins and spumigins families.

Although knowledge of bacteria able to degrade MCs for a potential biological treatment is increasing, few studies have explored the ability of bacteria to degrade other potentially toxic cyanobacterial metabolites besides the dynamics of compounds interaction on the efficiency of the biodegradation process.

Therefore, this present study aims to assess the ability of both MC-LR degrading bacteria to degrade many cyanobacterial peptides in individual or mix supplies. Besides that, we evaluated the MC-LR biodegradation rate along peptide mix or *Microcystis* crude extract as an approach for water treatment scenarios, since cyanobacterial cells can release many metabolites that could influence bacteria's capability to degrade them, especially the most toxic MC-LR. Moreover, we also test the general peptidase activity of *P. toxinivorans* against non-cyanobacterial peptides from different chemical structures and biolotical sources.

Methodology

Chemicals and reagents

All microcystins (MC-LR, DM-LR, MC-RR, MC-LF and MC-YR) and other cyanobacterial peptides such as Anabaenopeptin A and B (ANBP A and ANBP B, respectively), Aerucyclamide A and D (AERUCY A and AERUCY D, respectively) were obtained by purification from batch cultures of *Microcystis aeruginosa* PCC 7806 strain (Kreitz, 2016). The non-cyanobacterial peptides such as Cyclosporin A (CYCL A), [Glu^{1}]Fibrinopeptide-B (FIB), Leucine-Enkephalin (LEU-ENK) and Oxytocin (OXYT) as well as R2A bacterial culture media were purchased from SigmaAldrich® (United Kingdom). All peptides and R2A media were solubilised and prepared using ultrapure water at 18.2 MΩ.cm obtained by ELGA® ultrapure water systems (United Kingdom).

Bacterial strains and culture

Sphingosinicella microcystinivorans Y2 strain (Park et al., 2001) was kindly provided by Dr. Park from Shinshu University, Japan and *Paucibacter toxinivorans* 2C20 strain (Rapala et al., 2005) was obtained from Leibniz Institute DSMZ, the German Collection of Microorganisms and Cell Cultures GmbH (Germany). Both Y2 and 2C20 strains were streaked on R2A agar media (Reasoner and Geldreich, 1985) and incubated at 28º C over 72 hours. A single colony from each strain was initially transferred to 20 mL and grown at 150 rpm in a shaker incubator over 24 h at 28º C. Then, 1 mL was transferred to 100 mL and incubated again at the same conditions over 72 h in order to study their growth curve and respective mid log-phase by optical density at 600 nm (OD600).

To set all experiments, both strains were grown as subcultures in the same media and conditions (R2A media, 1:100 diluted in 100 mL of ultrapure water) over 24 h of incubation until they reached mid-log phase and OD were corrected to 0.4 with phosphate-buffer saline (PBS) before starting the experiment.

High throughput 96-wells microplate biodegradation experiments

Both OD-corrected strains were transferred to the 96-wells microplate in a solution with fresh culture media and respective peptide conditions. We applied two different

experimental set-ups considering cyanobacterial or non-cyanobacterial peptides in order to evaluate the biodegradation.

The first experimental set-up consisted of eight individual cyanobacterial peptides (DM-LR, MC-RR, MC-LF, MC-YR, ANBP A, ANBP B, AERUCY A and AERUCY D, with a final concentration of 10 μg mL^{-1} for each one) and an evaluation of MC-LR biodegradation rate (from the same concentration of 10 μg mL^{-1}) into three different metabolites supply such as:

1) only purified MC-LR;
2) a peptide mixture with all cyanopeptides previously tested (i.e., DM-LR, MC-RR, MC-LF, MC-YR, ANBP A, ANBP B, AERUCY A and AERUCY D) in a final concentration of 1 μg mL^{-1}. The peptide mix was pooled in R2A media to perform the experiment;
3) crude extract from *Microcystis aeruginosa* PCC 7806 obtained from a supernatant resulted by freezing-thawing (-80 ºC) and centrifuged over 15 minutes at 13,000 x g. The supernatant was diluted 1:10 in R2A media to perform the experiment.

The second experimental set-up consisted of individual biodegradation of four single non-cyanobacterial peptides (CYCL A, FIB, LEU-ENK and OXYT) in final concentrations of 10 μg mL^{-1}.

The final volume in each well was 5 μL of bacteria, 5 μL of purified peptides, and 140 μL of sterile R2A media, resulting in 150 μL total. For mixtures condition, the final 140 μL volume of fresh media were added already including the peptide mix or crude extract for both conditions. As negative control for biodegradation process, only peptides (5 μL on the same concentration) and media (145 μL) were added.

For all experimental conditions, three different microplates were set to get three different sampling times over 0, 3 and 7 days of incubation in a shaker incubator at 150 rpm and 28º C. This procedure was established in order to avoid multiple manipulations and consequent contamination. From each sampling time, 150 μL of methanol (80%) + formic acid (2%) were added to kill bacteria and stop their metabolism besides to precipitate large proteins, which could affect the analytical procedures. Thus, all volumes from each well were taken into clean 2 mL centrifuge tubes and centrifuged over 15 minutes at 13,000 x g. Supernatants were recovered and 1:10 diluted (100:900 μL) in

methanol 80% then stored at -20º C until UPLC-MS analysis. All experimental condition were carried out in triplicates (n=3).

UPLC-MS peptide analysis

All peptides studied here were analysed by UHPLC (Waters®, Manchester, UK) coupled to a Xevo TQ mass spectrometer (MS/MS) (Waters®, Manchester, UK). Chromatographic separation was carried out using a Waters Acquity UPLC BEH C18 column (1.7 µm, 2.1x100 mm) that was held at 60° C. Samples were kept in the sample manager at 10° C and the injection volume was 5 µL. The chromatographic run was conducted in a gradient mode with mobile phase of (A) water + 0.025% formic acid and (B) acetonitrile + 0.025% formic acid with a flow rate of 0.6 mL/min. The gradient consisted of 2% B initial condition rising to 25% B1 at 0.5 min holding until 1.5 min, rising to 40% B at 3.0 min, increasing further to 50% B at 4 min, a quick rise to 95% B and 4.1 min and held until 4.5 min before dropping back to 2% B at 5 min. The total run time was 5.5 min (Turner et al., 2017).

The Waters Xevo TQ parameters were 150° C source temperature, 600° C desolvation temperature, 600 L/hr desolvation gas flow, 150 L/hr cone gas flow and 0.15 mL/min of respective collision gas flow. Capillary voltage was held at 1.0 kV. Selected Reaction Monitoring (SRM) transitions (Supplementary material) were checked in the positive mode acquisition for all peptides.

The five MCs individually added into experiments were detected by UV-PDA considering 238 nm wavelength and a MC-LR calibration line while peptides in all other conditions were quantified considering MRM transitions (supplementary material).

Biodegradation rate, half-life and statistical analysis

Biodegradation of cyanobacterial peptides was also detailed from an exponential decay rate, the formula for which is represented by $Cy(t) = Cy_0 \times e^{-\lambda t}$; where Cy(t) is the respective cyanopeptide concentration ($ng.mL^{-1}$) at time t, Cy_0 is the concentration at day 0, and λ is the decay rate as decimal value (day^{-1}). In order to evaluate different responses besides degradation rate over 7 days of incubation, two calculations were made: over the first 3 days (t=3) and over the last 4 days of incubation (t=4).

Moreover, we also considered the half-life ($T_{1/2}$) for each cyanobacterial peptide when it reached approximately 50% of degradation according to biodegradation charts.

For MC-LR, biodegradation rate was considered in different conditions: purified MC-LR, MC-LR in the peptide mix, and MC-LR in the crude extract. ANOVA was applied to test the null hypothesis which was that the biodegradation rate between these conditions was the same; the alternative hypothesis considered them to be different ($p<0.05$). For non-cyanobacterial peptides, a pairwise t test comparison was applied considering conditions (treatment with bacteria and negative control with no bacteria) at time 0 and time 7 ($p<0.05$). All statistical analyses were carried out on Graphpad Prism 8.4.

Results

Throughout this study, we investigated the biodegradation of multiple cyanobacterial and non-cyanobacterial peptides over 7-days incubation by two bacterial strains already described as microcystins biodegraders. Additionally, we also carried out an evaluation regarding the biodegradation rate (day^{-1}) over 7 days of incubation (Supplementary Table 1) which we divided into the first three days and the last 4 days (Supplementary Table 2). Besides that, we evaluated a MC-LR biodegradation rate considering different conditions of metabolite supply.

Cyanobacterial peptide biodegradation

The cyanobacterial peptides were completely degraded by *Paucibacter toxinivorans* (2C20 strain) over 7 days when individually supplied, such as DM-LR, MC-LF, MC-YR (Figure 1B, D, and E, respectively) and ANBP A, B, AERUCY A, D (Figure 2A, B, C and D, respectively). However, MC-LR and MC-RR were not completely degraded and *Paucibacter toxinivorans* reached about 85-90% of biodegradation, respectively, over the time (Figure 1A and C).

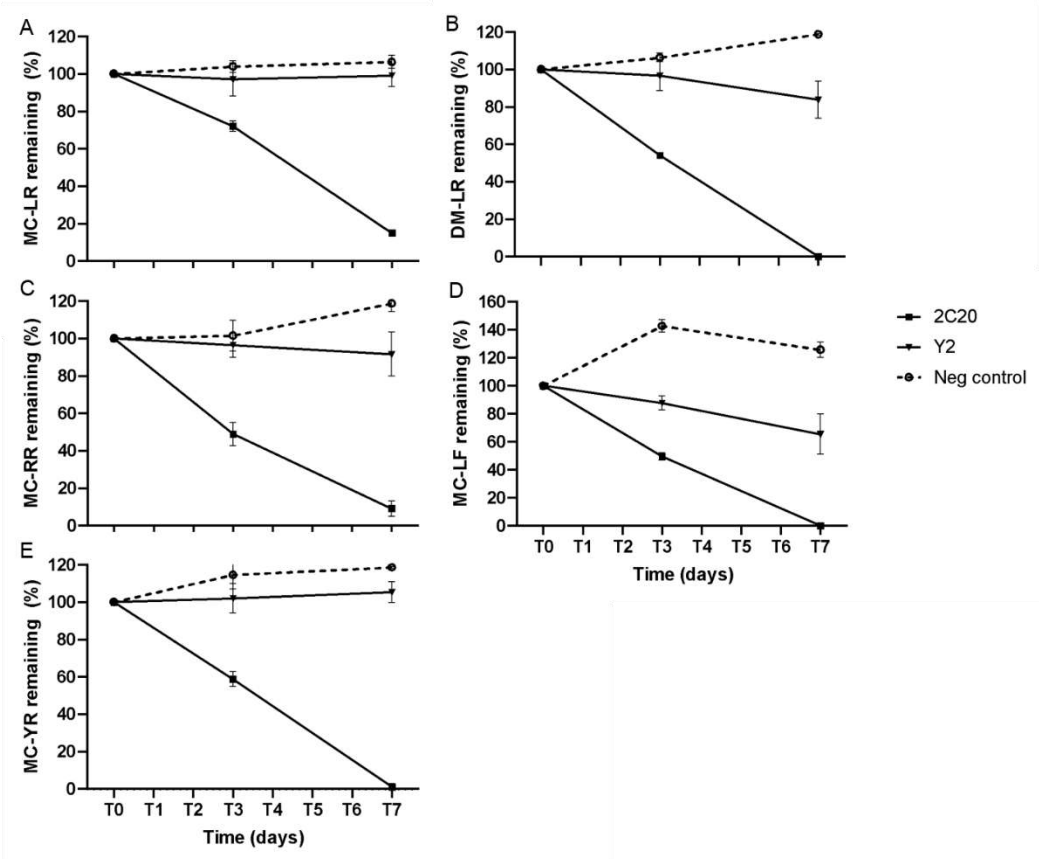

Figure 1: Biodegradation of five MCs by *Paucibacter toxinivorans* 2C20 strain and *Sphingosinicella microcystinivorans* Y2 strain over 7 days incubation. A) MC-LR, B) DM-LR, C) MC-RR, D) MC-LF and E) MC-YR. The data are expressed in percentages of the remaining concentrations of MCs, considering the average and standard deviation. The samples were taken in triplicate (n=3).

All non-microcystin peptides were degraded by 2C20 strain at a greater biodegradation rate (d^{-1}) than microcystins over 7 days (Supplementary Table 1), where AERUCY D was the most quickly degraded (λ= 1.117±0.02) whereas MC-LR was the least one (λ= 0.272±0.01) (Supplementary Table 1). Within MCs variants, MC-YR had the highest biodegradation rate (λ= 0.544±0.04 – Supplementary Table 1) with $T_{1/2}$ = 3.5 days while MC-LR had the lowest biodegradation rate as cited above with a $T_{1/2}$ of about 4.5 days (Figure 1).

Interestingly, ANBP A, ANBP B, AERUCY A, and AERUCY D were completely degraded in the first three days (Figure 2), which could also be seen from a very high biodegradation rate over this time (ANBP A: λ=2.363±0.007; ANBP B: λ=2.350±0.037; AERUCY A: λ=1.643±0.002 and AERUCY D: λ=2.607±0.044) (Supplementary Table 2). On the other hand, all MCs were intensely degraded in the last 4 days (DM-LR: λ=0.719±0.003; MC-RR: λ=0.435±0.095; MC-LF: λ=0.478±0.012 and λ=0.819±0.092) rather than in the first three days (DM-LR: λ=0.203±0.005; MC-RR: λ=0.240±0.04; MC-LF: λ=0.233±0.017 and λ=0.177±0.023) (Supplementary Table 2).

Regarding the biodegradation capability of *Sphingosinicella microcystinivorans* (Y2 strain), we observed a much lower or non-existent ability to degrade them. For DM-LR and MC-RR, it reached an average of 15% for both respectively (Figure 1A and B, respectively) while for MC-LF, the Y2 strain reached a biodegradation of 20% over the time. Y2 bacteria was not able to degrade any amount of MC-LR or MC-RR.

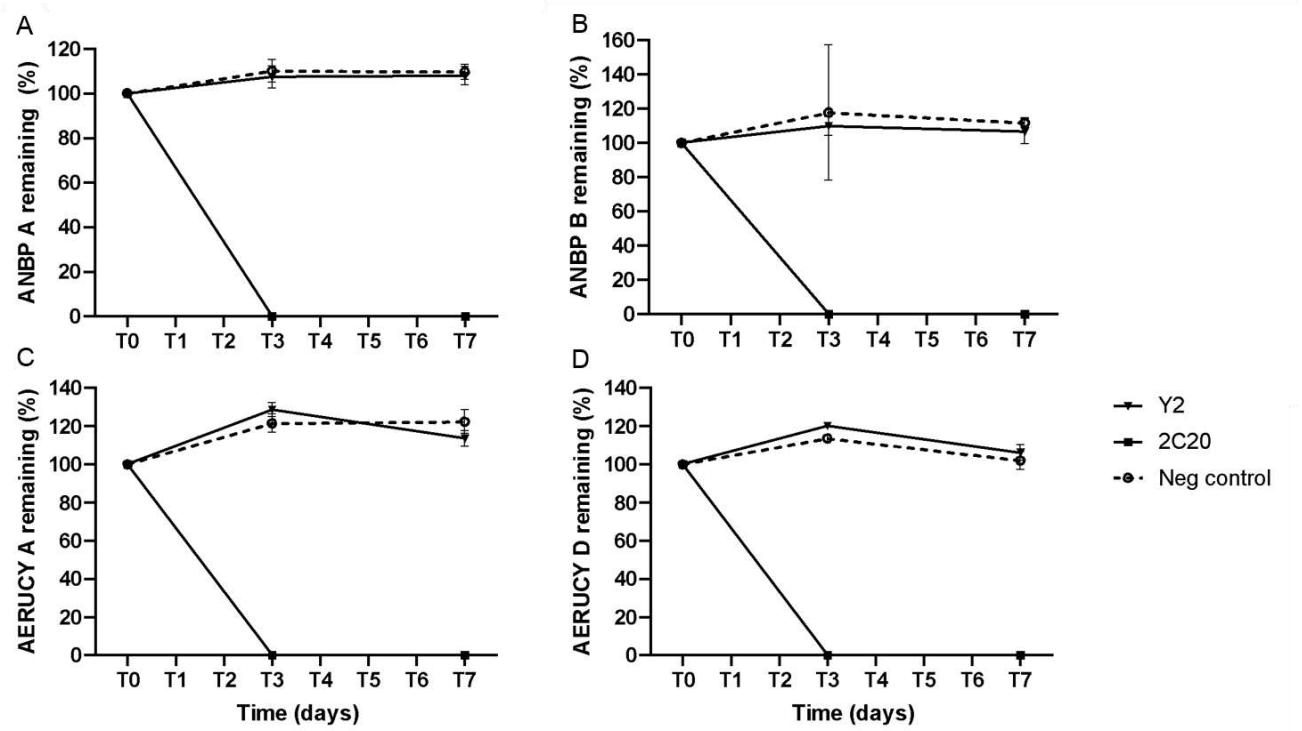

Figure 2: Biodegradation of four non-microcystin cyanobacterial peptides by *Paucibacter toxinivorans* 2C20 strain and *Sphingosinicella microcystinivorans* Y2 strain over 7 days in incubation. A) Anabaenopeptin A, B) Anabaenopeptin B, C) Aerucyclamide A, D) Aerucyclamide D. The data are expressed in percentage of remained concentration of peptides considering the average and standard deviation. The samples were taken in triplicate (n=3).

MC-LR biodegradation in different metabolites supply

As seen before, when MC-LR was the single peptide added to the *Paucibacter toxinivorans* degrader, there was about 85% of degradation over 7 days (Figure 1A) with a respective decay rate of λ=0.272±0.01 and $T_{1/2}$=4.5 days. Besides that, we could also observe almost four times the amount of degradation in the last 4 days (λ=0.394±0.002) as in the first three days (λ=0.109±0.013) of incubation. Y2 was not able to degrade individual MC-LR over 7 days.

Nonetheless, MC-LR was offered to both bacteria from the same concentration (10 μg mL^{-1}) into two different conditions: i) in a peptide mixture consisting of all cyanobacterial previously tested in a final concentration of 1 μg mL^{-1}; and ii) in a *Microcystis aeruginosa* crude extract. MC-LR in the peptide mix reached about 60% biodegradation by *Paucibacter toxinivorans* over the given amount of time (Figure 3A) and had a lower

decay rate (λ=0.162±0.008) compared to the conditions when it was the only cyanobacterial peptide added (λ=0.272±0.01) (Supplementary Table 1). Based on this, MC-LR half-life has increased in peptide mix to about 5.5 days.

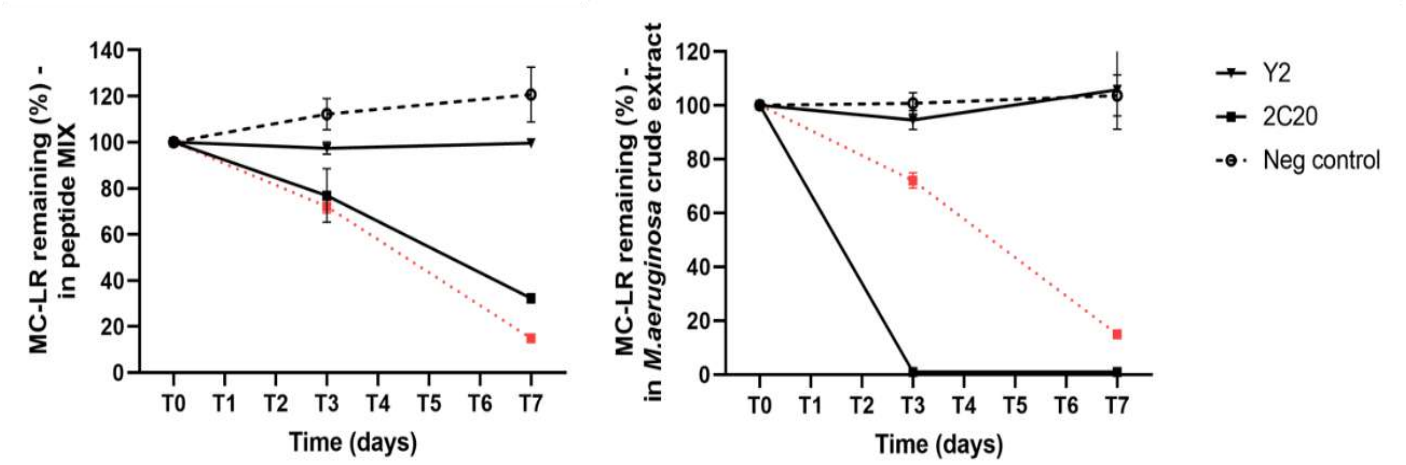

Figure 3: Biodegradation of MC-LR in different condition as peptide mix (A) and *Microcystis aeruginosa* PCC 7806 crude extract (B) over 7 days incubation *by Paucibacter toxinivorans* 2C20 strain and *Sphingosinicella microcystinivorans* Y2 strain. The peptide mix consisted of eight cyanobacterial peptides (four MCs and four non-MCs) used in the experiments. The dashed red line represents biodegradation of a single MC-LR by *Paucibacter toxinivorans*. The data are expressed in percentage of remained concentration of peptides considering the average and standard deviation. The samples were taken in triplicate (n=3).

From the peptide mix conditions, we assessed not only MC-LR biodegradation but also each peptide that was spiked in a final concentration of 1 μg mL^{-1} (Figure 4). We observed that not all MCs were completely degraded over 7 days by *Paucibacter toxinivorans* and MC-YR had the highest degradation. MC-YR and DM-LR (MC-LR with a demethylation on MeAsp residue) both reached about 70% while MC-RR and MC-LF had on average 45% and 35% of degradation respectively (Figure 4A). The biodegradation rate dropped greatly for all MCs and particularly for MC-LF whose rate decreased almost 7 times (λ=0.054±0.007). Y2 bacteria did not show any biodegradation capability for the four MCs tested.

Interestingly, we could not detect any non-microcystin peptides (ANBP A and B, AERUCY A and D) over 7 days even at time 0 from *P. toxinivorans* conditions; yet, from

Y2 strain, a slight degradation was observed just for AERUCY A and D (10 and 20%, respectively). We can consider a very quick biological degradation of all non-microcystins peptides by *P. toxinivorans* since all of them were detected in Y2 and negative control. The peptide mix had been prepared in a single vial and then added to each well. Moreover, all three microplates were simultaneously set up, thus initial sampling times (T0) were taken in an interval of 20-30 minutes.

Concerning the MC-LR spiked into *Microcystis aeruginosa* crude extract, we observed a most intense degradation by *P. toxinivorans* that was able to degrade completely over 3 days at an elevated decay rate ($\lambda = 2.33 \pm 0.007$). Nonetheless, the MC-LR half-life decreased substantially, reaching 1.5 days as opposed to 5.5 days (peptide mix) or 4.5 days (single condition). The Y2 strain retained its slight to non-existent biodegradation capability in both the peptide mix as well as in the *Microcystis* crude extract.

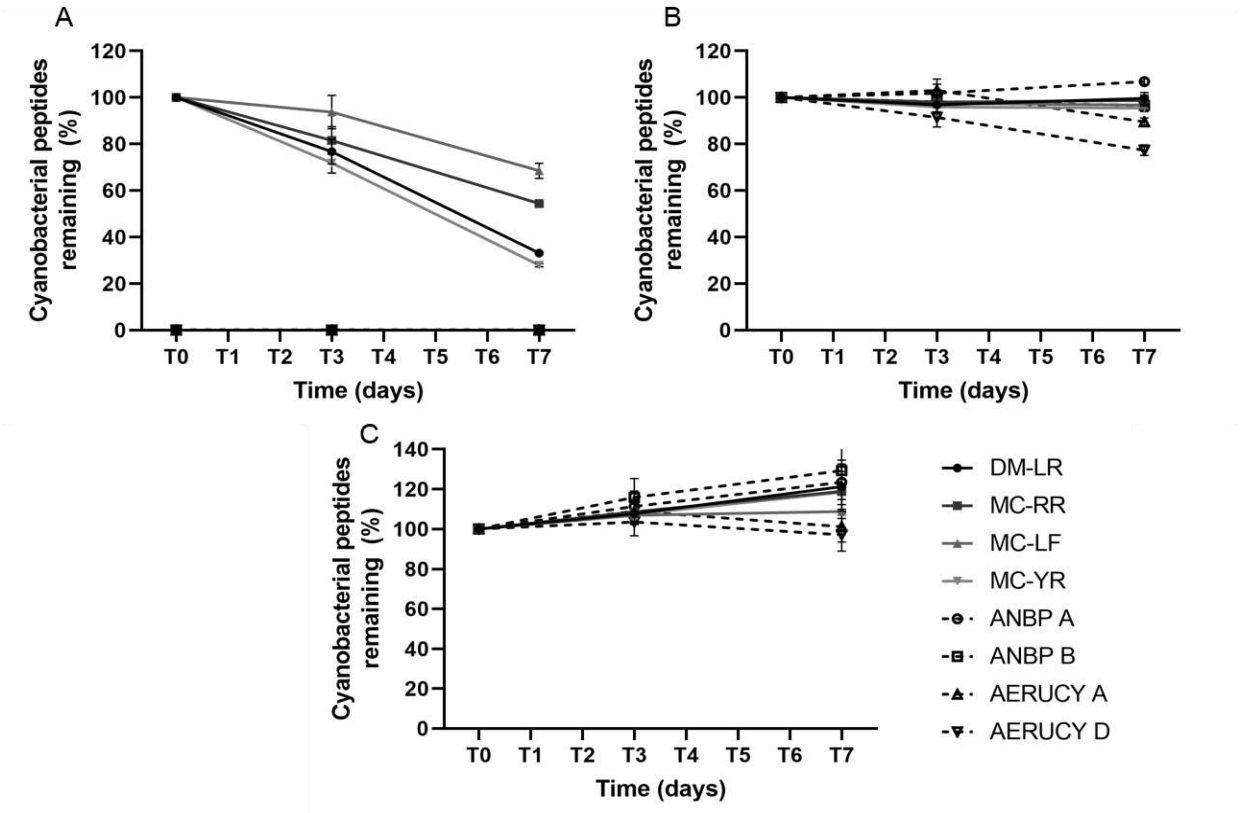

Figure 4: Biodegradation of each cyanobacterial peptide in mix condition by (A) *Paucibacter toxinivorans* 2C20 strain, (B) *Sphingosinicella microcystinivorans* Y2 strain and (C) in negative control. The data are expressed in percentage of remained concentration of peptides considering the average and standard deviation. The samples were taken in triplicate (n=3).

Moreover, Figure 5 summarises the MC-LR biodegradation rates between conditions from the peptide mix to the crude extract over both the first three days (A) and the total incubation time (B). Although MC-LR was completely degraded over 3 days in the crude extract, we can still observe a large difference in decay rates if we consider the calculation using the total incubation time (Figure 5B).

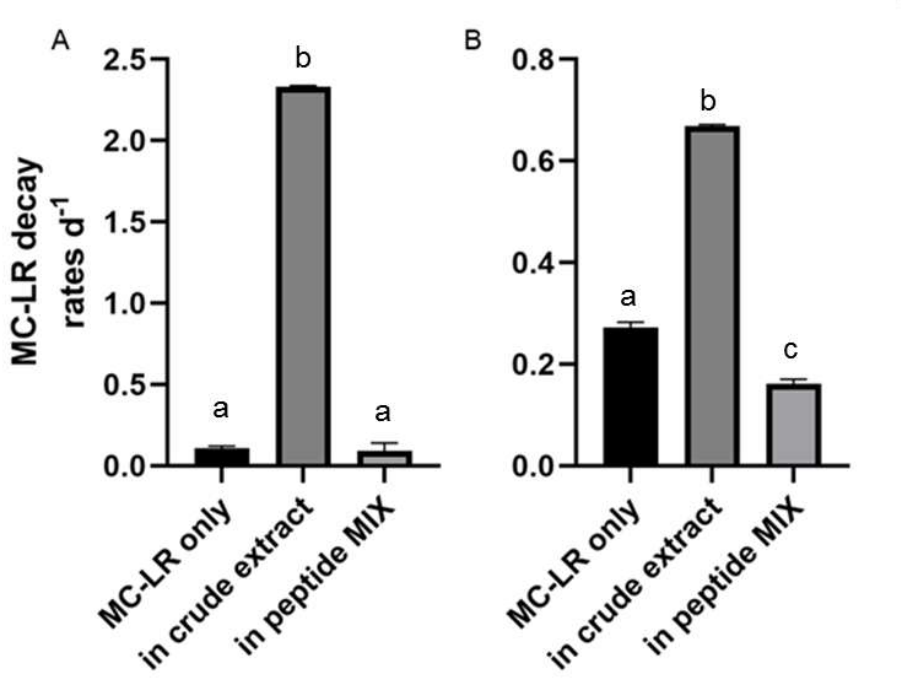

Figure 5: Exponential decay rate λ (d^{-1}) of MC-LR by *Paucibacter toxinivorans* in different conditions such as single MC-LR, in peptide mix, and in *Microcystis* crude extract over the first three days (A) and over the total incubation time (B). Different small letters mean statistical difference between conditions according to one-way ANOVA ($p<0.05$) and Tukey's *post hoc.*

Non-cyanobacterial peptides biodegradation by *Paucibacter toxinivorans*

Since *P. toxinivorans* successfully degraded all cyanobacterial peptides, we carried out an evaluation of its capability to degrade other peptides of different sources and chemical structures.

As well as cyanobacterial peptides, *P. toxinivorans* was able to degrade completely fibrinopeptide B, leucine-enkephalin, and oxytocin over 7 days of incubation. For cyclosporin A, the degradation was about 50% over the course of the incubation time.

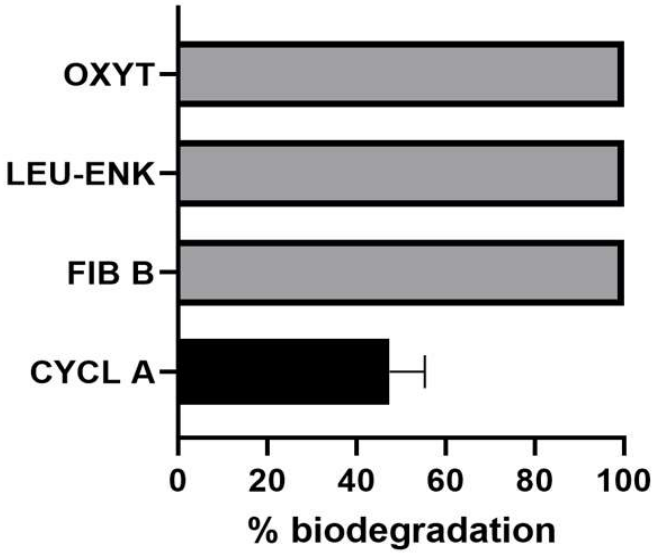

Figure 6: Biodegradation of non-cyanobacterial peptides by *Paucibacter toxinivorans* over 7 days incubation. The different colors represent complete degradation (black) or partial degradation (grey) over the incubation time. The data are expressed in percentage of remained concentration of peptides considering the average and standard deviation. The samples were taken in triplicate (n=3).

Discussion

In this current study, we evaluated the capability of two different bacteria to degrade a range of peptides. Both were previously described as MC degraders (Park et al., 2001; Rapala et al., 2005; Maruyama et al., 2006) as well as described by the presence of *mlr* pathway in studies regarding MC biodegradation, which they were used as positive controls (Lawton et al., 2011; Lezcano et al., 2016; Móron-Lopez et al., 2017).
Sphingosinicella microcystinivorans (Y2 strain) had been classified as *mlr* + (Saito et al., 2003) and was able to degrade MC-LR, -RR, and –YR over an incubation time of 3 to 7 days; moreover, it demonstrated strong biodegradation capability at high temperatures, eg.: 30˚ C and 35º C (Park et al., 2001; Maruyama et al., 2006). In addition, Lezcano et al., (2016) observed degradation from an initial concentration of 1 mg L^{-1} equivalent of MC-LR in different nutrient conditions over a course of 5 days. In addition, Y2 completely degraded MC-LR over 10 hours in a high TOC and TN, unlike *Paucibacter toxinivorans* (2C20 strain) which took 120 hours to degrade in these same conditions. The

latter was able to degrade successfully over 50 hours in low nutrient conditions (i.e., reservoir water and minimal salt medium). However, in our experiments, Y2 did not efficiently degrade any cyanobacterial peptides in different nutritional supplies such as the peptide mix or *Microcystis aeruginosa* crude extract. An interesting hypothesis is that the Y2 bacteria possibly diminished its ability to degrade MCs since it was maintained for a long time on successive cultures in the laboratory.

P. toxinivorans (2C20), on the other hand, has other biodegradation pathway than *mlr* because it does not have the corresponding genes (Lezcano et al., 2016). *Mlr* cluster genes were, until now, the unique enzymatic pathways described for MCs (Bourne et al., 1996 and 2001), although many researchers have been pointing to other possible pathways not yet described (Edwards et al., 2008; Manage et al., 2009; Mou et al., 2013; Lezcano et al., 2016, Moron-Lopez et al., 2017). Nevertheless, a microorganism should not necessarily have an enzymatic pathway to degrade a specific compound, and a single microbe can be responsible for the degradation of a broad range of substances (Seo et al., 2009; Wackett, 2013).

Then, *P. toxinivorans* was able to degrade successfully all peptides when they were individually offered. In addition, we can observe a bi-phasic degradation of MCs in that degradation from the last four days was much higher than during the first three days. Our results also support that idea that MC-LR degrades less than other MCs over 7 days, an observation which opposes other authors who have suggested MC-LR as the more easily degradable MCs compared to MC-RR, -LF, and -YR (Yang et al., 2014; Kreitz, 2016). Previously, Lawton et al. (2011) observed a higher biodegradation of MC-LF, compared to that of MC-LR and MC-RR, by *P. toxinivorans*, a similar observation by our findings. However, the 2C20 strain took a long time to degrade (i.e., 10 days to reach 50% degradation). This was much slower than our current results, which showed that all single microcystins were effectively degraded over 7 days with a half-life of approximately 4 days.

However, its biodegradation capability decreased when cyanobacterial peptides were disposed as a mix, reaching about 45-35% for MC-RR and MC-LF, respectively. Edwards et al. (2008) observed different behavior in MC-LR biodegradation by a natural microbial community when only MC-LR was added compared to a mix with the three other MCs ([D-Asp^3]MC-RR, MC-LF and MC-LW) and nodularin. When the mix was added to Rescobie Loch water, MC-LR half-life increased from 4.5 to 13 days; it was completely degraded in Forfar Loch water over 11 days. When MC-LR was the only peptide added

to the Forfar Loch water, only 30% was degraded in eleven days. In the *Bordetella sp.* strain MC-LTH1, Yang et al. (2014) observed a similar biodegradation rate for both MC-RR and MC-LR in mix over 42h; however, degradation occurred more quickly when both MCs were individually added (MC-RR: 30h and MC-LR: 36h). According to Li et al. (2015), biodegradation of MCs by biofilms-forming bacteria did not show any difference when exclusively offered or in a mix condition. Here, MC-LR had a slower decay rate when added in a peptide mix instead individual one. About this, MC-LR had the second highest biodegradation rate within MCs in peptide mix, falling behind MC-YR, which was the most degraded in both individual and mixed-in conditions. Even at one tenth less than the initial concentration of MC-LR, all four MCs in mix were degraded at a lesser rate by *P. toxinivorans.* This could be attributed to the structure of MCs, multiple toxins supplied, or even to a high energetic effort necessary to produce multiple enzymes to act at specific amino acid bonds simultaneously. Nevertheless, *P. toxinivorans* showed strong biodegradation capability at a higher concentration of toxins. Remarkably, when MC-LR was added into a *Microcystis* crude extract it was completely degraded over 3 days with a half-life of 1.5 days and showed the highest decay rate considering all conditions. Rapala et al. (1994) had previously observed a rapid MC biodegradation when crude extracts of microcystin-containing *Microcystis* were incubated in water or sediment samples taken from a eutrophic lake throughout a cyanobacterial-bloom. According to the authors, a bacterial community was able to degrade both MC-LR and [D-Asp3]MC-LR within 4 days in bloom-lysate conditions. Similarly, Christoffersen et al. (2002) observed a very quick degradation in cyanobacterial crude extract from a concentration of 54 μg L^{-1}, reaching complete removal in 4 days. This increased capability to degrade MC-LR can be subsequently because a wide variety of organic compounds not only peptides are released after cell disruption and it can stimulate a faster degradation. This fact was already observed in superior organisms as root exudates in the presence of carbon in soil, which stimulated bacteria to degrade specific organic compounds (Sarma and Prasad, 2016). This fact might be interesting for water treatment purposes when metabolite-releasing cyanobacterial blooms require rapid treatment and conventional treatments are not applicable or sufficient.

Irrespective of MC degradation, *P. toxinivorans* completely degraded four other cyanobacterial peptides over 3 days in incubation at a higher degradation rate than MCs using the same culture conditions (28º C, 150 rpm, and initial concentration of 10 μg mL^{-1}). Aerucyclamides have a cyclic hexapeptide structure of three azole or azoline rings

likely derived from cysteine and threonine modification (Portmann et al., 2008) while anabaenopeptins have cyclic peptides with a characteristic ureido bond connecting the primary amine group with the carboxyl group of the neighboring amino acid to form an amide bond (Harada et al., 1995; Welker et al., 2006).

For the first time, we are showing a complete biodegradation of other phosphatase inhibitors in the anabaenopeptin family. Kato et al. (2007) and Kreitz (2016) showed a very low to non-existent degradation for variants of this family. Moreover, Kreitz (2016) evaluated biodegradation from the same *P. toxinivorans* 2C20 strain and recorded biodegradation of 4 and 37% for anabaenopeptin A and B, respectively. The difference between the Kreitz' findings and those of this current study could be attributed to the culture maintenance or culture media since nutrient broth was previously used while we used R2A broth in all experiments.

Moreover, from a cytoplasmic extract obtained by MC-degrading *Sphingomonas* bacteria, Kato et al. (2007) also observed a degradation of other non-microcystin cyanobacterial peptides such as microviridin, microcyclamide, aeruginopeptin, and microcystin. Furthermore, they used broad acting enzymes from *mlr* containing-*Sphingomonas* on biodegradation of those non-microcystin peptides since bacterial cell extract was applied to evaluate it. Nevertheless, we showed that peptides other than microcystins – such as anabaenopeptin A, B and aerucyclamide A, D for example – were quickly degradable by *non-mlr* bacteria cultured along all peptides, suggesting no relation to the enzymatic pathway previously described. Moreover, these peptides were completely degraded after 3 days, degrading at a higher decay rate. Curiously, they might degrade in an interval of 30 minutes in peptide mix as they were not detected even at time 0 within *P. toxinivorans* condition.

We also evaluated the ability of *P. toxinivorans* to degrade not only peptides from cyanobacterial organisms but also from other sources and chemical structures such as cyclosporine A (cyclic peptide from eukaryote), [Glu^1]fibrinopeptide B (linear peptide from human), leucine-enkephalin (linear pentapeptide from eukaryote), and oxytocin (linear peptide vasopressin human hormone). With that exception of cyclosporine A that was ~50% degraded after 7 days, all three peptides were completely degraded. Cyclosporine is a cyclic peptide containing a disulfide bond between its Cys residues in cyclic structure as well as different amino acids bonds than MCs such as Tyr-Ile-Gln-Asn (Du Vigneaud et al., 1953; Wisniewski et al., 2013) that can be more complex to degrade than linear peptides. Nonetheless, it was also able to degrade non-cyanobacterial peptides

such as human peptides, which shows its large metabolic diversity and capability to be used for remediation purposes.

Furthermore, *P. toxinivorans* was able to grow broad-spectrum antibiotics like gramicidin C and polymyxin B over 7 days in incubation (data not shown) but we could not evaluate its degradation capability. This information may be important for the safe utilization of bacteria in water treatment as many antibiotics are released into the water daily (Guha Roy, 2019) and could disturb the efficiency of the biological treatment.

However, because water bodies worldwide are increasingly being polluted with a range of potentially harmful substances, it is extremely important to expand the research into biodegradation and remediation approaches in order to evaluate the bacterial capabilities for degrading a wide range of compounds.

Conclusion

From this study, we investigated the capability of already known microcystin-degraders to degrade both other cyanobacterial peptides as well as non-cyanobacterial peptides. In our study, *Sphingosinicella microcystinivorans* (Y2 strain) lost its efficient capability to degrade MCs and was unable to degrade other peptides under laboratory maintenance conditions. Meanwhile *Paucibacter toxinivorans* (2C20 strain) demonstrated a high biodegradation rate, degrading all peptides over the 7 days of incubation and thereby showing its wide physiological capability to degrade peptides with different chemical structures and production sources.

Moreover, the 2C20 strain was able to degrade MC-LR at a higher rate from a *Microcystis aeruginosa* PCC 7806 crude extract condition than purified MC-LR and MC-LR in a peptide mixture. Thus, it could be successfully used for water treatment purposes when there is a MC-producing cyanobacterial bloom and a possible senescence phase as many chemical metabolites besides peptides are released into the water body. However, other studies are needed in order to better understand the biodegradation and consequent non-toxicity of those metabolites that can be released by cyanobacterial species.

References

Beijerinck, M.W. (1901). Ueber oligonitrophile Mikroben. Zentr. Bakt. Parasitenk., II, 7, 561-582.

Briand, E., Humbert, J.F., Tambosco, K., Bormans, M., Gerwick, H. (2016). Role of bacteria in the production and degradation of Microcystis cyanopeptides. Microbiologyopen. Jun; 5(3): 469–478. doi: 10.1002/mbo3.343

Bouaïcha, N., Miles, C.O., Beach, D.G., Labidi, Z., Djabri, A., Benayache, N.Y., Nguyen-Quang, T., (2019). Structural Diversity, Characterization and Toxicology of Microcystins. Toxins, 11(12), 714. https://doi.org/10.3390/toxins11120714

Bourne, D.G., Jones, G.J., Blakeley, R.L., Jones, G.J., Negri, A.P., Riddles, P., (1996). Enzymatic pathway for the bacterial degradation of the cyanobacterial cyclic peptide toxin microcystin LR. Appl. Environ. Microbiol. 62, 4086–4094.

Bourne, D.G., Riddles, P., Jones, G.J., Smith, W., Blakeley, R.L., (2001). Characterization of a gene cluster involved in bacterial degradation of the cyanobacterial toxin microcystin LR. Environ. Toxicol. 16, 523–534.

Christoffersen, K., Lyck, S., Winding, A. (2002). Microbial activity and bacterial community structure during degradation of microcystins. Aquat. Microb. Ecol. 27, 125–136. doi:10.3354/ame027125

Du Vigneaud, V., Ressler, C., Trippett, S. (1953). The sequence of amino acids in oxytocin, with a proposal for the structure of oxytocin. J Biol Chem. 205(2):949-957.

Edwards, C., Graham, D., Fowler, N., Lawton, L.A. (2008). Biodegradation of microcystins and nodularin in freshwaters. Chemosphere 73:1315-132. https://doi.org/10.1016/j.chemosphere.2008.07.015

Guha Roy, A. (2019). Antibiotics in water. Nature Sustainability 2, 356 https://doi.org/10.1038/s41893-019-0295-1

Harada, K., Fujii, K., Shimada, T., Suzuki, M., Sano, H., Adachi, K., et al. (1995). 2 cyclic-peptides, anabaenopeptins, a 3rd group of bioactive compounds from the cyanobacterium Anabaena-flos-aquae NRC-525-17 Tetrahedron Lett, 36 (1995), pp. 1511-1514

Harada, K., Imanishi, S., Kato, H., Mizuno, M., Ito, E., Tsuji, K. (2004). Isolation of Adda from microcystin-LR by microbial degradation. Toxicon 44:107-109. https://doi.org/10.1016/j.toxicon.2004.04.003

Kato, H., Imanishi, S.Y., Tsuji, K., Harada, K-I. (2007). Microbial degradation of cyanobacterial cyclic peptides. Water research 41, 1754 – 1762. doi: 10.1016/j.watres.2007.01.003

Kreitz, J. (2016). Evidence for functional drift of bacterial isolates in response to cyanobacterial microcystin-lr and multiple peptide degradation in paucibacter toxinivorans. Robert Gordon University, MPhil thesis.

Kumar, P., Hegde, K., Brar, S.K., Cledon, M., Kermanshahi-Pour, A. (2019). Potential of biological approaches for cyanotoxin removal from drinking water: A review. Ecotoxicol Environ Saf. 172:488-503. doi:10.1016/j.ecoenv.2019.01.066

Lezcano, M.A., Moron-Lopez, J., Agha, R., Lopez-Heras, I., Nozal, L., Quesada, A., El-Shehawy, R. (2016). Presence or absence of mlr genes and nutrient concentrations co-determine the microcystin biodegradation efficiency of a natural bacterial community. Toxins 8:E318. doi: 10.3390/toxins8110318

Li, J.M., Shimizu, K., Akasako, H., Lu, Z.J., Akiyama, S., Goto, M., Utsumi, M., Sugiura, N. (2015). Assessment of the factors contributing to the variation in microcystins biodegradability of the biofilms on a practical biological treatment facility. Bioresour. Technol. 175, 463–472. doi: 10.1016/j.biortech.2014.10.047

Meriluoto, J., Spoof, L., Codd, G.A. (Eds.) (2017). Handbook of Cyanobacterial Monitoring and Cyanotoxin Analysis, 1st edition. Wiley 576p. ISBN: 978-1-119-06868-6.

Morón-López, J., Nieto-Reyes, L., El-Shehawy, R. (2017). Assessment of the influence of key abiotic factors on the alternative microcystin degradation pathway(s) (mlr −): A detailed comparison with the mlr route (mlr +). Sci. Total Environ. 599, 1945–1953. https://doi.org/10.1016/j.scitotenv.2017.04.042. 600.

Mou, X., Lu, X., Jacob, J., Sun, S., Heath, R. (2013). Metagenomic identification of bacterioplankton taxa and pathways involved in microcystin degradation in lake erie. PLoS One. 2013;8(4):e61890. doi:10.1371/journal.pone.0061890

Paerl, H.W. and Otten, T.G. (2013). Harmful cyanobacterial blooms: causes, consequences, and controls. Microb Ecol. 65(4):995-1010. doi:10.1007/s00248-012-0159-y

Parikh, A., Shah, V., Madamwar, D. (2006). Cyanobacterial Flora from Polluted Industrial Effluents. Environ Monit Assess 116, 91–102 . https://doi.org/10.1007/s10661-006-7229-x

Portmann, C., Blom, J.F., Gademann, K., Jüttner, F. (2008). Aerucyclamides A and B: isolation and synthesis of toxic ribosomal heterocyclic peptides from the cyanobacterium Microcystis aeruginosa PCC 7806. J Nat Prod.71(7):1193-1196. doi:10.1021/np800118g

Qin, B., Li, W., Zhu, G., Zhang, Y., Wu, T., Gao, G. (2015). Cyanobacterial bloom management through integrated monitoring and forecasting in large shallow eutrophic Lake Taihu (China). J Hazard Mater. 287:356-363. doi:10.1016/j.jhazmat.2015.01.047

Rapala, J., Lahti, K., Sivonen, K., Niemela¨, S. I. (1994). Biodegradability and adsorption on lake sediments of cyanobacterial hepatotoxins and anatoxin-a. Lett. Appl. Microbiol. 19, 423–428.

Rapala, J., Berg, K. A., Lyra, C., Niemi, R. M., Manz, W., Suomalainen, S., Paulin, L., and Lahti, K. (2005). Paucibacter toxinivorans gen. nov., sp. nov., a bacterium that degrades cyclic cyanobacterial hepatotoxins microcystins and nodularins. Int. J. Syst. Evol. Microbiol. 55, 1563–1568. doi:10.1099/ijs.0.63599-0

Reasoner, D.J. and Geldreich, E.E. (1985). A new medium for the enumeration and subculture of bacteria from potable water. Applied Environmental Microbiology, 49(1): 1–7

Sarma, H., and Prasad, M.N.V. (2016). Phytomanagement of Polycyclic Aromatic Hydrocarbons and Heavy Metals-Contaminated Sites in Assam, North Eastern State of India, for Boosting Bioeconomy. Bioremediation and Bioeconomy, 609–626. doi:10.1016/b978-0-12-802830-8.00024-1

Seo, J.S., Keum, Y.S., Li, Q.X. (2009). Bacterial degradation of aromatic compounds. Int J Environ Res Public Health. 6(1):278-309. doi:10.3390/ijerph6010278

Szlag, D.C., Sinclair, J.L., Southwell, B., Westrick, J.A. (2015) Cyanobacteria and Cyanotoxins Occurrence and Removal from Five High-Risk Conventional Treatment

Drinking Water Plants. Toxins (Basel). 7(6):2198-2220. Published 2015 Jun 12. doi:10.3390/toxins7062198

Turner, A.D., Waack, J., Lewis, A., Edwards, C., Lawton, L. (2018). Development and single-laboratory validation of a UHPLC-MS/MS method for quantitation of microcystins and nodularin in natural water, cyanobacteria, shellfish and algal supplement tablet powders. Journal of Chromatography B, 1074-1075, 111–123. doi:10.1016/j.jchromb.2017.12.03

Toruńska-Sitarz, A., Kotlarska, E., Mazur-Marzec, H. (2018). Biodegradation of nodularin and other nonribosomal peptides by the Baltic bacteria. International Biodeterioration & Biodegradation 134:48-57. doi:10.1016/j.ibiod.2018.08.004

Wackett, L.P. (2013). The Metabolic Pathways of Biodegradation. The Prokaryotes, 383–393. doi:10.1007/978-3-642-31331-8_76

Welker, M., Marsálek, B., Sejnohová, L., von Döhren, H. (2006). Detection and identification of oligopeptides in Microcystis (cyanobacteria) colonies: toward an understanding of metabolic diversity. Peptides. 27(9):2090-2103. doi:10.1016/j.peptides.2006.03.014

Welker, M. and von Döhren, H. (2006). Cyanobacterial peptides - nature's own combinatorial biosynthesis. FEMS Microbiol Rev. 30(4):530-563. doi:10.1111/j.1574-6976.2006.00022.x

Winogradsky, S. (1889). Recherches physiologiques sur les sulphobacteries. Annales de I'Institut Pasteur 3:49-60

Winogradsky, S. (1890a). Sur les organisms de la nitrification. Comptes Rendus de l'Academie des Sciences 110:1013-1016

Wiśniewski, K., Finnman, J., Flipo, M., Galyean, R., Schteingart, C. D. (2013). On the mechanism of degradation of oxytocin and its analogues in aqueous solution. Biopolymers, 100(4), 408–421. doi:10.1002/bip.22260

Yang, F., Zhou, Y., Sun, R., Wei, H., Li, Y., Yin, L., Pu, Y. (2014). Biodegradation of MC-LR and –RR by a novel microcystin-degrading bacteria isolated from Taihu lake. Biodegradation, 25:447-457. doi:10.1007/s10532-013-9673-y

5 DISCUSSÃO GERAL

O presente trabalho contemplou o estudo de possíveis estratégias no controle de florações de cianobactérias e remediação de seus metabólitos, um problema que tem sido amplamente reportado ao redor do mundo. Dentro desse contexto, este trabalho apresenta os efeitos do uso do peróxido de hidrogênio nos parâmetros limnológicos e na comunidade microbiana de um reservatório de água usado para abastecimento público, impactado de maneira recorrente por florações de cianobactérias. Além de avaliar a supressão específica de cianobactérias, apresentamos informações sobre a alteração da composição da comunidade bacteriana decorrente do tratamento. Em paralelo, também exploramos um outro aspecto relevante para a melhoria da qualidade de corpos d'água impactados por florações de cianobactérias, a degradação biológica de metabólitos secundários produzidos por esses organismos. Mais especificamente, caracterizamos uma comunidade microbiana originária de um ambiente impactado por florações de cianobactérias e capaz de degradar MC-LR. Também foi investigada a capacidade de linhagens bacterianas degradarem cianopeptídeos diversos e peptídeos de diferentes estruturas químicas e origens biológicas.

5.1 Mitigação de uma floração de cianobactérias em um reservatório de água para abastecimento e efeitos no bacterioplâncton

No estudo realizado no reservatório do Gavião (Fortaleza, Ceará) foi possível observar, a partir da aplicação de 10 mg L^{-1} de H_2O_2 na escala de mesocosmos, que o tratamento causou a supressão de grupos fitoplanctônicos como cianobactérias, algas verdes e diatomáceas (de acordo com estimativa da concentração de clorofila para cada um desses grupos) nas primeiras 24 e 72h após a aplicação, sendo este último o tempo de extinção do H_2O_2 no sistema. A composição inicial da comunidade de cianobactérias foi identificada por análise de metagenômica baseada nas sequências do gene que codificam a região 16S do rRNA, o que evidenciou a dominância de *Planktothrix sp.*, com a contribuição de outros gêneros em menor proporção: *Raphidiopsis sp. (Cylindrospermopsis sp.), Microcystis sp.*, e *Cyanobium sp.*. Todos eles apresentaram uma diminuição do número de sequências, e também a abundância relativa, ao longo do tempo na condição com H_2O_2.

Em simultâneo, parâmetros físicos da água, como transparência e turbidez, foram alterados de modo significativo ao longo do tratamento, em comparação a condição controle. Ambos, ainda, foram correlacionados respectivamente de maneira negativa ou positiva, com a presença de cianobactérias. A contribuição relativa de cianobactérias se manteve baixa até o último tempo amostral (120h) na condição com H_2O_2, enquanto um aumento na abundância de algas verdes foi observado na condição controle. Tal fato também foi observado por outros autores que avaliaram alterações na composição da comunidade fitoplanctônica após o uso do H_2O_2, com a consequente dominância de organismos da classe *Chlorophyta* (MATTHIJS et al., 2012; WEENINK et al., 2015; YANG et al., 2018).

A maior sensibilidade de cianobactérias ao tratamento com H_2O_2, em comparação a outros representantes do fitoplâncton, poderia ser explicada pela capacidade reduzida ou ineficiente destes microrganismos em produzir enzimas do aparato anti-oxidativo capazes de conferir uma resistência ao oxidante, como por exemplo peroxidases (PASSARDI et al., 2007; BERNROITNER et al., 2009). Tal fato também poderia ser explicado uma vez que cianobactérias produzem uma quantidade reduzida de H_2O_2, ou qualquer outro tipo de EROs ao longo da cadeia transportadora de elétrons, em comparação ao fitoplâncton eucarionte. Algas verdes, assim como vegetais superiores, através de um processo conhecido como reação de Mehler, produzem o radical O_2^- com a redução de O_2 a partir de elétrons provenientes da atividade do fotossistema I. Esse radical sofre seguidas etapas de redução se transformando em H_2O_2, pela ação da enzima superóxido dismutase, e posteriormente em H_2O, pela ação da catalase (ASADA, 2006; LATIFI et al., 2009; ALLAHVERDIYEVA et al., 2011). Assim, para diminuir os efeitos do estresse oxidativo produzido ao longo da atividade fotossintética, algas verdes e eucariotos fototróficos apresentariam um aparato enzimático mais eficaz. Já em cianobactérias, algumas flavoproteínas (do tipo *flv1p* e *flv3p*) seriam responsáveis por mediar a foto-redução de O_2 com elétrons do fotossistema I, sem a formação de radicais livres ou qualquer substância intermediária que resultasse na produção destes, acarretando diretamente na formação de H_2O (HELMAN et al., 2003; 2005; ALLAHVERDIYEVA et al., 2011; 2013; 2015). Logo, cianobactérias contariam com um aparato anti-oxidativo mais limitado para enfrentar um estresse oxidativo exógeno, principalmente nas concentrações de oxidantes aplicadas para o tratamento alternativo.

Matthijs et al. (2012) realizaram experimentos com a aplicação de H_2O_2 em uma lagoa recreacional na Holanda, dominada pela cianobactéria *Planktothrix agardhii*, tanto na

escala de mesocosmos como de modo *in situ*. Nos mesocosmos, após o tratamento com 2,3 mg L^{-1}, houve uma redução de ~98% na abundância da cianobactéria ao longo de 10 dias com uma consequente alteração da composição fitoplanctônica, registrado pelo aumento substancial do fitoplâncton eucarionte (clorofíceas, criptofíceas, diatomáceas, crisófitas e euglenófitas), além de uma diminuição de 30% na abundância do zooplâncton (*Daphnia sp* e *Diaphanosoma sp.*). Utilizando a mesma concentração em experimentos *in situ*, foi observado que a supressão da cianobactéria dominante se manteve ao longo de 7 semanas, além do rápido declínio da concentração de MCs (2 dias após aplicação). Enquanto isso, a composição da comunidade fitoplanctônica eucarionte permaneceu inalterada e a abundância de representantes do zooplâncton se manteve estável ao longo de 2 meses, sendo 3 vezes mais abundantes do que nos experimentos realizados em mesocosmos. A princípio, a preservação do grupo zooplanctônico contribuiria para manter um equilíbrio do sistema, controlando a abundância do fitoplâncton resistente ao H_2O_2, e sua consequente dominância após a supressão das cianobactérias (DEMOTT et al., 2001; WILSON et al., 2006).

Um dos pontos cruciais a considerar ao se aplicar H_2O_2 para a supressão de cianobactérias é o tempo de permanência do oxidante na água e a consequente geração de EROs (MATTHIJS et al., 2012; BURSON et al., 2014). De acordo com os nossos resultados, enquanto a abundância relativa de cianobactérias foi reduzida ao longo do tempo, em comparação ao controle, algumas bactérias heterotróficas se mostraram extremamente resistentes ao tratamento e apresentaram um aumento substancial em suas respectivas abundâncias relativas enquanto o oxidante ainda estava presente no sistema. Foi possível notar um aumento de OTUs (do inglês *operational taxonomic units*) classificadas como pertencentes ao gênero *Exiguobacterium*, em que uma única OTU atingiu cerca de 50% da abundância relativa nas primeiras 24h após a adição do H_2O_2. Essa alteração da composição do bacterioplâncton foi acompanhada também pelo aumento da abundância relativa de representantes dos gêneros *Deinococcus* e *Paracoccus*, sendo estes três gêneros os que mais fortemente contribuíram para a diferenciação entre as condições de tratamento e controle ao longo das 72h, de acordo com a análise de LEfSe e LDA. Esses três gêneros de bactérias heterotróficas já foram descritos como organismos bastante resistentes a oxidação, apresentando um aparato enzimático altamente desenvolvido para se proteger do estresse oxidativo promovido por EROs (WANG e SCHELLHORN, 1995; BAKER et al., 1998; TAKEBE et al., 2007).

Representantes do gênero *Exiguobacterium* (família *Bacillaceae*), que apresentou a maior abundância relativa na condição de tratamento, têm uma distribuição cosmopolita desde ambientes de água doce até ambientes marinhos, com uma ampla capacidade de adaptação a variações na temperatura, pH e salinidade, e até a elevadas doses de radiação UV (WHITE et al., 2013a; WHITE et al., 2019; STRAHSBURGER et al., 2018). Além dessa tolerância perante a radiação UV, esses organismos apresentam intensa atividade de enzimas relacionadas à resposta ao estresse oxidativo, como a catalase, o que pode estar diretamente relacionado à resistência ao H_2O_2 ao longo de 72h de exposição em nosso sistema (YUMOTO et al., 2004; PITT et al., 2007; TAKEBE et al., 2007).

Em um outro estudo realizado por Tian et al. (2012) foi possível observar um efeito direto da presença de uma linhagem de *Exiguobacterium sp.,* isolada do Taihu, China, na inibição do crescimento de diferentes gêneros de cianobactérias como *Planktothrix*, *Synechococcus* e *Chroococcus,* acarretando em uma diminuição de ~80% da abundância destas espécies em apenas dois dias, sem qualquer efeito significativo em representantes das algas verdes (*Chlamydomonas sp.* e *Chlorophyta sp.*). O efeito inibitório sobre cianobactérias se relacionou tanto com a quantidade da biomassa inicial de *Exiguobacterium sp*. como com a fase de crescimento das cianobactérias, na qual as células em fases lag e exponencial de crescimento seriam mais susceptíveis em comparação àquelas em fase estacionária. Em paralelo, os autores isolaram dois possíveis compostos com atividade algicida obtidos a partir do sobrenadante dessa linhagem de *Exiguobacterium sp*. com efeito negativo em espécies de *Microcystis* e *Synechococcus*.

No nosso caso, simultaneamente ao efeito direto do H_2O_2, o aumento na abundância de *Exiguobacterium sp*. se correlacionou de modo significativo com o decaimento das cianobactérias. No entanto, após o período de extinção do H_2O_2 (72h) foi observada uma tendência de recuperação do crescimento das cianobactérias, vista tanto pela análise de clorofilas (com distinção dos grupos fitoplanctônicos), como pela abundância relativa de sequências de DNA atribuídas as OTUs classificadas dentro do filo *Cyanobacteria*.

No último tempo amostral, 120h, foi identificada uma possível retomada do crescimento de cianobactérias, apontada pelo aumento discreto na proporção de sequências do gênero *Cyanobium,* uma picocianobactéria (PCy), isto é, um tipo de cianobactéria de tamanho reduzido (< 2,0 µm de diâmetro) (SIEBURTH et al., 1978; CALLIERI et al., 2012). Representantes de PCy estão presentes em grande parte das florações de cianobactérias, porém são subestimados na análise convencional de microscopia óptica utilizada para identificação e contagem de cianobactérias. No entanto,

análises moleculares ou metodologias que façam uso de fluorescência são adequadas para evidenciar essas cianobactérias menores (CALLIERI, 2007; GUEDES et al., 2018). Em uma condição ambiental favorável, esses organismos podem dominar a zona fótica de corpos d'água oligotróficos, seja nas camadas superiores ou no hipolímnio, sendo a transparência da água um fator importante para o seu estabelecimento (REYNOLDS et al, 2002).

Apesar de ter sido inicialmente afetado pela presença de H_2O_2, ao final do experimento *Cyanobium* se mostrou mais abundante em relação aos demais representantes do filo *Cyanobacteria*. Isso pode estar relacionado a sua maior taxa de crescimento, seu biovolume reduzido e a sua capacidade de se adaptar rapidamente às novas condições após o tratamento, em comparação com outras cianobactérias. Além disso, *Cyanobium* pode ter se beneficiado em detrimento dos demais grupos principalmente pela elevada quantidade de nutrientes (CALLIERI, 2010), uma vez que as concentrações de amônia, nitrito, nitrato e ortofosfato se mantiveram inalteradas com o tratamento ao longo do tempo.

Embora os efeitos do processo oxidativo numa potencial liberação e/ou degradação de toxinas no corpo d'água não tenham sido avaliados neste trabalho, se faz necessária a investigação deste ponto em uma perspectiva de aplicação do tratamento e suas consequências para a saúde pública. No entanto, nada impede que processos que afetem exclusivamente o crescimento de cianobactérias sejam conciliados com outros para a remediação de cianotoxinas, principalmente quando o método empregado para a mitigação de cianobactérias não for eficiente para eliminar suas toxinas até um limite estabelecido como seguro (WANG et al., 2017; KUMAR et al., 2019; SPOOF et al., 2020).

5.2 Comunidade microbiana associada a florações de cianobactérias, degradação de MC-LR e de outros peptídeos produzidos por cianobactérias

Em trabalhos anteriores do nosso grupo, nos quais atuei durante a iniciação científica e o mestrado, obtivemos resultados positivos para a degradação da MC-LR por uma comunidade microbiana recuperada da água intersticial coletada na lagoa de Jacarepaguá, RJ. Essas amostras de água intersticial foram previamente filtradas em membrana de poro 0.45 µm e a comunidade remanescente na fração filtrada foi caracterizada (SANTOS et al., 2020). Investigamos o processo de degradação da MC-LR ao longo de 7 dias em

condições de laboratório, com variações de temperatura, pH e aeração (SANTOS et al., 2020). Durante este estudo, observamos a degradação da toxina em algumas amostras de água recuperada após filtração em membranas de poro 0.22 µm, que eram utilizadas como controle negativo.

No presente trabalho, demos continuidade a esta linha de pesquisa e exploramos as comunidades microbianas de tamanho reduzido que foram obtidas da água superficial da lagoa de Jacarepaguá (RJ) usando duas frações de filtrados: < 0.45 µm e < 0.22 µm, a partir de amostras de água coletadas em dois períodos (novembro de 2016 e 2017). Evidenciamos a atividade metabólica de microrganismos presentes nestas comunidades de tamanho reduzido, o que foi especialmente interessante para aquelas frações < 0.22 µm. Em paralelo, exploramos a composição taxonômica das comunidades, bem como a morfologia de seus representantes. Além disso, comparamos essas características no tempo 0 e após 7 dias de incubação no laboratório, com ou sem a presença da MC-LR.

Enquanto a fração < 0.45 µm apresentou células com morfologias compatíveis com bactérias e típicas de bacilli no tempo 0, a fração < 0.22 µm mostrou poucas estruturas compatíveis com a aparência de células e possíveis fragmentos, por exemplo em formato filamentoso. Essa escassez de células de tamanho reduzido poderia estar relacionada com um estado de resistência ou dormência dos microrganismos (GINGICHASHVILI et al., 2019; GRAY et al., 2019).

Foi possível observar alterações na morfologia de células contidas em ambas as frações de tamanho após incubação durante 7 dias, com ou sem a presença da MC-LR. Essas alterações não indicaram um estado de limitação nutricional, pois evidenciam processos de reprodução (formação de septo), crescimento celular, motilidade (presença de flagelos) e excreção de uma matriz polissacarídica. Ghuneim et al. (2018) sugerem três possíveis causas para que microrganismos apresentem um tamanho reduzido ou sejam capazes de ultrapassar os menores poros de filtros usados nas etapas de filtração das amostras brutas, como os utilizados aqui: i) características morfológicas específicas dos organismos que são classificados como "*ultramicrobacteria*"; ii) ausência de uma parede celular rígida, o que permite a passagem pelos poros pequenos da membrana de filtração; iii) um estado de privação de nutrientes ou senescência celular, o que acarretaria numa diminuição de seu biovolume.

Além da alteração morfológica ao longo do período de incubação, foi evidenciada a modificação na composição da comunidade por meio de alterações na abundância relativa de determinados grupos taxonômicos, principalmente mediante a presença da MC-LR.

As amostras obtidas no tempo inicial (T0) para ambas as frações de tamanho tiveram a presença majoritária de representantes dos filos *Proteobacteria* e *Actinobacteria*, e estes são os filos mais comumente descritos para ambientes de água doce (NEWTON et al., 2011). Luef et al. (2015), a partir de amostras de água subterrânea, observaram uma composição distinta das comunidades bacterianas com tamanho entre 1,2 e 0,2 μm de diâmetro em comparação aquelas menores que 0,2 μm. *Proteobacteria* apareceu mais abundante nos filtrados provenientes do poro maior ao passo que representantes de filos candidatos a divisão como *WWE3, OP11* e *OD1* estiveram mais abundantes na fração de tamanho menor. Além disso, representantes do filo *Parcubacteria*, candidato a divisão e integrante do superfilo *Patescibacteria,* como bactérias que apresentam um tamanho < 0.45 μm (BROWN et al., 2015; PROCTOR et al., 2018; TIAN et al., 2020) contribuíram com 30% da abundância relativa de uma comunidade bacteriana de tamanho reduzido obtida de uma estação de tratamento de água (BRUNO et al., 2017). Tais diferenças na composição e diversidade taxonômica de comunidades bacterianas de tamanho reduzido observada por estes trabalhos pode ser explicada devido às variadas características dos ambientes de estudo (LUEF et al., 2015). Especificamente em relação à fração < 0,22 μm, além dos filos mais abundantes *Proteobacteria* e *Actinobacteria*, identificamos a presença de representantes dos filos *Bacteroidetes*, *Tenericutes* e *Spirochaetes*, que ocupam nichos nos mais variados ambientes aquáticos e apresentam biovolume reduzido em comparação a outras espécies bacterianas, atingindo um diâmetro < 0,4 μm com morfologia filamentosa, ovóide ou bacilar (GARRITY, 2012; RICHARDS et al., 2016; WIRTH et al., 2016; WIESE et al., 2018; BOWMAN, 2020).

Alguns táxons descritos como degradadores de MCs por outros autores foram identificados aqui com a abundância aumentada após a incubação de 7 dias das amostras de ambos os filtrados com a toxina. Após a adição da MC-LR, observamos uma modificação considerável na estrutura das comunidades bacterianas com a redução da abundância relativa de representantes do filo *Actinobacteria* a quase zero e o aumento de *Proteobacteria*. Ademais, no caso das comunidades incubadas sem a presença da toxina, foi mantido o padrão de dominância de *Actinobacteria* e *Proteobacteria*. Nas amostras incubadas com MC-LR, dentre as OTUs pertencentes ao filo *Proteobacteria,* observamos um aumento expressivo na abundância relativa da ordem *Methylophilales*. Além disso, neste cenário, as ordens *Pseudomonadales* e *Burkholderiales* também apresentaram um aumento na abundância relativa em relação a condição sem toxina, contribuindo para uma estrutura distinta entre ambas as condições. Mais especificamente pudemos notar que na

presença de MC-LR houve uma contribuição acentuada de gêneros como *Methylophilus* e *Methylovorus* (ordem *Methylophilales*), *Acinetobacter* (ordem *Pseudomonadales*), além de *Acidovorax* e *Comamonas* (ordem *Burkholderiales*). Tais gêneros ou representantes dessas ordens já foram identificados na água intersticial da lagoa de Jacarepaguá (SANTOS et al., 2020), e em diferentes corpos d'água (HO et al., 2012; LI et al., 2016; DING et al., 2020; MASSEY e YANG, 2020) sendo relacionados com a degradação de MCs. Neste trabalho não observamos aumento na abundância relativa de OTUs classificadas na família *Sphingomonadaceae*, cujos representantes têm sido isolados e de maneira recorrente associados à degradação de MC-LR em ambientes historicamente impactados com florações de cianobactérias (KUMAR et al., 2019; MASSEY e YANG, 2020). O mesmo já foi relatado em outros estudos, demonstrando a diversidade de microrganismos distribuídos em diferentes ambientes capazes de degradar MCs e que não pertencem a esse grupo em especial (BUKOWSKA et al., 2018). Alterações na comunidade bacteriana já tinham sido observadas, independentemente do tamanho das células, em estudo anterior, no qual MC teve influência direta na estrutura da comunidade favorecendo a dominância de alguns grupos taxonômicos específicos (LI et al., 2016).

Logo, a alteração da estrutura da comunidade bacteriana mediada pela presença de MC-LR em comparação àquelas comunidades incubadas sem a toxina, evidenciou um enriquecimento de táxons já descritos na literatura como capazes de degradar essa molécula. Mas também foi possível identificar outros táxons abundantes nesta condição que podem ter contribuído com o processo ou, então, podem ter sido indiretamente favorecidos pela nova composição da comunidade. A partir dos nossos resultados conseguimos revelar que microrganismos de tamanho reduzido constituem uma fração diversa, comumente subestimada, que podem contribuir para a dinâmica e função de comunidades microbianas. Estes organismos podem participar ativamente na degradação de microcistina em ambientes aquáticos e, em paralelo, podem ser capazes de metabolizar outras moléculas, sendo uma potencial ferramenta para o tratamento biológico da água ou mesmo de diferentes tipos de efluentes. Além disso, a organização dos microrganismos sob a forma de consórcios microbianos já foi apontada como crucial para uma maior eficiência na degradação de MCs em ambientes impactados por florações de cianobactérias, onde os microrganismos poderiam desempenhar funções diferentes e complementares ao longo deste processo (MOU et al., 2013; KUMAR et al., 2019).

Embora consórcios microbianos tenham um grande potencial na degradação de metabólitos de cianobactérias, é também importante investigar a capacidade de degradação de linhagens isoladas, dentre bactérias ou até fungos, devido a maior facilidade de manutenção dos cultivos e mesmo de manipulação genética, visando sua otimização para aplicação em larga escala. Além disso, as linhagens isoladas permitem aprofundar o conhecimento sobre vias metabólicas específicas envolvidas nos processos de degradação. Do ponto de vista biotecnológico, é interessante investigar a capacidade de um único microrganismo em degradar uma ampla diversidade de cianotoxinas, ou metabólitos de um modo geral, visando uma potencial utilização como tratamento alternativo. Este tópico foi abordado na parte final deste trabalho.

A partir de uma linhagem de *Paucibacter toxinivorans* (2C20) isolada de um ambiente impactado por florações de cianobactérias da Finlândia (RAPALA et al., 2005), na qual a via de degradação *mlr* está ausente (*mlr*-), foi possível avaliar a degradação de diversos peptídeos produzidos por cianobactérias ou de outros peptídeos de diferentes origens. Esta linhagem foi capaz de degradar, além da MC-LR, outras quatro variantes (DM-LR, MC-LF, MC-RR, MC-YR) ao longo de 7 dias em condições de laboratório. Também foi detectada a degradação de outros peptídeos produzidos por cianobactérias com potencial citotoxicidade (anabaenopeptina A e B, aeruciclamida A e D). A biodegradação destes últimos, em paralelo a outras moléculas classificadas como cianopeptídeos que não a MC, ainda é pouco explorada. Kato et al. (2007) observaram uma baixa degradação de variantes de anabaenopeptinas promovida pelo extrato celular de uma linhagem de *Sphingomonas sp*. que sintetiza enzimas responsáveis pela degradação de microcistinas. No entanto, Briand et al. (2016) evidenciaram a degradação de peptídeos da classe das aeruciclamidas e cianopeptolinas mediada por uma comunidade microbiana aderida à mucilagem da cianobactéria *Microcystis aeruginosa* e mantida em condição de cultivo misto ao longo de 3 anos. Aqui, os resultados suportam a ampla capacidade de *Paucibacter toxinivorans* em degradar uma variedade de cianopeptídeos purificados. Porém, foi observada uma menor capacidade de degradação das MCs por esta linhagem quando todos os cianopeptídeos utilizados nos experimentos (microcistinas, anabaenopeptinas e aeruciclamidas) foram oferecidos sob a forma de mistura, em comparação à degradação das MCs isoladas. Um fato que podemos elucidar futuramente, a partir dos resultados, é a possibilidade da utilização de vias enzimáticas distintas na degradação das microcistinas, anabaenopeptinas e aeruciclamidas, uma vez que quando todos estes peptídeos foram adicionados ao mesmo tempo a linhagem 2C20 apresentou

taxas de degradação completamente diferentes. Na condição de mistura, as MCs foram degradadas mais lentamente em comparação a condição em que estas foram adicionadas como única fonte de peptídeo para a bactéria. Enquanto isso, em mistura, as anabaenopeptinas e aeruciclamidas foram degradadas em aproximadamente 30 minutos em comparação a degradação observada ao longo de 3 dias, quando estes foram adicionados separadamente como única fonte de peptídeo. Ou seja, a oferta dos peptídeos em mistura promoveu uma diminuição da capacidade de degradação da linhagem 2C20 sobre as MCs enquanto aumentou consideravelmente sobre as anabaenopeptinas e aeruciclamidas.

Conforme relatado por alguns pesquisadores, as taxas de degradação de MCs diferem de acordo como as linhagens bacterianas utilizadas ou dos consórcios microbianos testados. Por exemplo, Edwards et al. (2008) observaram diferentes taxas de degradação da MC-LR quando oferecida em uma mistura com outras variantes de MCs ([D-Asp^3]MC-RR, MC-LF e MC-LW) e nodularina (cianopeptídeo tóxico). Essas capacidades distintas foram observadas a partir de comunidades microbianas obtidas de diferentes corpos d'água. Por exemplo, uma comunidade do lago Forfar (Escócia) se mostrou capaz de degradar a MC-LR mais rapidamente quando adicionada na condição de mistura com outras MCs e nodularina, se comparado a condição de MC-LR como única fonte de peptídeo. Já uma comunidade microbiana obtida do lago Rescobie (Escócia) respondeu de modo contrário, apresentando uma menor taxa de degradação da MC-LR na condição de mistura do que na condição individual. Em relação a linhagens isoladas, *Bordetella sp.* degradou tanto MC-LR como MC-RR mais rapidamente quando adicionadas sob a forma exclusiva do que sob a forma de mistura contendo ambas as MCs (YANG et al., 2014). Essas respostas distintas podem estar relacionadas com a quantidade de peptídeos ofertados e as concentrações disponíveis, além da capacidade de resposta de cada microrganismo ou comunidade perante aos efeitos sinérgicos dessas moléculas quando adicionadas como misturas.

No nosso estudo, foi avaliada a capacidade de degradação da linhagem de *P. toxinivorans* (2C20) sobre a MC-LR adicionada em diferentes condições, como: única fonte de peptídeo, sob a forma de mistura com todos os cianopeptídeos utilizados nos experimentos (citado anteriormente), ou adicionada ao extrato bruto de *Microcystis aeruginosa* (cianobactéria produtora de microcistina e outros peptídeos). Foi observado que a linhagem 2C20 apresentou uma taxa de degradação de MC-LR mais elevada quando adicionada a um extrato bruto de *Microcystis aeruginosa*, em relação às demais

condições. Tal cenário poderia mimetizar um processo de lise celular ou senescência de floração de cianobactérias no ambiente natural, que tende a liberar muitos compostos nos corpos d'água. Christoffersen et al. (2002) sugeriram que a presença do carbono orgânico dissolvido, oriundo de extrato bruto, poderia influenciar de modo positivo na eficiência de degradação de MC-LR. A rápida remoção de MC-LR nestas circunstâncias poderia ser um objeto facilitador para a remediação desta molécula nos corpos d'água impactados com florações de cianobactérias, fazendo uso da degradação biológica.

No entanto, mais estudos são necessários acerca da degradação de outros compostos produzidos por cianobactérias diferentes da classe dos peptídeos, e que apresentam toxicidade no âmbito da saúde pública, como por exemplo as saxitoxinas e cilindrospermopsina (carbamatos e alcalóides). Além disso, é importante avaliar a toxicidade dos possíveis subprodutos gerados a partir do processo de degradação dos metabólitos de cianobactérias, em paralelo aos metabólitos gerados pela bactéria responsável pelo processo de degradação biológica.

6 CONCLUSÃO GERAL E PERSPECTIVAS

O tratamento com peróxido de hidrogênio sob um sistema de mesocosmos instalado em um reservatório do semiárido brasileiro ocasionou alterações em parâmetros limnológicos, como fatores físicos, físico-químicos e biológicos. O tratamento acarretou inicialmente uma supressão do fitoplâncton, com o grupo das cianobactérias sendo mais sensíveis que o grupo das algas verdes ao longo do tempo. Alguns gêneros de bactérias heterotróficas se mostraram resistentes ao processo oxidativo como *Exiguobacterium*, *Deinococcus* e *Paracoccus*, que dominaram o sistema até a extinção do H_2O_2. Apesar de não avaliar a potencial degradação de toxinas, se faz necessário otimizar a aplicação de um tratamento alternativo *in situ* de modo que contemple o controle do crescimento de cianobactérias e também a degradação de toxinas, além de investigar a potencial toxicidade em representantes de diferentes níveis tróficos acarretada pela geração de produtos de decomposição em consequência do processo de oxidação. Em paralelo, se faz necessário determinar o tempo em que cianobactérias restabelecem a dominância do sistema aquático após a aplicação do tratamento, estimando a necessidade de repetidas intervenções, o que poderia vir a promover a resistência de microrganismos no ecossistema.

Comunidades microbianas obtidas da lagoa de Jacarepaguá, ambiente historicamente impactado pela poluição e dominado por cianobactérias, foram capazes de degradar microcistina. Pela primeira vez foi relatado que essa degradação foi mediada por comunidades microbianas de tamanho reduzido, obtidas por filtração (<0.45 e <0.22 µm). A presença da toxina promove alterações na composição taxonômica dessas comunidades microbianas, enriquecendo a abundância relativa de táxons já descritos como capazes de degradá-la em outros sistemas aquáticos, principalmente por representantes das ordens *Methylophilales* e *Pseudomonadales*. As comunidades microbianas apresentaram mudanças em sua morfologia ao longo de 7 dias de incubação, independente da presença da toxina. A partir dessa observação é possível otimizar condições para manutenção dessas comunidades de tamanho reduzido em cultivo no laboratório para que a capacidade de biodegradação de seus componentes possa ser considerada em potenciais tratamentos alternativos, conciliando com a investigação da capacidade de degradação de outros compostos orgânicos poluentes.

A bactéria *Paucibacter toxinivorans* degradou diferentes microcistinas, além de outros cianopeptídeos e peptídeos de diferentes origens biológicas ao longo de 7 dias.

Além disso, a bactéria apresentou diferentes taxas de degradação da MC-LR quando esta toxina foi adicionada em um sistema de misturas com todos os cianopeptídeos testados e em um extrato bruto de *Microcystis aeruginosa*. Outra área promissora do ponto de vista biotecnológico é otimizar o cultivo de *Paucibacter toxinivorans* de modo a diminuir o tempo de degradação dos metabólitos produzidos por cianobactérias para que seja aplicada em biorreatores ou até mesmo em um tratamento em escala real.

7 REFERÊNCIAS BIBLIOGRÁFICAS

Alexander, J., Karaolia, P., Fatta-Kassinos, D., Schwartz, T. (2015). Impacts of advanced oxidation processes on microbiomes during wastewater treatment. In: Fatta-Kassinos, D., Dionysiou, D., Kümmerer, K. (eds) Advanced treatment technologies for urban wastewater reuse. The handbook of environmental chemistry, vol 45. Springer, Cham. https://doi.org/10.1007/698_2015_359

Allahverdiyeva Y., Ermakova M., Eisenhut M., Zhang P., Richaud P., Hagemann M., Cournac L., Aro E.M. (2011). Interplay between flavodiiron proteins and photorespiration in Synechocystis sp. PCC 6803. J. Biol. Chem.286:24007–24014. doi: 10.1074/jbc.M111.223289

Allahverdiyeva, Y., Mustila, H., Ermakova, M., Bersanini, L., Richaud, P., Ajlani, G., Battchikova, N., Cournac, L., Ero, E-M. (2013). Flavodiiron proteins Flv1 and Flv3 enable cyanobacterial growth and photosynthesis under fluctuating light. Proc. Natl. Acad. Sci. U.S.A. 110,4111–4116. doi: 10.1073/pnas.1221194110

Allahverdiyeva, Y., Isojärvi, J., Zhang, P., & Aro, E. M. (2015). Cyanobacterial Oxygenic Photosynthesis is Protected by Flavodiiron Proteins. Life (Basel, Switzerland), 5(1), 716–743. https://doi.org/10.3390/life5010716

Allison, S.D. & Martiny, J.B.H. (2008). Colloquium paper: Resistance, resilience, and redundancy in microbial communities. Proc. Natl. Acad. Sci. U.S.A. 105 Suppl 1(Suppl 1):11512-11519. doi:10.1073/pnas.0801925105

A.P, H.R., Mishra, A., Lundborg, C.S., Tripathy, S.K. (2020). Advanced oxidation process-based water disinfection – the microbiology beyond bacterial inactivation. Preprints, 2020080291. doi: 10.20944/preprints202008.0291.v1

Asada, K. (2006). Production and scavenging of reactive oxygen species in chloroplasts and their functions. Plant Physiol. 141(2):391-396. doi:10.1104/pp.106.082040

Baker, S.C., Ferguson, S.J., Ludwig, B., Page, M.D., Richter, O.M., van Spanning, R.J. (1998). Molecular genetics of the genus Paracoccus: metabolically versatile bacteria with bioenergetic flexibility. Microbiology and molecular biology reviews: MMBR, 62(4), 1046–1078.

Barrington, D.J., Reichwaldt, E.S., Ghadouani, A. (2013). The use of hydrogen peroxide to remove cyanobacteria and microcystins from waste stabilization ponds and hypereutrophic systems. Ecological Engineergin, 50:86-94. https://doi.org/10.1016/j.ecoleng.2012.04.024

Bernroitner, M., Zamocky, M., Furtmüller, P.G., Peschek, G.A., Obinger, C. (2009). Occurrence, phylogeny, structure, and function of catalases and peroxidases in cyanobacteria, Journal of Experimental Botany, 60:(2) 423–440, https://doi.org/10.1093/jxb/ern309

Bister, B., Keller, S., Baumann, H.I., Nicholson, G., Weist, S., Jung, G., Süssmuth, R.D., Jüttner, F. (2004). Cyanopeptolin 963A, a chymotrypsin inhibitor of Microcystis PCC 7806. J Nat Prod. 67(10):1755-1757. doi:10.1021/np049828f

Bruno, A., Sandionigi, A., Rizzi, E., Bernasconi, M., Vicario, S., Galimberti, A., Cocuzza, C., Labra, M., Casiraghi, M. (2017). Exploring the under-investigated "microbial dark matter" of drinking water treatment plants. Sci. Rep. 7. https://doi.org/10.1038/srep44350.

Bonné, P.A., Hofman, J.A., van der Hoek J.P. (2002). Long term capacity of biological activated carbon filtration for organics removal. Water Supply. 2 (1): 139–146. doi: https://doi.org/10.2166/ws.2002.0018

Botha, N, Van De Venter, M., Downing, T. G., et al. (2004). The effect of i.p.ly administered microcystin-LR on the gastrointestinal tract of Balb/c mice. Toxicon, 43(3): 251-254.

Bourne, D.G., Jones, G.J., Blakeley, R.L., Jones, G.J., Negri, A.P., Riddles, P. (1996).Enzymatic pathway for the bacterial degradation o;f the cyanobacterial cyclic peptide toxin microcystin LR. Appl. Environ. Microbiol. 62, 4086–4094.

Bourne, D. G., Riddles P., Jones G. J., Smith W. & Blakeley R. L. (2001) Characterization of a gene cluster involved in bacterial degradation of the cyanobacterial toxin microcystin LR. Environ. Toxicol.16:523–34.

Bowman, J.P. (2020). Out From the Shadows–Resolution of the Taxonomy of the Family Cryomorphaceae. Frontiers in Microbiology, 11, 795. https://doi.org/10.3389/fmicb.2020.00795

Bukowska, A., Kaliński, T., Chróst, R.J. (2018). Degradation of microcystins by water and bottom sediment bacterial communities from a eutrophic freshwater lake. Aquat. Microbl. Ecol. 82, 129–144. doi: 10.3354/ame01887

Burson, A., Matthijs, H.C., de Bruijne, W., Talens, R., Hoogenboom, R., Gerssen, A., Vusser, P.M., Stomp, M., Steur, K., van Scheppingen, Y., Huisman, J. (2014). Termination of a toxic Alexandrium bloom with hydrogen peroxide. Harmful Algae. 31:125-135. doi:10.1016/j.hal.2013.10.017

BRASIL. Ministério da Saúde. Portaria 2.914, de 12 de dezembro de 2011. Dispõe sobre os procedimentos de controle e vigilância da qualidade da água para o consumo humano e seu padrão de potabilidade. Brasília: Ministério da Saúde, 2011. Disponível em: <http://bvsms.saude.gov.br/bvs/saudelegis/gm/2011/prt2914_12_12_2011.html>. Acesso em: 05 de agosto de 2020.

Briand, E., Humber, J.F., Tambosco, K., Bormans, M., Gerwick, W.H. (2016). Role of bacteria in the production and degradation of Microcystis cyanopeptides. Microbiology Open, 5(3):469-478. Doi: 10.1002/mbo3.343.

Brown, C.T., Hug, L.A., Thomas, B.C., Sharon, I., Castelle, C.J., Singh, A., Wilkins, M.J., Wrighton, K.C., Williams, K.H., Banfield, J.F. (2015). Unusual biology across a group comprising more than 15% of domain Bacteria. Nature. 523(7559):208-211. doi:10.1038/nature14486

Callieri, C. (2007). Picophytoplankton in freshwater ecosystems : the importance of small-sized phototrophs. Freshw. Rev. 1, 1–28. doi: 10.1608/FRJ-1.1.1

Callieri, C. (2010). Single cells and microcolonies of freshwater picocyanobacteria: a common ecology. J. Limnol. 69:257–277. https://doi.org/10.4081/jlimnol.2010.257

Callieri, C., Cronberg, G., Stockner, J.G. (2012). ”Freshwater picocyanobacteria: single cells, microcolonies and colonial forms,” in Ecology of Cyanobacteria II: Their Diversity in Time and Space 2nd Edn ed. Whitton B. A. (Berlin: Springer;) 229–269.

Carmichael W.W. (2001). Health Effects of Toxin-Producing Cyanobacteria: "The CyanoHABs". Human and Ecological Risk Assessment 7: 1393-1407. https://doi.org/10.1080/20018091095087

Chen, W., Song, L., Peng, L., Wan, N., Zhang, X., Gan, N. (2008). Reduction in microcystin concentrations in large and shallow lakes: Water and sediment-interface contributions. Water Research 42:763 – 773. https://doi.org/10.1016/j.watres.2007.08.007

Christoffersen, K., Lyck, S., and Winding, A. (2002). Microbial activity and bacterial community structure during degradation of microcystins. Aquat. Microb. Ecol. 27, 125–136.

Cory, R.M., Davis, T.W., Dick, G.J., Johengen, T., Denef, V.J., Berry, M.A., Page, S.E., Watson, S.B., Yuhas, K., Kling, G.W. (2016). Seasonal Dynamics in Dissolved Organic Matter, Hydrogen Peroxide, and Cyanobacterial Blooms in Lake Erie. Front. Mar. Sci. 3:54. doi: 10.3389/fmars.2016.00054

Cruz, B.N. e Neuer, S. (2019). Heterotrophic Bacteria Enhance the Aggregation of the Marine Picocyanobacteria Prochlorococcus and Synechococcus. Frontiers in microbiology, 10, 1864. https://doi.org/10.3389/fmicb.2019.0186

DeMott, W.R., Gulati, R.D., Van Donk, E. (2001). Daphnia food limitation in three hypereutrophic Dutch lakes: Evidence for exclusion of large-bodied species by interfering filaments of cyanobacteria. Limnology and Oceanography 46: 2054–2060. https://doi.org/10.4319/lo.2001.46.8.2054

Dietrich, D. e Hoeger, S. (2005). Guidance values for microcystins in water and cyanobacterial supplement products (blue-green algal supplements): a reasonable or misguided approach? Toxicol. Appl. Pharmacol., 203 pp. 273-289. doi: 10.1016/j.taap.2004.09.005.

Ding, Q., Liu, K., Song, Z., Sun, R., Zhang, J., Yin, L., Pu, Y. (2020). Effects of Microcystin-LR on Metabolic Functions and Structure Succession of Sediment Bacterial Community under Anaerobic Conditions. Toxins (Basel) 12(3):183. doi:10.3390/toxins12030183

Donovan, C.J., Ku, J.C., Quilliam, M.A., Gill, T.A. (2008). Bacterial degradation of paralytic shellfish toxins. Toxicon 52, 91–100. doi: 10.1016/j.toxicon.2008.05.005

Dziga, D., Wasylewski, M., Wladyka, B., Nybom, S., Meriluoto, J. (2013). Microbial degradation of microcystins. Chem. Res. Toxicol. 26, 841–852. https://doi.org/10.1021/tx4000045

Dziga, D., Kokocinski, M., Maksylewicz, A., Czaja-Prokop, U., & Barylski, J. (2016). Cylindrospermopsin Biodegradation Abilities of Aeromonas sp. Isolated from Rusałka Lake. Toxins, 8(3), 55. https://doi.org/10.3390/toxins8030055

Edwards, C., Graham, D., Fowler, N., Lawton, L.A. (2008). Biodegradation of microcystins and nodularin in freshwaters. Chemosphere 73:1315-132. https://doi.org/10.1016/j.chemosphere.2008.07.015

Ersmark, K., Del Valle, J. R., Hanessian. S. (2008). Chemistry and biology of the aeruginosin family of serine protease inhibitors. Angew. Chem. Int. Ed. 47:1202–1223. https://doi.org/10.1002/anie.200605219.

Fan, X. & Song, Y. (2020). Advanced oxidation process as a postharvest decontamination technology to improve microbial safety of fresh produce. J. Agric. Food Chem. xxxx, xxx, xxx-xxx https://doi.org/10.1021/acs.jafc.0c01381

Garrity, G.M. (2012). Bergey's manual of systematic bacteriology: Volume one: the Archaea and the deeply branching and phototrophic bacteria. Springer Science & Business Media.

Ghuneim L-A. J., Jones D. L., Golyshin, P. N., Golyshina, O. V. (2018). Nano-sized and filterable Bacteria and Archaea: Biodiversity and function. Frontiers in Microbiology 9: 1971. doi: 10.3389/fmicb.2018.01971

Gingichashvili, S., Duanis-Assaf, D., Shemesh, M., Featherstone, J.D.B., Feuerstein, O., Steinberg, D. (2019). The Adaptive Morphology of Bacillus subtilis Biofilms: A Defense Mechanism against Bacterial Starvation. Microorganisms. 2019;8(1):62. doi:10.3390/microorganisms8010062

Gray, D.A., Dugar, G., Gamba, P., Strahl, H., Jonker, M.J., Hamoen, L.W. (2019). Extreme slow growth as alternative strategy to survive deep starvation in bacteria. Nat Commun 10, 890. https://doi.org/10.1038/s41467-019-08719-8

Guan, R., Yuan, X., Wu, Z., Jiang, L., Li, Y., Zeng, G. (2018). Principle and application of hydrogen peroxide based advanced oxidation processes in activated sludge treatment: A review, Chemical Engineering Journal. doi: https://doi.org/10.1016/j.cej.2018.01.153

Guedes, I.A., Rachid, C., Rangel, L.M., Silva, L., Bisch, P.M., Azevedo, S., Pacheco, A. (2018). Close Link Between Harmful Cyanobacterial Dominance and Associated Bacterioplankton in a Tropical Eutrophic Reservoir. Frontiers in microbiology, 9, 424. https://doi.org/10.3389/fmicb.2018.00424

Helbling, E.W., Villafañe, V., Buma, A., Andrade, M., Zaratti, F. (2001). DNA damage and photosynthetic inhibition induced by solar ultraviolet radiation in tropical phytoplankton (Lake Titicaca, Bolivia). European Journal of Phycology 36: 157–166. https://doi.org/10.1017/S0967026201003122

Helman Y., Tchernov D., Reinhold L., Shibata M., Ogawa T., Schwarz R., Ohad I., Kaplan A. Genes encoding A-type flavoproteins are essential for photoreduction of $O2^{-}$ in cyanobacteria. Curr. Biol. 2003;13:230–235. doi: 10.1016/S0960-9822(03)00046-0.

Ho, L., Sawade, E., Newcombe, G. (2012). Biological treatment options for cyanobacteria metabolite removal - A review. Water Research, 46(5), 1536–1548. https://doi.org/10.1016/j.watres.2011.11.018.

Ho, L., Tang, T., Hoefel, D., Vigneswaran, B. (2012). Determination of rate constants and half-lives for the simultaneous biodegradation of several cyanobacterial metabolites in Australian source waters. Water Research, 46(17), 5735–5746. doi:10.1016/j.watres.2012.08.003

Ho, L., Tang, T., Monis, P. T., & Hoefel, D. (2012). Biodegradation of multiple cyanobacterial metabolites in drinking water supplies. Chemosphere, 87(10), 1149–1154. doi:10.1016/j.chemosphere.2012.02.020

Instituto Trata Brasil. Saneamento é Saúde. Website: http://www.tratabrasil.org.br/

Janssen, E.M. (2019). Cyanobacterial peptides beyond microcystins - A review on co-occurrence, toxicity, and challenges for risk assessment. Water Res. 151:488-499. doi:10.1016/j.watres.2018.12.048

Jia, Y., Du, J., Song, F., Zhao, G., Tian, X. (2012). A fungus capable of degrading microcystin-LR in the algal culture of Microcystis aeruginosa PCC7806. Appl. Biochem. Biotechnol. 166, 987−996. DOI: 10.1007/s12010-011-9486-6

Jin, Y., Zhang, S., Xu, H., Ma, C., Sun, J., Li, H., Pei, H. (2019). Application of N-TiO2 for visible-light photocatalytic degradation of Cylindrospermopsis raciborskii - More difficult than that for photodegradation of Microcystis aeruginosa?. Environ Pollut.245:642-650. doi:10.1016/j.envpol.2018.11.056

Jochimsen, E. M., Carmichael, W.W.; An, J., Cardo, D.M., Cookson, S.T., Holmes, C.E., Antunes, M.B., De Melo Filho, D.A., Lyra, T.M., Barreto, V.S.T., Azevedo, S.M., Jarvis, W.R. (1998): Liver Failure and Death after Exposure to Microcystins at a Hemodialysis Center in Brazil. New England J. of Med., 338(13):873–878. doi: 10.1056/NEJM199803263381304

Jones, G.J., Bourne, D.G., Blakeley, R.L., Doelle, H. (1994). Degradation of the cyanobacterial hepatotoxin microcystin by aquatic bacteria. Nat. Toxins 2, 228– 35. Doi: 10.1002/nt.2620020412

Kato, H., Imanishi, S.Y., Tsuji, K., Harada, K. (2007). Microbial degradation of cyanobacterial peptides. Water Research. 41:1754–1762. Doi: 10.1016/j.watres.2007.01.003

Kehr, J.C. e Dittmann, E. (2015). Biosynthesis and function of extracellular glycans in cyanobacteria. Life 5:164–180. doi:10.3390/life5010164

Kleinteich, J., Puddick, J., Wood, S. A., Hildebrand, F., Laughinghouse, H. D., IV, Pearce, D. A., Dietrich, D. R., Wilmotte, A. (2018). Toxic Cyanobacteria in Svalbard: Chemical Diversity of Microcystins Detected Using a Liquid Chromatography Mass Spectrometry Precursor Ion Screening Method. Toxins, 10(4), 147. https://doi.org/10.3390/toxins10040147

Kumar, P., Hegde, K., Brar, S.K., Cledon, M., Kermanshahi-Pour, A. (2019). Potential of biological approaches for cyanotoxin removal from drinking water: A review. Ecotoxicol Environ Saf. 172:488-503. doi:10.1016/j.ecoenv.2019.01.066

Latifi, A., Ruiz, M., Zhang, C.C. (2009). Oxidative stress in cyanobacteria. FEMS Microbiol Rev. 33(2):258-278. doi:10.1111/j.1574-6976.2008.00134.x

Lawton, L.A., Robertson, P.K.J., Cornish, B.J.P.A., Marr, I.L., Jaspars, M. (2003). Processes infuencing surface interaction and photocatalytic destruction of microcystins on titanium dioxide photocatalysts. J. Catal. 213, 109–113. https://doi.org/10.1016/S0021-9517(02)00049-0

Leão, P.N., Pereira, A.R., Liu, W.T., Julio, N.G., Pevzner, P.A., Dorrestein, P.C., König, G.M., Vasconcelos, V.M., Gerwick., W.H. (2010). Synergistic allelochemicals from a freshwater cyanobacterium. Proc Natl Acad Sci U S A. 107(25):11183-11188. doi:10.1073/pnas.0914343107

Lekkerkerker-Teunissen, K., Chekol, E.T., Maeng, S. K., Ghebremichael, K., Houtman, C. J., Verliefde, A.R.D., Verberk, J.Q., Amy, G.L., van Dijk J.C. (2012). Pharmaceutical removal during managed aquifer recharge with pretreatment by advanced oxidation. Water Supply. 12 (6): 755–767. doi:https://doi.org/10.2166/ws.2012.050

Lemes, G.A.F., Kersanach, R., Pinto, L.S., Dellagostin, O.A., Yunes, J.S., Matthiensen, A. (2008). Biodegradation of microcystins by aquatic Burkholderia sp. from a South Brazilian coastal lagoon. Ecotoxicology and Environmental Safety 69, 358-365. https://doi.org/10.1016/j.ecoenv.2007.03.013

Lezcano, M.Á., Velázquez, D., Quesada, A., El-Shehawy, R. (2017). Diversity and temporal shifts of the bacterial community associated with a toxic cyanobacterial bloom: An interplay between microcystin producers and degraders, Water Researc. doi: 10.1016/j.watres.2017.08.025.

Li, J., Shi, G., Mei, Z., Wang, R., Li, D. (2016). Discerning biodegradation and adsorption of microcystin-LR in a shallow semi-enclosed bay and bacterial community shifts in response to associated process. Ecotoxicol. Environ. Saf. 132, 123–131. https://doi.org/10.1016/j.ecoenv.2016.05.033

Li, J., Li, R., Li, J. (2017). Current research scenario for microcystins biodegradation - A review on fundamental knowledge, application prospects and challenges. Sci Total Environ. 595:615-632. doi:10.1016/j.scitotenv.2017.03.285

Li, Q., Lin, F., Yang, C., Wang, J., Lin, Y., Shen, M., Zhao, J., (2018). A large-scale comparative metagenomic study reveals the functional interactions in six bloom- forming microcystis-epibiont communities. Frontiers in microbiology, 9, 746

Liu, J., Li, B., Wang, Y., Zhang, G., Jiang, X., Li, X. (2019). Passage and community changes of filterable bacteria during microfiltration of a surface water supply. Environment International 131: 104998. doi: 10.1016/j.envint.2019.104998

Lowe, J., Souza-Menezes, J., Freire, D.S., Mattos, L.J., Castiglione, R.C., Barbosa, C.M.L., Santiago, L., Ferrão, F.M., Cardoso, L.H.D., da Silva, R.T., Vieira-Beiral, H.J., Vieyra, A., Morales, M.M., Azevedo, S.M.F.O. Soares, R.M. (2012). Single sublethal

dose of microcystin-LR is responsible for different alterations in biochemical, histological and physiological renal parameters . Toxicon 59 :p.601-609. doi: 10.1016/j.toxicon.2012.02.003

Luef, B., Frischkorn, K., Wrighton, K., Holman, H-Y., Birarda, G., Thomas, B., Singh, A., Williams, K., Siegerist, C., Tringe, S., Downing, K., Comolli, L., Banfield, J. (2015). Diverse uncultivated ultra-small bacterial cells in groundwater. Nat Commun 6, 6372. https://doi.org/10.1038/ncomms7372

Magalhães, V.F., Soares, R.M., Azevedo, S.M.F.O (2001). Microcystin contamination in fish from the Jacarepaguá Lagoon (Rio de Janeiro, Brazil): ecological implication and human health risk. Toxicon, 39(7), 10077-1085. Doi: 10.1016/s0041-0101(00)00251-8

Magalhães, V.F., Marinho, M.M., Domingos, P., Oliveira, A.C., Costa, S.M., Azevedo, L.O., Azevedo, S.M.F.O. (2003). Microcystins (Cyanobacteria hepatotoxins) bioaccumulation in fish and crustaceans from Sepetiba Bay (Brasil, RJ). Toxicon. 42:89-295. https://doi.org/10.1016/S0041-0101(03)00144-2.

Martijn, A.J. e Kruithof, J.C. (2012). UV and UV/H2O2 Treatment: The Silver Bullet for by-product and Genotoxicity Formation in Water Production, Ozone: Science & Engineering, 34:2, 92-100, DOI: 10.1080/01919512.2012.649596

Massey, I.Y. e Yang, F. (2020). A Mini Review on Microcystins and Bacterial Degradation. Toxins, 12(4), 268. https://doi.org/10.3390/toxins12040268

Matthijs, H.C.P., Visser, P.M., Reeze, B., Meeuse, J., Slot, P.C., Wijn, G., Talens, R., Huisman, J. (2012). Selective suppression of harmful cyanobacteria in an entire lake with hydrogen peroxide. Water Res 46:1460–1472. https://doi.org/10.1016/j.watres.2011.11.016

Meriluoto, J., Spoof, L., Codd, G.A. (Eds.) (2017). Handbook of Cyanobacterial Monitoring and Cyanotoxin Analysis, 1st edition. Wiley 576p. ISBN: 978-1-119-06868-6.

Moraes, A.C.N., Magalhães, V.F. (2018). Renal tubular damage caused by cylindrospermopsin (cyanotoxin) in mice. Toxicol Lett. 286:89-95. doi:10.1016/j.toxlet.2017.12.028

Moreno, I.M., Mate, A., Repetto, G., Vazquez, C.M., Camean, A.M. (2003). Influence of microcystin-LR on the activity of membrane enzymes in rat intestinal mucosa. Journal of Physiology and Biochemistry, 59:293-299. https://doi.org/10.1007/BF03179887

Morón-López, J., Nieto-Reyes, L., El-Shehawy, R.. (2017). Assessment of the influence of key abiotic factors on the alternative microcystin degradation pathway(s) (mlr-): A detailed comparison with the mlr route (mlr+). Sci Total Environ. 599-600:1945-1953. doi:10.1016/j.scitotenv.2017.04.042

Morris, R.J., Williams, D.E., Luu, H.A., Holmes, C.F.B., Andersen, R.J., Calvert, S.E. (2000). The adsorption of microcystin-LR by natural clay particles. Toxicon. 38:303-308. doi: 10.1016/s0041-0101(99)00149-x

Mostofa, K.M.G., Liu, C-Q., Sakugawa, H., Vione, D., Minakata, D., Wu, F. (2013). Photoinduced and microbial generation of hydrogen peroxide and organic peroxides in natural waters. In: Mostofa KMG, Yoshioka T, Mottaleb A, Vione D (eds) Photobiochemistry of organic matter: principles and practices in water environments. Springer, Berlin, pp 139–207

Mou X, Lu X, Jacob J, Sun S, Heath R (2013). Metagenomic identification of bacterioplankton taxa and pathways involved in microcystin degradation in Lake Erie. PLoS ONE 8(4): e61890. doi:10.1371/journal.pone.0061890

Newton, R.J., Jones, S.E., Eiler, A., Mcmahon, K.D., Bertilsson, S. (2011). A guide to the natural history of freshwater lake Bacteria. Microbiol. Mol. Biol. Rev. 75 (1), 14–49.https://doi.org/10.1128/MMBR.00028-10.

Niedermeyer, T. H. (2015). Anti-infective natural products from Cyanobacteria. Planta Med. 81:1309–1325. doi: 10.1055/s-0035-1546055

Nobre, A.C.L., Coelho, G.R., Coutinho, M.C.M., Silva, M.M.M., Angelim, E.V., Menezes, D.B., Fonteneles, M.C., Monteiro, H.S.A. (2001). The role of phospholipase A(2) and cyclooxygenase in renal toxicity induced by microcystin-LR. Toxicon, 39(5): 721-724. https://doi.org/10.1016/S0041-0101(00)00193-8

Nybom, S.M., Dziga, D., Heikkila, J.E., Kull, T.P., Salminem, S.J., Meriluoto, J.A (2012). Characterization of microcystin-LR removal process in the presence of probiotic bacteria. Toxicon 59:171–181. https://doi.org/10.1016/j.toxicon.2011.11.008

Oller, I., Malato, S., Sánchez-Pérez, J.A. (2011). Combination of Advanced Oxidation Processes and biological treatments for wastewater decontamination--a review. Sci Total Environ. 409(20):4141-4166. doi:10.1016/j.scitotenv.2010.08.061

O'Neil, J., Davis, T.W., Burford, A., Gobler, C.J., (2012). The rise of harmful cyanobacteria blooms: The potential roles of eutrophication and climate change. Harmful Algae 313–334.

Paerl H. (2008). Nutrient and other environmental controls of harmful cyanobacterial blooms along the freshwater-marine continuum. Adv Exp Med Biol. 619:217-237. doi:10.1007/978-0-387-75865-7_10

Paerl, H.W. e Otten, T.G. (2013). Harmful Cyanobacterial Blooms: Causes, Consequences, and Controls. Environmental Microbiology. 65(4):995-1010. doi: 10.1007/s00248-012-0159-y.

Park, J.A., Yang, B., Park, C., Choi, J.W., van Genuchten, C.M., Lee, S-H. (2017). Oxidation of microcystin-LR by the Fenton process: Kinetics, degradation intermediates, water quality and toxicity assessment. Chemical Engineering Journal, 309, 339-348. https://doi.org/10.1016/j.cej.2016.10.083

Passardi, F., Zamocky, M., Favet, J., Jakopitsch, C., Penel, C., Obinger, C., et al. (2007). Phylogenetic distribution of catalase-peroxidases: are there patches of order in chaos? Gene 397, 101–113. doi: 10.1016/j.gene.2007.04.016

Pestana, C.J., Edwards, C., Prabhu, R., Robertson, P.K.J., Lawton, L.A (2015). Photocatalytic degradation of eleven microcystin variants and nodularin by TiO2 coated glass microspheres, Journal of Hazardous Materials http://dx.doi.org/10.1016/j.jhazmat.2015.07.016

Pitt, T.L., Malnick, H., Shah, J., Chattaway, M.A., Keys, C.J., Cooke, F.J., Shah, H.N. (2007). Characterisation of Exiguobacterium aurantiacum isolates from blood cultures of six patients. Clin Microbiol Infect.13(9):946-948. doi:10.1111/j.1469-0691.2007.01779.x

Polle, A. (1996). Mehler reaction: Friend or foe in photosynthesis? Botanica Acta. 109:2 https://doi.org/10.1111/j.1438-8677.1996.tb00546.x

Proctor, C.R., Besmer, M.D., Langenegger, T., Beck, K., Walser, J.C., Ackermann, M., Bürgmann, H., Hammes, F. (2018). Phylogenetic clustering of small low nucleic acid-content bacteria across diverse freshwater ecosystems. ISME J 12, 1344–1359 (2018). https://doi.org/10.1038/s41396-018-0070-8

Rapala, J., Berg, K. A., Lyra, C., Niemi, R. M., Manz, W., Suomalainen, S., Paulin, L., and Lahti, K. (2005). Paucibacter toxinivorans gen. nov., sp. nov., a bacterium that degrades cyclic cyanobacterial hepatotoxins microcystins and nodularins. Int. J. Syst. Evol. Microbiol. 55, 1563–1568. doi:10.1099/ijs.0.63599-0

Reynolds, C.S. (1987). Cyanobacterial water-blooms. In: J. Callow [ed.] Advances in botanical research. Academic Press. London. p. 67-143.

Reynolds, C.S., Huszar, V., Kruk, C., Naselli-Flores, L., Melo, S. (2002). Towards a functional classification of the freshwater phytoplankton. J. Plankton Res. 24, 417–428. 10.1093/plankt/24.5.417.

Reynolds, C.S. (2006). Ecology of Phytoplankton. Cambridge. p.535. https://doi.org/10.1017/CBO9780511542145.002.

Richards, G.P., Fay, J.P., Uknalis, J., Olanya, O.M., Watson, M.A. (2016). Purification and host specificity of predatory Halobacteriovorax isolates from seawater. Applied and environmental microbiology, 82(3), 922-927. doi: 10.1128/AEM.03136-15

Roberty, S., Bailleul, B., Berne, N., Franck, F., Cardol, P. (2014). PSI Mehler reaction is the main alternative photosynthetic electron pathway in Symbiodinium sp., symbiotic dinoflagellates of cnidarians. New Phytol. 204(1):81-91. doi:10.1111/nph.12903

Santos, A.A., Rachid, C., Pacheco, A.B., Magalhães, V.. (2020). Biotic and abiotic factors affect microcystin-LR concentrations in water/sediment interface. Microbiol Res. 236:126452. doi:10.1016/j.micres.2020.126452

Schopf, J. W. e Walter, M.R. (1982). Origin and early evolution of cyanobacteria: the geological evidence In N.G. Carr, & B. A. Whitton (eds), The Biology of Cyanobacteria. Blackwell, Oxford:543–564.

Schneider, M. e Bláha, L. (2020). Advanced oxidation processes for the removal of cyanobacterial toxins from drinking water. Environ Sci Eur 32, 94. https://doi.org/10.1186/s12302-020-00371-0

Shade, A., Peter, H., Allison, S.D., Baho, D.L., Berga, M., Bürgmann, H., Huber, D.H., Langenheder, S., Lennon, J.T., Martiny, J.B.H., Matulich, K.L., Schmidt, T.M., Handelsman, J. (2012). Fundamentals of microbial community resistance and resilience. Front Microbiol. 3:417. doi:10.3389/fmicb.2012.00417

Sieburth, J.M., Smetacek, V., Lenz, J. (1978). Pelagic ecosystem structure: Heterotrophic compartments of the plankton and their relationship to plankton size fractions, Limnology and Oceanography, 23, doi: 10.4319/lo.1978.23.6.1256.

Sivonen, K., Leikoski, N., Fewer, D. P, Jokela, J. (2010). Cyanobactins – ribosomal cyclic peptides produced by cyanobacteria. Appl. Microbiol. Biotechnol. 86:1213–1225. Doi: 10.1007/s00253-010-2482-x

Smith, V.H. e Schindler, D.W. (2009). Eutrophication science: where do we go from here?. Trends Ecol Evol. 24(4):201-207. doi:10.1016/j.tree.2008.11.009

Smith, M.J., Shaw, G.R., Eaglesham, G.K., Ho, L., Brookes, J.D. (2008). Elucidating the factors influencing the biodegradation of cylindrospermopsin in drinking water sources. Environ Toxicol. 23(3):413-421. doi:10.1002/tox.20356

Sistema Nacional de Informações sobre Saneamento (2019), Ministério das Cidades, Brasil. Diagnóstico dos serviços de águas e esgotos em 2018. Disponível em: http://www.snis.gov.br/diagnostico-anual-agua-e-esgotos/diagnostico-dos-servicos-de-agua-e-esgotos-2018

Soares, R.M., Cagido, V., Ferraro, R.B., Meyer-Fernandes, J.R., Rocco, P.R., Zin, W.A., Azevedo, S.M. (2007). Effects of microcystin-LR on mouse lungs. Toxicon, 50(3): 330-338. doi: 10.1016/j.toxicon.2007.04.003

Soina, V.S., Lysak, L.V., Konova, I.A., Lapygina, E.V., Zvyagintsev. Study of Ultramicrobacteria (Nanoforms) in Soils and Subsoil Deposits by Electron Microscopy. Eurasian Soil Science, 2012, Vol.45, Nº11, p.1048-1056

Song, H.H., Reichwaldt, E.S., Ghadouani,A. (2014). Contribution of sediments in the removal of microcystin-LR from water.Toxicon 83,84–90. Doi: 10.1016/j.toxicon.2014.02.019.

Spoof, L., Jaakkola, S., Važić, T., Häggqvist, K., Kirkkala, T., Ventelä, A-M., Kirkkala, T., Svircev, Z., Meriluoto, J. (2020). Elimination of cyanobacteria and microcystins in irrigation water—effects of hydrogen peroxide treatment. Environ Sci Pollut Res 27, 8638–8652. https://doi.org/10.1007/s11356-019-07476-x

Strahsburger, E., Zapata, F., Pedroso, I., Fuentes, D., Tapia, P., Ponce, R., Valdes, J. (2018). Draft genome sequence of Exiguobacterium aurantiacum strain PN47 isolate from saline ponds, known as “Salar del Huasco”, located in the Altiplano in the North of Chile. Brazilian Journal of Microbiology, 49(1), 7-9. https://doi.org/10.1016/j.bjm.2017.03.011

Suri, R.P.S., Liu, J., Hand, D.W., Crittenden, J.C., Perram, D.L., Mullins, M.E. (1993). Heterogeneous photocatalytic oxidation of hazardous organic contaminants in water. Water Environmental Research, 65(5):665-673. www.jstor.org/stable/25044356.

Svirčev, Z., Lalić, D., Bojadžija Savić, G., Tokodi, N., Drobac, D., Chen, L., Meriluoto, J., Codd, G. (2019). Global geographical and historical overview of cyanotoxin distribution and cyanobacterial poisonings. Arch Toxicol. 93(9):2429-2481. doi:10.1007/s00204-019-02524-4

Takebe, F., Hara, I., Matsuyama, H., Yumoto, I. (2007). Effects of H2O2 under low- and high-aeration-level conditions on growth and catalase activity in Exiguobacterium oxidotolerans T-2-2T. J Biosci Bioeng. 104(6):464-469. doi:10.1263/jbb.104.464.

Tian, C., Liu, X., Tan, J., Lin, S., Li, D., Yang, H. (2012). Isolation, identification and characterization of an algicidal bacterium from Lake Taihu and preliminary studies on its algicidal compounds. J Environ Sci (China).24(10):1823-1831. doi:10.1016/s1001-0742(11)60983-2

Tian, R., Ning, D., He, Z., Zhang, P., Spencer, S., Gao, S., Shi, W., Wu, L., Zhang, Y., Yang, Y., Adams, B., Rocha, A., Detienne, B., Lowe, K., Joyner, D., Klingeman, D., Arkin, A., Fields, M., Hazen, T., Stahl, D., Alm, E., Zhou, J. (2020). Small and mighty: adaptation of superphylum Patescibacteria to groundwater environment drives their genome simplicity. Microbiome 8, 51. https://doi.org/10.1186/s40168-020-00825-w

Tonietto, A.E., Lombardi, A.T., Vieira, A.A.H., Parrish, C.C., Choueri, R.B. (2014). Cylindrospermopsis raciborskii (Cyanobacteria) exudates: chemical characterization and complexation capacity for Cu, Zn, Cd and Pb. Water Reserach. 49:381–390. https://doi.org/10.1016/j.watres.2013.10.025

Vincent, W.F. (2000). Cyanobacterial Dominance in the Polar Regions. In: Whitton B.A., Potts M. (eds) The Ecology of Cyanobacteria. Springer, Dordrecht. https://doi.org/10.1007/0-306-46855-7_12

Waggoner, D.C., Wozniak, A.S., Cory, R.M., Hatcher, P.G. (2017). The role of reactive oxygen species in the degradation of lignin derived dissolved organic matter. Geochimica et Cosmochimica Acta 208:171–184. https://doi.org/10.1016/j.gca.2017.03.036

Wang, P. e Schellhorn, H.E. (1995). Induction of resistance to hydrogen peroxide and radiation in Deinococcus radiodurans. Can J Microbiol.41:170–176

Wang, F., van Halem, D., Liu, G., Lekkerkerker-Teunissen, K., van der Hoek, J.P. (2017). Effect of residual H2O2 from advanced oxidation processes on subsequent biological water treatment: A laboratory batch study. Chemosphere. 185:637-646. doi: 10.1016/j.chemosphere.2017.07.073.

Weenink, E.F., Luimstra, V.M., Schuurmans, J.M., Van Herk, M.J., Visser, P.M., Matthijs, H.C. (2015). Combatting cyanobacteria with hydrogen peroxide: a laboratory study on the consequences for phytoplankton community and diversity. Front Microbiol. 6:714. doi:10.3389/fmicb.2015.00714

White, R.A. III, Grassa, C.J., Suttle, C.A. (2013a). Draft genome sequence of Exiguobacterium pavilionensis strain RW-2, with wide thermal, salinity, and pH tolerance, isolated from modern freshwater microbialites. Genome Announc. 1:e00597-13. doi: 10.1128/genomeA.00597-13

White, R.A. III., Soles, S.A., Gavelis, G., Gosselin, E., Slater, G.F., Lim, D., Leander, B., Suttle, C.A. (2019). The Complete Genome and Physiological Analysis of the Eurythermal Firmicute Exiguobacterium chiriqhucha Strain RW2 Isolated From a Freshwater Microbialite, Widely Adaptable to Broad Thermal, pH, and Salinity Ranges. Frontiers in microbiology, 9, 3189. https://doi.org/10.3389/fmicb.2018.03189

Wiese, J., Saha, M., Wenzel-Storjohann, A., Weinberger, F., Schmaljohann, R., Imhoff, J.F. (2018). Vicingus serpentipes gen. nov., sp. nov., a new member of the Flavobacteriales from the North Sea. International journal of systematic and evolutionary microbiology, 68(1), 333-340. doi: 10.1099/ijsem.0.002509

Williams, D. E., Craig, M., Dawe, S. C., et al. (1997). Evidence for a covalently 'bound form of microcystin-LR in salmon larvae and dungeness crab larvae. Chemical Research in Toxicology, 10:463-469.

Wilson, A.E., Sarnelle, O., Tillmanns, A.R. (2006). Effects of cyanobacterial toxicity and morphology on the population growth of freshwater zooplankton: Meta-analyses of laboratory experiments, Limnology and Oceanography, 51, doi: 10.4319/lo.2006.51.4.1915.

Wirth, R., Ugele, M., Wanner, G. (2016). Motility and Ultrastructure of Spirochaeta thermophila. Frontiers in Microbiology, 7, 1609. doi: 10.3389/fmicb.2016.01609

World Health Organisation (2003) disponível em: http://www.who.int/water_sanitation_health/resourcesquality/toxcyanbegin.pdf

Wörmer L., Cirés, S., Quesada, A. (2011). Importance of natural sedimentation in the fate of microcystins. Chemosphere 82:1141–1146. https://doi.org/10.1016/j.chemosphere.2010.11.024

Wu, S., Lv, J., Wang, F., Duan, N., Li, Q., Wang, Z. (2017). Phtocatalytic degradation of microcystin- LR with a nanostructured photocatalyst based on upconversion nanoparticles@TiO2 composite under simulated solar lights. Scientific Reports (7):14435. https://doi.org/10.1038/s41598-017-14746-6

van Der Hoek, W., Konradsen, F., Jehangir., W.A. (1999) Domestic use of irrigation water: health hazard or opportunity? International Journal of Water Resources Development 15, 107-119.

Yang, F., Zhou, Y., Sun, R., Wei, H., Li, Y., Yin, L., Pu, Y. (2014). Biodegradation of MC-LR and –RR by a novel microcystin-degrading bacteria isolated from Taihu lake. Biodegradation, 25:447-457. doi:10.1007/s10532-013-9673-y

Yang, Z., Buley, R.P., Fernandez-Figueroa, E.G., Barros, M.U.G., Rajendran, S., Wilson, A.E. (2018). Hydrogen peroxide treatment promotes chlorophytes over toxic cyanobacteria in a hyper-eutrophic aquaculture pond. Environ Pollut.240:590-598. doi:10.1016/j.envpol.2018.05.012

Yoshizawa, S., Matsushima, R., Watanabe, M.F., Harada, K-I., Ichihara, A., Carmichael, W.W., Fujiki, H. (1990). Inhibition of protein phosphatases by microcystin and nodularin associated with hepatotoxicity. Journal of Cancer Research and Clinical Oncology 116: 609-614

Yumoto, I., Hishinuma-Narisawa, M., Hirota, K., Shingyo, T., Takebe, F., Nodasaka, Y. (2004). Exiguobacterium oxidotolerans sp nov., a novel alkaliphile exhibiting high catalase activity. Int. J. Syst. Evol. Microbiol. 54, 2013–2017. doi: 10.1099/ijs.0.63129-0

8 MATERIAL SUPLEMENTAR

8.1 Capítulo 1 (Improving water quality and controlling cyanobacterial bloom using hydrogen peroxide in a semiarid region reservoir used for drinking water)

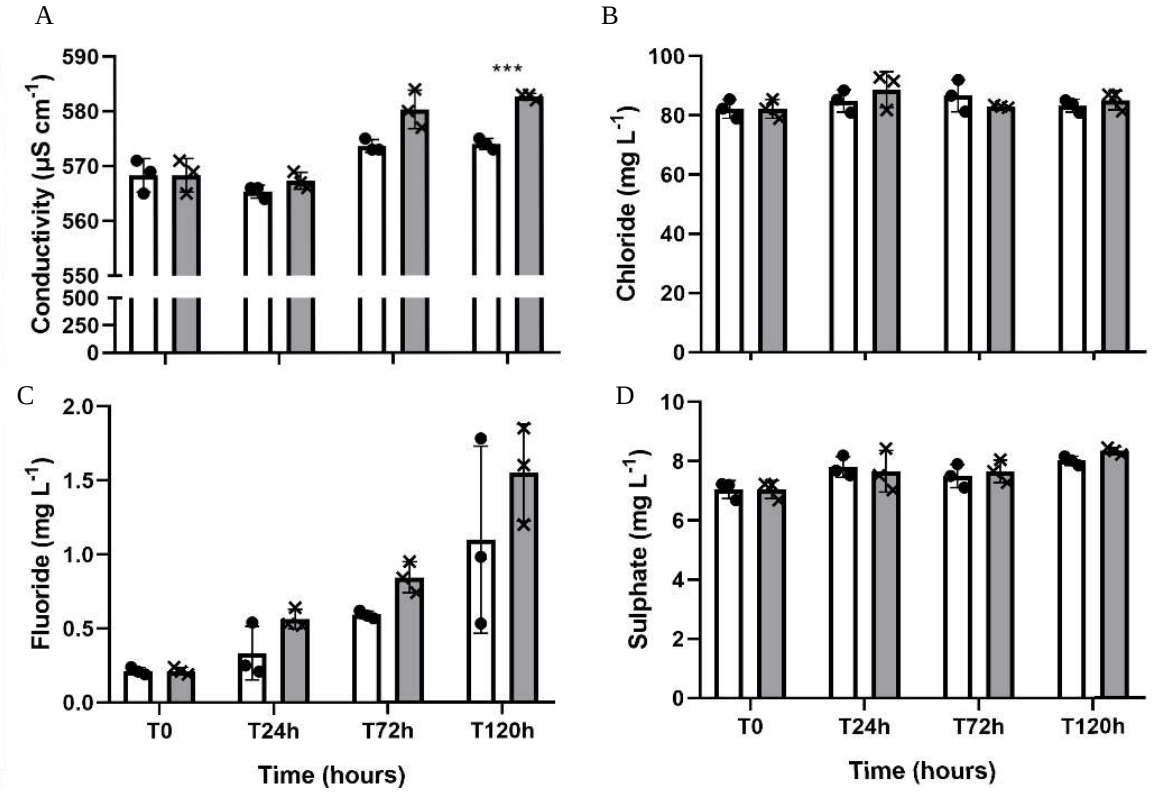

Supplementary Figure 1: Effect of H_2O_2 on conductivity (A), chloride (B), fluoride (C) and sulphate (D) over the time. Results are expressed as the mean ± SD. Grey bars and white bars are representing the treatment and control condition, respectively. In the figure A the y-axis was divided in two segments to identify the difference between both respective bars from control and treatment condition. The asterisks represent statistical difference between treatment and control ($p<0.001$).

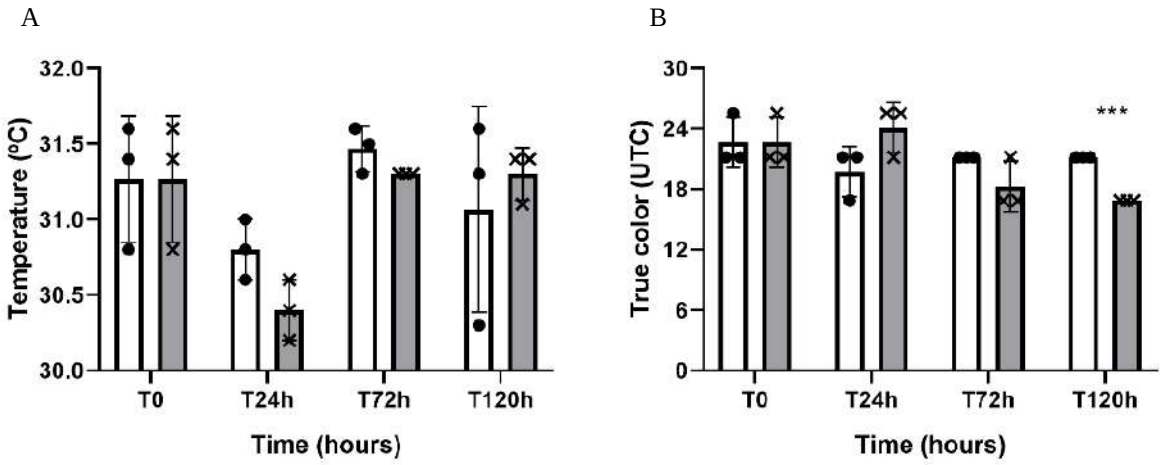

Supplementary Figure 2: Effect of H_2O_2 on temperature (A) and true colour (B) over the time. Results are expressed as the mean ± SD. Grey bars and white bars are representing the treatment and control condition, respectively. The asterisks represent statistical difference between treatment and control ($p<0.001$).

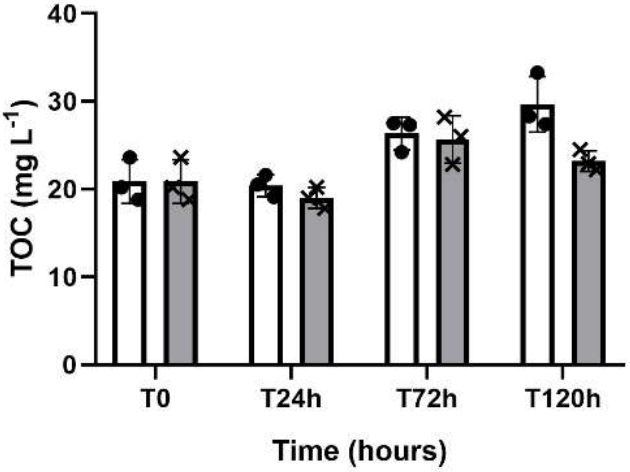

Supplementary Figure 3: Effect of H_2O_2 on TOC over the time. Results are expressed as the mean ± SD. Grey bars and white bars are representing the treatment and control condition, respectively.

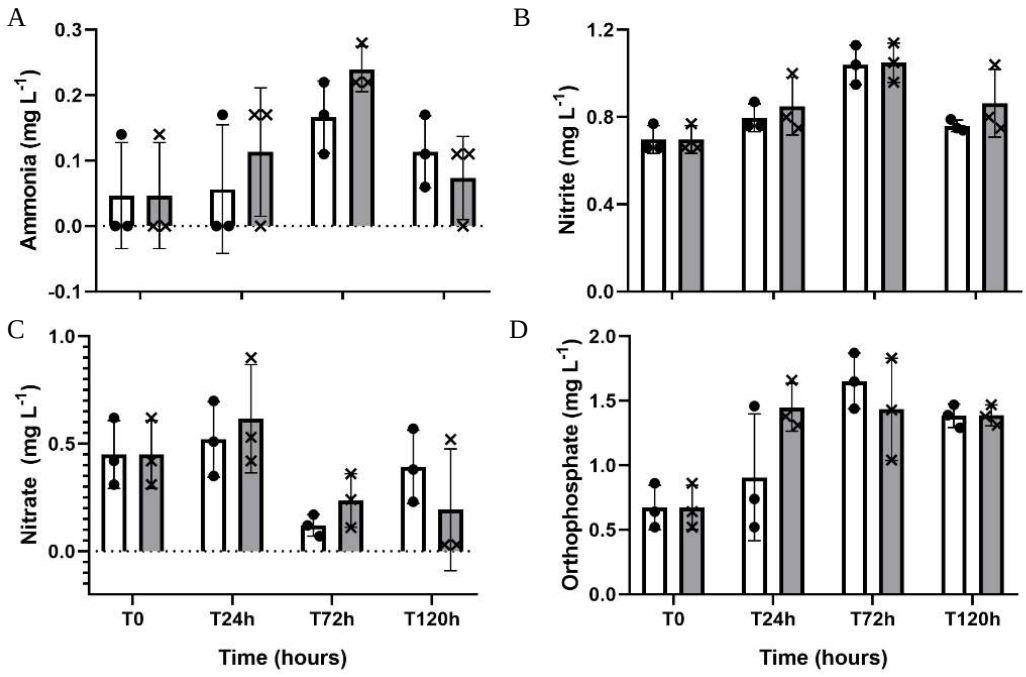

Supplementary Figure 4: Effect of H_2O_2 on ammonia (A), nitrite (B), nitrate (C) and orthophosphate (D) over the time. Results are expressed as the mean ± SD. Grey bars and white bars are representing the treatment and control condition, respectively

Supplementary Table 1: Pearson correlation analysis between all parameters. The significant ($p<0.05$) p-value are labelled in bold (A) and r-values are labelled according negative (in red) or positive (in green) correlation (B).

A)

p value	Transparency	Turbidity	True Color	Temperature	pH	Conductivity	DO	TOC	DOC	Ammonia	Nitrite	Nitrate	Orthophosphate	Sulfate	Fluoride	Chloride	Chl Cyano	Chl Green Algae	Chl Diatoms
Transparency	0	**1.47963E-06**	0.0093469 37	0.9205474	**1.48E-06**	**6.73E-06**	**0.000138**	**0.01071**	0.6067469	0.8406510 67	0.0734098 7	**0.041779**	0.2330527	**0.040132**	0.0704275 4	**0.0050497 88**	0.9456645 1	**2.623E-12**	0.7474234 9	0.8534705 57
Turbidity	**1.47963E-06**	0	0.0716285	0.6906019	**1.31E-06**	**0.012471**	**0.000533**	0.2316176	**0.0234275 88**	0.6379091 9	0.3836496 3	0.9323935	0.7880374 8	0.2341102 5	0.0788628 36	0.8832749 8	**2.36E-07**	0.8757558 1	0.1589397 95
True Color	**0.0093469 37**	0.0716285	0	0.218314	**0.032759**	**0.019985**	0.12291	0.4689782	0.5160282 81	0.2394363 5	0.5953592 5	**0.014861**	0.7728156 3	0.3862405 6	**0.0396621 68**	0.3311955 1	**0.0358954**	**0.0461092**	0.1102991 82
Temperature	0.9205474 23	0.6906019	0.218314	0	0.2251431	**0.024092**	0.3052711	**0.014116**	**0.0387725 09**	0.562764	0.2433320 2	**0.029454**	0.8421153 3	0.6687524 6	0.1781930 1	0.5106076 6	0.8114377 7	0.1737042 9	0.4449780 95

Nitrite	Ammonia	DOC	TOC	DO	Conductivity	pH
0.041778551	0.073409866	0.840651067	0.606746927	**0.010710449**	**0.000137674**	**6.72865E-06**
0.3836496	0.6379092	**0.023428**	0.2316176	**0.000533**	**0.012471**	**1.31E-06**
0.5953593	0.2394363	0.5160283	0.4689782	0.12291	**0.019985**	**0.032759**
0.243332	0.562764	0.0387725	**0.014116**	0.3052711	**0.024092**	0.2251431
0.1198274	0.123407	0.4622969	0.6242501	**1.73E-06**	**3.61E-05**	0
0.031176	0.1867829	0.1334629	0.0219219	**0.016578**	0	**3.61E-05**
0.6042402	0.2782	0.2356161	0.5729477	0	**0.016578**	**1.73E-06**
0.1727151	0.1300714	**7.45E-05**	0	0.5729477	**0.021922**	0.6242501
0.263025563	0.122357557	0	**7.4477E-05**	0.235616099	0.133462943	0.462296896
0.002314	0	0.12235756	0.13007139	0.27820002	0.18678286	0.123407
0	**0.002314**	0.26302556	0.17271513	0.60424024	**0.031176**	0.11982741
0.026931	**0.001141**	**0.040385**	0.06669225	0.55968477	**0.011544**	0.17467151
0.009462	0.03450931	0.06220945	0.05128865	0.54046115	**0.046706**	0.66974565
0.2224397	0.97257572	0.62615468	0.20372788	0.63508494	**0.032563**	0.30851723
0.374115403	0.561620945	0.108157168	0.092324755	0.191398571	9.00574E-05	**0.034738455**
0.4727983	0.90454817	0.97152451	0.25938582	0.09423407	0.62504704	0.54492116
0.0353419	0.13056683	0.70543036	0.75211818	**0.0068838**	**0.0001703**	**5.178E-06**
0.76925606	0.15332594	0.30971149	0.46201044	0.6872145	**0.0415825**	0.79111016
0.137290739	**0.02439428**	0.158796835	0.341471261	0.152018275	0.234827723	0.176439532

Chl Green Algae	Chl Cyano	Chloride	Fluoride	Sulfate	Orthophosphate	Nitrate
0.747423486	**2.62323E-12**	0.945664514	**0.005049788**	0.070427545	**0.040132**	0.233052703
0.8757558	**2.36E-07**	0.883275	0.0788628	0.2341102	0.7880375	0.9323935
0.046109	**0.035895**	0.3311955	**0.039662**	0.3862406	0.7728156	**0.014861**
0.1737043	0.8114378	0.5106077	0.178193	0.6687525	0.8421153	**0.029454**
0.7911102	**5.18E-06**	0.5449212	**0.034738**	0.3085172	0.6697456	0.1746715
0.041583	**0.00017**	0.625047	**9.01E-05**	**0.032563**	**0.046706**	**0.011544**
0.6872145	**0.006884**	0.0942341	0.1913986	0.6350849	0.5404611	0.5596848
0.4620104	0.7521182	0.2593858	0.0923248	0.2037279	0.0512887	0.0666922
0.309711491	0.705430356	0.97152451	0.108157168	0.626154684	0.062209452	**0.040385066**
0.15332594	0.13056683	0.90454817	0.56162094	0.97257572	**0.034509**	**0.001141**
0.76925606	**0.035342**	0.4727983	0.3741154	0.2224397	**0.009462**	**0.026931**
0.16316409	0.36256805	0.30592575	0.0793796	0.77757672	**0.033404**	0
0.65005131	**0.040543**	0.91517804	**0.022243**	0.22847353	0	**0.033404**
0.034508	0.14322601	0.58986535	**0.007356**	0	0.22847353	0.77757672
0.003324598	**0.004169653**	0.936886587	0	**0.007356157**	**0.022243489**	0.079379604
0.98872658	0.67544484	0	0.93688659	0.58986535	0.91517804	0.30592575
0.69602161	0	0.67544484	**0.0041697**	0.14322601	**0.0405429**	0.36256805
0	0.69602161	0.98872658	**0.0033246**	**0.0345078**	0.65005131	0.16316409
0.0004079	0.829246494	0.417938098	0.144712776	0.256790953	**0.04888505**	0.833163594

Chl Diatoms
0.853470557
0.1589398
0.1102992
0.4449781
0.1764395
0.2348277
0.1520183
0.3414713
0.158796835
0.024394
0.13729074
0.83316359
0.04888505
0.25679095
0.144712776
0.4179381
0.82924649
0.0004079
0

B)

Conductivity	pH	Temperature	True Color	Turbidity	Transparency	r value
0.74	-0.82	0.02	-0.55	-0.84	1.00	**Transparency**
-0.53	0.85	0.09	0.40	1.00	-0.84	**Turbidity**
-0.50	0.47	-0.28	1.00	0.40	-0.55	**True Color**
0.49	-0.28	1.00	-0.28	0.09	0.02	**Temperature**
-0.78	1.00	-0.28	0.47	0.85	-0.82	**pH**
1.00	-0.78	0.49	-0.50	-0.53	0.74	**Conductivity**
-0.52	0.84	-0.23	0.35	0.69	-0.54	**DO**
0.50	-0.11	0.53	-0.17	0.27	0.12	**TOC**
0.34	0.17	0.45	-0.15	0.49	-0.05	**DOC**
0.30	-0.35	0.13	-0.27	-0.11	0.40	**Ammonia**
0.47	-0.35	0.27	-0.12	-0.20	0.45	**Nitrite**
-0.54	0.31	-0.48	0.52	-0.02	-0.27	**Nitrate**
0.44	-0.10	0.05	-0.07	-0.06	0.45	**Orthophosphate**
0.47	-0.23	-0.10	-0.20	-0.27	0.40	**Sulfate**
0.75	-0.46	0.31	-0.45	-0.39	0.59	**Fluoride**
-0.11	0.14	-0.15	0.22	-0.03	0.02	**Chloride**
-0.73	0.82	-0.06	0.46	0.87	-0.96	**Chl Cyano**
0.45	-0.06	0.31	-0.44	-0.04	0.07	**Chl Green Algae**
0.27	-0.31	0.18	-0.36	-0.32	0.04	**Chl Diatoms**

Orthophosphate	Nitrate	Nitrite	Ammonia	DOC	TOC	DO
0.45	-0.27	0.45	0.40	-0.05	0.12	-0.54
-0.06	-0.02	-0.20	-0.11	0.49	0.27	0.69
-0.07	0.52	-0.12	-0.27	-0.15	-0.17	0.35
0.05	-0.48	0.27	0.13	0.45	0.53	-0.23
-0.10	0.31	-0.35	-0.35	0.17	-0.11	0.84
0.44	-0.54	0.47	0.30	0.34	0.50	-0.52
0.14	0.13	-0.12	-0.25	0.27	-0.13	1.00
0.43	-0.41	0.31	0.34	0.76	1.00	-0.13
0.41	-0.45	0.26	0.35	1.00	0.76	0.27
0.46	-0.66	0.63	1.00	0.35	0.34	-0.25
0.55	-0.48	1.00	0.63	0.26	0.31	-0.12
-0.47	1.00	-0.48	-0.66	-0.45	-0.41	0.13
1.00	-0.47	0.55	0.46	0.41	0.43	0.14
0.27	-0.07	0.28	-0.01	0.11	0.29	-0.11
0.50	-0.39	0.20	0.13	0.36	0.38	-0.30
-0.02	0.23	0.17	-0.03	0.01	-0.26	0.37
-0.45	0.21	-0.46	-0.34	0.09	-0.07	0.57
0.11	-0.32	-0.07	-0.32	0.23	0.17	0.09
-0.43	-0.05	-0.34	-0.49	-0.32	-0.22	-0.32

Chl Diatoms	Chl Green Algae	Chl Cyano	Chloride	Fluoride	Sulfate
0.04	0.07	-0.96	0.02	0.59	0.40
-0.32	-0.04	0.87	-0.03	-0.39	-0.27
-0.36	-0.44	0.46	0.22	-0.45	-0.20
0.18	0.31	-0.06	-0.15	0.31	-0.10
-0.31	-0.06	0.82	0.14	-0.46	-0.23
0.27	0.45	-0.73	-0.11	0.75	0.47
-0.32	0.09	0.57	0.37	-0.30	-0.11
-0.22	0.17	-0.07	-0.26	0.38	0.29
-0.32	0.23	0.09	0.01	0.36	0.11
-0.49	-0.32	-0.34	-0.03	0.13	-0.01
-0.34	-0.07	-0.46	0.17	0.20	0.28
-0.05	-0.32	0.21	0.23	-0.39	-0.07
-0.43	0.11	-0.45	-0.02	0.50	0.27
0.26	0.46	-0.33	0.12	0.57	1.00
0.33	0.61	-0.60	0.02	1.00	0.57
-0.19	0.00	-0.10	1.00	0.02	0.12
-0.05	-0.09	1.00	-0.10	-0.60	-0.33
0.70	1.00	-0.09	0.00	0.61	0.46
1.00	0.70	-0.05	-0.19	0.33	0.26

Sample	Condition	Time (h)	Transparency (cm)	Turbidity (NTU)	True Color (mg L^{-1})	Temperature (^{o}C)	pH	Conductivity (µS cm^{-1})	DO (mg L^{-1})	TOC (mg L^{-1})	DOC (mg L^{-1})	Ammonia (mg L^{-1})	Nitrite (mg L^{-1})	Nitrate (mg L^{-1})	Orthophosphate (mg L^{-1})	Sulfate (mg L^{-1})	Fluoride (mg L^{-1})	Chloride (mg L^{-1})	Chl Cyano (µg L^{-1})	Chl Green Algae (µg L^{-}	Chl Diatoms (µg L^{-1})
T1M3	Control	24	67	11.6	16.85	30.6	9.07	564	10.18	21.6	17	0.17	0.76	0.35	0.74	7.69	0.21	88.45	34.03	10.16	1.17
T1M1	Control	24	58	11.4	21.19	31	9.15	566	10.1	20.5	17	0	0.87	0.7	0.52	8.2	0.25	85.31	35.05	9.67	1.5
T0	Control	0	51	11	21.19	30.8	8.98	569	8.09	20.2	15.5	0	0.66	0.42	0.86	7.23	0.24	78.97	34.95	8.29	1.83
T0	Control	0	46	11.4	21.19	31.4	8.84	565	8.2	18.8	16.5	0.14	0.66	0.31	0.64	6.69	0.19	85.45	33	8.03	1.17
T0	Control	0	45	11.1	25.53	31.6	8.62	571	7.7	23.6	16.3	0	0.77	0.62	0.52	7.2	0.21	82.31	36.71	9.09	2.23

T5M5	T5M3	T5M1	T3M5	T3M2	T3M1	T1M5
Control	Control	Control	Control	Control	Control	Control
120	120	120	72	72	72	24
67	72	67	67	63	58	68
12.6	12.6	14	14.4	14	14.7	11.4
21.19	21.19	21.19	21.19	21.19	21.19	21.19
31.6	30.3	31.3	31.5	31.6	31.3	30.8
9.01	8.92	8.99	9.2	9.07	9.15	9.2
574	573	575	573	575	573	566
8.6	9.56	9.25	10.6	12.71	11.03	10.78
33.3	27.4	28.3	27.5	24.2	27.3	19.1
20.8	20.6	24.1	22.3	22.1	21.8	15.6
0.06	0.11	0.17	0.17	0.11	0.22	0
0.79	0.74	0.75	1.04	0.95	1.13	0.76
0.57	0.38	0.23	0.12	0.17	0.07	0.51
1.39	1.29	1.47	1.65	1.44	1.87	1.46
8.16	7.86	8.03	7.5	7.11	7.9	7.53
0.98	0.53	1.78	0.59	0.62	0.57	0.54
85.1	80.9	83.98	86.68	92.08	81.28	80.97
24.09	25.92	30.07	26.55	27.68	31.2	29.47
11.33	11.64	13.02	12.24	12.57	13.8	10.67
0	0.63	0.86	0	0	0	0.67

T5M2	T3M6	T3M4	T3M2	T1M6	T1M4	T1M2
Treatment	Treatment	Treatment	Treatment	Treatment	Treatment	Treatment
120	72	72	72	24	24	24
108	112	115	119	84	83	78
4	6.5	4.7	5.4	8.3	8.6	7.9
16.85	16.85	16.85	21.19	21.19	25.53	25.53
31.1	31.3	31.3	31.3	30.6	30.4	30.2
8.34	8.17	8.13	7.97	8.97	9.02	8.81
583	577	580	584	566	567	569
8.14	6.65	6.35	6.25	9.54	10.84	9.36
22.2	26	22.8	28.2	20.2	19	17.8
17.8	18.5	19.5	17.4	16.1	16.6	15.3
0	0.22	0.22	0.28	0.17	0	0.17
0.8	1.05	0.96	1.14	0.8	0.75	1
0.52	0.24	0.36	0.11	0.42	0.9	0.53
1.31	1.43	1.04	1.83	1.66	1.38	1.31
8.45	7.66	7.28	8.05	7.03	7.53	8.43
1.6	0.84	0.74	0.95	0.64	0.53	0.52
86.86	83.08	83.56	82.59	81.86	91.61	92.91
0	1.87	0.28	0	15.36	14.15	18.18
26.99	3.18	2.7	3.65	3.82	4.08	3.57
2.88	0.29	0.1	0.18	0	0	0

T5M6	T5M4
Treatment	Treatment
120	120
102	105
7.3	5.3
16.85	16.85
31.4	31.4
8.37	8.26
582	583
8.71	7.29
24.5	22.9
18.5	17.2
0.11	0.11
0.75	1.04
0.03	0.03
1.38	1.47
8.34	8.21
1.2	1.85
81.32	86.75
14.26	0
19.01	24.54
2.3	2.9

8.2 Capítulo 2 (Effect of hydrogen peroxide on the bacterioplankton community from a drinking water reservoir in Brazilian semiarid region)

Supplementary Table 1: Sample identification, sequencing data and diversity indexes

			Number of sequences			Richness	Diversity	Evenness
Sample	Description	DNA concentration (ng/uL)	Before trim qual	After trim qual	Coverage	Sobs	Shannon (H')	ShannonEven
T0a	Time 0	10.8	103444	32221	0.975	1617	5.08	0.688
T0b	Time 0	13.106	50162	32221	0.973	1711	5.14	0.691
T0c	Time 0	7.762	84658	32221	0.974	1653	5.19	0.700
T1M1	No H_2O_2 (T 24h)	24.855	220482	32221	0.973	1687	4.98	0.671
T1M2	H_2O_2 (T 24h)	21.904	65561	32221	0.979	1245	2.74	0.385
T1M3	No H_2O_2 (T 24h)	15.593	96268	32221	0.980	1410	4.98	0.687
T1M4	H_2O_2 (T 24h)	17.373	89357	32221	0.985	883	2.41	0.356
T1M5	No H_2O_2 (T 24h)	12.076	266828	32221	0.977	1447	4.95	0.681
T1M6	H_2O_2 (T 24h)	12.487	134237	32221	0.982	1114	3.13	0.446
T3M1	No H_2O_2 (T 72h)	26.633	100340	32221	0.975	1571	5.12	0.696
T3M2	H_2O_2 (T 72h)	8.088	149253	32221	0.982	1025	3.36	0.485
T3M3	No H_2O_2 (T 72h)	23.73	38774	32221	0.978	1438	4.97	0.683
T3M4	H_2O_2 (T 72h)	5.693	363589	32221	0.982	991	3.21	0.466

T3M6	H_2O_2 (T 72h)	8.584	98866	32221	0.975	1373	3.18	0.440
T5M1	No H_2O_2 (T 120h)	20.208	86240	32221	0.974	1548	4.83	0.658
T5M2	H_2O_2 (T 120h)	23.88	155713	32221	0.975	1587	4.69	0.636
T5M3	No H_2O_2 (T 120h)	22.109	102664	32221	0.981	1276	4.58	0.641
T5M4	H_2O_2 (T 120h)	17.982	84591	32221	0.983	1165	4.22	0.598
T5M5	No H_2O_2 (T 120h)	26.747	100176	32221	0.980	1308	4.61	0.642
T5M6	H_2O_2 (T 120h)	18.224	165810	32221	0.978	1427	5.13	0.707

Supplementary Table 2: Analysis of two way PERMANOVA considering condition (control or treatment) and time (0, 24, 72 and 120h) as groups and using Bray-Curtis matrix distance of similarity and $p<0.05$ for hypothesis test.

Two-way PERMANOVA

Permutation N: 9999					
Source	Sum of square roots	df	Mean square	F	P
Condition	1.9493	1	1.9493	26.562	0.0001
Time	0.99428	3	0.33143	4.5162	0.0001
Interaction	-0.036183	3	-0.012061	-0.16435	0.037
Residual	0.88064	12	0.073386		
Total	3.788	19			

Supplementary Table 3: Relative abundance (%) of bacterial phyla in control and treatment samples over the time 0 (A), 24h (B), 72 (C) and 120h (D). Average values of replicates are also shown. (n=3).

(A)

	Time 0a	Time 0b	Time 0c	**average**
Actinobacteria	20.3	21.2	22.2	21.2
Bacteria_unclassified	4.4	5.3	5.6	5.1
Bacteroidetes	7.0	6.5	6.8	6.8
Chloroflexi	7.6	7.5	7.9	7.7
Cyanobacteria	24.2	21.6	15.6	20.4
Deinococcota	0.0	0.0	0.0	0.015
Firmicutes	0.1	0.2	0.3	0.2
Patescibacteria	1.0	1.5	1.5	1.3
Planctomycetes	13.7	14.8	15.2	14.6
Proteobacteria	10.7	11.3	11.6	11.2
Verrucomicrobia	8.5	7.9	10.6	9.0
Others	2.4	2.2	2.4	2.3

(B)

	No H2O2 (M1)	No H2O2 (M3)	No H2O2 (M5)	H2O2 (M2)	H2O2 (M4)	H2O2 (M6)	**avg no H2O2**	**avg H2O2**
Actinobacteria	17.2	20.0	20.1	4.0	5.4	10.8	19.1	6.7
Bacteria_unclassified	4.9	4.2	4.6	0.8	0.9	2.3	4.6	1.3
Bacteroidete	6.4	7.0	6.8	1.2	1.0	2.5	6.7	1.6
Chloroflexi	9.6	6.9	5.9	0.9	1.1	2.4	7.5	1.5
Cyanobacteria	29.1	24.5	22.0	0.5	0.9	2.2	25.2	1.2
Deinococcota	0.0	0.1	0.0	29.7	4.5	0.2	0.1	11.5
Firmicutes	0.2	0.5	0.1	37.1	52.5	53.7	0.3	47.7
Patescibacteria	1.0	1.2	1.3	0.3	0.7	1.1	1.2	0.7
Planctomycetes	12.1	13.2	14.5	4.0	5.7	11.5	13.3	7.1
Proteobacteria	10.8	11.4	11.6	19.0	24.0	7.6	11.3	16.9
Verrucomicrobia	6.3	8.6	11.0	2.3	3.0	4.6	8.6	3.3
Others	2.3	2.1	2.0	0.2	0.2	0.9	2.1	0.5

(C)

	No H2O2 (M1)	No H2O2 (M3)	H2O2 (M2)	H2O2 (M4)	H2O2 (M6)	**avg no H2O2**	**avg H2O2**
Actinobacteria	13.9	15.1	4.8	5.2	5.3	14.5	5.1
Bacteria_unclassified	4.8	4.1	1.6	2.1	2.0	4.4	1.9
Bacteroidete	7.7	6.6	14.8	6.5	11.9	7.2	11.1
Chloroflexi	9.0	9.2	0.7	0.7	0.7	9.1	0.7
Cyanobacteria	26.4	27.8	0.7	0.7	1.6	27.1	1.0
Deinococcota	0.1	0.0	8.0	7.6	7.0	0.0	7.5
Firmicutes	0.2	0.4	32.4	37.6	48.9	0.3	39.6
Patescibacteria	1.1	0.9	0.3	0.4	0.4	1.0	0.4
Planctomycetes	14.3	13.4	4.5	5.3	5.7	13.8	5.2
Proteobacteria	10.5	9.5	28.4	29.9	11.4	10.0	23.2
Verrucomicrobia	9.2	10.2	3.6	3.8	4.6	9.7	4.0
Others	2.6	2.6	0.2	0.3	0.4	2.6	0.3

D)

	No H2O2 (M1)	No H2O2 (M3)	No H2O2 (M5)	H2O2 (M2)	H2O2 (M4)	H2O2 (M6)	**avg no H2O2**	**avg H2O2**
Actinobacteria	12.0	10.6	10.2	6.4	3.5	8.0	10.9	6.0
Bacteria_unclassified	3.5	3.5	3.2	2.5	1.9	2.9	3.4	2.4
Bacteroidetes	8.1	9.2	12.6	15.5	23.5	17.4	10.0	18.8
Chloroflexi	9.6	9.2	10.0	2.6	1.1	2.4	9.6	2.0
Cyanobacteria	24.8	20.1	14.4	4.6	4.2	13.3	19.8	7.4
Deinococcota	0.1	0.0	0.0	0.8	1.4	0.2	0.0	0.8

Firmicutes	0.4	0.2	0.1	6.8	8.3	2.2	0.3	5.8
Patescibacteria	0.8	0.8	0.4	0.1	0.1	0.2	0.7	0.2
Planctomycetes	13.5	11.8	13.4	4.3	2.9	8.3	12.9	5.2
Proteobacteria	9.9	9.5	8.7	30.9	24.0	23.6	9.4	26.2
Verrucomicrobia	15.0	23.2	24.9	23.7	28.5	20.1	21.0	24.1
Others	2.2	1.7	1.9	1.7	0.5	1.4	1.9	1.2

Supplementary Table 4: Main OTUs that contributed to the difference between control and treatment at each time: 24h (a), 72h (b) and 120 (c) according to SIMPER analysis. OTUs were selected considering a contribution above 1% or a cumulative contribution of 50%

(A)

24h (treatment vs control)					
Overall dissimilarity: 75.04					
Taxon	Av. dissim	Contrib. %	Cumulative %	Mean control	Mean h2o2
Otu000001	23.02	30.67	30.67	40	1.45E+04
Otu000003	5.239	6.982	37.66	3,32E+03	14
Otu000008	5.121	6.824	44.48	14,3	3.24E+03
Otu000047	3.191	4.252	48.73	47	2.04E+03
Otu000005	2.006	2.673	51.4	6	1.27E+03
Otu000009	1.428	1.903	53.31	950	49.7
Otu000007	1.168	1.557	54.86	881	145
Otu000016	1.159	1.544	56.41	779	48.7
Otu000010	0.9891	1.318	57.73	946	323
Otu000006	0.9642	1.285	59.01	1,08E+03	469
Otu000014	0.9547	1.272	60.28	818	216

Otu00002 8	0.9193	1.225	61.51	633	53.3
Otu00000 2	0.8747	1.166	62.68	1.20E+03	680

(B)

72h (treatment vs control)					
Overall dissimilarity: 81.62					
Taxon	Av. dissim	Contrib. %	Cumulative %	Mean control	Mean h2o2
Otu00000 1	18.75	22.98	22.98	2.00E+01	1.18E+04
Otu00000 5	4.522	5.541	28.52	3.50E+00	2.85E+03
Otu00000 3	3.355	4.111	3.26E+01	2.12E+03	7.33
Otu00000 8	3.317	4.064	36.69	1.25E+01	2.10E+03
Otu00002 5	2.263	2.773	39.47	1.50E+00	1.43E+03
Otu00001 6	1.757	2.152	41.62	1.14E+03	30
Otu00002 1	1.523	1.866	4.35E+01	967	6.67
Otu00000 9	1.478	1.81	45.29	993	61.3
Otu00001 4	1.47	1,801	47.09	959	32
Otu00002 3	1.368	1.675	48.77	863	0.667
Otu00004 2	1.236	1.514	50.28	1.5	780

Otu000039	1.158	1.418	51.7	1.5	731
Otu000002	1.115	1.366	53.07	1.54E+03	835
Otu000028	0.8843	1.083	54.15	587	29.7
Otu000006	0.8404	1.03	5.52E+01	875	345

(C)

120h (treatment vs control)					
Overall dissimilarity: 72.79					
Taxon	Av. dissim	Contrib. %	Cumulative %	Mean control	Mean h2o2
Otu000017	6.955	9.554	9.554	8.33	4.39E+03
Otu000002	5.984	8.221	17.78	4.53E+03	756
Otu000003	3.373	4.634	22.41	2.43E+03	303
Otu000001	2.592	3.561	25.97	19.7	1.65E+03
Otu000009	1.737	2.386	28.36	1.27E+03	178
Otu000037	1.542	2.118	30.48	0.667	972
Otu000029	1.466	2.013	32.49	30	954
Otu000088	1.456	2	34.49	5	922
Otu000023	1.292	1.774	36.26	846	31.7

Otu000006	1.13	1.552	37.81	934	222
Otu000081	1.113	1.529	39.34	2.33	704
Otu000016	1.089	1.495	40.84	1.04E+03	351
Otu000014	1.082	1.486	42.33	797	116
Otu000160	0.9758	1.341	43.67	1.33	616
Otu000025	0.9362	1.286	44.95	1.67	592
Otu000028	0.8992	1.235	46.19	608	41.3
Otu000065	0.7712	1.059	47.25	4	490
Otu000042	0.7236	0.994	48.24	1.67	458
Otu000005	0.7151	0.9824	49.22	4	455
Otu000010	0.6141	0.8436	50.07	576	189

Supplementary Table 5: Spearman correlation between the main OTUs, which contributed to the difference between control and treatment over the time, with physical chemical parameters that showed difference over the treatment according to Guedes et al., 2020. Spearman r values are labeled considering a negative (in red) or positive (in green) correlation, from a significant p-value ($p<0.01$).

(r) Sperman	Transparency	Turbidity	pH	Conductivity	DO_2	DOC	Chl Cyano	Chl Green Algae	Chl Diatoms
Otu000001	0.775	-0.658	-0.407	0.264	-0.206	-0.139	-0.712	-0.399	-0.252
Otu000002	-0.472	0.760	0.467	-0.173	0.344	0.406	0.497	0.280	-0.150
Otu000003	-0.702	0.810	0.710	-0.485	0.592	0.171	0.772	0.410	0.138
Otu000005	0.803	-0.722	-0.577	0.530	-0.384	0.022	-0.747	-0.240	-0.042
Otu000006	-0.774	0.708	0.646	-0.628	0.358	-0.119	0.821	0.035	0.027
Otu000007	-0.719	0.356	0.465	-0.492	0.287	-0.278	0.730	0.389	0.531
Otu000008	0.797	-0.687	-0.520	0.447	-0.318	-0.045	-0.755	-0.350	-0.239
Otu000009	-0.622	0.764	0.559	-0.242	0.317	0.250	0.622	0.378	0.017
Otu000010	-0.823	0.664	0.596	-0.679	0.325	-0.153	0.893	-0.032	0.085
Otu000014	-0.915	0.791	0.669	-0.531	0.459	-0.029	0.887	0.308	0.096
Otu000016	-0.622	0.846	0.588	-0.158	0.481	0.445	0.551	0.624	0.013
Otu000017	0.265	-0.477	-0.393	0.473	-0.549	-0.015	-0.306	0.323	0.567
Otu000021	-0.881	0.767	0.643	-0.492	0.481	0.059	0.885	0.296	0.103
Otu000023	-0.735	0.839	0.538	-0.133	0.390	0.489	0.661	0.587	0.091
Otu000025	0.666	-0.551	-0.683	0.777	-0.530	0.337	-0.595	-0.002	0.221
Otu000028	-0.803	0.752	0.706	-0.541	0.462	-0.034	0.783	0.200	-0.027
Otu000029	-0.107	-0.128	0.081	0.074	-0.042	-0.163	0.090	0.600	0.736
Otu000037	0.683	-0.717	-0.748	0.821	-0.729	0.190	-0.714	0.102	0.338
Otu000039	0.734	-0.656	-0.626	0.601	-0.475	0.122	-0.708	-0.245	-0.026
Otu000042	0.604	-0.746	-0.806	0.550	-0.757	-0.104	-0.593	-0.223	0.255
Otu000047	0.310	-0.286	-0.092	0.051	0.017	-0.054	-0.215	-0.369	-0.254

Otu000065	0.804	-0.564	-0.711	0.848	-0.527	0.410	-0.829	0.148	0.090
Otu000081	0.760	-0.581	-0.638	0.759	-0.536	0.409	-0.771	0.230	0.310
Otu000088	-0.255	-0.088	0.187	-0.162	0.105	-0.299	0.205	0.569	0.742
Otu000160	0.723	-0.626	-0.713	0.806	-0.620	0.368	-0.757	0.199	0.298

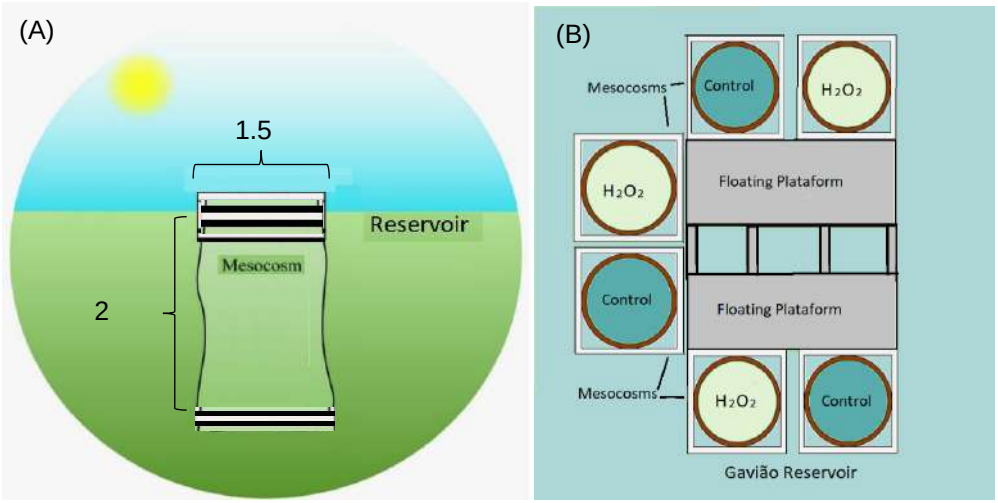

Supplementary Figure 1: The experimental set-up of the mescosms structure (A) maintained in a PVC-based floating platform (B). Adapted from Guedes et al., 2020

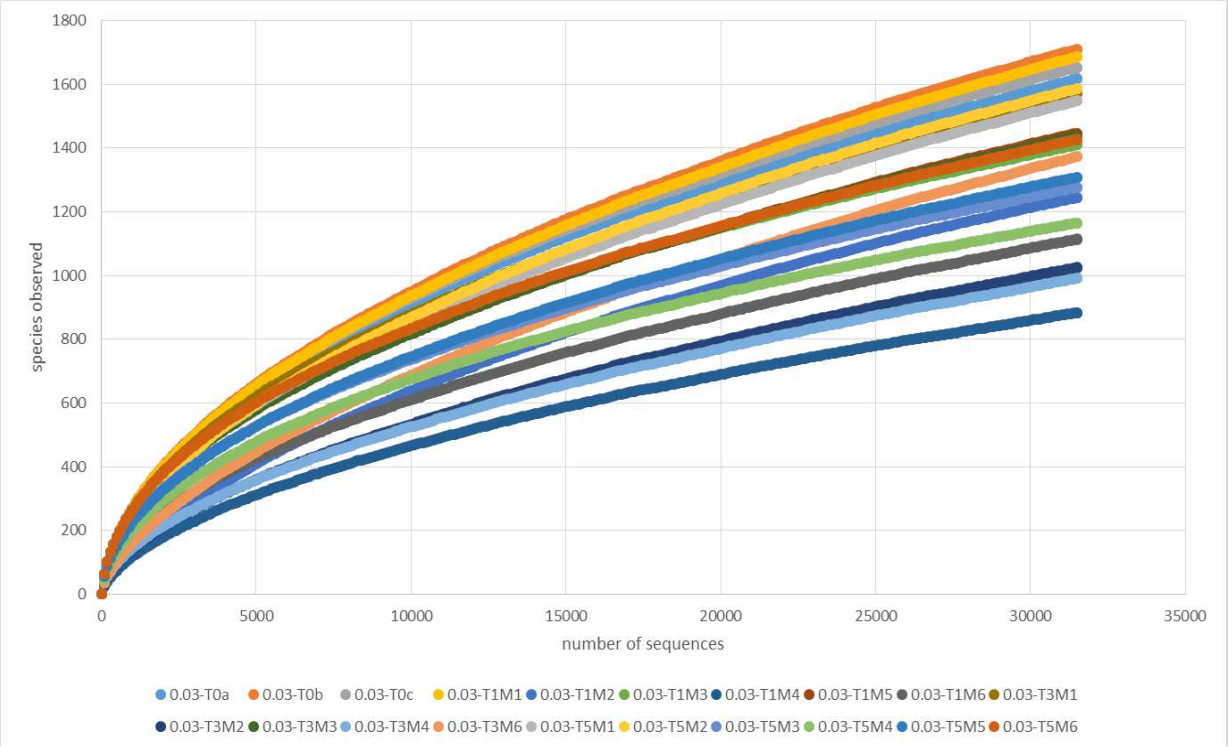

Supplementary Figure 2: Rarefaction curves relating observed species with the number of sequences for all samples after normalization.

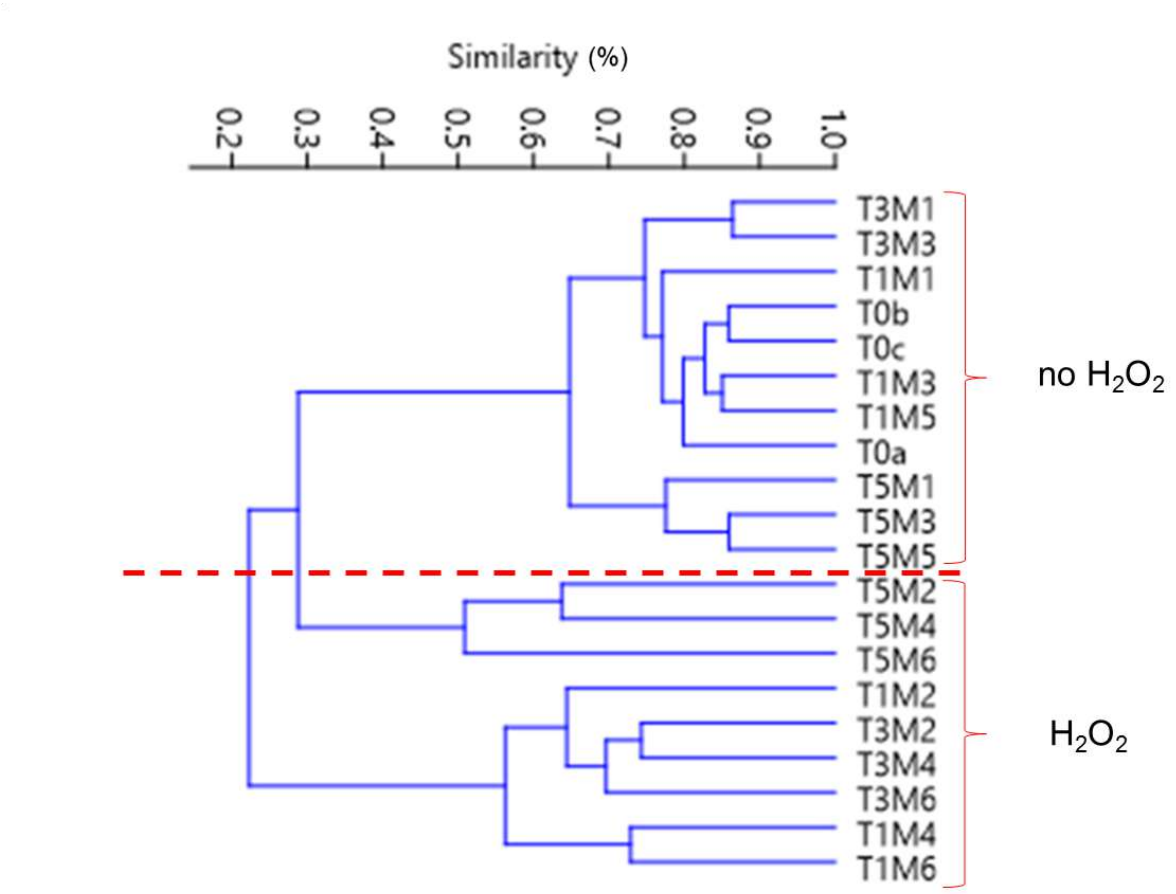

Supplementary Figure 3: Hierarchical clustering of samples considering a matrix using Bray-Curtis distance. The dashed red line separates treatment and control groups.

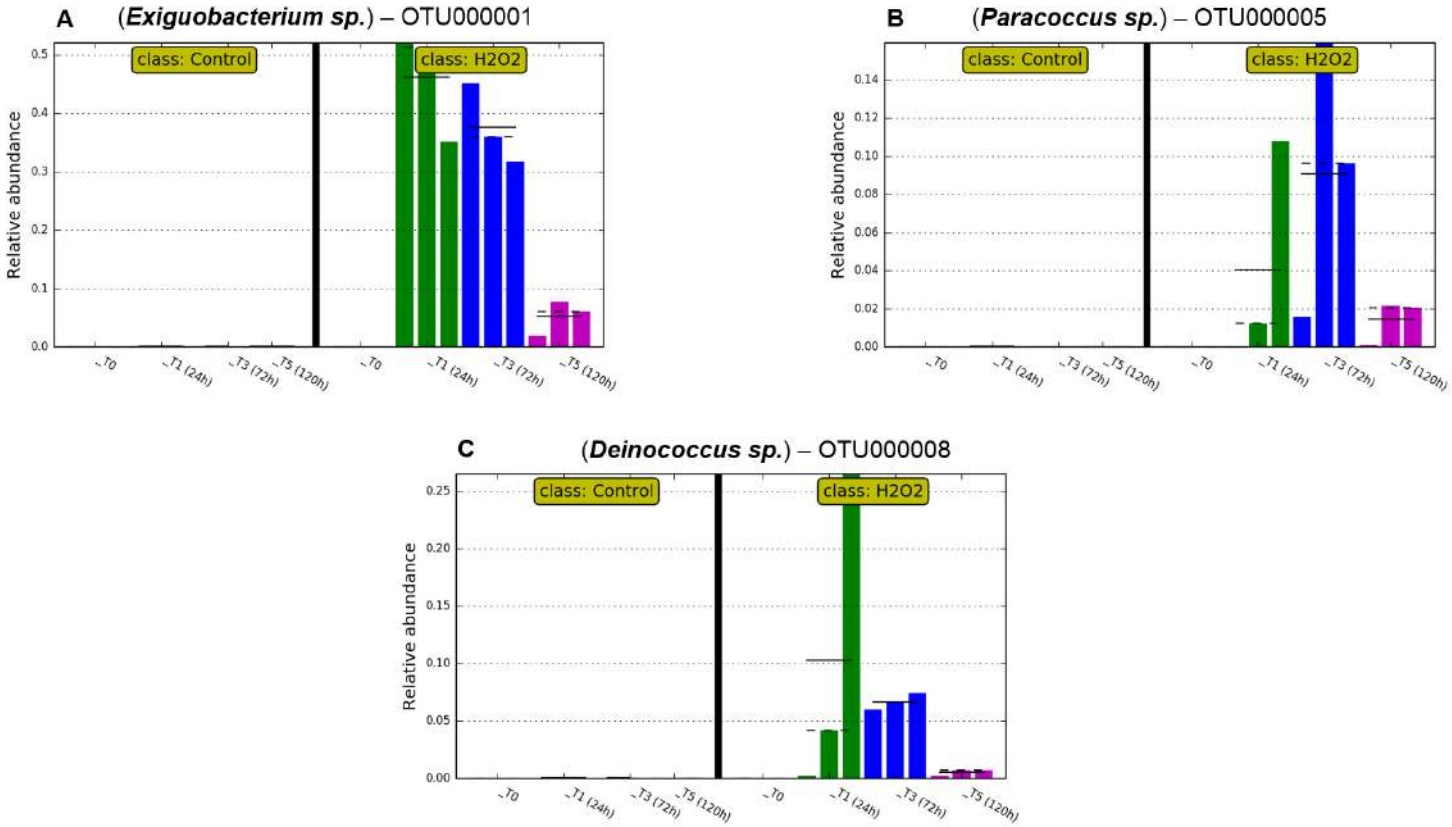

Supplementary Figure 4: Relative abundance of the three main bacterial genera that contributed to the difference between treatment and control in each sampling time according to LEfSe analysis, considering in A) *Exiguobacterium sp.* B) *Deinococcus sp.* and C) *Paracoccus sp.*

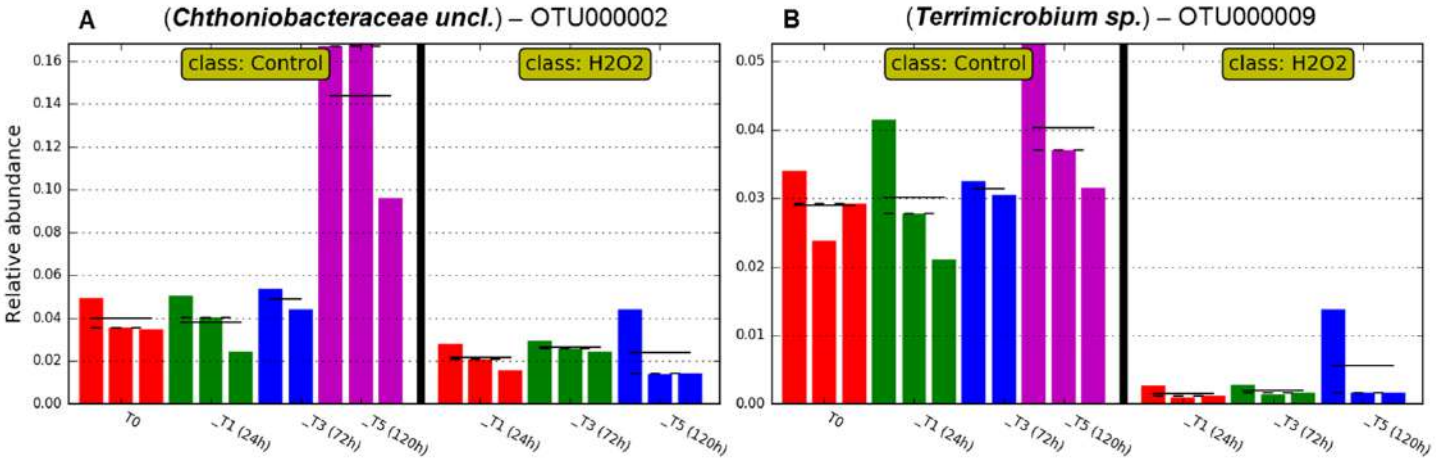

Supplementary Figure 5: Relative abundance of the two main heterotrophic bacteria that contributed to the difference between treatment and control in each sampling time according to LEfSe analysis, considering in A) *Chthoniobacteraceae unclassified* and B) *Terrimicrobium sp.*

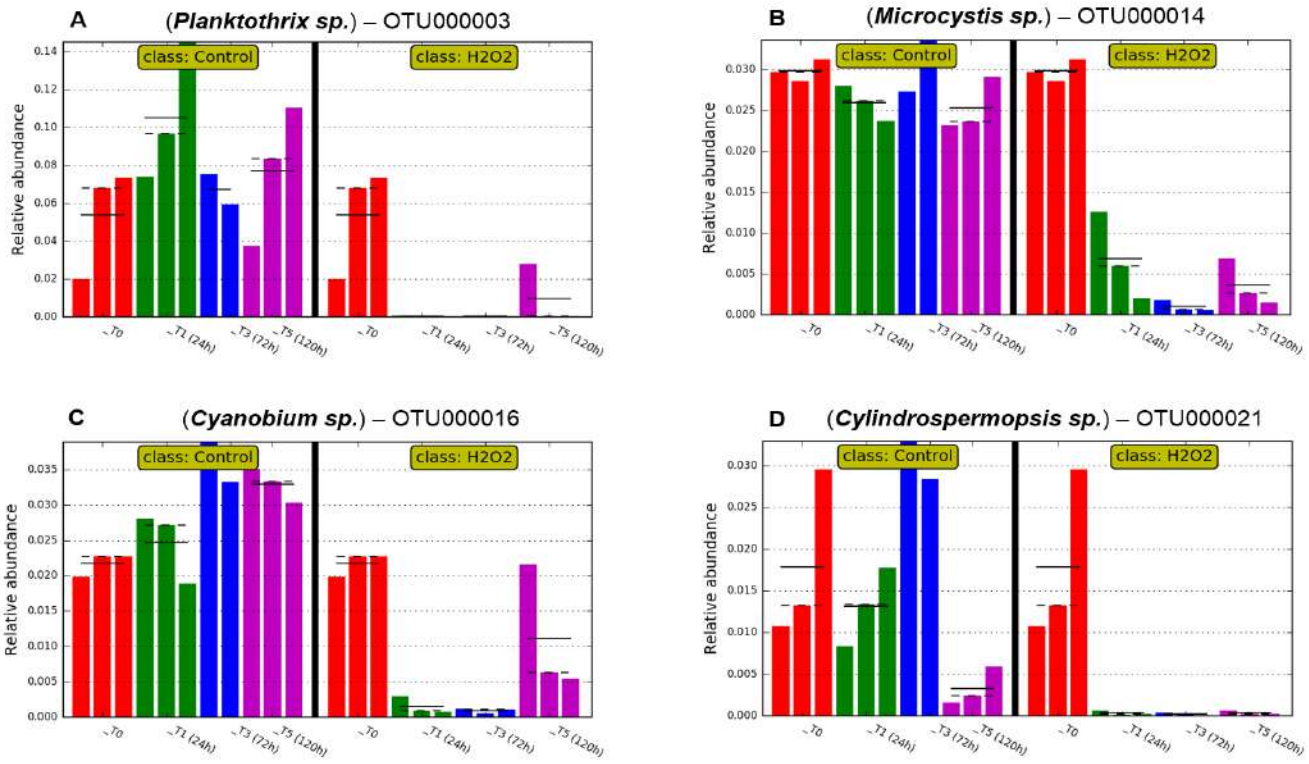

Supplementary Figure 6: Relative abundance of the four main cyanobacterial genera present in the reservoir considering control and treatment conditions over the time. (A) *Planktothrix sp.* (B) *Microcystis sp.* (C) *Cyanobium sp.* and (D) *Cylindrospermopsis sp.* now *Raphidiopsis sp.*

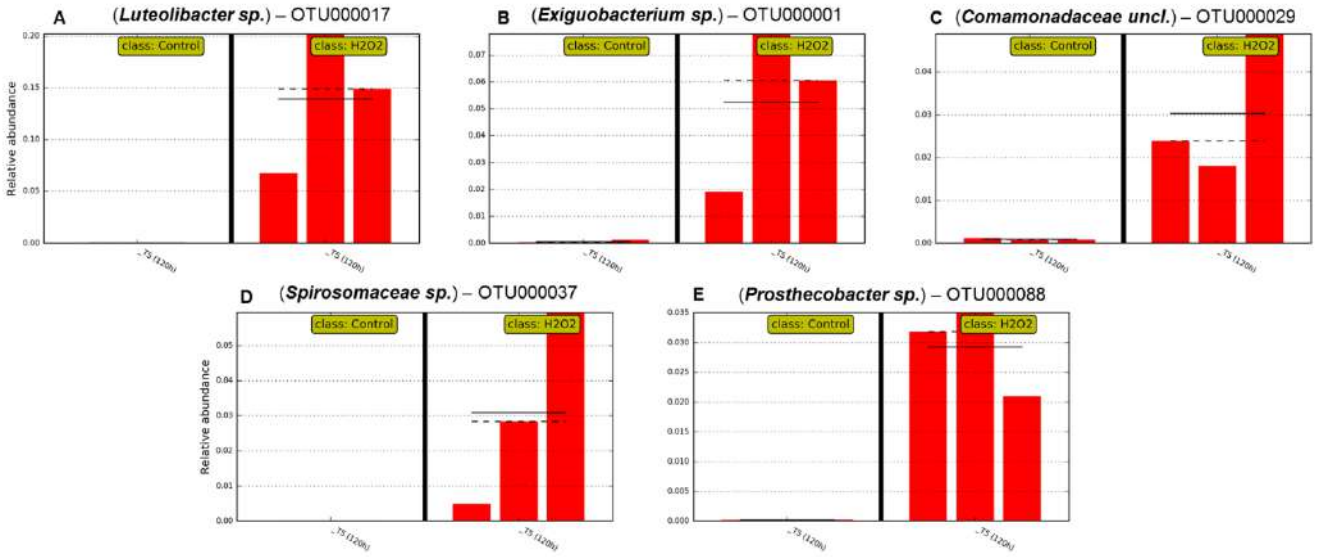

Supplementary Figure 7: Relative abundance of the top five bacteria in treatment and control condition at 120h sampling time according to LEfSe analysis, where A) *Luteolibacter sp.*, B) *Exiguobacterium sp.*, C) *Comamonadaceae unclassified.*, D) *Spirosomaceae sp.* and E) *Prosthecobacter sp.*

8.3 Capítulo 3 (Filterable bacterioplankton able to degrade microcystin)

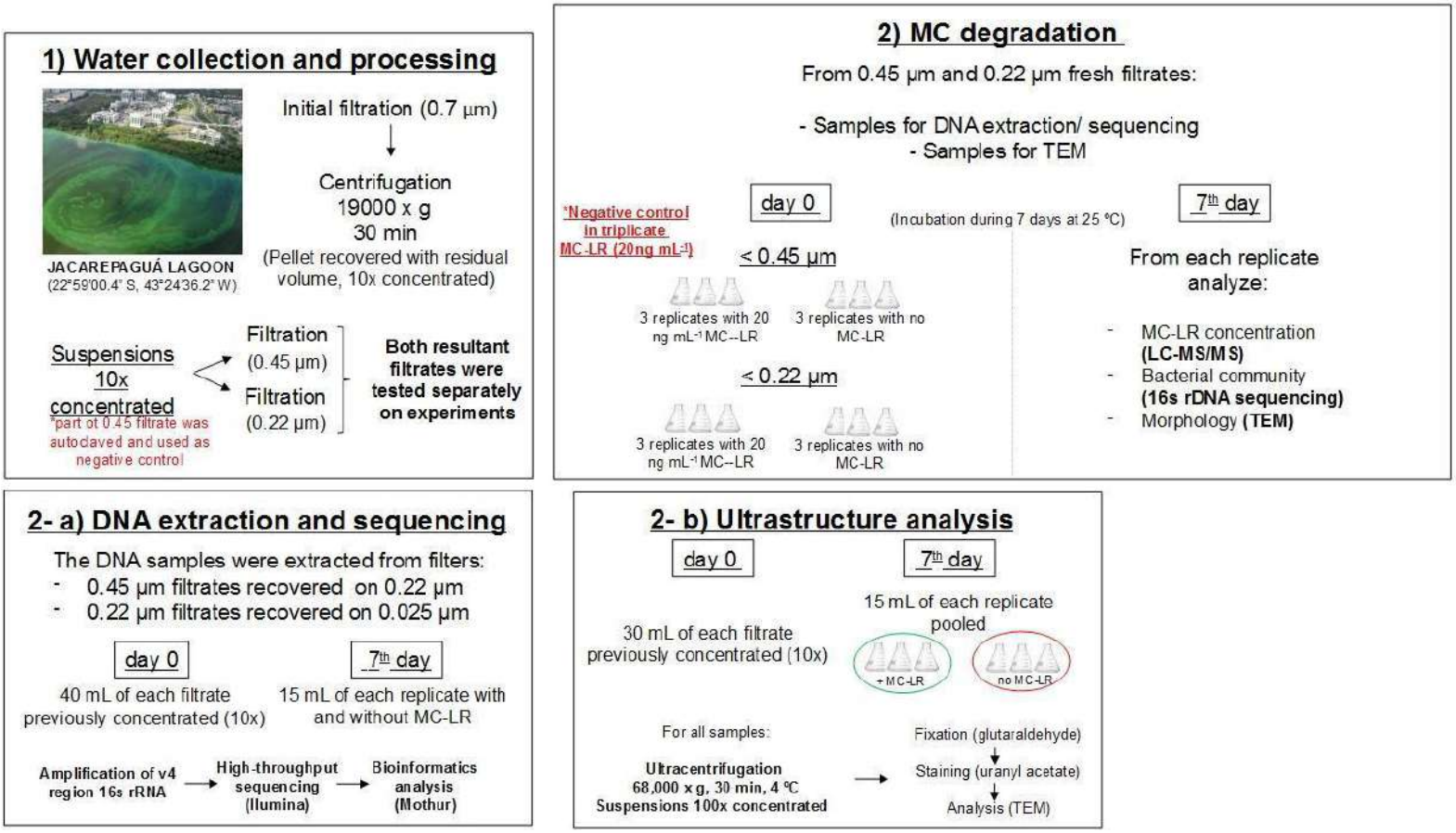

Supplementary Figure 1: Overview of the experimental setup

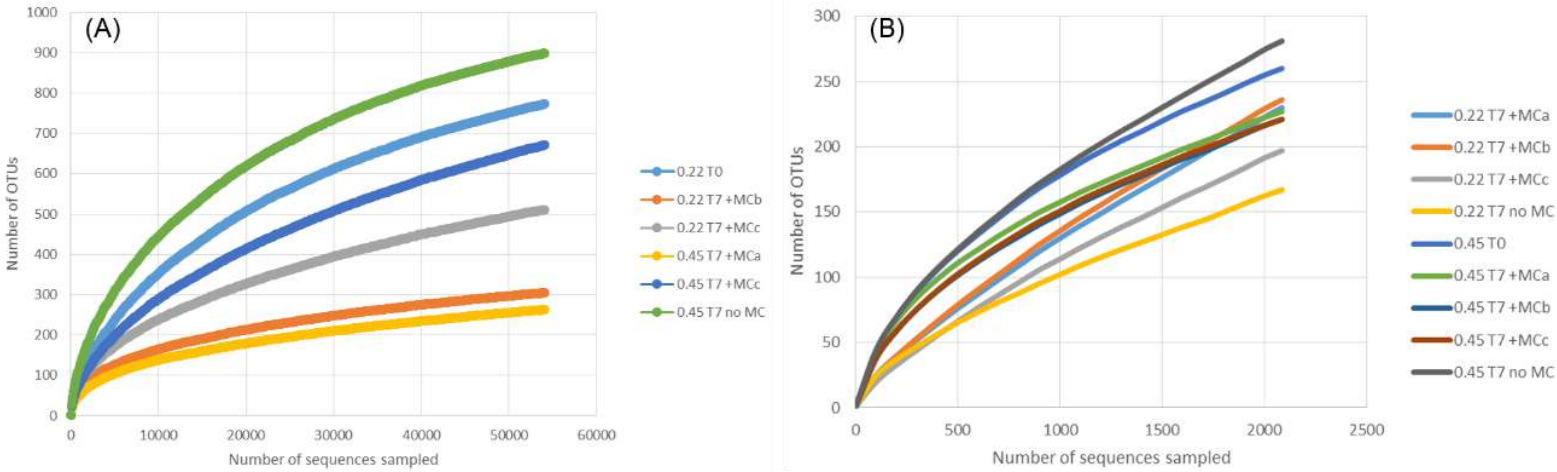

Supplementary Figure 2: Rarefaction curves (number of OTUs per number of sequences) of sequenced samples collected in (A) November 2016 and (B) November 2017. Bacterial communities originally selected by different pore size filters (<0.45 or <0.22 μm) at time 0 (T_0) and after 7 days (T_7), with or without MC-LR. +MC a, b, c refers to replicates maintained with MC-LR.

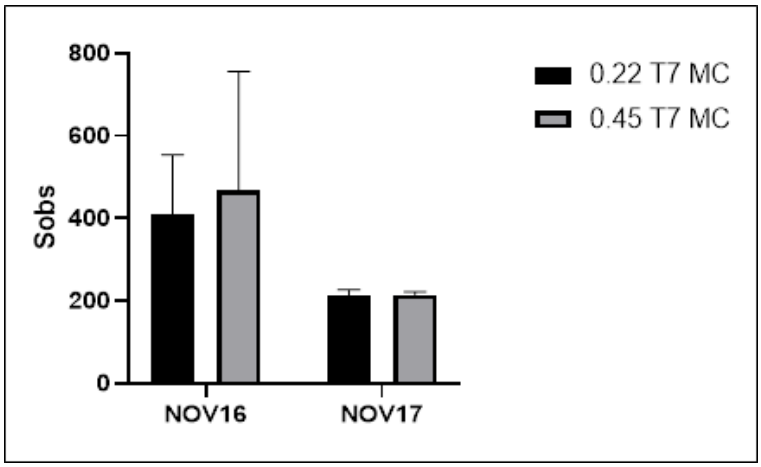

Two-way ANOVA Ordinary
Alpha 0.05

Source of Variation	% of total variation	P value	P value summary	Significant?
Interaction	0.8727	0.747	ns	No
YEAR	52.59	0.0395	*	Yes
SIZE	0.9553	0.7359	ns	No

ANOVA table	SS (Type III)	DF	MS	F (DFn, DFd)	P value
Interaction	1995	1	1995	F (1, 6) = 0.1141	P=0.7470
YEAR	120243	1	120243	F (1, 6) = 6.877	P=0.0395
SIZE	2184	1	2184	F (1, 6) = 0.1249	P=0.7359
Residual	104911	6	17485		

Supplementary Figure 3: Richness estimated from the number of observed species (sobs) for samples that degraded MC-LR (MC) after 7 days (T7). Samples originally selected according to size (<0.45 μm and <0.22 μm) and collected in different dates (Nov 2016 and Nov 2017). Statistical analysis considering the two tested groups by two-way ANOVA and Tukey's *post hoc.*

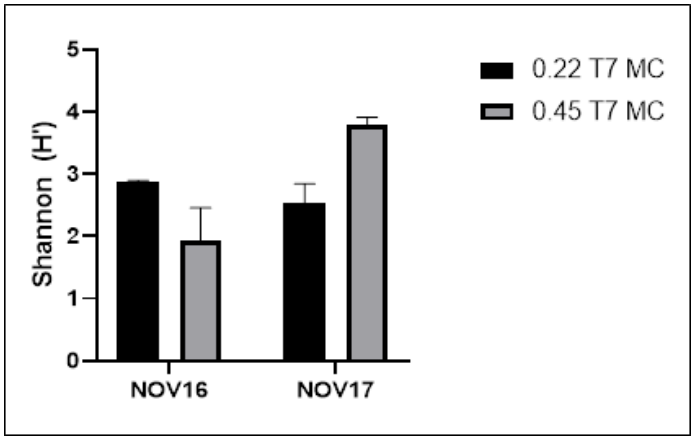

Source of Variation	% of total variation	P value	P value summary	Significant?
Interaction	56.66	0.0012**		Yes
YEAR	26.49	0.0074**		Yes
SIZE	1.074	0.4553ns		No

ANOVA table	SS (Type III)	DF	MS	F (DFn, DFd)	P value
Interaction	2.913	1	2.913	F (1, 6) = 33.60	P=0.0012
YEAR	1.362	1	1.362	F (1, 6) = 15.71	P=0.0074
SIZE	0.05521	1	0.05521	F (1, 6) = 0.6368	P=0.4553
Residual	0.5202	6	0.08669		

Tukey's multiple comparisons test	Mean Diff.	95.00% CI of diff.	Significant?	Summary	Adjusted P Value
NOV16:0.45 T7 MC vs. NOV17:0.45 T7 MC	-1.855	-2.785 to -0.9245	Yes	**	0.0019
NOV17:0.22 T7 MC vs. NOV17:0.45 T7 MC	-1.253	-2.086 to -0.4211	Yes	**	0.0079

Supplementary Figure 4: Diversity estimated by by Shannon index (H') for samples that degraded MC-LR (MC) after 7 days (T7). Samples originally selected according to size (<0.45 μm and <0.22 μm) and collected in different dates (Nov 2016 and Nov 2017). Statistical analysis considering the two tested groups by two-way ANOVA and Tukey's *post hoc.*

(A)

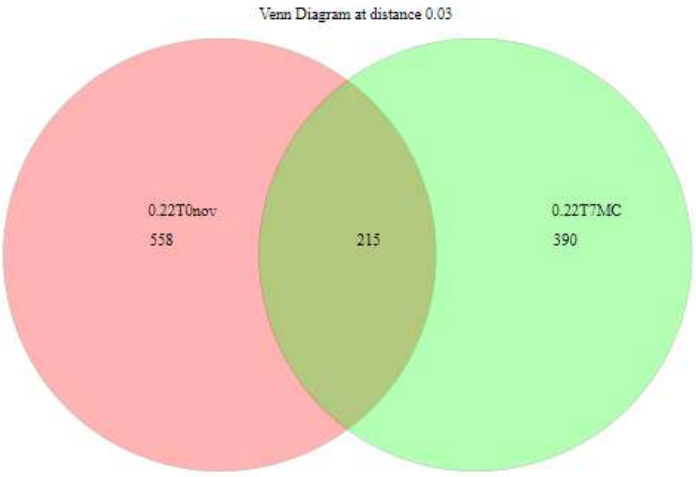

The number of species in group 0.22T0nov is 773
The number of species in group 0.22T7MC is 605
The number of species shared between groups 0.22T0nov and 0.22T7MC is 215
Percentage of species that are shared in groups 0.22T0nov and 0.22T7MC is 18.4867
The total richness for all groups is 1163

.

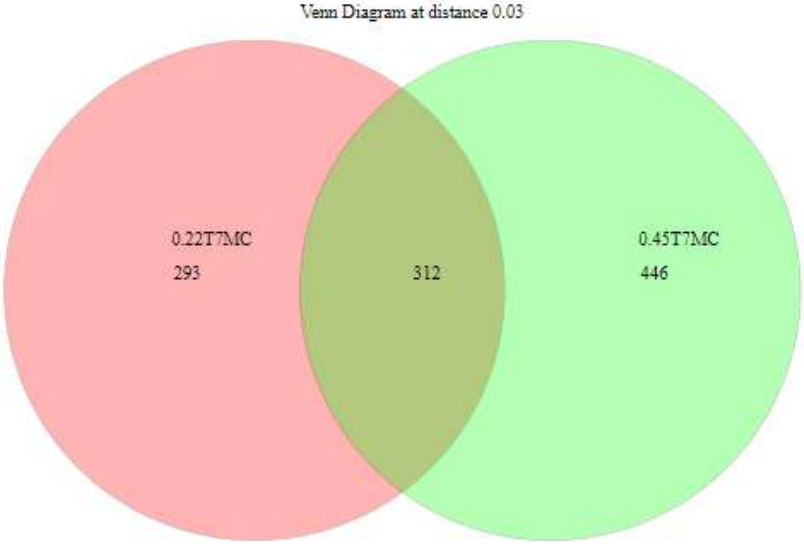

The number of species in group 0.22T7MC is 605

The number of species in group 0.45T7MC is 758

The number of species shared between groups 0.22T7MC and 0.45T7MC is 312

Percentage of species that are shared in groups 0.22T7MC and 0.45T7MC is 29.686

The total richness for all groups is 1051

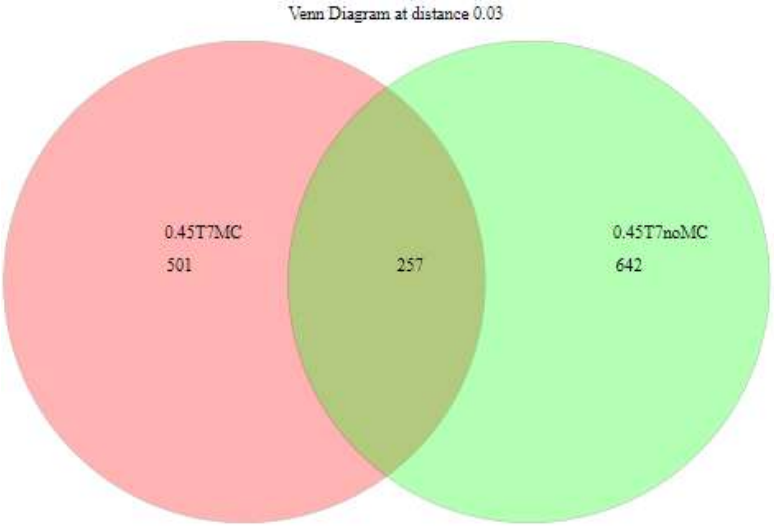

The number of species in group 0.45T7MC is 758

The number of species in group 0.45T7noMC is 899

The number of species shared between groups 0.45T7MC and 0.45T7noMC is 257

Percentage of species that are shared in groups 0.45T7MC and 0.45T7noMC is 18.3571

The total richness for all groups is 1400

(B)

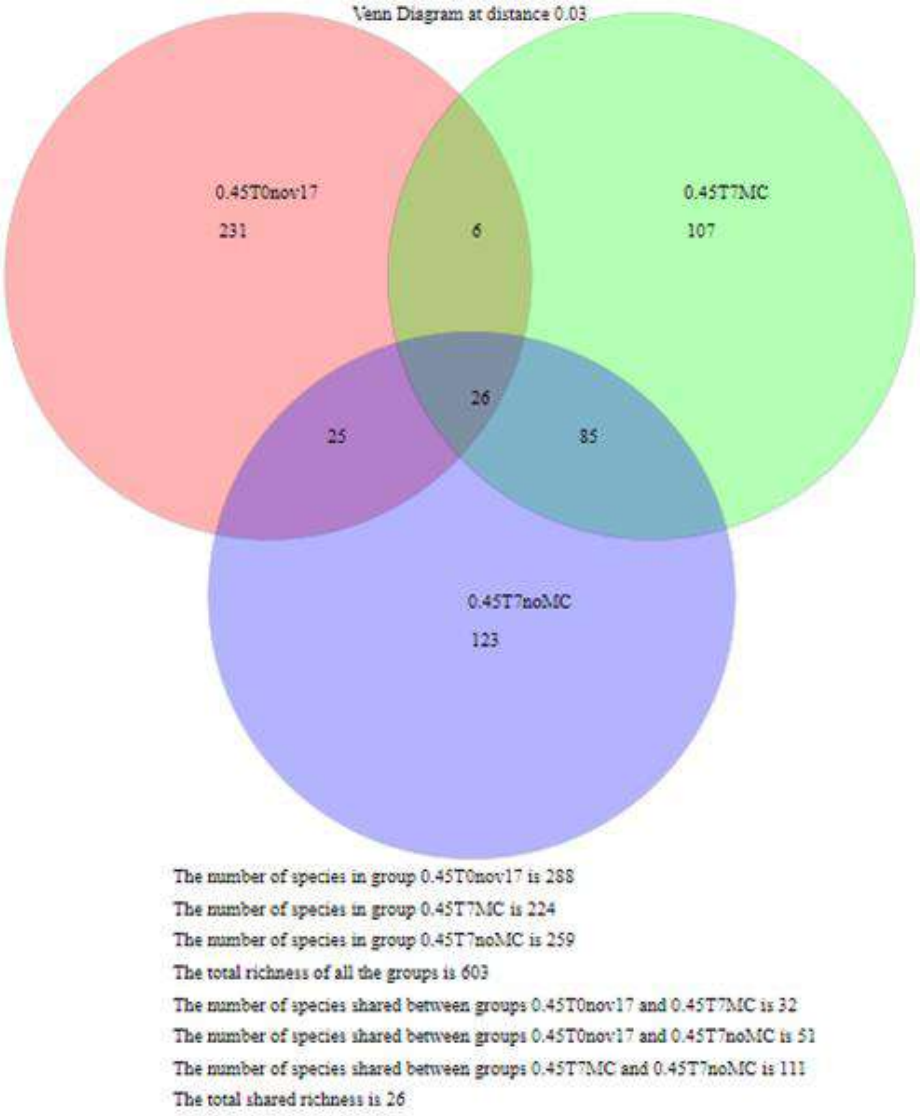

Supplementary Figure 5: Venn diagrams representing comparisons of bacterial community composition based on sobs richness for samples collected in (A) November 2016, and (B) November 2017. In November 2016, pairwise contrasts are shown between <0.22 µm communities at initial (T0) and final (T7) times with MC, between <0.45 µm communities incubated for 7 days with (MC) and without (noMC) MC, and between <0.45 µm and 0.22 µm communities incubated for 7 days with MC. The diagrams show the number of unique species and the number of commonly shared species.

Supplementary Table 1: DNA concentrations recovered from samples used in biodegradation assays. Microbial communities originally selected by different sizes (<0.45 or <0.22 μm) at time 0 (T0) and after 7 days (T7) with or without MC-LR. The sequencing analysis was performed with samples collected in November 2016 and November 2017 (< 0.45 μm and < 0.22 μm fractions). +MCa,b, c refers to replicates maintained with MC-LR.

	DNA concentration (ng/μL)	
Sample	Nov 2016	Nov 2017
<0.45 T0	0.7 (too low)	3.06
<0.45 T7 +MCa	15	9.86
<0.45 T7 +MCb	- (lost)	10.2
<0.45 T7 +MCc	10	9.48
<0.45 T7 no MC	5.6	8.96
<0.22 T0	2.7	0.2 (too low)
<0.22 T7 +MCa	- (lost)	7.84
<0.22 T7 +MCb	52	10.4
<0.22 T7 +MCc	33	11.6
<0.22 T7 no MC	0.9 (too low)	8.6

Supplementary Table 2: Two-way PERMANOVA results for (A) November 2016 (A) and November 2017 (B) samples considering groups by size and presence of MC-LR. (C) Comparison of groups maintained in the presence of MC-LR considering size and year of collection.

(A)

Two-way PERMANOVA

Permutation N: 9999

Source	Sum of sqrs	df	Mean square	*F*	*p*
SIZE	0.39902	1	0.39902	7.3108	0.0113
MC-LR	0.72819	1	0.72819	13.342	0.0223
Interaction	0.33195	1	0.33195	6.082	0.0223
Residual	0.10916	2	0.05458		
Total	1.5683	5			

Similarity index

Bray-Curtis

Permutation N:

9999

Recompute

(B)

Two-way PERMANOVA

Permutation N: 999

Source	Sum of sqrs	df	Mean square	*F*	*p*
size	0.87001	1	0.87001	3.4541	0.001
mc-lr	0.36794	1	0.36794	1.4608	0.047
Interaction	0.034003	1	0.034003	0.135	0.039
Residual	1.2594	5	0.25188		
Total	2.5313	8			

Similarity index

Bray-Curtis

Permutation N:

999

Recompute

(C)

Two-way PERMANOVA

Permutation N: 9999

Source	Sum of sqrs	df	Mean square	*F*	*p*
size	0.7321	1	0.7321	4.8128	0.0001
year	0.83531	1	0.83531	5.4912	0.0002
Interaction	0.19584	1	0.19584	1.2874	0.0022
Residual	0.9127	6	0.15212		
Total	2.676	9			

Similarity index

Bray-Curtis

Permutation N:

9999

Recompute

Supplementary Table 3: Pairwise comparison of samples collected in (A) November 2016 and (B) November 2017. Comparison based on the composition of communities recovered from biodegradation assays. Microbial communities originally selected by different sizes (<0.45 or <0.22 μm) at time 0 (T0) and after 7 days (T7) with (MC) or without MC-LR (noMC). Results of Wilcoxon-Mann-Whitney test ($p<0.05$). In the case of replicates maintained with MC-LR for 7 days, the average composition was considered.

(A)

0.22 T0 vs. 0.22 T7MC	0.45 T7noMC vs. 0.45 T7MC	0.45 T7MC vs. 0.22 T7MC
Mann Whitney test P value: <0.0001 Exact or approximate P value?: Approximate P value summary: **** Significantly different (P < 0.05)?: YES One- or two-tailed P value?: Two-tailed Sum of ranks in column A,B: 5346119 , 4817167 Mann-Whitney U: 2275782	Mann Whitney test P value: <0.0001 Exact or approximate P value?: Approximate P value summary: **** Significantly different (P < 0.05)?: YES One- or two-tailed P value?: Two-tailed Sum of ranks in column A,B: 4885662 , 5286643 Mann-Whitney U: 2342022	Mann Whitney test P value: <0.0001 Exact or approximate P value?: Approximate P value summary: **** Significantly different (P < 0.05)?: YES One- or two-tailed P value?: Two-tailed Sum of ranks in column A,B: 4843134 , 5329171 Mann-Whitney U: 2299494
 **0.22** **T0 x T7 MC**	 **0.45** **T7 MC x T7 no MC**	 **0.22 x 0.45** **T7 MC**

(B)

0.22 T7noMC vs. 0.22 T7MC	0.45 T7MC vs. 0.45 T0	0.45 T7noMC vs. 0.45 T0	0.45 T7noMC vs. 0.45 T7MC	0.22 T7MC vs. 0.45 T7MC
Mann Whitney test P value: 0.8383 Exact or approximate P value?: Approximate P value summary: NS Significantly different (P < 0.05)? NO One- or two-tailed P value?: Two-tailed Sum of ranks in column A,B: 1649654 , 1654082 Mann-Whitney U: 823399	Mann Whitney test P value: 0.0017 Exact or approximate P value?: Approximate P value summary: ** Significantly different (P < 0.05)?: YES One- or two-tailed P value? Two-tailed Sum of ranks in column A,B: 1693498 , 1610237 Mann-Whitney U: 783982	Mann Whitney test P value: 0.4638 Exact or approximate P value?: Approximate P value summary: NS Significantly different (P < 0.05)?: NO One- or two-tailed P value?: Two-tailed Sum of ranks in column A,B: 1661964 , 1641771 Mann-Whitney U: 815516	Mann Whitney test P value: 0.014 Exact or approximate P value?: Approximate P value summary: * Significantly different (P < 0.05)?: YES One- or two-tailed P value?: Two-tailed Sum of ranks in column A,B: 1619568 , 1684167 Mann-Whitney U: 793313	Mann Whitney test P value: <0.0001 Exact or approximate P value?: Approximate P value summary: **** Significantly different (P < 0.05)?: YES One- or two-tailed P value?: Two-tailed Sum of ranks in column A,B: 1700768 , 1602968 Mann-Whitney U: 776713
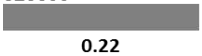 **0.22** **T7 x T7 no MC**	 **0.45** **T0 x T7 MC**	 **0.45** **T0 x T7 no MC**	 **0.45** **T7 MC x T7 no MC**	 **0.22 x 0.45** **T7 MC**

Supplementary Table 4: Composition of bacterial communities (Phylum) based on the relative abundance (%) of OTUs. The composition of samples collected at different dates (Nov 2016 and Nov 2017), originally selected by size (< 0.45 μm or < 0.22 μm) and recovered at initial (T0) or final (7 days, T7) times after incubation with MC-LR (+MC) or without MC-LR (no MC).

November 2016						
Taxon	**0.22 T0**	**0.22 T7 +MCb**	**0.22 T7 +MCc**	**0.45 T7 +MCa**	**0.45 T7 +MCc**	**0.45 T7 no MC**
Actinobacteria	63%	0%	0%	0%	0%	7%
Bacteria_unclassified	3%	0%	0%	0%	0%	0%
Bacteroidetes	1%	10%	9%	1%	1%	3%
Firmicutes	1%	1%	0%	0%	0%	0%
Proteobacteria	31%	86%	85%	99%	98%	89%
Spirochaetes	1%	0%	0%	0%	0%	0%
Tenericutes	0%	3%	5%	0%	0%	0%
Verrucomicrobia	0%	0%	0%	0%	0%	0%
Gemmatimonadetes	0.00%	0.00%	0.00%	0.00%	0.00%	0.00%
Parcubacteria	0.00%	0.00%	0.00%	0.00%	0.00%	0.00%
Planctomycetes	0.00%	0.00%	0.00%	0.00%	0.00%	0.00%
Candidatus Saccharibacteria	0.00%	0.00%	0.00%	0.00%	0.00%	0.00%
Chlamydiae	0.00%	0.00%	0.00%	0.00%	0.00%	0.00%
Deinococcus-Thermus	0.00%	0.00%	0.00%	0.00%	0.00%	0.00%
Fusobacteria	0.00%	0.00%	0.00%	0.00%	0.00%	0.00%
total	100%	100%	100%	100%	100%	100%

November 2017									
Taxon	**0.22 T7 +MCa**	**0.22 T7 +MCb**	**0.22 T7 +MCc**	**0.22 T7 noMC**	**0.45 T0**	**0.45 T7 +MCa**	**0.45 T7 +MCb**	**0.45 T7 +MCc**	**0.45 T7 no MC**
Actinobacteria	0.05%	0.00%	0.10%	0.05%	61.65%	3%	0.19%	0.58%	3.74%
Unclassified	0.10%	0.10%	0.00%	0.10%	14.67%	2%	0.24%	0.58%	0.62%
Bacteroidetes	3.21%	0.58%	3.26%	2.35%	2.21%	8%	10.31%	10.69%	1.49%
Firmicutes	0.00%	0.43%	0.14%	0.00%	3.50%	0%	0.10%	0.38%	0.10%
Planctomycetes	0.00%	0.00%	0.05%	0.00%	1.82%	0%	0.14%	0.24%	0.24%
Proteobacteria	96.64%	98.85%	96.45%	97.51%	14.67%	85%	67.16%	82.74%	89.69%
Tenericutes	0.00%	0.05%	0.00%	0.00%	0.05%	0%	0.38%	0.14%	0.00%
Verrucomicrobia	0.00%	0.00%	0.00%	0.00%	1.44%	2%	21.48%	4.65%	4.12%
total	100.0%	100.0%	100.0%	100.0%	100.0%	100.0%	100.0%	100.0%	100.0%

Supplementary Table 5: SIMPER analysis of the main OTUs (top 20) contributing for the differentiation of bacterial communities according to (A) size (0.22 and 0.45 µm) and (B) presence of MC-LR (1 = presence of MC-LR and 0 = absence of MC-LR) for samples collected in November 2016.

(A)

Nov 2016 SIMPER (considering SIZE)					
Taxon	**Av. dissim**	**Contrib. %**	**Cumulative %**	**Mean 0.22**	**Mean 0.45**
Otu00001	19.32	24.2	24.2	4.61E+03	2.27E+04
Otu00004	8.176	10.24	34.44	9.37E+03	1.57E+03
Otu00003	8.162	10.22	44.66	1.40E+03	1.01E+04
Otu00002	4.466	5.593	50.25	5.75E+03	2.23E+03
Otu00010	3.654	4.576	54.83	3.96E+03	23.7
Otu00012	2.24	2.805	57.63	2.38E+03	168
Otu00006	2.1	2.629	60.26	2.26E+03	60
Otu00020	1.899	2.379	62.64	733	1.82E+03
Otu00011	1.621	2.03	64.67	1.77E+03	34.3
Otu00007	1.441	1.804	66.47	1.56E+03	46.3
Otu00016	1.439	1.801	68.27	191	1.75E+03
Otu00017	1.416	1.773	70.05	1.57E+03	76.7
Otu00013	1.366	1.71	71.76	1.47E+03	38.7
Otu00032	1.247	1.562	73.32	1.16E+03	606
Otu00026	1.145	1.434	74.75	1.25E+03	25
Otu00029	0.9415	1.179	75.93	1.04E+03	66
Otu00019	0.775	0.9704	76.9	132	943
Otu00009	0.7439	0.9316	77.83	815	22.7
Otu00025	0.719	0.9004	78.73	779	24.7
Otu00027	0.715	0.8954	79.63	96	813

(B)

Nov 2016 SIMPER (considering MC-LR)					
Taxon	Av. dissim	Contrib. %	Cumulative %	Mean 0	Mean 1
Otu00001	18.53	20.12	20.12	275	2.03E+04
Otu00003	12.08	13.11	33.23	1.36E+04	1.80E+03
Otu00004	7.541	8.187	41.42	40	8.19E+03
Otu00010	5.475	5.944	47.36	5.94E+03	20.8
Otu00002	5.147	5.588	52.95	282	5.85E+03
Otu00012	3.496	3.796	56.75	3.79E+03	14.5
Otu00006	3.179	3.451	60.2	3.45E+03	15.5
Otu00020	3.137	3.406	63.6	3.54E+03	145
Otu00032	2.423	2.63	66.24	2.63E+03	8
Otu00007	2.184	2.371	68.61	2.38E+03	15.8
Otu00013	2.054	2.23	70.84	2.24E+03	16.3
Otu00011	1.245	1.352	72.19	3	1.35E+03
Otu00016	1.211	1.315	73.5	1.49E+03	709
Otu00017	1.075	1.167	74.67	120	1.17E+03
Otu00025	1.071	1.162	75.83	1.17E+03	18.8
Otu00026	0.8632	0.9371	76.77	30.5	941
Otu00059	0.8437	0.916	77.68	912	0
Otu00029	0.7202	0.7819	78.47	47.5	808
Otu00019	0.6314	0.6855	79.15	102	756
Otu00033	0.6284	0.6822	79.83	686	6.25

Supplementary Table 6: SIMPER analysis of the main OTUs (top 20) contributing for the differentiation of bacterial communities according to (A) size (0.22 and 0.45 µm) and (B) presence of MC-LR (1 = presence of MC-LR and 0 = absence of MC-LR) for samples collected in November 2017.

(A)

November-17 SIMPER (considering SIZE)					
Taxon	Av. dissim	Contrib. %	Cumulative %	Mean 0.22	Mean 0.45
Otu0001	10.22	12.14	12.14	488	116
Otu0002	9.163	10.88	23.03	401	18.2
Otu0003	5.352	6.357	29.38	247	99
Otu0005	3.585	4.258	33.64	164	14.2
Otu0004	3.207	3.809	37.45	139	72.4
Otu0006	2.728	3.24	40.69	0	114
Otu0007	2.681	3.184	43.87	0.25	112
Otu0008	2.049	2.434	46.31	104	23.4
Otu0009	1.846	2.192	48.5	0	77
Otu0011	1.761	2.091	50.59	1.25	74.4
Otu0013	1.548	1.839	52.43	0	64.6
Otu0014	1.411	1.675	54.11	0.25	59
Otu0015	1.376	1.634	55.74	0	57.4
Otu0012	1.369	1.626	57.36	13.5	64
Otu0016	1.33	1.58	58.94	2	55.4
Otu0017	1.29	1.532	60.48	0	53.8
Otu0010	1.185	1.408	61.88	54.8	32.8
Otu0018	0.906	1.076	62.96	0	37.8
Otu0021	0.8593	1.021	63.98	37.3	1.4

Otu0019	0.791	0.9395	64.92	0	33
Otu0020	0.6915	0.8213	65.74	23.8	13.6

(B)

November-17 SIMPER (considering MC-LR)					
Taxon	**Av. dissim**	**Contrib. %**	**Cumulative %**	**Mean 1**	**Mean 0**
Otu0001	7.801	9.709	9.709	352	140
Otu0002	5.857	7.289	17	249	66.3
Otu0003	4.834	6.017	23.02	228	39
Otu0006	4.205	5.234	28.25	6.67	176
Otu0004	3.859	4.803	33.05	65	176
Otu0005	3.603	4.485	37.54	44.7	153
Otu0016	2.18	2.713	40.25	1.5	92
Otu0009	1.836	2.286	42.54	30.8	66.7
Otu0007	1.818	2.262	44.8	75.8	35.3
Otu0011	1.694	2.108	46.91	32.7	60.3
Otu0008	1.505	1.873	48.78	64.3	49
Otu0018	1.348	1.677	50.46	3.33	56.3
Otu0019	1.318	1.641	52.1	0	55
Otu0013	1.29	1.606	53.7	53.8	0
Otu0012	1.244	1.548	55.25	58.3	8
Otu0010	1.222	1.522	56.77	59	9.67
Otu0015	1.087	1.352	58.13	45.3	5
Otu0014	1.073	1.336	59.46	41	16.7
Otu0017	1.051	1.308	60.77	43.8	2
Otu0032	0.6711	0.8353	61.61	0	28
Otu0020	0.6125	0.7624	62.37	25.7	3

Supplementary Table 7: Exclusive OTUs in < 0.22 μm communities considering those that contributed with ≥10 sequences in both November 2016 and November 2017 samples. Numbers in parentheses correspond to the classification confidence (%) according to the database.

Taxon
Actinobacteria(100);Actinobacteria(100);Actinomycetales(100);Mycobacteriaceae(100);**Mycobacterium**(100)
Actinobacteria(100);Actinobacteria(100);**Actinomycetales**(100);Actinomycetales_unclassified(100);Actinomycetales_unclassified (100)
Actinobacteria(100);Actinobacteria(100);**Actinomycetales**(100);Actinomycetales_unclassified(100);Actinomycetales_unclassified (100;
Actinobacteria(100);Actinobacteria(100);**Actinomycetales**(100);Actinomycetales_unclassified(100);Actinomycetales_unclassified (100)
Actinobacteria(100);Actinobacteria(100);**Actinomycetales**(100);Actinomycetales_unclassified(100);Actinomycetales_unclassified (100)
Actinobacteria(100);Actinobacteria(100);**Actinomycetales**(100);Actinomycetales_unclassified(100);Actinomycetales_unclassified (100)
Actinobacteria(100);Actinobacteria(100);**Actinomycetales**(100);Actinomycetales_unclassified(100);Actinomycetales_unclassified (100)

Actinobacteria(100);**Actinobacteria**(100);Actinobacteria_unclassified(100);Actinobacteria_unclassified(100);Actinobacteria_unclassified(100)
Actinobacteria(77);**Actinobacteria**(54);Actinobacteria_unclassified(54);Actinobacteria_unclassified(54);Actinobacteria_unclassified(54)
Actinobacteria(61);**Actinobacteria**(56);Actinobacteria_unclassified(56);Actinobacteria_unclassified(56);Actinobacteria_unclassified(56)
Bacteroidetes(100);Bacteroidia(84);**Bacteroidales**(84);Bacteroidales_unclassified(84);Bacteroidales_unclassified(84)
Bacteroidetes(100);Flavobacteriia(100);Flavobacteriales(100);**Cryomorphaceae**(100);Cryomorphaceae_unclassified(100)
Bacteroidetes(100);Flavobacteriia(100);Flavobacteriales(100);**Cryomorphaceae**(100);Cryomorphaceae_unclassified(100)
Bacteroidetes(100);Bacteroidetes_unclassified(100);Bacteroidetes_unclassified(100);Bacteroidetes_unclassified(100);Bacteroidetes_unclassified(100)
Proteobacteria(100);Alphaproteobacteria(100);Rhodospirillales(100);Rhodospirillaceae(100);**Azospirillum**(100)

Proteobacteria(100);Alphaproteobacteria(100);Rhodospirillales(100);Rhodospirillaceae(100);**Insolitispirillum**(100)
Proteobacteria(100);Betaproteobacteria(100);Methylophilales(100);**Methylophilaceae**(100);Methylophilaceae_unclassified(100)
Proteobacteria(100);Betaproteobacteria(100);Methylophilales(100);**Methylophilaceae**(100);Methylophilaceae_unclassified(100)
Proteobacteria(100);Betaproteobacteria(100);Methylophilales(100);**Methylophilaceae**(100);Methylophilaceae_unclassified(100)
Proteobacteria(100);Betaproteobacteria(100);Rhodocyclales(100);Rhodocyclaceae(100);**Zoogloea**(78)
Proteobacteria(100);Deltaproteobacteria(100);Desulfuromonadales(100);Geobacteraceae(100);**Geobacter**(100)
Proteobacteria(100);Deltaproteobacteria(100);Bdellovibrionales(100);Bacteriovoracaceae(100);**Halobacteriovorax**(100)
Proteobacteria(100);Gammaproteobacteria(100);Pseudomonadales(100);Moraxellaceae(100);**Acinetobacter**(100)
Proteobacteria(100);Gammaproteobacteria(100);Alteromonadales(100);Alteromonadaceae(100);**Catenovulum**(100)
Proteobacteria(100);Gammaproteobacteria(100);Thiotrichales(100);Piscirickettsiaceae(100);**Thioalkalimicrobium**(100)

Proteobacteria(86);**Gammaproteobacteria**(58);Gammaproteobacteria_unclassified(58);Gammaproteobacteria_unclassified(58);Gammaproteobacteria_unclassified(58)
Spirochaetes(100);Spirochaetia(100);Spirochaetales(100);Spirochaetaceae(100);**Spirochaeta**(100)
Spirochaetes(100);Spirochaetia(100);Spirochaetales(100);Spirochaetaceae(100);**Spirochaeta**(100)
Spirochaetes(100);Spirochaetia(100);Spirochaetales(100);Spirochaetaceae(100);**Spirochaeta**(100)
Spirochaetes(100);Spirochaetia(100);Spirochaetales(100);**Spirochaetaceae**(100);Spirochaetaceae_unclassified(100)
Tenericutes(75);Mollicutes(75);Acholeplasmatales(67);Acholeplasmataceae(67);**Acholeplasma**(67)
Tenericutes(100);Mollicutes(100);Acholeplasmatales(100);Acholeplasmataceae(100);**Acholeplasma**(100)
Tenericutes(100);Mollicutes(100);Acholeplasmatales(100);Acholeplasmataceae(100);**Acholeplasma**(100)
Tenericutes(100);Mollicutes(100);Acholeplasmatales(94);Acholeplasmataceae(94);**Acholeplasma**(94)
Tenericutes(100);Mollicutes(100);Acholeplasmatales(100);Acholeplasmataceae(100);**Acholeplasma**(100)

Bacteria_unclassified(84);Bacteria_unclassified(84);Bacteria_unclassified(84);Bacteria_unclassified(84);Bacteria_unclassified(84)
Bacteria_unclassified(100);Bacteria_unclassified(100);Bacteria_unclassified(100);Bacteria_unclassified(100);Bacteria_unclassified(100)
Bacteria_unclassified(100);Bacteria_unclassified(100);Bacteria_unclassified(100);Bacteria_unclassified(100);Bacteria_unclassified(100)
Bacteria_unclassified(100);Bacteria_unclassified(100);Bacteria_unclassified(100);Bacteria_unclassified(100);Bacteria_unclassified(100)
Bacteria_unclassified(58);Bacteria_unclassified(58);Bacteria_unclassified(58);Bacteria_unclassified(58);Bacteria_unclassified(58)
Bacteria_unclassified(91);Bacteria_unclassified(91);Bacteria_unclassified(91);Bacteria_unclassified(91);Bacteria_unclassified(91)
Bacteria_unclassified(92);Bacteria_unclassified(92);Bacteria_unclassified(92);Bacteria_unclassified(92);Bacteria_unclassified(92)
Bacteria_unclassified(100);Bacteria_unclassified(100);Bacteria_unclassified(100);Bacteria_unclassified(100);Bacteria_unclassified(100)
Bacteria_unclassified(67);Bacteria_unclassified(67);Bacteria_unclassified(67);Bacteria_unclassified(67);Bacteria_unclassified(67)
Bacteria_unclassified(90);Bacteria_unclassified(90);Bacteria_unclassified(90);Bacteria_unclassified(90);Bacteria_unclassified(90)

Bacteria_unclassified(100);Bacteria_unclassified(100);Bacteria_unclassified(100);Bacteria_unclassified(100);Bacteria_unclassified(100)
Bacteria_unclassified(100);Bacteria_unclassified(100);Bacteria_unclassified(100);Bacteria_unclassified(100);Bacteria_unclassified(100)
Bacteria_unclassified(100);Bacteria_unclassified(100);Bacteria_unclassified(100);Bacteria_unclassified(100);Bacteria_unclassified(100)

8.4 Capítulo 4 (Biodegradation of cyanobacterial and non-cyanobacterial peptides by *Paucibacter toxinivorans*)

Supplementary Table 1: Exponential decay rate calculated as percent per day (d^{-1}) for each cyanopeptide and respective condition evaluated from *Sphingosinicella microcystinivorans* Y2 strain and *Paucibacter toxinivorans* strain 2C20 biodegradation capacity besides negative control.

	Decay rate of cyanopeptides		
	Over 7 days		
	Y2	2C20	Neg Control
Purified cyanopeptides			
MC-LR	0.001 ± 0.008	0.272 ± 0.010	-0.008 ± 0.004
DM-LR	0.025 ± 0.016	0.498 ± 0.001	-0.024 ± 0.0005
MC-RR	0.013 ± 0.018	0.351 ± 0.066	-0.024 ± 0.005
MC-LF	0.062 ± 0.029	0.372 ± 0.002	-0.032 ± 0.006
MC-YR	-0.006 ± 0.007	0.544 ± 0.044	-0.024 ± 0.0004
ANBP A	-0.010 ± 0.005	1.012 ± 0.003	-0.013 ± 0.004
ANBP B	-0.009 ± 0.009	1.007 ± 0.016	-0.015 ± 0.003
Aerucycl. A	-0.018 ± 0.005	0.704 ± 0.0009	-0.028 ± 0.007
Aerucycl. D	-0.005 ± 0.007	1.117 ± 0.018	-0.012 ± 0.004
Cyanopeptides in mix			
MC-LR + mix	0.0006 ± 0.0008	0.162 ± 0.008	-0.026 ± 0.013
DM-LR in mix	0.0005 ± 0.003	0.157 ± 0.005	-0.027 ± 0.013
MC-RR in mix	0.002 ± 0.003	0.086 ± 0.0012	-0.024 ± 0.011
MC-LF in mix	0.005 ± 0.002	0.054 ± 0.007	-0.012 ± 0.01
MC-YR in mix	0.006 ± 0.001	0.182 ± 0.004	-0.024 ± 0.012
ANBP A in mix	-0.009 ± 0.001	*	-0.03 ± 0.012
ANBP B in mix	0.005 ± 0.004	*	-0.036 ± 0.016
Aerucycl. A in mix	0.016 ± 0.002	*	-0.001 ± 0.01

Aerucycl. D in mix	0.036 ± 0.004	*	0.004 ± 0.013
MC-LR + *M.aeruginosa* 7806 crude extract	-0.007 ± 0.019	0.668 ± 0.003	-0.0049 ± 0.01

*respective cyanopeptide was not detected at any time, even time 0.

Supplementary Table 2: Exponential decay rate (d^{-1}) for each cyanopeptide in different condition (purified and into the mix) from *Paucibacter toxinivorans* 2C20 strain degradation capability. The decay rates are represented over the first three days of incubation and over the last four days of incubation.

	Decay rate of cyanopeptides	
	First 3 days	Last 4 days
Purified cyanopeptide		
MC-LR	0.109 ± 0.013	0.394 ± 0.02
DM-LR	0.203 ± 0.005	0.719 ± 0.003
MC-RR	0.240 ± 0.04	0.435 ± 0.095
MC-LF	0.233 ± 0.017	0.478 ± 0.012
MC-YR	0.177 ± 0.023	0.819 ± 0.092
ANBP A	2.363 ± 0.007	**
ANBP B	2.350 ± 0.037	**
Aerucycl. A	1.643 ± 0.002	**
Aerucycl. D	2.607 ± 0.044	**
Cyanopeptides in mix		
MC-LR + mix	0.09 ± 0.05	0.215 ± 0.045
DM-LR in mix	0.088 ± 0.023	0.209 ± 0.013
MC-RR in mix	0.068 ± 0.024	0.100 ± 0.015
MC-LF in mix	0.022 ± 0.025	0.077 ± 0.009
MC-YR in mix	0.110 ± 0.02	0.236 ± 0.02
ANBP A in mix	*	*
ANBP B in mix	*	*
Aerucycl. A in mix	*	*
Aerucycl. D in mix	*	*
MC-LR + *M.aeruginosa* 7806 crude extract	2.33 ± 0.007	**

*respective cyanopeptide was not detected at any time even time 0, which makes an unattainable decay rate calculation

**respective cyanopeptide was completely degraded over 3rd day, so there was no decay rate for the last 4 days

Supplementary Material: Selected Reaction Monitoring (SRM) transitions and retention time used for detection of all peptides studied

Peptide	[M+H]* or [M+2H]** (and daughter ion)	Retention time
DM-LR	981.596>135.239	2.81
MC-RR	520>135.24**	1.83
MC-LF	986.596>135.245	4.40
MC-YR	1045.568>135.303	2.57
MC-LR	995.6>135.239	2.78
ANBP A	844.48>83.96	1.85
ANBP B	837.521>201.021	1.56
AERUCY A	535..287>140.907	2.58
AERUCY D	587.13>539.125	2.32
CYCL A	1224.841>1112.809	3.57
FIB	786.075>119.95	1.25
LEU-ENK	556.313>119.951	1.43
OXYT	1007.458>723.307	1.30